In Vivo Biomechanics of Cruciate Ligament Injuries

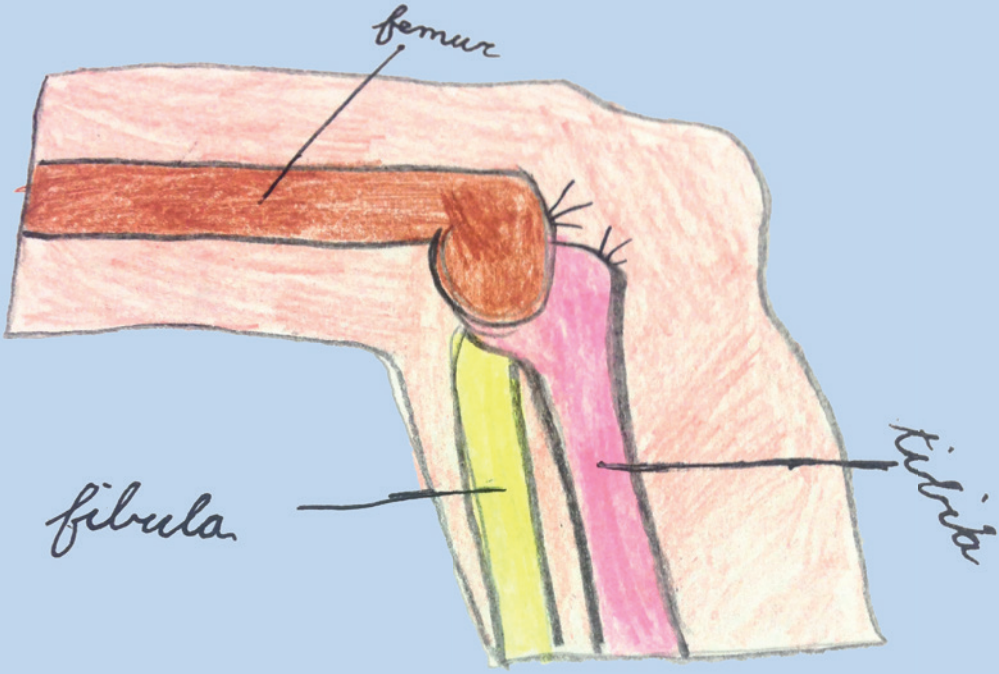

Samuel K. Van de Velde

Stellingen behorende bij het proefschrift

In Vivo Biomechanics of Cruciate Ligament Injuries

1. The widely accepted assumption that abnormal kinematics and consequent abnormal loading within the knee initiate osteoarthritis underlies much of current osteoarthritis research and orthopedic practice. (*This thesis*)
2. An MRI scanner, two fluoroscopes, and a group of keen students with computers suffice for the accurate analysis of in vivo knee biomechanics. (*This thesis*)
3. A minimal shift in tibiofemoral kinematics in cruciate ligament deficiency results in a considerable change in cartilage loading distribution within the knee joint. (*This thesis*)
4. Injury of the posterior cruciate ligament is not be as benign as previously thought. (*This thesis*)
5. Cruciate ligament deficiency upsets the entire in vivo knee homeostasis with changes in patellofemoral biomechanics and elongation patterns of the collateral ligaments. (*This thesis*)
6. Of the various lateral extra-articular reconstructions, an anatomic anterolateral ligament reconstruction might be the least biomechanically favorable option. (*This thesis*)
7. The study of in vivo knee biomechanics documents more than just common sense. (*This thesis*)
8. Evidence based medicine is not restricted to randomized trials and meta-analyses. Sometimes the evidence we need will come from the basic sciences [...]. (*David L. Sackett*)
9. Orthopaedic sports medicine extends far beyond the boundaries of the intercondylar notch. (*Robert E. Leach*)
10. The knee anterolateral ligament may be fiction, but we thought it fact. (*James H. Lubowitz, Editor-in-Chief, Arthroscopy*)
11. Never include too many articles about the anterior cruciate ligament in any one issue of the Journal. (*The ACL Rule, the American Journal of Sports Medicine*)
12. Dad, you should become a pediatric orthopaedic surgeon. Children's bones are smaller so you are home sooner. (*Svea Van de Velde*)

In Vivo Biomechanics of Cruciate Ligament Injuries

Samuel Van de Velde

In Vivo Biomechanics of Cruciate Ligament Injuries

PhD thesis, Leiden University Medical Center, Leiden, the Netherlands

ISBN: 978-94-6299-443-0

Cover design: Svea Van de Velde

Lay-out and printing: Ridderprint BV

The digital version of this thesis is available at www.orthopeden.org or by scanning the QR-code.

Funding for this thesis was provided by the Henri Benedictus - Fellow of the King Baudouin Foundation and the Belgian American Educational Foundation (BAEF); National Institutes of Health (NIH) R01AR052408-01, R21AR051078-01, R01AR055612-01, and the NIH Ruth L. Kirschstein National Research Service Award Postdoctoral Fellowship F32AR056451-01A1.

The publication of this thesis was supported by the Nederlandse Orthopaedische Vereniging, Haaglanden Medisch Centrum, Nederlandse Vereniging voor Arthroscopie, KBC Haaglanden Fysiotherapie, Bauerfeind Benelux, Anna Foundation|NOREF, en Van Dinter Den Haag.

In Vivo Biomechanics of Cruciate Ligament Injuries

Proefschrift

ter verkrijging van
de graad van Doctor aan de Universiteit van Leiden,
op gezag van Rector Magnificus prof. mr. C.J.J.M. Stolker,
volgens besluit van het College voor Promoties
te verdedigen op dinsdag 29 november 2016
klokke 15:00 uur
door

Samuel Karel Van de Velde
Geboren te Mechelen, België
in 1978

Promotor:	Prof. dr. R.G.H.H. Nelissen
Co-promotores:	Assoc. Prof. Guoan Li (Harvard Medical School, USA)
	Dr. E.R.A. van Arkel (HMC, Den Haag)
Leden promotiecommissie:	Prof. dr. G. Kloppenburg
	Prof. dr. B.P.F. Lelieveldt
	Prof. dr. G.M.M.J. Kerkhoffs (AMC, Amsterdam)
	Dr. D.E. Meuffels (Erasmus MC, Rotterdam)

To my wife Jolie and children Svea, Finnegan and Beckett

TABLE OF CONTENTS

CHAPTER 1

General introduction

"Biomechanics is mechanics applied to biology. Biomechanics seeks to understand the mechanics of living systems. The motivation for research in this area comes from the realization that biology can no more be understood without biomechanics than an airplane can without aerodynamics. For an airplane, mechanics enables us to design its structure and predict its performance. For an organism, biomechanics helps us to understand its normal function, predict changes due to alterations, and propose methods of artificial intervention. Thus diagnosis and treatment are closely associated with biomechanics."

Y.C. Fung, 1981

Injury during sports is a constant threat and, of all injuries, those of the knee fulfill the athlete's greatest fear of spending a long time out of action.[5] The most common disabling injury of the knee is rupture of the anterior cruciate ligament (ACL), with an estimated annual incidence of one in 1,750 in patients under 30 years of age.[19] The tell-tale 'pop' of the ligament (and accompanying pain) means the end of the athlete's season and the beginning of approximately a year of rehabilitation before a full recovery is possible. Acute injury of the ACL is associated with meniscal tears, chondral damage, and injury to the medial collateral ligament (MCL).[9,20,28,33] As the ACL injury becomes more chronic, an increasing incidence of joint swelling, instability, and meniscal tears is found.[1,14,31,32] Ultimately, an increased incidence,[14,36] an earlier onset,[36] and a faster progression[22] of knee osteoarthritis (OA) is seen in ACL deficient patients.

Rupture of the posterior cruciate ligament (PCL) – which compared to the ACL has received much less attention in the literature despite its incidence of up to 37% in patients presenting with knee hemarthrosis after a sports or traffic accident – might not be as benign as previously thought.[13,18,24,40] Even though many PCL deficient patients do relatively well with nonoperative treatment fairly long term, several studies have shown that as an isolated PCL deficiency becomes chronic, persistent pain, swelling, and instability are prevalent, eventually resulting in joint degeneration.[10-13,24,40,41]

According to a survey of orthopaedic surgeons that were randomly selected from the American Academy of Orthopaedic Surgeons (AAOS) directory, the standard of care for a ruptured ACL in persons who place a high demand on the ligament is an arthroscopic autograft reconstruction of the damaged ligament.[29] Each year ~200,000 patients opt for ACL reconstruction in the United States,[7] drawn by the excellent postoperative stability and health-related quality of life.[3] Serious adverse events such as infection and deep vein thrombosis are rare (<1%),[8,17] and the most distressing complication of ACL reconstruction, i.e. failure of the reconstructed ACL graft, occurs in less than 6%.[26,42] Yet, despite the generally high patient-reported satisfaction and function, less than 50% of patients return to

their preinjury level of play after uncomplicated ACL reconstruction.[2,37] Interestingly, more than 50% of patients might be able to cope with the loss of ACL function when they are provided with structured rehabilitation supervised by a physical therapist, without compromising the clinical results.[15] Even at 5-years, clinical results and radiographic measures did not differ between knees surgically reconstructed early or late and those with an ACL deficient knee treated with rehabilitation alone, indicating that not every young, active adult necessarily requires surgical reconstruction of the ACL.[16] Eventually, no long-term difference in OA prevalence has been detected between patients that opted for conservative treatment and those that opted for surgery.[27]

The optimal treatment of isolated PCL injuries is even more controversial than that of ACL injuries. Whereas some clinicians have traditionally advocated nonoperative treatment of a torn PCL because many patients with PCL deficiency have good functional results,[12,34] others have supported surgical reconstruction based on long-term follow-up studies revealing an association between the increased posterior displacement of the tibia and joint degeneration in PCL deficient knees.[6,11,25,38] Unfortunately, analogous to the inability of ACL reconstruction to prevent long-term joint degeneration, OA has been reported in 20% to 60% of patients after PCL reconstruction as well.[4,11,21,35]

The etiology of the variable perception of disability following cruciate ligament deficiency, the reduced reintegration in sports participation after surgical reconstruction, and the inability of either ACL or PCL reconstruction to prevent OA is multifaceted and goes beyond the scope of the present thesis. For one, lifestyle naturally changes with increasing age, and so do the physical demands of the knee. No relationship has been found between knee function and activity level. Rather, most patients who were less active after cruciate ligament reconstruction at a young age indicated a change in interest with advancing age.[37] Fear of reinjury or further damage is cited as an additional critical factor for not returning to play at any level of competition in a different cohort.[30] Another factor in the variable disability perception might be the plastic changes in brain activation patterns following cruciate ligament rupture. For example, functional MR imaging of patients with chronic ACL deficiency has shown a reorganization of the central nervous system, suggesting that ACL injury might be regarded as a neurophysiologic dysfunction with altered propriocepsis and centrally controlled balance disturbances.[23] Finally, the loss of cruciate ligament integrity directly causes direct biomechanical modifications of the injured lower limb – modifications which might persist even after clinically successful reconstruction. It is the latter topic that will be the focus of the present thesis.

The ***aim of this thesis*** is to explore the complexity of biomechanics of a rupture of either the ACL or the PCL complex.

Measuring biomechanics of the knee with an acceptable degree of accuracy is difficult. When the in vivo knee joint motion is analyzed in all its six degrees-of-freedom without

compromising on physiological loading conditions, the task becomes even more challenging. This thesis offers a brief overview of the development, validation and application of a non-invasive imaging methodology to capture the in vivo biomechanics of ACL deficient and PCL deficient knees.

By combining dual fluoroscopy to capture the in vivo joint motion and magnetic resonance (MR) imaging to reconstruct the joint anatomy, we obtained a comprehensive insight in both tibiofemoral as well as patellofemoral kinematics and cartilage biomechanics of healthy knees under various loading conditions. These baseline measurements helped us comprehend the alterations in biomechanics seen in knees after injury of either ACL or PCL, which in turn generated clinically useful data for the improvement of our surgical reconstruction techniques.

The thesis is organized in several chapters, with the first chapters focusing on the measurement methodology and its validation, the next chapters covering the biomechanical sequelae of ACL injury and PCL injury, and the final chapters concentrating on the ACL complex as it affects the entire knee joint.

In ***Chapter 2***, we present a rationale for the measurement of in vivo knee biomechanics. In ***Chapter 3***, we describe the step-by-step approach to the measurement of in vivo knee biomechanics with the combined MR and dual fluoroscopic imaging system. Results are only as strong as the validity of the measurement system that generates the data. Therefore, we outline in ***Chapter 4*** our validation study of the combined MR and dual fluoroscopic imaging system for the measurement of tibiofemoral kinematics.

The biomechanical data of ACL deficient and PCL deficient knees that were obtained with the combined MR and dual fluoroscopic imaging system are presented in the subsequent chapters. ***Chapters 5 and 6*** demonstrate how minimal alterations in tibiofemoral kinematics in ACL deficient and PCL deficient knees result in abnormal cartilage contact biomechanics. Since the tibiofemoral and patellofemoral kinematics are linked, it is not surprising to see that rupture of either ACL or PCL also affects the patellofemoral joint (***Chapters 7 and 8***). That deficiency of one of the knee joint structures upsets the in vivo knee homeostasis is demonstrated by the changes seen in the collateral ligaments in ACL injured knees (***Chapter 9***).

We contend that the study of in vivo knee biomechanics is more than an esoteric basic science field, and can generate clinically useful data. For example, in ***Chapter 10,*** based on our biomechanics analysis we argue against performing an anatomic reconstruction of the anterolateral ligament (ALL), and instead make a case for reconsidering the more traditional lateral extra-articular reconstructions in patients with increased anterolateral laxity following ACL injury.

REFERENCES

1. Aichroth PM, Patel DV, Zorrilla P. The natural history and treatment of rupture of the anterior cruciate ligament in children and adolescents: a prospective review. J Bone Joint Surg Br. 2002;84:38-41.
2. Ardern CL, Taylor NF, Feller JA, Webster KE. Return-to-sport outcomes at 2 to 7 years after anterior cruciate ligament reconstruction surgery. Am J Sports Med. 2012 Jan;40(1):41-8.
3. Barenius B, Nordlander M, et al. Quality of life and clinical outcome after ACL reconstruction using patellar tendon graft or quadrupled semitendinosus graft: an 8-year follow-up of a randomized controlled trial. Am J Sports Med. 2010; 38:1533–1541.
4. Becker R, Ropke M, Nebelung W. Clinical outcome of arthroscopic posterior cruciate ligament-plasty. Unfallchirurg. 1999;102(5):354-358.
5. Bollen S. Epidemiology of knee injuries: diagnosis and triage. Br J Sports Med 2000;34:227-228
6. Boynton MD, Tietjens BR. Long-term followup of the untreated isolated posterior cruciate ligament-deficient knee. Am J Sports Med. 1996;24(3):306-310.
7. Brophy RH, Wright RW, et al. Cost analysis of converting from single-bundle to double-bundle anterior cruciate ligament reconstruction. Am J Sports Med. 2009; 37:683–687.
8. Brophy RH, Wright RW, Huston LJ, Nwosu SK; MOON Knee Group, Spindler KP. Factors associated with infection following anterior cruciate ligament reconstruction. J Bone Joint Surg Am. 2015 Mar 18;97(6):450-4.
9. Butler JC, Andrews JR. The role of arthroscopic surgery in the evaluation of acute traumatic hemarthrosis of the knee. Clin Orthop Relat Res. 1988;228:150-152.
10. Clancy WG Jr, Shelbourne KD, Zoellner GB, Keene JS, Reider B, Rosenberg TD. Treatment of knee joint instability secondary to rupture of the posterior cruciate ligament: report of a new procedure. J Bone Joint Surg Am. 1983;65(3):310-322.
11. Cross MJ, Powell JF. Long-term followup of posterior cruciate ligament rupture: a study of 116 cases. Am J Sports Med. 1984; 12(4):292-297.
12. Dandy DJ, Pusey RJ. The long-term results of unrepaired tears of the posterior cruciate ligament. J Bone Joint Surg Br. 1982;64(1):92-94.
13. Dejour H, Walch G, Peyrot J, Eberhard P. The natural history of rupture of the posterior cruciate ligament. Rev Chir Orthop Reparatrice Appar Mot. 1988;74(1):35-43.
14. Fithian DC, Paxton LW, Goltz DH. Fate of the anterior cruciate ligament-injured knee. Orthop Clin North Am. 2002;33:621-636.
15. Frobell RB, Roos EM, Roos HP, Ranstam J, Lohmander LS. A randomized trial of treatment for acute anterior cruciate ligament tears. N Engl J Med. 2010 Jul 22;363(4):331-42 A randomized trial of treatment for acute anterior cruciate ligament tears.
16. Frobell RB, Roos HP, Roos EM, Roemer FW, Ranstam J, Lohmander LS. Treatment for acute anterior cruciate ligament tear: five year outcome of randomised trial. Br J Sports Med. 2015 May;49(10):700.

17. Gaskill T, Pullen M, Bryant B, Sicignano N, Evans AM, DeMaio M. The Prevalence of Symptomatic Deep Venous Thrombosis and Pulmonary Embolism After Anterior Cruciate Ligament Reconstruction. Am J Sports Med. 2015 Nov;43(11):2714-9.

18. Geissler WB, Whipple TL. Intraarticular abnormalities in association with posterior cruciate ligament injuries. Am J Sports Med. 1993;21(6):846-849.

19. Griffin LY, Agel J, Albohm MJ, et al. Noncontact anterior cruciate ligament injuries: risk factors and prevention strategies. J Am Acad Orthop Surg. 2000;8(3):141-150.

20. Hardaker WT Jr, Garrett WE Jr, Bassett FH III. Evaluation of acute traumatic hemarthrosis of the knee joint. South Med J. 1990;83:640-644.

21. Hughston JC, Bowden JA, Andrews JR, Norwood LA. Acute tears of the posterior cruciate ligament: results of operative treatment. J Bone Joint Surg Am. 1980;62(3):438-450.

22. Kannus P, Jarvinen M. Posttraumatic anterior cruciate ligament insufficiency as a cause of osteoarthritis in a knee joint. Clin Rheumatol 1989;8:251–60.

23. Kapreli E, Athanasopoulos S, Gliatis J, et al. Anterior cruciate ligament deficiency causes brain plasticity: a functional MRI study. Am J Sports Med. 2009 Dec;37(12):2419-26.

24. Keller PM, Shelbourne KD, McCarroll JR, Rettig AC. Nonoperatively treated isolated posterior cruciate ligament injuries. Am J Sports Med. 1993;21(1):132-136.

25. L'Insalata JC, Harner CD. Treatment of acute and chronic posterior cruciate ligament deficiency: new approaches. Am J Knee Surg. 1996;9(4):185-193.

26. Lind M, Menhert F, Pedersen AB. Incidence and outcome after revision anterior cruciate ligament reconstruction: results from the Danish registry for knee ligament reconstructions. Am J Sports Med. 2012 Jul;40(7):1551-7.

27. Lohmander LS, Englund PM, et al. The long-term consequence of anterior cruciate ligament and meniscus injuries: osteoarthritis. Am J Sports Med. 2007; 35:1756–1769.

28. Maffulli N, Binfield PM, King JB, Good CJ. Acute haemarthrosis of the knee in athletes: a prospective study of 106 cases. J Bone Joint Surg Br. 1993;75:945-949.

29. Marx RG, Jones EC, Angel M, Wickiewicz TL, Warren RF. Beliefs and attitudes of members of the American Academy of Orthopaedic Surgeons regarding the treatment of anterior cruciate ligament injury. Arthroscopy. 2003;19(7):762–770.

30. McCullough KA, Phelps KD, Spindler KP, et al. MOON Group Return to high school- and college-level football after anterior cruciate ligament reconstruction: A Multicenter Orthopaedic Outcomes Network (MOON) cohort study. Am J Sports Med. 2012;40(11):2523–2529.

31. Murrell GA, Maddali S, Horovitz L, Oakley SP, Warren RF. The effects of time course after anterior cruciate ligament injury in correlation with meniscal and cartilage loss. Am J Sports Med. 2001;29:9-14.

32. Nebelung W, Wuschech H. Thirty-five years of follow-up of anterior cruciate ligament-deficient knees in high-level athletes. Arthroscopy. 2005;21:696-702.

33. Noyes FR, Bassett RW, Grood ES, Butler DL. Arthroscopy in acute traumatic hemarthrosis of the knee: incidence of anterior cruciate tears and other injuries. J Bone Joint Surg Am. 1980;62:687-695, 757.

34. Patel DV, Allen AA, Warren RF, Wickiewicz TL, Simonian PT. The nonoperative treatment of acute, isolated (partial or complete) posterior cruciate ligament-deficient knees: an intermediate-term follow-up study. HSS J. 2007;3(2):137-146.

35. Richter M, Kiefer H, Hehl G, Kinzl L. Primary repair for posterior cruciate ligament injuries: an eight-year followup of fifty-three patients. Am J Sports Med. 1996;24(3):298-305.

36. Roos H, Adalberth T, Dahlberg L, Lohmander LS. Osteoarthritis of the knee after injury to the anterior cruciate ligament or meniscus: the influence of time and age. Osteoarthritis Cartilage 1995;3:261–7.

37. Schmale GA, Kweon C, Larson RV, Bompadre V. High satisfaction yet decreased activity 4 years after transphyseal ACL reconstruction. Clin Orthop Relat Res. 2014 Jul;472(7):2168-74.

38. Schulte KR, Chu ET, Fu FH. Arthroscopic posterior cruciate ligament reconstruction. Clin Sports Med. 1997;16(1):145-156.

39. Shelbourne KD, Wilckens JH, Mollabashy A, DeCarlo M. Arthrofibrosis in acute anterior cruciate ligament reconstruction. The effect of timing of reconstruction and rehabilitation. Am J Sports Med. 1991 Jul-Aug;19(4):332-6.

40. Strobel MJ, Weiler A, Schulz MS, Russe K, Eichhorn HJ. Arthroscopic evaluation of articular cartilage lesions in posterior-cruciate-ligament deficient knees. Arthroscopy. 2003;19(3):262-268.

41. Torg JS, Barton TM, Pavlov H, Stine R. Natural history of the posterior cruciate ligament-deficient knee. Clin Orthop Relat Res. 1989;246:208-216.

42. Wright RW, Magnussen RA, Dunn WR, Spindler KP. Ipsilateral graft and contralateral ACL rupture at five years or more following ACL reconstruction: A systematic review. J Bone Joint Surg Am. 2011;93(12):1159–1165.

2

CHAPTER

Evaluation of knee biomechanics with three-dimensional modeling techniques.

Samuel K. Van de Velde
Thomas J. Gill, IV
Guoan Li

J Bone Joint Surg Am. 2009 Feb;91 Suppl 1:108-14.

In orthopaedic surgery, the central pathology motivating the study of biomechanics is osteoarthritis (OA). The stiffness, pain and loss of movement attributed to OA affect nearly 27 million people in the United States and increase its total health care costs by $186 billion each year.[20] The knee, the principal large joint to be targeted by OA, results in disabling knee symptoms in an estimated 10% of the UK population older than 55, a quarter of whom are severely disabled.[28] Despite decades of research, OA continues to be viewed as an irreversible degradation of the joint. Upon diagnosis, the patient is resigned to either palliative medical care or – if conservative management fails – surgical replacement of the diseased joint. Current orthopaedic practice and its attempts at preventing OA are to a large extent based on the widely accepted assumption that abnormal joint kinematics, with consequent abnormal loading within the joint, initiate detrimental processes such as the progressive degeneration of articular cartilage and the subchondral bone next to it. The biomechanics of the various musculoskeletal articulations are therefore studied so that treatment protocols could be developed that create optimal joint environments: the creation of an optimal biomechanical joint environment, whether it is done through reconstructing a ruptured ligament or modifying the joint alignment by bracing or osteotomy is believed to avert long-term complications of OA.

The predicament is that any research, biomechanics or not, directed at OA and its prevention is complicated by the fact that the pathogenesis of OA is likely multifactorial and remains unclear to a large extent. The long-held belief that knee OA is a straightforward "wear and tear" disease of cartilage has been abandoned by many experts.[2] Instead, the metabolic and structural changes that are seen in the osteoarthritic joint are currently viewed as the adaptive response of the synovial joint to a variety of genetic, constitutional, or biomechanical insults.[6] Nevertheless, it remains widely accepted that knee joint instability is an important risk factor in the aetiopathogenesis of the disease[11,12,30] – an assumption bolstered, for example, by the success of the instability-inducing transection of the anterior cruciate ligament (ACL), a well-established animal model to study OA.[7,24] Analogous to the study of osteoarthritic changes following ACL deficiency in dogs, sheep or horses, the biomechanical examination of patients that are seen in the orthopaedic practice with an instability-inducing injury, such as rupture of the ACL or posterior cruciate ligament (PCL), has been compelling to OA researchers for several reasons. Rupture of one of the cruciate ligaments is a common and acute injury (annually one in every 1750 people between 15 and 25 years old could become ACL-deficient[15] and up to 40% of patients evaluated for knee hemarthrosis have an associated PCL injury[10]), and is associated with rapid cartilage degeneration and a very high risk for developing knee OA in the affected knee.[30] In other words, patient recruitment is relatively easy, the time of disease onset could be clearly determined, and the contralateral knee could be used as an intra-subject control.[19]

Even though OA is now widely believed to result in part from local mechanical factors acting within the context of systemic susceptibility, very little is known about the

biomechanical response of healthy articular cartilage to physiologic loading or about the extent of the mechanical alteration in the knee joint once one of the cruciate ligaments is ruptured. Even less is known about the impact of surgical reconstruction on the biomechanics of articular cartilage. In addition, most research has been directed predominantly at the tibiofemoral joint. In contrast, little is attention has been paid to the patellofemoral joint – the knee compartment with often the predominant clinical complaints following cruciate ligament injury. Finally, few quantitative data have been reported on the effect of cruciate ligament deficiency on the soft tissue structures surrounding the knee joint – structures critical for the maintenance of the knee joint homeostasis. We believe that these critical gaps in knowledge are due to the difficulty in analyzing with an acceptable accuracy the in vivo biomechanics of the both the tibiofemoral and patellofemoral joint with its corresponding cartilage layers and soft tissue structures.

Historically, the joint kinematics have been studied using cadaveric specimens. For example, in our laboratory a robotic testing system is used which applies various external loads on a human cadaver knee and measures the corresponding changes in knee kinematics as well as in situ forces in the native ACL and reconstruction grafts (Figure 1). Knowledge obtained from these studies has been vital for our current approach to the treatment of

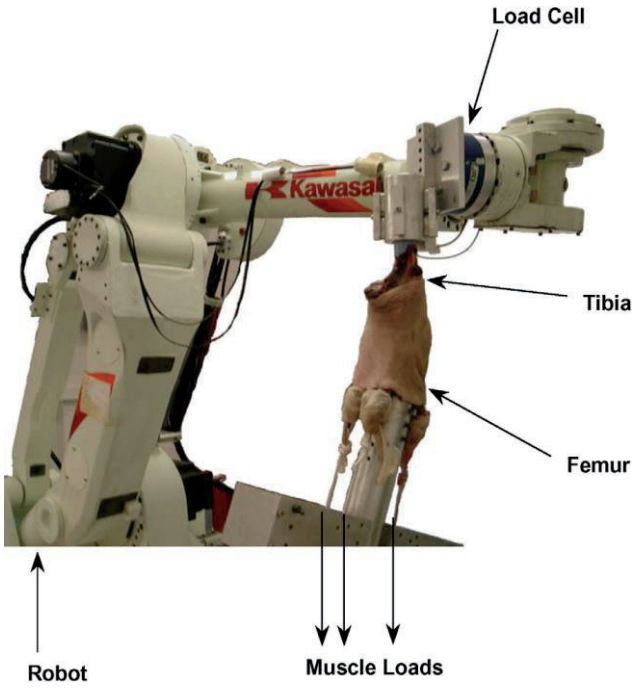

Figure 1. The robotic testing system with pulleys for the application of muscle loads.

various articular pathologies. However, due to the complexity of muscle loading patterns, the simulation of the human joint function under physiological loads remains difficult in in-vitro conditions. Furthermore, factors such as graft healing and postoperative rehabilitation cannot be addressed in-vitro. Out of this context, the quest for an accurate, minimally invasive method to analyze the in vivo joint biomechanics was initiated.

In brief, measuring the in vivo joint biomechanics in six degrees-of-freedom (6DOF) with an acceptable accuracy has been proven to be technically challenging. Multiple video cameras have been used to track the three-dimensional (3D) motions of reflective markers fixed to the skin.[8,29] Due to the relative motion between the skin and the underlying bones, as well as the difficulty in identifying external landmarks on the tested joint, there is a certain degree of inaccuracy associated with this technique.[4] One solution that has been proposed to reduce the artifact associated with non-rigid body movement of points placed on the skin during gait analysis was based on uniformly distributing a cluster of points on the limb segment.[1] To entirely eliminate the effect of skin motion, reflective markers have been fixed directly to knee or ankle bones using intracortical pins.[21,35] Another technique, roentgen stereophotogrammatric analysis (RSA), was developed to measure the motion of roentgen opaque markers embedded within bone, which are captured using dual X-ray images.[23,33] The accuracy of kinematic measurements greatly improved. Unfortunately the enhanced precision could only be attained through disruption of the joint, limiting the clinical implementations. Another highly accurate but intrinsically invasive analysis technique which has greatly enhanced our understanding of in vivo joint contact forces was the placement of instrumented joint prostheses that measure the in vivo dynamic loads experienced by for example the shoulder,[5] hip,[17] or knee[9] during daily activities. Unfortunately, the technique is obviously limited to patients scheduled for joint arthroplasty surgery.

Recently, computed tomography (CT) and magnetic resonance (MR) imaging techniques have been introduced into in vivo musculoskeletal joint biomechanics studies.[16,26,31] These techniques offer 3D quantification of in vivo morphology and positions of the joint without using invasive markers – qualifications of particular value in the examination of the human spine with its complicated anatomy[13,27] or for the study of the complex glenohumeral and thoracoscapular motion patterns in the shoulder.[14] Within the imaging equipment however, joint motion is restricted, thereby limiting the flexibility to study various functional activities.

Fluoroscopy, the radiology technique that allows still or moving digital images of internal structures on a monitor or TV screen, has been used extensively for the analysis of in vivo knee joint and total knee arthroplasty (TKA) kinematics,[3,18,32,34,36] due to its relative accessibility, easiness to operate, and low radiation dosage compared to traditional X-rays.

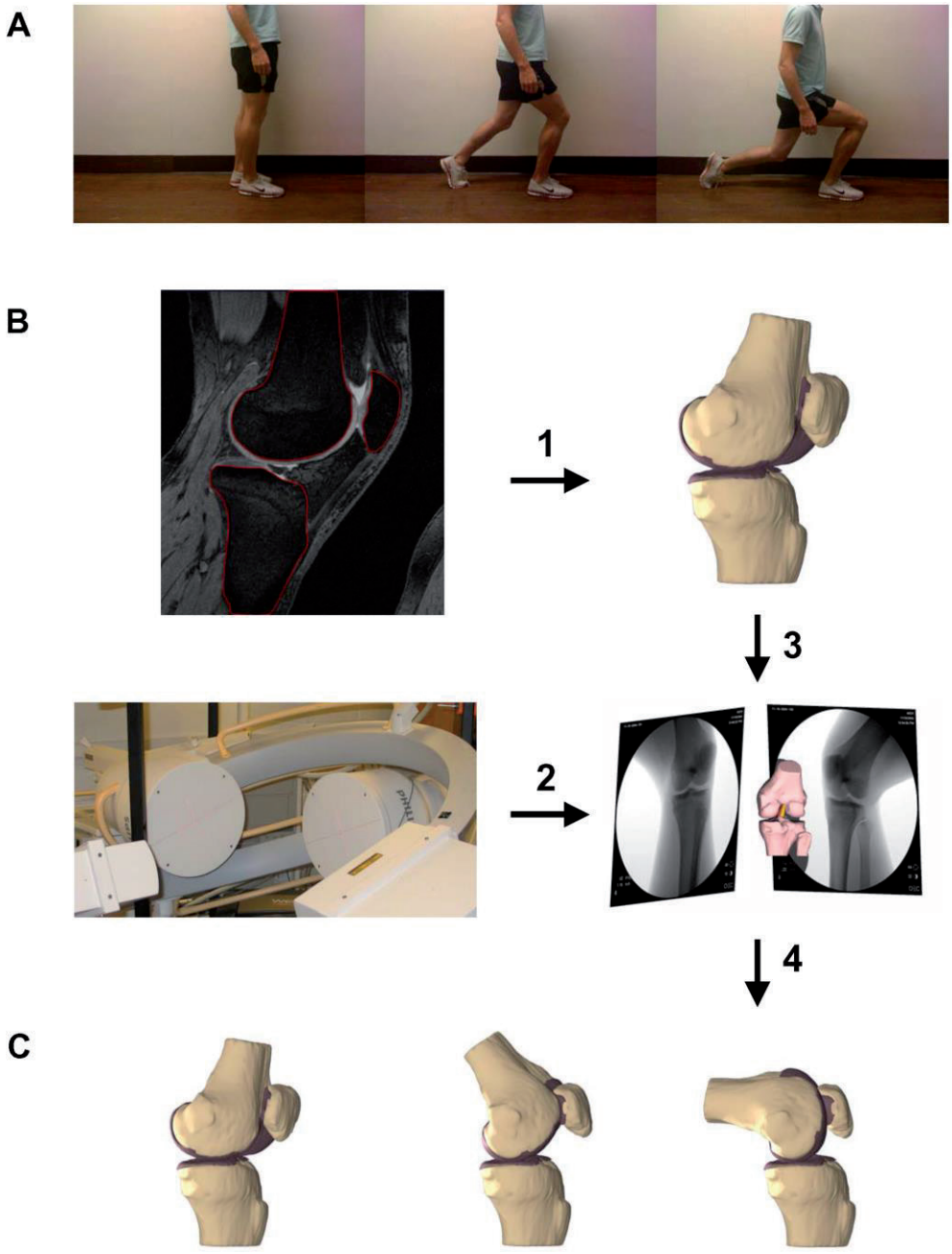

Figure 2. A concise overview of the methodology. The kinematics during a single-leg lunge (**A**) were analyzed using a combined MR and dual fluoroscopic imaging technique (**B**), in which an MR-based 3D model (1) and fluoroscopic images (2) are combined and manipulated in six degrees-of-freedom (3), resulting in a series of knee models (4) which accurately reproduce the performed in vivo activity (**C**).

The widespread availability of mobile digital fluoroscopic systems with dynamic imaging capabilities and adjustable configurations ("C-arms") has placed this type of motion analysis now within reach of many research groups. Both single- and double-plane fluoroscopic systems are utilized with excellent results. For the examination of tissue responses under in vivo loading conditions, single-plane fluoroscopy provides experimental flexibility and relatively large viewing volumes, besides the lower radiation and cost.[188] Although 3D model matching could theoretically be achieved using a single image, certain studies have found that the use of only a single image may not result in the same accuracy in the out-of-plane degrees-of-freedom compared to the in-plane motion.[18,22] To eliminate this critical source of error, our laboratory has added the additional fluoroscope, thereby creating a dual fluoroscopic imaging system for the analysis of in vivo knee joint motion in all degrees-of-freedom.

Over the past decade, the research of joint biomechanics in our laboratory has gone through an evolution from in-vitro simulation to in vivo measurements. The overall goal of our project was to develop a non-invasive methodology that would not only be capable of capturing joint kinematics in all degrees-of-freedom, but would also be sufficiently accurate for the detailed analysis of subtle articular contact changes during physiologic loading. Furthermore, the methodology would incorporate unmodified and commercially available imaging hardware, so that – once automated algorithms for the various processes are refined – the in vivo analysis of joint biomechanics could be employed in routine clinical settings. Our approach was to combine the benefits of fluoroscopy (i.e. in vivo joint motion) and MR imaging (i.e. joint anatomy), while reducing the innate limitations of the techniques in isolation (Figure 2).

REFERENCES

1. Andriacchi, T. P.; Alexander, E. J.; Toney, M. K.; Dyrby, C.; and Sum, J.: A point cluster method for in vivo motion analysis: applied to a study of knee kinematics. J Biomech Eng, 120(6): 743-9, 1998.
2. Aspden, R. M.; Scheven, B. A.; and Hutchison, J. D.: Osteoarthritis as a systemic disorder including stromal cell differentiation and lipid metabolism. Lancet, 357(9262): 1118-20, 2001.
3. Banks, S. A., and Hodge, W. A.: Accurate measurement of three-dimensional knee replacement kinematics using single-plane fluoroscopy. IEEE Trans Biomed Eng, 43(6): 638-49, 1996.
4. Benoit, D. L.; Ramsey, D. K.; Lamontagne, M.; Xu, L.; Wretenberg, P.; and Renstrom, P.: Effect of skin movement artifact on knee kinematics during gait and cutting motions measured in vivo. Gait Posture, 24(2): 152-64, 2006.
5. Bergmann, G.; Graichen, F.; Bender, A.; Kaab, M.; Rohlmann, A.; and Westerhoff, P.: In vivo glenohumeral contact forces--measurements in the first patient 7 months postoperatively. J Biomech, 40(10): 2139-49, 2007.
6. Brandt, K.; Lohmander, L.; and Doherty, M.: The concept of osteoarthritis as failure of the diarthrodial joint. In Osteoarthritis, pp. 70-74. Edited by Brandt, K.; Doherty, M.; and Lohmander, L., 70-74, Oxford, Oxford University Press, 1998.
7. Brandt, K. D.; Myers, S. L.; Burr, D.; and Albrecht, M.: Osteoarthritic changes in canine articular cartilage, subchondral bone, and synovium fifty-four months after transection of the anterior cruciate ligament. Arthritis Rheum, 34(12): 1560-70, 1991.
8. Chao, E. Y.: Biomechanics of the human gait. Frontiers in Biomechanics, in Zweifach B, New York, NY: Springer-Verlag: 225-219, 1986.
9. D'Lima, D. D.; Steklov, N.; Patil, S.; and Colwell, C. W., Jr.: The Mark Coventry Award: in vivo knee forces during recreation and exercise after knee arthroplasty. Clin Orthop Relat Res, 466(11): 2605-11, 2008.
10. Fanelli, G. C.; Giannotti, B. F.; and Edson, C. J.: The posterior cruciate ligament arthroscopic evaluation and treatment. Arthroscopy, 10(6): 673-88, 1994.
11. Felson, D. T. et al.: Osteoarthritis: new insights. Part 1: the disease and its risk factors. Ann Intern Med, 133(8): 635-46, 2000.
12. Fithian, D. C.; Paxton, L. W.; and Goltz, D. H.: Fate of the anterior cruciate ligament-injured knee. Orthop Clin North Am, 33(4): 621-36, v, 2002.
13. Fujii, R.; Sakaura, H.; Mukai, Y.; Hosono, N.; Ishii, T.; Iwasaki, M.; Yoshikawa, H.; and Sugamoto, K.: Kinematics of the lumbar spine in trunk rotation: in vivo three-dimensional analysis using magnetic resonance imaging. Eur Spine J, 16(11): 1867-74, 2007.
14. Graichen, H.; Stammberger, T.; Bonel, H.; Karl-Hans, E.; Reiser, M.; and Eckstein, F.: Glenohumeral translation during active and passive elevation of the shoulder - a 3D open-MRI study. J Biomech, 33(5): 609-13, 2000.

15. Griffin, L. Y. et al.: Noncontact anterior cruciate ligament injuries: risk factors and prevention strategies. J Am Acad Orthop Surg, 8(3): 141-50, 2000.

16. Hirsch, B. E.; Udupa, J. K.; and Roberts, D.: Three-dimensional reconstruction of the foot from computed tomography scans. J Am Podiatr Med Assoc, 79(8): 384-94, 1989.

17. Hodge, W. A.; Fijan, R. S.; Carlson, K. L.; Burgess, R. G.; Harris, W. H.; and Mann, R. W.: Contact pressures in the human hip joint measured in vivo. Proc Natl Acad Sci U S A, 83(9): 2879-83, 1986.

18. Komistek, R. D.; Dennis, D. A.; and Mahfouz, M.: In vivo fluoroscopic analysis of the normal human knee. Clin Orthop, (410): 69-81, 2003.

19. Kozanek, M.; Van de Velde, S. K.; Gill, T. J.; and Li, G.: The contralateral knee joint in cruciate ligament deficiency. Am J Sports Med, 36(11): 2151-7, 2008.

20. Lawrence, R. C. et al.: Estimates of the prevalence of arthritis and other rheumatic conditions in the United States. Part II. *Arthritis Rheum,* 58(1): 26-35, 2008.

21. Lafortune, M. A.; Cavanagh, P. R.; Sommer, H. J., 3rd; and Kalenak, A.: Three-dimensional kinematics of the human knee during walking. J Biomech, 25(4): 347-57, 1992.

22. Li, G.; Wuerz, T. H.; and DeFrate, L. E.: Feasibility of using orthogonal fluoroscopic images to measure in vivo joint kinematics. J Biomech Eng, 126(2): 314-8, 2004.

23. Lundberg, A.; Goldie, I.; Kalin, B.; and Selvik, G.: Kinematics of the ankle/foot complex: plantarflexion and dorsiflexion. Foot Ankle, 9(4): 194-200, 1989.

24. Marshall, K. W., and Chan, A. D.: Arthroscopic anterior cruciate ligament transection induces canine osteoarthritis. J Rheumatol, 23(2): 338-43, 1996.

25. Moro-oka, T. A.; Hamai, S.; Miura, H.; Shimoto, T.; Higaki, H.; Fregly, B. J.; Iwamoto, Y.; and Banks, S. A.: Dynamic activity dependence of in vivo normal knee kinematics. J Orthop Res, 26(4): 428-34, 2008.

26. Nakagawa, S.; Kadoya, Y.; Todo, S.; Kobayashi, A.; Sakamoto, H.; Freeman, M. A.; and Yamano, Y.: Tibiofemoral movement 3: full flexion in the living knee studied by MRI. J Bone Joint Surg Br, 82(8): 1199-200, 2000.

27. Ochia, R. S.; Inoue, N.; Renner, S. M.; Lorenz, E. P.; Lim, T. H.; Andersson, G. B.; and An, H. S.: Three-dimensional in vivo measurement of lumbar spine segmental motion. Spine, 31(18): 2073-8, 2006.

28. Peat, G.; McCarney, R.; and Croft, P.: Knee pain and osteoarthritis in older adults: a review of community burden and current use of primary health care. *Ann Rheum Dis,* 60(2): 91-7, 2001.

29. Reinschmidt, C.; van Den Bogert, A. J.; Murphy, N.; Lundberg, A.; and Nigg, B. M.: Tibiocalcaneal motion during running, measured with external and bone markers. Clin Biomech (Bristol, Avon), 12(1): 8-16, 1997.

30. Roos, H.; Adalberth, T.; Dahlberg, L.; and Lohmander, L. S.: Osteoarthritis of the knee after injury to the anterior cruciate ligament or meniscus: the influence of time and age. Osteoarthritis Cartilage, 3(4): 261-7, 1995.

31. Sheehan, F. T.; Zajac, F. E.; and Drace, J. E.: Using cine phase contrast magnetic resonance imaging to non-invasively study in vivo knee dynamics. J Biomech, 31(1): 21-6, 1998.

32. Stiehl, J. B.; Komistek, R. D.; Dennis, D. A.; Paxson, R. D.; and Hoff, W. A.: Fluoroscopic analysis of kinematics after posterior-cruciate-retaining knee arthroplasty. J Bone Joint Surg Br, 77(6): 884-9, 1995.

33. van Dijk, R.; Huiskes, R.; and Selvik, G.: Roentgen stereophotogrammetric methods for the evaluation of the three dimensional kinematic behaviour and cruciate ligament length patterns of the human knee joint. J Biomech, 12(9): 727-31, 1979.

34. Varadarajan, K. M.; Moynihan, A. L.; D'Lima, D.; Colwell, C. W.; and Li, G.: In vivo contact kinematics and contact forces of the knee after total knee arthroplasty during dynamic weight-bearing activities. J Biomech, 41(10): 2159-68, 2008.

35. Westblad, P.; Hashimoto, T.; Winson, I.; Lundberg, A.; and Arndt, A.: Differences in ankle-joint complex motion during the stance phase of walking as measured by superficial and bone-anchored markers. Foot Ankle Int, 23(9): 856-63, 2002.

36. Zihlmann, M. S.; Gerber, H.; Stacoff, A.; Burckhardt, K.; Szekely, G.; and Stussi, E.: Three-dimensional kinematics and kinetics of total knee arthroplasty during level walking using single plane video-fluoroscopy and force plates: a pilot study. Gait Posture, 24(4): 475-81, 2006.

3

CHAPTER

Application guidelines for dynamic knee joint analysis with a dual fluoroscopic imaging system.

Samuel K. Van de Velde
Ali Hosseini
Michal Kozanek
Thomas J. Gill, IV
Harry E. Rubash
Guoan Li

Acta Orthop Belg. 2010 Feb;76(1):107-13.

ABSTRACT

The widespread availability of mobile digital fluoroscopic systems with dynamic imaging capabilities places this type of motion analysis within reach of many research groups. With the addition of the second fluoroscope though, and the incorporation of a treadmill to analyze gait, the fluoroscopic analysis technique, which was once a rather straightforward method, has become more complex. Therefore, the purpose of the present manuscript was to provide a comprehensive review of the various processes that are associated with the dynamic knee joint motion analysis, including patient selection, construction of three-dimensional knee models, fluoroscopic scanning, and matching.

INTRODUCTION

Fluoroscopy has been used extensively for the analysis of in vivo knee joint and total knee arthroplasty (TKA) kinematics.[2,13,22,23,25] The fluoroscopic images, taken by either one or two fluoroscopes, can be combined with three-dimensional (3D) anatomic models of the knee joint, created based on computerized tomography (CT) or magnetic resonance (MR) images. When analyzing TKA kinematics, 3D computer-aided design (CAD) models of the TKA components (supplied by the manufacturer) are usually used. Both single- and double-plane fluoroscopic systems are utilized with excellent results. For the examination of tissue responses under in vivo loading conditions, single-plane fluoroscopy provides experimental flexibility and relatively large viewing volumes, besides the lower radiation and cost.[18]

Although 3D model matching could theoretically be achieved using a single image, certain studies have found that the use of only a single image may not result in the same accuracy in the out-of-plane degrees-of-freedom compared to the in- plane motion.[13,17] For this reason, our laboratory has added the additional fluoroscope, thereby creating a dual fluoroscopic imaging system (DFIS) for the analysis of in vivo knee joint motion.[17]

In a recent validation study, we compared the reproduction of dynamic knee flexion by our combined MR-DFIS technique to the kinematics measured by a methodology similar to the highly accurate but invasive Roentgen Stereophotogrammatric Analysis (RSA),[16] and found an excellent agreement in all degrees-of-freedom that were determined by the two methods. Additionally, the feasibility of the DFIS for the application of in vivo knee joint kinematic analysis was demonstrated by measuring the six degrees-of freedom (6DOF) knee joint motion of one living subject during a step ascent and treadmill gait.

With the addition of the second fluoroscope however, and the incorporation of a treadmill to analyze gait, the analysis technique has become more complex. Therefore, the purpose of the present manuscript was to provide a clear, illustrated, and comprehensive review of our experience to date with the DFIS technique.[14,15]

METHODOLOGY

1. Patient Selection

The first steps of the combined MR and DFIS technique are the inclusion, instruction, and protection of the patient. First, the treadmill gait of patients with a body mass index (BMI) greater than 30 is difficult to investigate, because the contralateral leg may obstruct the imaging of the studied knee joint and thus hamper the analysis of treadmill gait.

Second, during participation in the study, each patient's knee is MR scanned, which is necessary for the construction of a 3D anatomic knee model (see below). As with every

MRI scanner, patients with metal implants (such as surgical clips, fixation screws and plates, and pacemakers) are excluded from the study.

Finally, although low compared to traditional X-rays, a minimal amount of radiation exposure to the patient is intrinsic to the DFIS. The Radiation Safety Committee at our institute has calculated that the amount of radiation the patient is exposed to is 13 millirem during our dynamic imaging of the knee joint. For the protection against unnecessary radiation exposure, each patient is provided with a lead skirt and vest and a lead thyroid shield. Any woman of childbearing potential is questioned and urine or serum tested to determine whether she is possibly pregnant. If found pregnant, she is excluded from the study.

2. MRI scan and construction of 3D knee model

The next step following patient selection is the acquirement of MR images of the studied knee joint (8). When studying cartilage deformation, we ask the patient to refrain from all

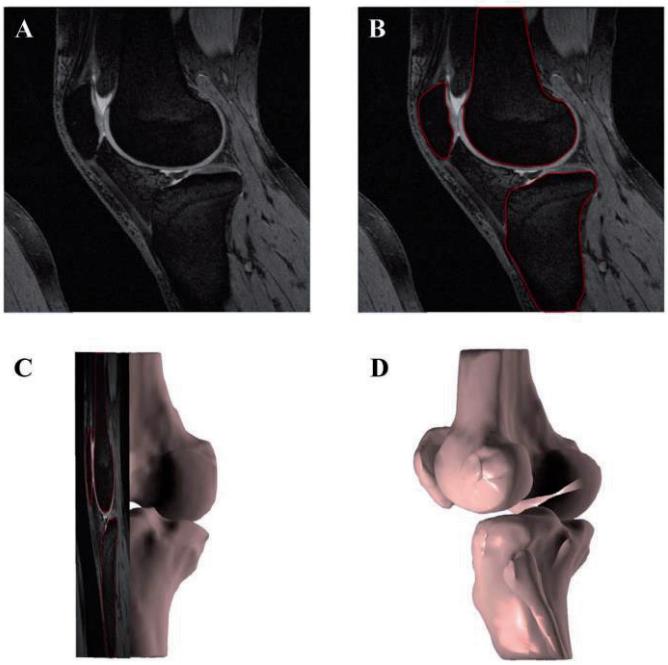

Figure 1. An illustration of the creation of a 3D MR image based model of the knee joint. Within each MR image of the knee (**A**), the contours of the tibia, fibula, femur and patella are digitized (**B**). Using the contour lines created in the individual MR images, meshes are assembled (**C**), resulting in a 3D model of the knee (**D**).

strenuous activity for at least four hours prior to their visit, and to remain non-weight bearing for one hour prior to the MR imaging of the knee.[5] During scanning, each patient is asked to lay supine with the knee in a relaxed, extended position while sagittal and coronal plane images are acquired with a 3.0 Tesla MR scanner. Each knee scanning lasts approximately twelve minutes per plane.

The MR images are then imported into commercially available solid modeling software (Rhinoceros®, McNeel, Seattle, WA) to construct 3D surface mesh models of the tibia, fibula, femur and articulating cartilage. The 3D models are created by digitizing the contours of the tibia, fibula, femur and articulating cartilage within each MR image. Unfortunately, delineations between bone and soft tissue in MR images do not always lend themselves to unique contours. Numeric routines to locate "edges" (boundary regions based on the gradient in image intensity), combined with a human operator reviewing these contours to determine that faulty contours are not added to the model, have been developed.[6] However, based on our experience, for the time being a trained researcher can accomplish the digitizing task most reliably manually. The digitized data (x, y, z coordinates) are then linked using B-Spline curves to reproduce the contours of the tibia, fibula, femur, and articulating cartilage. Meshes are assembled using the contour lines with a point density of 80 vertices/cm2 and triangular facets with an average aspect ratio of 2, creating geometric bony models. A typical 3D knee joint model is shown in figure 1. Following one week of supervised training, the construction of one complete knee model requires on average eight hours.

3. Fluoroscopic Scanning

In order to capture simultaneous images of the knee at different flexion angles, two fluoroscopes (BV Pulsera®, Philips, Bothell, WA) are used. The fluoroscopes use a pulsed snapshot X-ray to capture images (1024 X 1024 pixels with voxel size 0.28 X 0.28 mm). A snap shot in our system takes a pulse interval of 8 milliseconds (ms). Therefore, by setting up 25.33 ms rest time between two X-ray pulses, we can obtain 30 snapshot images in one second. If we set up 58.67 ms between two X-ray pulses, we can obtain 15 snapshot images in one second.[16] The fluoroscopes we use are commercially available and unmodified.

The fluoroscope has a clearance of approximately one meter between the X-ray source and the image intensifier, allowing the patient to be imaged by the fluoroscopes simultaneously as he or she performs dynamic weightbearing activities throughout the entire range of motion. A treadmill is incorporated within the DFIS to study the knee motion during walking. In theory, a force-plate instrumented treadmill could be used to capture the ground reaction forces in all three coordinates during walking.[21] For the purpose of accurately differentiating the heel-strike and toe-off instances at a moderate cost though, we use two thin dynamic TekScan pressure sensors, fixed to the heel and the toe of the shoes. The

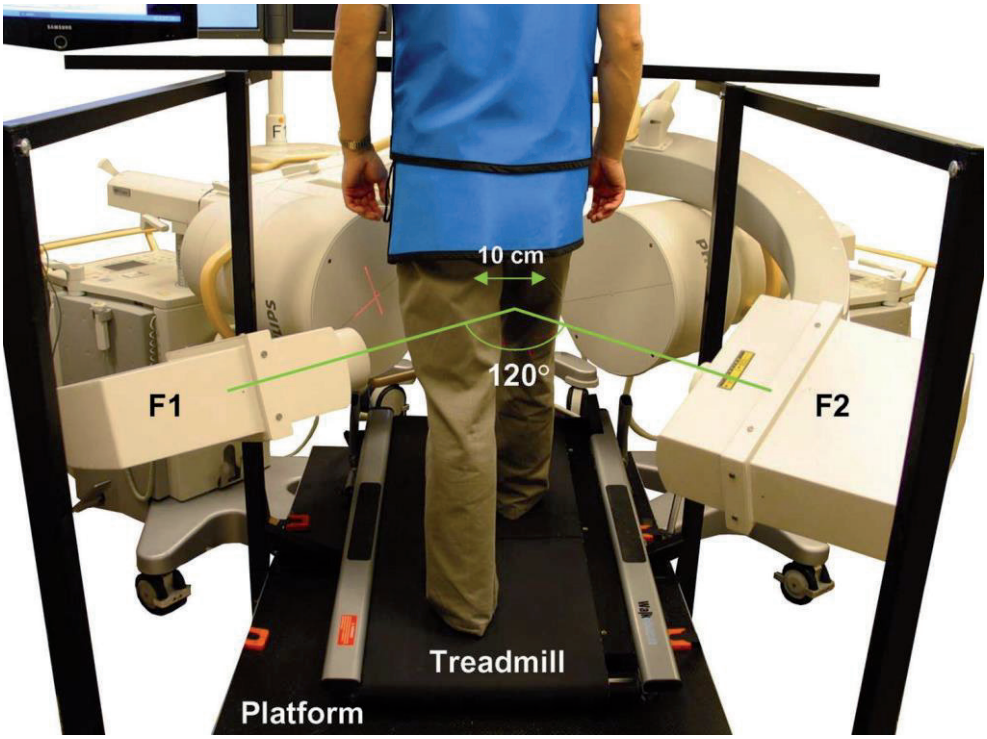

Figure 2. Overview of one of the activities that could be analyzed with the dual fluoroscopes, namely treadmill gait. For capturing the entire gait cycle, the fluoroscopes (**F1** and **F2**) were oriented with a 120° angle between the fluoroscopic intensifiers, spaced 10 cm apart (measured between the closest diameter point of the intensifiers), and with the radiation beams parallel to the ground.

treadmill is placed on a platform so that it can be easily centered between the fluoroscopes (figure 2). In general, the range of knee motion during the treadmill gait (~ 350 mm) is larger than the diameter of the image intensifier of the fluoroscopes (~ 295 mm). We therefore re-orientate the two fluoroscopes so that the knee motion can be captured within a field of view of ~ 450 mm by both fluoroscopes during the gait.

In our preliminary experience, the optimal fluoroscope setup for treadmill gait analysis is a 120° angle between the planes of the fluoroscopic intensifiers, spaced 10 cm apart, and with the radiation beams parallel to the ground (figure 2). Two laser-positioning devices, attached to the fluoroscopes, helped to align the target knee within the field of view of the fluoroscopes during the stance phase. In addition, a radiopaque marker taped to the skin of the studied knee joint facilitates the centering the studied joint during imaging on the display monitor. With this setup, we are capable of capturing the full gait cycle,[16] and

walking speeds up to 1.3 m/s could be analyzed without significant motion blur.[15] The knee is then imaged during three consecutive strides. Our entire dynamic analysis of the knee joint, which includes treadmill gait, step ascent, chair rise, and lunge, takes less than 30 minutes.

4. Matching

The relative location and orientation of the X-ray sources and image intensifiers of the two fluoroscopes are reproduced as points in 3D space in the modeling software (Rhinoceros®, McNeel, Seattle, WA) (fig 3).[7] The fluoroscopic images are then corrected for distortion

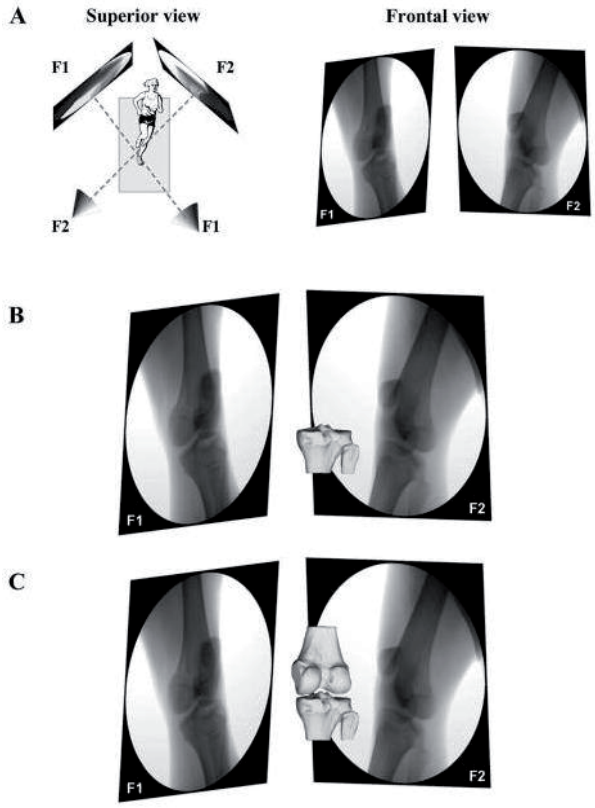

Figure 3. The fluoroscopic images are imported into the solid modeling software and placed in the planes based on the position of the respective fluoroscopes during the imaging of the patient (**A**, superior and frontal view of "virtual fluoroscopic system", with illustrative person on treadmill for orientation). The 3D MR image–based knee models of tibia (**B**), femur (**C**), and patella are imported into the same software and independently manipulated in six degrees-of-freedom inside the software until the projections of the model matched the outlines of the fluoroscopic images.

using the method of Gronenschild,[10] imported in the solid modeling software and placed in the position of the intensifiers of the virtual DFIS. The bony contours of the femur, tibia, fibula, and patella are outlined on the fluoroscopic images. These curves representing the projections of the knee will aid in matching the 3D knee model to the fluoroscopic images (see below).

Next, the 3D knee model is imported in the same modeling file, placed in the 3D space between the points that replicate the respective fluoroscopes, and viewed from the source points (by setting at origin of the view at the source point and directed at the intensifier point), effectively projecting the 3D model onto the fluoroscopic images (figure 3).[17] With the modeling file's viewing screen set to multiple panes, the 3D model can be simultaneously translated and rotated in all degrees-of-freedom in a controlled manner in indefinitely small increments. Once the 3D model's position in space approaches the bony contours of the fluoroscopic images though, the latter contours become difficult to detect, because the model blocks the viewing of the fluoroscopic images. To resolve this, we first outline the bony contours of the femur, tibia, fibula, and patella on the fluoroscopic images – these outlines can be highlighted and remain visible while the 3D model shifts over the bony contours on the fluoroscopic images. When the 3D model matches the bony contours on both fluoroscopic images, a 'match' is made. This matching process is repeated for each desired instance of the dynamic activity.

Manually matching the 3D model to the fluoroscopic images remains the gold standard at our laboratory, until automated algorithms have been further refined and validated.[4] Following one week of supervised training, the entire matching process including image correction, virtual environment setup, and reproduction of the in vivo knee activities (treadmill gait, step ascent, chair rise, and lunge, totaling approximately 12 fluoroscopic image pairs per activity) requires on average eight hours.

5. Measuring Kinematics

When describing knee kinematics, we typically use either a coordinate system based on the transepicondylar axis of the femur,[9,20,24] or a coordinate system utilizing the geometric center axis of the femur (figure 4) in which the various tibial and femoral axes are drawn manually based on the bony geometry of the MR model.[9]

The tibial coordinates are identical for both coordinate systems. The long axis of the tibial shaft is drawn first by creating a line parallel to the posterior wall of the tibial shaft in the sagittal plane. An anterior-posterior axis and a medial-lateral axis are then drawn perpendicular to the long axis of the tibia. The axes intersect at the center of the tibial plateau to form a Cartesian coordinate system.

In the coordinate system based on the trans-epicondylar axis of the femur, two axes are drawn on the femur : the long axis of the femur (parallel to the posterior wall of the femoral shaft in the sagittal plane) and the transepicondylar line (flexion axis). In the coordinate system based on the geometric center axis of the femur, the geometric center axis (flexion axis) is constructed by fitting circles to the medial and lateral condyles and by connecting the centers of these circles with a line.[19] The middle point of the flexion axis is used as the

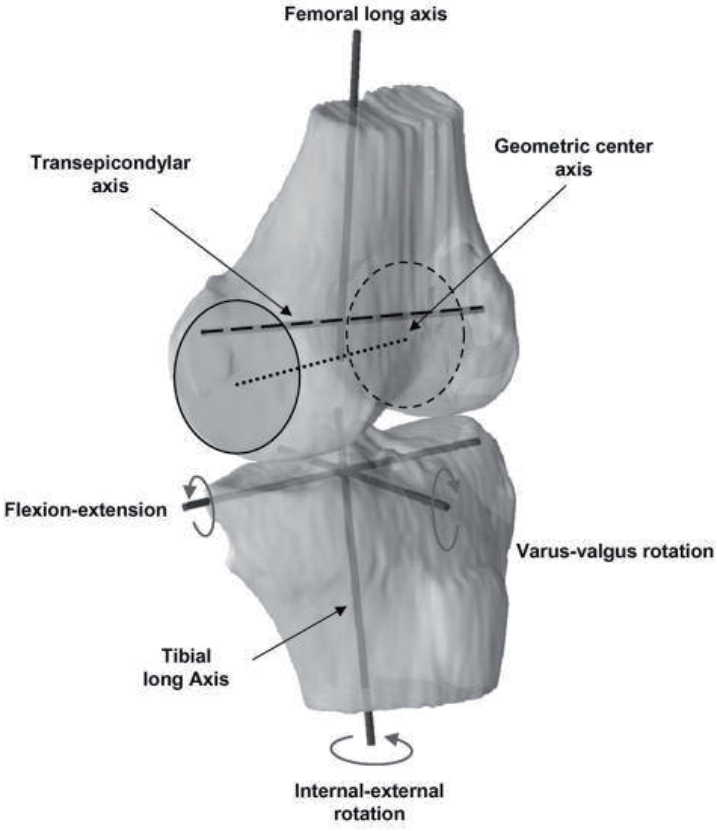

Figure 4. Coordinate systems used to define knee joint motion.

origin of the femoral coordinate system.

Translation is defined as the motion of the midpoint of the femoral flexion axis relative to the tibial coordinate system.[19] Femoral translations are then converted to tibial translations (anteroposterior, mediolateral, and proximodistal) so the data can be reported in a manner consistent with previous studies. The rotation of the knee is measured in a fashion similar to that described by Grood and Suntay.[11] Flexion is defined as the angle between the long axes of the femur and tibia, projected onto the sagittal plane of the tibia. Internal-external rotation is defined as the rotation of the femoral flexion axis in the transverse plane of the tibia (perpendicular to the long axis of the tibia). Varus-valgus rotation is defined as the angle between the long axis of the tibia and the femoral flexion axis projected onto the coronal plane of the tibia. Each knee position along the in vivo activity path is recorded using these six variables. Following one instruction session, the kinematics measurement of the in vivo knee activities (tread- mill gait, step ascent, chair rise, and lunge) requires on average four hours.

VALIDATION

A thorough understanding of the capabilities and limitations of the analysis system is necessary to investigate the dynamic knee joint motion with the technique.[16] When comparing the results of the DFIS technique with the 'gold standard' in joint kinematics analysis, namely the highly accurate but invasive RSA technique, we found an excellent agreement in all degrees-of-freedom that were determined by the two methods. The difference in reproduction of tibiofemoral kinematics during dynamic flexion-extension between the DFIS technique and the RSA method was $0.1 \pm 0.65°$/second in flexion speed ; 0.24 ± 0.16 mm in posterior femoral translation; and $0.16 \pm 0.61°$ in internal- external tibial rotation.[16] When measuring the tibiofemoral kinematics of a living subject during the stance phase of gait and subsequently reproducing the positions of the tibia and femur five times using the matching procedure, excellent intraobserver repeatability was found.[15]

CONCLUDING REMARKS

When asked about the accuracy of the current non-invasive technologies to measure joint kinematics, it is important to always take into account the balance between 'accuracy of measurement' and 'accuracy of reproduction of natural activity'. Fluoroscopy has a sub-millimeter accuracy to measure joint translations.[16] However, natural, unrestricted motion is difficult to perform within the constraints of the fluoroscopes. On the other hand, the kinematics of virtually all daily activities could be assessed using gait laboratory technology,[1] unfortunately at the expense of a certain degree of accuracy (rotational errors up to 4.4° and translational errors of up to 13.0 mm for walking have been reported).[3] Knee

kinematics are greatly activity dependent, and should therefore be interpreted in the context of the test modality.[12,14,18] For instance, we noted that motion of the medial femoral condyle in the transverse plane measured with the DFIS was greater than that of the lateral femoral condyle during the stance phase of gait – a trend opposite to what has been observed during non-weightbearing flexion or single-leg lunge in previous studies.[14]

The dynamic knee joint analysis using the DFIS with current technology is time-consuming and laborious, and therefore not yet applicable in the routine clinical practice. Significant advances in the development and validation of automated algorithms of the processes are therefore needed, so that the cost of manual labor could be reduced and the size of study samples increased. Ultimately, the DFIS could then be employed in routine clinical practice, assessing the impact of joint diseases and the efficacy of its various treatments. At this point, we believe that the increased accuracy of the DFIS already outweighs the time-cost associated with the technique when performing the analysis of the cartilage biomechanics following cruciate ligament deficiency, where the smallest errors in measurement are required to detect the often-subtle changes. The main advantage though of the dual fluoroscopic technique is that, in addition to its high accuracy, relatively low radiation, and non-invasive nature, it places the in vivo analysis of the various musculoskeletal joints, such as the knee, ankle, wrist, hip, and shoulder, as well as the human spine, within reach of virtually every researcher working in a routine clinical setting: an MR scanner, two fluoroscopes, and a group of keen (pre-) medical students with computers suffice.

REFERENCES

1. Andriacchi TP, Dyrby CO, Johnson TS. The use of functional analysis in evaluating knee kinematics. Clin Orthop Relat Res 2003; 410: 44-53.
2. Banks SA, Hodge WA. Accurate measurement of three- dimensional knee replacement kinematics using single-plane fluoroscopy. IEEE Trans Biomed Eng 1996; 43: 638-649.
3. Benoit DL, Ramsey DK, Lamontagne M et al. Effect of skin movement artifact on knee kinematics during gait and cutting motions measured in vivo. Gait Posture 2006; 24: 152-164.
4. Bingham J, Li G. An optimized image matching method for determining in-vivo TKA kinematics with a dual-orthogonal fluoroscopic imaging system. J Biomech Eng 2006; 128: 588-595.
5. Bingham JT, Papannagari R, Van de Velde SK et al. In vivo cartilage contact deformation in the healthy human tibiofemoral joint. Rheumatology (Oxford) 2008; 47: 1622-1627.
6. Bingham JT, Rubash HE, Li G. Orthogonal Segmentation of NMR Images For Precision Models of the Knee Cartilage. Trans ORS 2006 ;31 (Chicago, Il).
7. DeFrate LE, Papannagari R, Gill TJ, Moses JM, Pathare NP, Li G. The 6 degrees of freedom kinematics of the knee after anterior cruciate ligament deficiency: an in vivo imaging analysis. Am J Sports Med 2006; 34: 1240- 1246.
8. DeFrate LE, Sun H, Gill TJ, Rubash HE, Li G. In vivo tibiofemoral contact analysis using 3D MRI-based knee models. J Biomech 2004; 37: 1499-1504.
9. Eckhoff DG, Dwyer TF, Bach JM, Spitzer VM, Reinig KD. Three-dimensional morphology of the distal part of the femur viewed in virtual reality. J Bone Joint Surg 2001; 83-A, Suppl 2: 43-50.
10. Gronenschild E. Correction for geometric image distortion in the x-ray imaging chain: local technique versus global technique. Med Phys 1999; 26: 2602-2616.
11. Grood ES, Suntay WJ. A joint coordinate system for the clinical description of three-dimensional motions: application to the knee. J Biomech Eng 1983;105: 136-144.
12. Iwata S, Suda Y, Nagura T et al. Clinical disability in posterior cruciate ligament deficient patients does not relate to knee laxity, but relates to dynamic knee function during stair descending. Knee Surg Sports Traumatol Arthrosc 2007; 15: 335-342.
13. Komistek RD, Dennis DA, Mahfouz M. In vivo fluoroscopic analysis of the normal human knee. Clin Orthop Relat Res 2003; 410: 69-81.
14. Kozanek M, Hosseini A, Liu F et al. Tibiofemoral kinematics and condylar motion during the stance phase of gait. J Biomech 2009; 42: 1877-1884.
15. Li G, Kozanek M, Hosseini A, Liu F, Van de Velde SK, Rubash HE. New fluoroscopic imaging technique for investigation of 6DOF knee kinematics during treadmill gait. J Orthop Surg Res 2009; 4: 6.
16. Li G, Van de Velde SK, Bingham JT. Validation of a non- invasive fluoroscopic imaging technique for the measurement of dynamic knee joint motion. J Biomech 2008; 41: 1616-1622.

17. Li G, Wuerz TH, DeFrate LE. Feasibility of using orthogonal fluoroscopic images to measure in vivo joint kinematics. J Biomech Eng 2004;126: 314-318.

18. Moro-oka TA, Hamai S, Miura H, et al. Dynamic activity dependence of in vivo normal knee kinematics. J Orthop Res 2008; 26: 428-434.

19. Most E, Axe J, Rubash H, Li G. Sensitivity of the knee joint kinematics calculation to selection of flexion axes. J Biomech 2004; 37: 1743-1748.

20. Olcott CW, Scott RD. The Ranawat Award. Femoral component rotation during total knee arthroplasty. Clin Orthop Relat Res 1999; 367: 39-42.

21. Paolini G, Della Croce U, Riley PO, Newton FK, Casey Kerrigan D. Testing of a tri-instrumented-treadmill unit for kinetic analysis of locomotion tasks in static and dynamic loading conditions. Med Eng Phys 2007; 29: 404-411.

22. Stiehl JB, Komistek RD, Dennis DA, Paxson RD, Hoff WA. Fluoroscopic analysis of kinematics after posterior-cruciate-retaining knee arthroplasty. J Bone Joint Surg 1995; 77-B: 884-889.

23. Varadarajan KM, Moynihan AL, D'Lima D, Colwell CW, Li G. In vivo contact kinematics and contact forces of the knee after total knee arthroplasty during dynamic weight-bearing activities. J Biomech 2008; 41: 2159-2168.

24. Yoshino N, Takai S, Ohtsuki Y, Hirasawa Y. Computed tomography measurement of the surgical and clinical transepicondylar axis of the distal femur in osteoarthritic knees. J Arthroplasty 2001; 16: 493-497.

25. Zihlmann MS, Gerber H, Stacoff A et al. Three-dimensional kinematics and kinetics of total knee arthroplasty during level walking using single plane video-fluoroscopy and force plates: a pilot study. Gait Posture 2006; 24: 475-481.

4

CHAPTER

Validation of a non-invasive fluoroscopic imaging technique for the measurement of dynamic knee joint motion.

Guoan Li
Samuel K. Van de Velde
Jeffrey T. Bingham

J Biomech. 2008;41(7):1616-22.

ABSTRACT

The accurate measurement of the in vivo knee joint kinematics in six degrees-of-freedom (6DOF) remains a challenge in biomedical engineering. We have adapted a dual fluoroscopic imaging system (DFIS) to investigate the various in vivo dynamic knee joint motions. This paper presents a thorough validation of the accuracy and repeatability of the DFIS system when used to measure 6DOF dynamic knee kinematics. First, the validation utilized standard geometric spheres made from different materials to demonstrate the capability of the DFIS technique to determine the object positions under changing speeds. The translational pose of the spheres could be recreated to less than 0.15 ± 0.09 mm for velocities below 300 mm/s. Next, tantalum beads were inserted into the femur and tibia of two fresh frozen cadaver knees to compare the dynamic kinematics measured by matching knee models to the kinematics from the tantalum bead matching — a technique similar to Roentgen stereophotogrammetric analysis (RSA). Each cadaveric knee was attached to the crosshead of a tensile testing machine and vertically translated at a rate of 16.66 mm/s while images were captured with the DFIS. Subsequently, the tibia was held fixed and the femur manually flexed from full extension to 90° of flexion, as the DFIS acquired images. In vitro translation of the cadaver knee using the tensile testing machine deviated from predicted values by 0.08 ± 0.14 mm for the matched knee models. The difference between matching the knee and tantalum bead models during the dynamic flexion–extension motion of the knee was 0.1 ± 0.65°/s in flexion speed; 0.24 ± 0.16 mm in posterior femoral translation; and 0.16 ± 0.61° in internal–external tibial rotation. Finally, we applied the method to investigate the knee kinematics of a living subject during a step ascent and treadmill gait. High repeatability was demonstrated for the in vivo application. Thus, the DFIS provides an easy and powerful tool for accurately determining 6DOF positions of the knee when performing daily functional activities.

INTRODUCTION

Measuring the in vivo dynamic knee biomechanics in six degrees-of-freedom (6DOF) with an acceptable accuracy has been proven to be technically challenging. Multiple video cameras have been used to track the three-dimensional (3D) motions of reflective markers fixed to the skin.[9] Lafortune et al.[15] fixed reflective markers directly to bone using a thin rod in order to eliminate the effect of skin motion. Another technique measured the motion of roentgen opaque markers embedded within the bones, which are captured using dual X-ray images.[4,7,13,24,27] A point-cluster technique has also been proposed in order to reduce the effect of relative motion of the skin and bones.[1] Single plane fluoroscopy has been extensively used for the analysis of in vivo joint mechanics due to its relative accessibility, easiness to operate, and low radiation dosage compared to traditional X-rays.[5,26] Recently, a fluoroscope was moved together with the gait leg to capture the motion images of the knee.[30] However, the use of just a single image may not result in the same accuracy in the out-of-plane degrees-of-freedom compared to the in-plane motion.[14,17,29] Therefore, biplanar X-ray images,[3,29] sagittal plane magnetic resonance (MR) images,[21] and cine-MR imaging[25] have been used to measure in vivo knee motion. In our laboratory, we have utilized the cine function of two fluoroscopes to capture dynamic motion pictures of knee. By combining the fluoroscopic images captured during the dynamic motion with the 3D anatomic knee joint models, it is possible to quantitatively determine the 6DOF dynamic kinematics of the knee, similar to our studies of the quasi-static weight-bearing knee function.[10,11,18] However, a thorough understanding of the capabilities and limitations of the system is necessary to investigate the dynamic knee joint motion with the technique. This study presents a rigorous validation of the dynamic dual fluoroscopic imaging system (DFIS) for the measurement of in vivo human knee joint motion.

METHODOLOGY

Three validation sections and one application of the technique were carried out in this study. The first validation section used accurate spheres made from ceramic, steel and tungsten rolling down a slope. The second section used a tensile testing machine (QTest 5, MTS) to translate cadaveric knees at a known speed. The third section compared the results of the DFIS with those measured with a technique similar to the traditional Roentgen stereophotogrammetric analysis (RSA) method. Finally, the DFIS method was used to determine the knee kinematics during a step ascent and treadmill gait to determine the repeatability of the method when used under in vivo dynamic conditions.

1. Validation using spheres

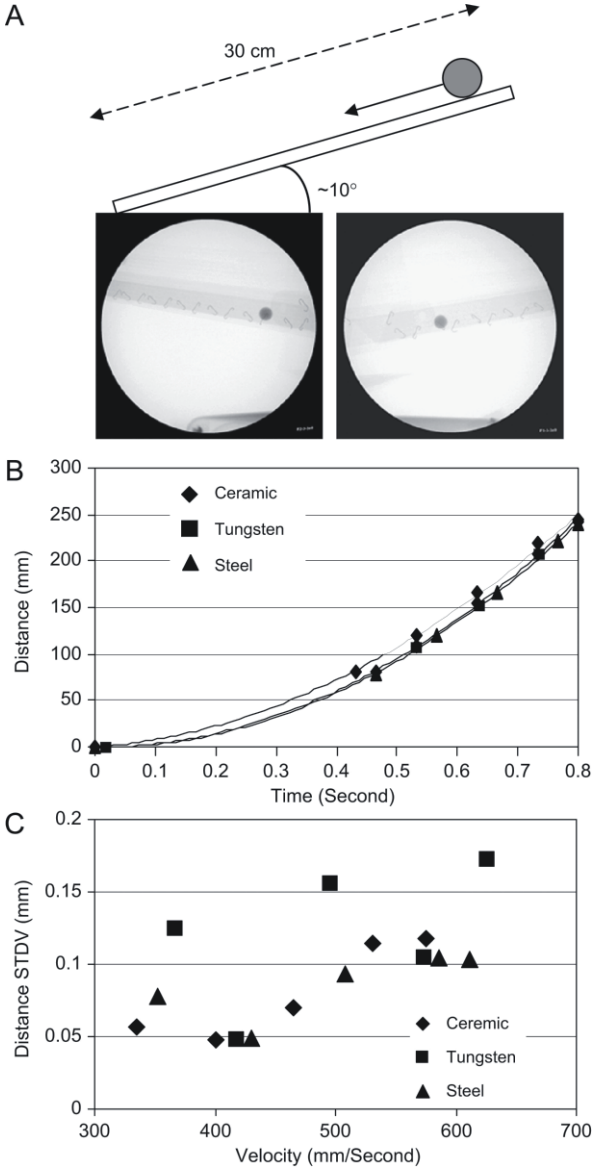

Figure 1. (**A**) Top: diagram showing the experimental setup of the rolling sphere. Bottom: two fluoroscopic images captured by the DFIS. (**B**) Oblique rolling distances of the spheres with time and their second order polynomial interpolations. (**C**) Standard deviations of the determined rolling distances as a function of rolling velocity.

Three spheres of 12.7 ± 0.016 mm in diameter made of ceramic, steel and tungsten, respectively, were allowed to roll down a ~10° inclined groove (Figure 1). All configurations began at rest and the spheres were allowed to travel 30 cm. The rolling spheres were imaged using the DFIS. The dual fluoroscopic setup and calibration was performed as previously published.[6] The DFIS consisted of two fluoroscopes (BV Pulsera, Philips) set to generate 8ms width X-ray pulses every 33 ms with a dose rate of 13 mGy/s. Therefore, the fluoroscopic system samples the object's motion at a frequency of 125 Hz (1000 ms/8 ms), but only takes 30 snap shots. In the actual setup, the snap shot can be generated every 67 ms, so that 15 images can be obtained at the actual frequency of 125 Hz.

The dual image set captured at each time point and solid models of the spheres were introduced into a virtual dual fluoroscopic system that reproduced the geometry of the actual DFIS. The position of the sphere model was manipulated manually in space until its projections matched the sphere's images on both fluoroscopic images (Fig. 1A). The sphere's positions along the rolling path on the groove were then reproduced by a series of sphere models.

Next, we determined the traveling distance of the sphere with time. Each sphere was matched five times to determine the repeatability of the methodology in determining the positions of objects moving with an increasing velocity. The repeatability was represented by the standard deviation of the distances of the sphere at different time intervals during its rolling. To further investigate the sensitivity of the system for the analysis of the velocity of the object, the distance and time relation of the spheres was interpolated using a second-order polynomial function and the sphere velocity was then estimated using the first derivative of the polynomial. The standard deviation of the distance as a function of the sphere velocity was analyzed to determine the effect of velocity on the sphere position determination.

2. Validation using cadaveric knees

The accuracy of reproducing the relative knee position during dynamic motion using the DFIS has been rigorously validated in this study. Three spherical ceramic beads (2.5 mm in diameter, <0.001 mm in manufacturing tolerance) were imbedded in the tibia and femur separately of two fresh frozen cadaver knees (male, 80 years, right knee; female, 67 years, left knee). Both knees were then MR scanned with all the surrounding soft tissues intact. The MR scan was performed using a 3.0T magnet (Siemens, Germany) with surface coil and a 3D spoiled gradient recalled acquisition in steady-state (SPGR) sequence. The scan was done in both the sagittal and coronal planes with a field-of-view of 160 x 160 mm. The scan was done with 1 mm in thickness and no gap between the scans. For each knee, the MR scanning time was approximately 12 min. The acquired MR images were used to reconstruct two 3D knee models, including the tibia, fibula, and femur, as well as the outlines of the tantalum beads in a solid-modeling software (Rhinoceros, Robert McNeel

and Associates, Seattle WA) using a protocol established in our laboratory.[17] A joint coordinate system that has been described previously was used to describe the 6DOF knee joint kinematics.[10]

2.1. Measurement of dynamic knee position

The knee was then attached to the crosshead of a materials testing machine (QTest 5, MTS, Minneapolis, MN) that has an accuracy of 0.001 mm in displacement control mode. Two fluoroscopes were positioned so that the knee specimen was within the view of both fluoroscopes. The knee was imaged from two orthogonal directions while the MTS machine moved the knee downwards at a constant speed of 16.66 mm/s, the maximal speed

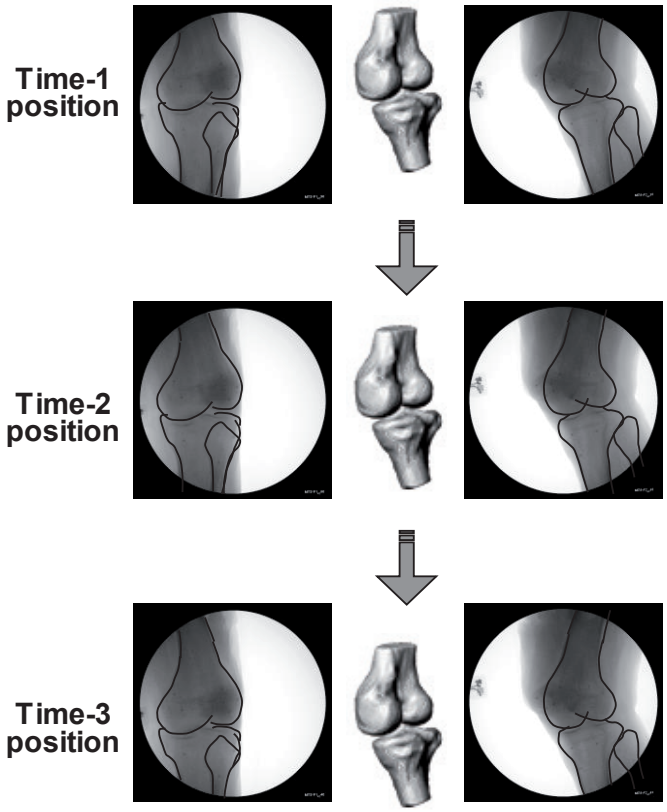

Figure 2. Diagram showing the knee positions captured using the dual fluoroscopic system at three time intervals while translated by the MTS machine at a constant velocity (16.66mm/sec). The moving distance of the knee between time 1 and time 2 is 2.78mm, between time 2 and time 3 is 8.33mm, and between time 1 and time 3 is 11.11mm.

achievable with this device. The knee motion was imaged with 30 frames per second with a frame rate of 125 Hz. Each frame was a snap shot with a pulse of 8 ms. Fig. 2 shows the positions of the knee captured at three different times during the dynamic motion. To validate the accuracy of the combined fluoroscopic and MR imaging technique in determination of dynamic knee motion, the fluoroscopic images and the 3D knee models were used to reproduce the dynamic knee positions, which were then used to calculate knee velocity.

To do this, three positions of each knee along the motion path were randomly selected (Figure 2). The fluoroscopic images and bony outlines were corrected using an algorithm based on the work of Gronenschild.[12] Next, the bony contours on the corresponding fluoroscopic images were automatically outlined using a modified Canny edge detection algorithm[8] and visually inspected to remove erroneous contours (Figure 2). The fluoroscopic images and 3D knee model were then imported into the solid-modeling software to create a virtual DFIS (Figure 3). The tibial and femoral models of the knee were initially placed in random positions and orientations for each trial. The models were then adjusted separately in 6DOF so that their projections matched the bony contours of the fluoroscopic images. A series of knee models therefore reproduced the motion of the knee.

To evaluate the accuracy of the image-matching method in reproducing the dynamic positions of the knee, the distances traveled by the femur and tibia were determined directly from the knee models using the time-1 position as a reference (Figure 2). The translational motions of the femur and tibia were represented by the origins of their coordinate systems. Each of the three knee positions was reproduced five times using the imaging matching process. The data for each knee were averaged and compared to the experimental measurements using the MTS machine.

2.2. Measurement of dynamic knee flexion

For the more complicated 6DOF flexion–extension of the knee, it is challenging to accurately determine the knee motion in space and use it as a gold standard to validate the DFIS. We, therefore, compared the DFIS with a method, similar to the RSA technique, using imbedded spherical beads for the determination of the 6DOF knee kinematics during dynamic flexion–extension of the knee. The method using spherical beads has been shown to have an accuracy of within 0.1 mm in translation and 0.11 in orientation.[6]

Each knee was then positioned inside the field view of the dual fluoroscopic system and manually flexed-extended throughout the full range of knee motion. The knee motion was imaged using the fluoroscopes with a frame rate of 30 Hz. The dual fluoroscopic images and the MR model of the knee, including the beads, were used to setup a virtual fluoroscopic system for reproducing the dynamic knee motions (Figure 3).

First, the knee positions during the dynamic flexion–extension were reproduced by matching the bead positions on the fluoroscopic images using the beads models constructed from the MR images. This method is similar to the RSA method in which roentgen opaque markers are embedded within the target bones.[24]

Next, the knee positions during the dynamic flexion–extension were reproduced using the 3D knee models through the model matching method. The dynamic knee positions obtained from these two methods were compared. In this study, we compared the flexion–extension angle; internal–external tibial rotation; varus–valgus rotation; anterior–posterior, medial–lateral and proximal–distal translations; and flexion speed of the knee obtained from the two methods along their flexion–extension paths.

3. Application of the method to measure living subject motion

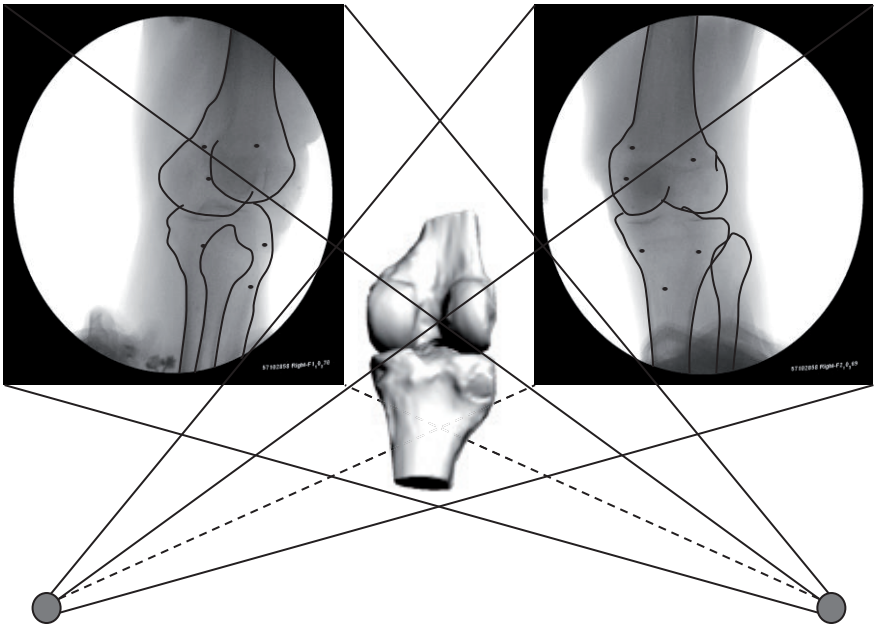

Figure 3. Virtual fluoroscopic system used to reproduce dynamic knee motion using the model matching method and the RSA method. Note the images of the beads used in RSA method.

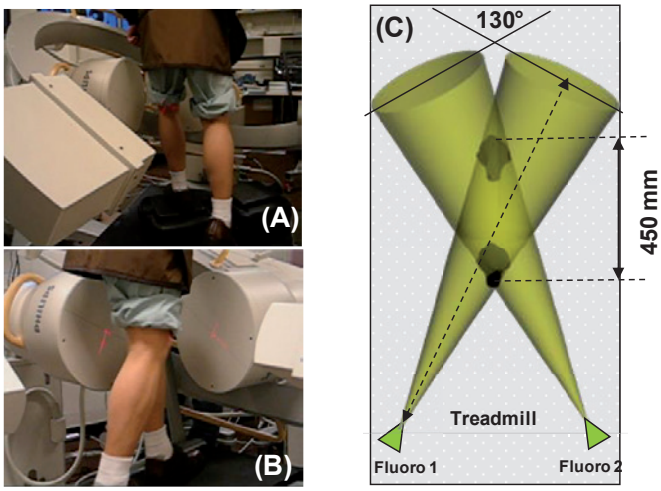

Figure 4. Setup of the fluoroscopes for capturing knee positions during (**A**) ascending a step and (**B**) a treadmill gait. (**C**) Schematic setup of the dual fluoroscopes on a treadmill that can capture a complete gait cycle of the knee (~450 mm) during treadmill gait.

The DFIS was used to measure the 6DOF knee kinematics of a living subject while ascending a step and during the stance phase of a gait cycle on a treadmill. One healthy subject (male, 45 years old) was recruited in this study. The left knee of the subject was MR scanned using the same protocol as used for the cadaveric knees above to create a 3D meshed model of the knee. The anatomic knee model included the bony geometry of the tibia, femur, and fibula. A joint coordinate system described in our previous publications was adopted for the measurement of 6DOF knee joint kinematics.[10]

The subject first performed a step ascent of 20 cm height, similar to stair climbing, inside the DFIS (Fig. 4A). The fluoroscopes imaged the entire rising motion using its cine-function. Thereafter, a treadmill was incorporated with the DFIS for the measurement of the knee position during treadmill gait (Fig. 4B). Since the knee motion during the treadmill gait (up to 350 mm) is larger than the diameter of the image intensifier of the fluoroscopes (~310mm), the two fluoroscopes were re-orientated to construct a common field of view with a length of ~450 mm, so that the entire knee motion could be captured by both fluoroscopes during the gait cycle (Fig. 4C). The subject practiced the gait on the treadmill for one minute (~1.2 mile/hour treadmill speed). Two laser-positioning devices were attached to both fluoroscopes to help the subject align his gait within the field of view of the fluoroscopes. The knee was then imaged from heel strike to toe-off.

The positions of the tibia and femur were reproduced five times using the matching procedure (Figure 3). The data on 6DOF knee kinematics, including knee flexion, internal-external tibial rotation, as well as medial-lateral translation and varus-valgus rotation, were analyzed using the tibial and femoral positions. The repeatability of the kinematics measurement by the DFIS is represented by standard deviation.

RESULTS

1. Validation using spheres

The travel distances of the spheres were interpolated using second-order polynomials with $R^2 < 0.99$ for all the spheres (Fig. 1B). On average, the translational pose of spheres could be reproduced with standard deviations to less than 0.15 ± 0.09 mm over a distance of 150 mm for velocities below 300 mm/s (Fig. 1C). No statistically significant difference was found between the repeatability of the spheres made of different materials. The velocity of the spheres reached up to 600 mm/s at end of the translation distance. In general, the standard deviation of the sphere poses increased with the velocity. However, for the maximal velocity tested in this study (velocities greater than 500 mm/s), the standard deviation was still below 0.2 mm (Fig. 1C).

2. Validation using cadaveric knees

2.1. Validation for measurement of dynamic knee position

Between time-1 and time-2 positions, the MTS machine translated the knee 2.78 mm (Table 1). Using the image-matching method, the femur of the first knee traveled in average 2.73 mm (0.04 mm less than the experimental data) and the tibia traveled in average 2.91 mm (0.13 mm more than the experimental data). Between time-1 and time-3 positions, the MTS machine translated the knee 11.11 mm. Using the image-matching method, the femur traveled in average 11.26 mm (0.15 mm more than the experimental data) and the tibia traveled in average 11.21 mm (0.18 mm more than the experimental data). Similar accuracy was observed for the second knee (Table 1). Overall, the mean error obtained from this

Experimental measurement	Reproduced using image matching method			
	Femur 1	Tibia 1	Femur 2	Tibia 2
2.78	2.75±0.07	2.92±0.08	2.89±0.03	2.80±0.09
8.33	8.43±0.19	8.26±0.10	8.32±0.09	8.42±0.18
11.11	11.20±0.20	11.20±0.22	11.21±0.07	11.22±0.14

Table 1. Travel distances of the two knees (mm) moved by the MTS machine in space and the distances reproduced using the image matching method.

		F/E(°)	IR/ER(°)	Var/Val(°)	AP(mm)	ML(mm)	PD(mm)	Speed (°/s)
Knee 1	Mean difference	0.37	-0.16	0.31	0.24	-0.13	-0.11	0.10
	Standard deviation	0.91	0.61	0.72	0.16	0.18	0.18	0.65
Knee 2	Mean difference	0.06	-0.01	-0.06	-0.03	0.01	0.04	-0.10
	Standard deviation	0.37	0.07	0.06	0.09	0.10	0.08	0.23

Table 2. Comparison of the 6DOF knee kinematics between the RSA and dual fluoroscopic methods. The differences between the two methods were represented using mean differences and the corresponding standard deviations along the flexion paths of the two knee specimens. F/E, flexion-extension; IR/ER, internal-external rotation; Var/Val, varus-valgus rotation; AP, anterior-posterior translation; ML, medial-lateral translation; PD, proximal-distal translation.

validation was less than 0.15 mm in the determination of the dynamic positions of the cadaveric knees. The speed of the knee was also calculated using the knee positions determined above. For knee 1, the moving speed was determined to be 16.72 ± 0.46 and 16.75 ± 0.31 mm/s for knee 2, both close to the experimental speed of 16.66 mm/s.

2.2. Measurement of dynamic knee flexion

The DFIS and the bead matching methods showed similar flexion–extension paths for the two knees (Figure 5). The difference was less than 0.24 ± 0.16mm in posterior femoral translation during the dynamic knee motion. The difference in internal–external tibial rotation was below 0.16 ± 0.61° between the two methods. Similar accuracy was observed in the other degrees-of-freedom (Table 2). On average, the difference of the two methods showed a difference of 0.1 ± 0.65°/s in flexion speed during the dynamic flexion–extension of the knee.

3. Application of the method to measure living subject motion

The tibiofemoral kinematics during a step ascent was plotted as a function of knee flexion angles. The knee extended from 66.57 ± 0.33° flexion at the beginning of the ascending motion to 8.81 ± 0.22° at the end of the ascending motion. An anterior femoral translation was observed from a 1.54 ± 0.13 mm anterior position to a 6.46 ± 0.15 mm anterior position. The knee was in an internal rotation position of 5.19 ± 0.30° initially and increased with the ascending motion. At the end of the ascending motion, the knee externally rotated to 3.27 ± 0.49°.

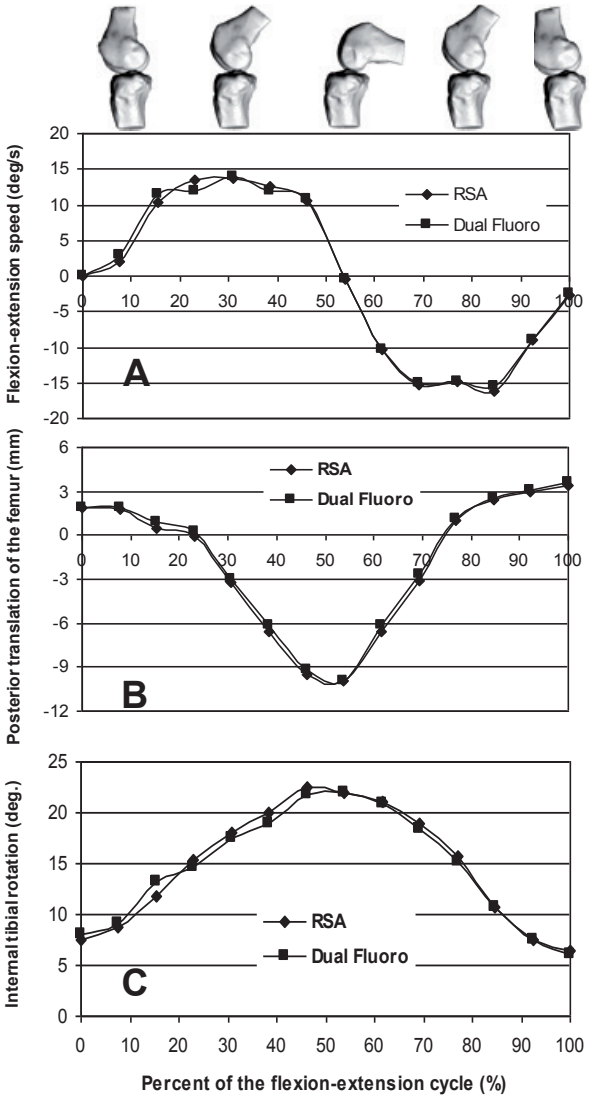

Figure 5. Dynamic knee flexion-extension determined using the two methods. **A**) Flexion speeds; **B**) posterior femoral translation; and **C**) internal tibial rotation.

The kinematics of the knee during one gait cycle on the treadmill could be repeatedly reproduced (Figure 6). After heel strike, the tibia showed an increase in flexion angle to 10.76 ± 0.5° and then returned towards to full extension in the mid stance phase. Thereafter, the flexion angle sharply increased in terminal extension and swing phases. The maximal flexion angle reached 54.72 ± 0.44° at swing phase. The range of posterior femoral

translation reached almost 20 mm during the entire cycle of the gait cycle and the femur also moved medially in a similar range. The knee was kept in a slightly valgus position throughout most of the gait cycle, but rotated to varus during swing phase. The tibia rotated internally after heel strike to 10.65 ± 0.49° and then rotated externally back to about 1.5° during the mid-stance and terminal extension phases, and showed increase in internal rotation during swing phase.

DISCUSSION

This paper presents a validation study of the DFIS for the measurement of 6DOF knee joint kinematics in a non-invasive manner. The validation utilized standard geometric spheres made from different materials to demonstrate the capability of the DFIS to determine the object positions under changing velocities. Cadaveric knees were used to determine both the knee positions translated at a known speed and the 6DOF knee kinematics during dynamic flexion–extension. Finally, we have applied the method to investigate the knee kinematics of a living subject during step ascent and treadmill gait to demonstrate the in vivo usage of the DFIS.

The DFIS has been extensively used to investigate the knee joint kinematics during a quasi-static weight-bearing flexion of the knee.[10,11,18] Under static conditions, the DFIS has been shown to have a high accuracy in translation (0.04 ± 0.06 mm) and orientation (<0.3°).[10] Under dynamic conditions, the sphere positions could be determined with a SD below 0.1 mm, which is slightly higher than those determined under static conditions using similar spheres.[6] The sphere materials were not shown to affect significantly the results under current testing conditions. The dynamic validation section using cadaveric knees on an accurate materials testing machine, demonstrated that the DFIS on average has an accuracy of less than 0.15 mm and 0.1 mm/s in translation and velocity, respectively. The dynamic flexion validation section using the cadaveric knees with embedded radio opaque beads showed that the DFIS produced similar results in knee kinematics analysis as a method similar to the traditional RSA method.

Validating measurement techniques of 6DOF knee kinematics has always been a challenge in biomechanics since a gold standard for the comparison is difficult to establish. Cine-MR imaging technique has been applied to study slow flexion and extension motion of the knee.[25] The apparent advantage of using an MR imaging scanner is the minimal radiation while the disadvantage is the limited scanning space that prevents imaging the physiological functional activities of the knee. Bi-plane high-speed X-ray scanners have also been used to investigate the dynamic joint function.[3,29] Most previous investigations using fluoroscopes have been focused on quasi-static motions of the knee.[5,10,17,26] Recently, one study performed a validation of using a single fluoroscope to obtain kinematic data from a total knee arthroplasty during level walking,[30] where the fluoroscope was moved to

follow the knee motion to overcome the limited field of view of the image intensifier. They estimated an accuracy of 0.2 mm for in-plane translation and of 3.25 mm for out-plane translation, and an accuracy of 1.57° for rotation. Our study positioned the two fluoroscopes so that their common image zone covers the knee motion during the complete gait cycle on a treadmill. In addition, the fluoroscope has a frame rate up to 125 Hz. Therefore, the system has a sufficient rate to image normal joint function such as gait, ascending a step, standing up from a chair, etc. We have demonstrated the feasibility of using the DFIS to investigate the dynamic motion of a living subject in this study.

There are many reports on treadmill gait kinematics and comparisons with overground gait.[20,23,28] In general, similar kinematics and kinetics were observed in sagittal plane flexion of the knee.[19,22,23] Our data reported the 6DOF knee kinematics during treadmill walking and ascending steps. The data on knee flexion during treadmill gait was similar to those by others on normal subjects during ambulatory activities.[2] The knee was close to full extension at heel strike, and then showed a quick increase in flexion to about 10° during the early segment of the mid stance phase. The knee maintained a full extension position during the mid-stance phase until toe off. A sharp increase in flexion was observed in the early swing phase. The DFIS system demonstrated a repeatable manner in producing the dynamic knee kinematics of one gait cycle as indicated by the standard deviation.

The DFIS has certain limitations. Because of the setup of the two fluoroscopes, motion within the system is restricted to activities such as treadmill gait, stair ascent/descent, and lunge. In addition, we found that the error in recreating dynamic motion might increase with increasing velocity, as was demonstrated using the translational poses of the spheres. However, for the maximal velocity tested in this study (velocities greater than 500 mm/s), the standard deviation was still below 0.2 mm.

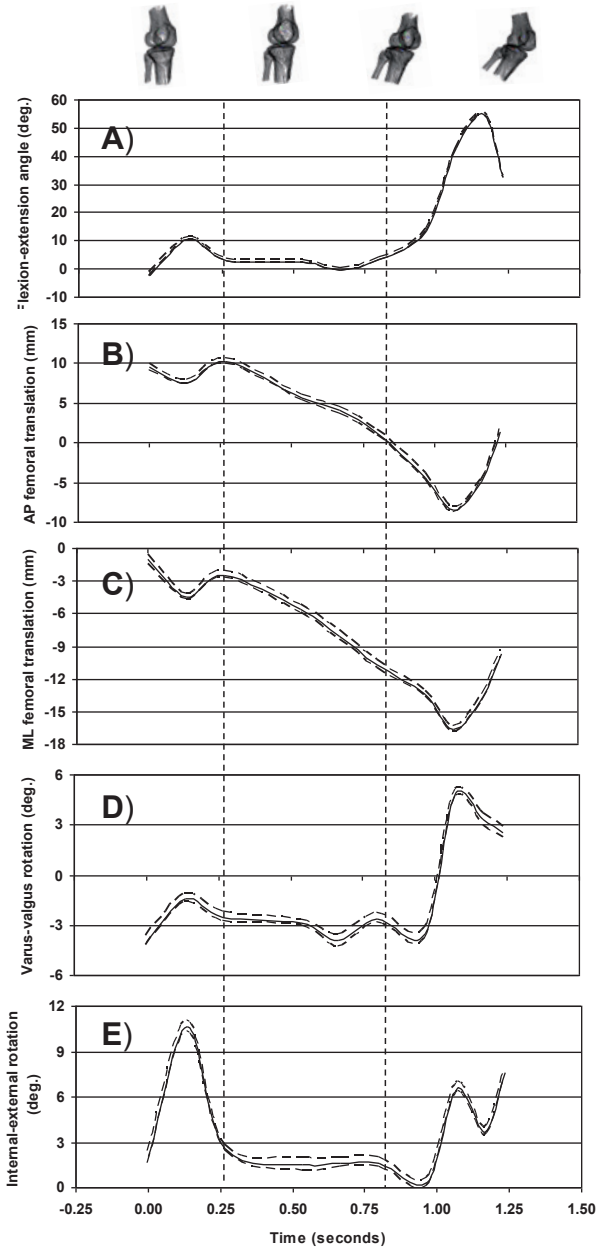

Figure 6. In vivo knee kinematics during a gait cycle on the treadmill. **A**) Flexion-extension angles; **B**) anterior-posterior femoral translation; **C**) medial-lateral femoral translation; **D**) varus-valgus rotation; and **E**) internal-external tibial rotation with time.

In summary, this paper presented a thorough validation of the accuracy and repeatability of the DFIS system when used to measure the 6DOF dynamic knee kinematics, and related the validation results to the data in the literature, obtained using the various functional analysis techniques. This validation demonstrated that the moving knee positions and velocities can be determined using the DFIS technique. The feasibility of this system for the application of in vivo knee joint kinematics analysis was demonstrated by measuring the 6DOF knee joint motion of one living subject during a step ascent and treadmill gait. The system is not only a viable solution for the investigation of fully dynamic weight-bearing joint kinematics, but also has a low radiation dosage, is non-invasive, and can be constructed using any pair of readily available fluoroscopes. Thus, the DFIS provides an easy and powerful tool for accurately determining 6DOF positions of healthy, injured, and surgically treated knees in 3D space.

REFERENCES

1. Andriacchi, T.P., Alexander, E.J., Toney, M.K., Dyrby, C., Sum, J., 1998. A point cluster method for in vivo motion analysis: applied to a study of knee kinematics. Journal of Biomechanical Engineering 120 (6), 743–749.
2. Andriacchi, T.P., Dyrby, C.O., Johnson, T.S., 2003. The use of functional analysis in evaluating knee kinematics. Clinical Orthopaedics and Related Research 410, 44–53.
3. Asano, T., Akagi, M., Tanaka, K., Tamura, J., Nakamura, T., 2001. In vivo three-dimensional knee kinematics using a biplanar imagematching technique. Clinical Orthopaedics and Related Research 388, 157–166.
4. Bach Jr., B.R., Mikosz, R.P., Andriacchi, T.P., 1988. The influence of changing femoral attachment positions on force displacement characteristics of the anterior cruciate ligament. Transactions on Orthopaedic Research Society 13, 129.
5. Banks, S.A., Hodge, W.A., 1996. Accurate measurement of three-dimensional knee replacement kinematics using single-plane fluoroscopy. IEEE Transactions on Biomedical Engineering 43 (6), 638–649.
6. Bingham, J., Li, G., 2006. An optimized image matching method for determining in-vivo TKA kinematics with a dual-orthogonal fluoroscopic imaging system. Journal of Biomechanical Engineering 128 (4), 588–595.
7. Blankevoort, L., Huiskes, R., de Lange, A., 1988. The envelope of passive knee joint motion. Journal of Biomechanics 21 (9), 705–720.
8. Canny, J.A., 1986. A computational approach to edge detection. IEEE Transactions on Pattern Analysis and Machine Intelligence 8, 679–698.
9. Chao, E.Y., 1986. Biomechanics of the human gait. In: Zweifach, B. (Ed.), Frontiers in Biomechanics. Springer, New York, NY, pp. 219–225.
10. DeFrate, L.E., Papannagari, R., Gill, T.J., Moses, J.M., Pathare, N.P., Li, G., 2006. The 6 degrees of freedom kinematics of the knee after anterior cruciate ligament deficiency: an in vivo imaging analysis. American Journal of Sports Medicine 34 (8), 1240–1246.
11. DeFrate, L.E., Nha, K.W., Papannagari, R., Moses, J.M., Gill, T.J., Li, G., 2007. The biomechanical function of the patellar tendon during in vivo weight-bearing flexion. Journal of Biomechanics 40 (8), 1716–1722.
12. Gronenschild, E., 1999. Correction for geometric image distortion in the X-ray imaging chain: local technique versus global technique. Medical Physics 26 (12), 2602–2616.
13. Karrholm, J., Elmqvist, L.G., Selvik, G., Hansson, L.I., 1989. Chronic anterolateral instability of the knee. A roentgen stereophotogrammetric evaluation. American Journal of Sports Medicine 17 (4), 555–563.
14. Komistek, R.D., Dennis, D.A., Mahfouz, M., 2003. In vivo fluoroscopic analysis of the normal human knee. Clinical Orthopaedics and Related Research 410, 69–81.

15. Lafortune, M.A., Cavanagh, P.R., Sommer 3rd, H.J., Kalenak, A., 1992. Three-dimensional kinematics of the human knee during walking. Journal of Biomechanics 25 (4), 347–357.

16. Li, G., DeFrate, L.E., Sun, H., Gill, T.J., 2004a. In vivo elongation of the anterior cruciate ligament and posterior cruciate ligament during knee flexion. American Journal of Sports Medicine 32 (6), 1415–1420.

17. Li, G., Wuerz, T.H., DeFrate, L.E., 2004b. Feasibility of using orthogonal fluoroscopic images to measure in vivo joint kinematics. Journal of Biomechanical Engineering 126 (2), 314–318.

18. Li, G., Moses, J.M., Papannagari, R., Pathare, N.P., DeFrate, L.E., Gill, T.J., 2006. Anterior cruciate ligament deficiency alters the in vivo motion of the tibiofemoral cartilage contact points in both the anteroposterior and mediolateral directions. Journal of Bone and Joint Surgery—American Volume 88 (8), 1826–1834.

19. Matsas, A., Taylor, N., McBurney, H., 2000. Knee joint kinematics from familiarised treadmill walking can be generalised to overground walking in young unimpaired subjects. Gait and Posture 11 (1), 46–53.

20. McKenna, M., Riches, P.E., 2007. A comparison of sprinting kinematics on two types of treadmill and over-ground. Scandinavian Journal of Medicine and Science in Sports 17 (6), 649–655.

21. Nakagawa, S., Kadoya, Y., Todo, S., Kobayashi, A., Sakamoto, H., Freeman, M.A., Yamano, Y., 2000. Tibiofemoral movement 3: full flexion in the living knee studied by MRI. Journal of Bone and Joint Surgery—British Volume 82 (8), 1199–1200.

22. Nymark, J.R., Balmer, S.J., Melis, E.H., Lemaire, E.D., Millar, S., 2005. Electromyographic and kinematic nondisabled gait differences at extremely slow overground and treadmill walking speeds. Journal of Rehabilitation Research and Development 42 (4), 523–534.

23. Riley, P.O., Paolini, G., Della Croce, U., Paylo, K.W., Kerrigan, D.C., 2007. A kinematic and kinetic comparison of overground and treadmill walking in healthy subjects. Gait and Posture 26 (1), 17–24.

24. Selvik, G., 1989. Roentgen stereophotogrammetry. A method for the study of the kinematics of the skeletal system. Acta Orthopaedica Scandinavica—Supplementum 232, 1–51.

25. Sheehan, F.T., Zajac, F.E., Drace, J.E., 1998. Using cine phase contrast magnetic resonance imaging to non-invasively study in vivo knee dynamics. Journal of Biomechanics 31 (1), 21–26.

26. Stiehl, J.B., Komistek, R.D., Dennis, D.A., Paxson, R.D., Hoff, W.A., 1995. Fluoroscopic analysis of kinematics after posterior-cruciate retaining knee arthroplasty. Journal of Bone and Joint Surgery—British Volume 77 (6), 884–889.

27. van Dijk, R., Huiskes, R., Selvik, G., 1979. Roentgen stereophotogrammetric methods for the evaluation of the three dimensional kinematic behaviour and cruciate ligament length patterns of the human knee joint. Journal of Biomechanics 12 (9), 727–731.

28. White, S.C., Yack, H.J., Tucker, C.A., Lin, H.Y., 1998. Comparison of vertical ground reaction forces during overground and treadmill walking. Medicine and Science in Sports and Exercise 30 (10), 1537–1542.

29. You, B.M., Siy, P., Anderst, W., Tashman, S., 2001. In vivo measurement of 3-D skeletal kinematics from sequences of biplane radiographs: application to knee kinematics. IEEE Transactions on Medical Imaging 20 (6), 514–525.

30. Zihlmann, M.S., Gerber, H., Stacoff, A., Burckhardt, K., Szekely, G., Stussi, E., 2006. Three-dimensional kinematics and kinetics of total knee arthroplasty during level walking using single plane videofluoroscopy and force plates: a pilot study. Gait and Posture 24 (4), 475–481.

5

CHAPTER

Increased tibiofemoral cartilage contact deformation in patients with anterior cruciate ligament deficiency.

Samuel K. Van de Velde
Jeffrey T. Bingham
Ali Hosseini
Michal Kozanek
Louis E. DeFrate
Thomas J. Gill, IV
Guoan Li

Arthritis Rheum. 2009 Dec;60(12):3693-702.

ABSTRACT

Objective. To investigate the in vivo cartilage contact biomechanics of the tibiofemoral joint following anterior cruciate ligament (ACL) injury.

Methods. Eight patients with an isolated ACL injury in 1 knee, with the contralateral side intact, participated in the study. Both knees were imaged using a specific magnetic resonance sequence to create 3- dimensional models of knee bone and cartilage. Next, each patient performed a lunge motion from 0° to 90° of flexion as images were recorded with a dual fluoroscopic system. The three-dimensional knee models and fluoroscopic images were used to reproduce the in vivo knee position at each flexion angle. With this series of knee models, the location of the tibiofemoral cartilage contact, size of the contact area, cartilage thickness at the contact area, and magnitude of the cartilage contact deformation were compared between intact and ACL- deficient knees.

Results. Rupture of the ACL changed the cartilage contact biomechanics between 0° and 60° of flexion in the medial compartment of the knee. Compared with the contralateral knee, the location of peak cartilage contact deformation on the tibial plateaus was more posterior and lateral, the contact area was smaller, the average cartilage thickness at the tibial cartilage contact area was thinner, and the resultant magnitude of cartilage contact deformation was increased. Similar changes were observed in the lateral compartment, with increased cartilage contact deformation from 0° to 30° of knee flexion in the presence of ACL deficiency.

Conclusion. ACL deficiency alters the in vivo cartilage contact biomechanics by shifting the contact location to smaller regions of thinner cartilage and by increasing the magnitude of the cartilage contact deformation.

INTRODUCTION

Many experts have abandoned the long-held belief that knee osteoarthritis (OA) is a straightforward "wear and tear" disease of cartilage.[1] Instead, the metabolic and structural changes of OA are currently viewed as the adaptive response of synovial joints to a variety of genetic, constitutional, or biomechanical insults.[2] Nevertheless, it remains widely accepted that knee joint instability is an important risk factor in the pathogenesis of the disease.[3,4,5]

The assumption that abnormal kinematics and consequent abnormal loading within the joint initiate knee OA underlies much of current OA research and orthopedic practice. Transection of the anterior cruciate ligament (ACL) is a well-established technique for inducing OA in animal models.[6,7] Reconstruction of the ruptured ACL has become one of the most frequently performed orthopedic procedures in an attempt to restore normal joint motion and prevent long-term complications.[3] A number of alignment-modifying therapeutic options, including bracing and osteotomy, might be used to alter the rate of OA progression.[8]

However, even though OA is widely believed to result in part from local mechanical factors acting within the context of systemic susceptibility, little is known about the extent of the mechanical alteration in the knee joint following rupture of the ACL. In general, the changes in kinematics that are observed in unstable knee joints are very minimal, on the order of millimeters.[9,10,11] Yet, these minimal alterations in kinematics are believed to trigger the devastating destruction of the articular cartilage.

Measuring articular cartilage function in the human knee joint with an acceptable degree of accuracy is technically challenging. The morphology of knee joint cartilage has been extensively investigated in knee specimens from cadaver donors and from living donors, using various techniques, such as needle probes, ultrasound, stereophotogrammetry, and magnetic resonance imaging (MRI).[12–18] Several recent studies have presented data on tibiofemoral contact kinematics in living subjects. Both open and closed MRI techniques have been used to determine tibiofemoral contact areas and locations for a variety of activities.[19,20,21] Other investigators have used a combination of either computed tomography (CT) or MRI with fluoroscopy to estimate cartilage contact locations during a lunge motion in healthy[22,23] and ACL-deficient[24,25] knees. In general, the cartilage contact location in these studies has been estimated based on the closest interarticular distance between the bony surfaces of the tibiofemoral joint[24] or the centroid of the tibiofemoral cartilage contact area.[25] While these previous studies have provided valuable data on the cartilage contact location, essential in vivo cartilage contact biomechanics, such as cartilage contact area, cartilage thickness, and cartilage contact deformation in a knee joint at risk of developing OA, remain unclear.

We hypothesized that rupture of the ACL changes the cartilage contact biomechanics of the tibiofemoral joint, with a resultant increase in the magnitude of cartilage contact deformation. In the present study, we used a combined dual fluoroscopic and MRI technique to analyze the effects of ACL deficiency on the location of tibiofemoral cartilage contact, the size of the contact area, the cartilage thickness at the contact area, and the magnitude of cartilage contact deformation during in vivo weight-bearing flexion of the knee from 0° to 90°.

PATIENTS AND METHODS

Patient selection. Eight patients (5 men and 3 women; age range 19–38 years) with complaints of knee laxity were included in the study. These patients had a diagnosis of acute, isolated ACL rupture, as documented by clinical examination findings (8-mm Lachman test with no end point, a grade 2 pivot-shift test measured by the same orthopedic surgeon [TJG], mean ± SD International Knee Documentation Committee[26] score 63.5 ± 8.7, mean ± SD manual maximum injured–minus–intact knee displacement score 4.2 ± 1.9 mm as measured with a KT-1000 knee ligament arthrometer [MEDmetric, San Diego, CA] by the same physical therapist) and findings on MRI. All patients had healthy contralateral knees. Patients had been injured within a mean ± SD of 4.4 ± 3 months of testing. Patients with injury to other ligaments, noticeable cartilage lesions, meniscal damage, and injury to the underlying bone were excluded from the study.

Five of these 8 patients were included in our previous studies of the 6 degrees-of-freedom tibiofemoral kinematics[9] as well as the motion of the tibiofemoral cartilage contact points in patients with ACL deficiency.[25] Each patient signed a consent form that had been approved by our Institutional Review Board.

Imaging procedure. The MRI and dual orthogonal fluoroscopic imaging techniques have been described in detail previously.[9,25,27] Briefly, both the left and the right knees were imaged with an MR scanner to create 3-dimensional (3-D) meshed models of the knees, using a protocol established in our laboratory.[9] To reduce the effects of load history on cartilage thickness, patients were asked to refrain from all strenuous activity, such as lifting, running, or stair climbing, for at least 4 hours prior to their visit and to remain non–weight bearing for ~1 hour prior to MRI of the knee. Patients were asked to lie supine, with the knee in a relaxed, extended position while sagittal plane images were acquired with a 3T MRI scanner (Siemens, Malvern, PA). The MR scanner was equipped with a surface coil and used a 3-D double-echo water excitation sequence (field of view 16 x 16 x 12 cm, voxel resolution 0.31 x 0.31 x 1.00 mm, repetition time [TR] 24 msec, echo time [TE] 6.5 msec, and flip angle 25°). Each scan lasted for ~12 minutes. The images were then imported into solid modeling software (Rhinoceros; Robert McNeel and Associates, Seattle, WA) to construct 3-D surface mesh models of the tibia, fibula, femur, and

articulating cartilage. The meshes were assembled using a point density of 80 vertices/cm^2 and triangular facets, with an average aspect ratio of 2.

After the MRI-based computer models were constructed, both knees of each patient were simultaneously imaged using 2 orthogonally placed fluoroscopes (OEC 9800; GE Healthcare, Salt Lake City, UT) as the patient performed a single-leg quasistatic lunge at 0°, 15°, 30°, 60°, and 90° of flexion. At each flexion angle, the patient was asked to pause for 5 seconds while simultaneous fluoroscopic images were taken. Throughout the experiment, the leg being tested supported the patient's body weight, while the other leg provided stability. The time elapsed between the MRI scan and the lunge activity was ~15 minutes.

Next, the fluoroscopic images were imported into solid modeling software and placed in the orthogonal planes based on the position of the fluoroscopes during imaging of the patient. Finally, the 3-D MRI–based knee model of each patient was imported into the same software, viewed from the 2 orthogonal directions corresponding to the orthogonal fluoroscopic setup used to acquire the images, and independently manipulated in 6 degrees of freedom inside the software until the projections of the model matched the outlines of the fluoroscopic images. When the projections matched the outlines of the images taken during in vivo knee flexion, the model reproduced the in vivo position of the knee. This system has an error of <0.1 mm and 0.3° in measuring tibiofemoral joint translations and rotations, respectively.[9] When comparing the dual fluoroscopic model matching technique with tantalum bead matching, a technique similar to Roentgen stereophotogrammetric analysis, the difference between the 2 techniques in the proximodistal direction (i.e., analogous to the measured apparent penetration) was 0.075 ± 0.13 mm (mean ± SD).[28]

Statistical analysis. In this study, cartilage thickness was calculated by finding the smallest Euclidian distance connecting a vertex of the articular surface to the cartilage–bone interface of the 3-D surface mesh models. The size of the contact area between the tibia and femur was determined by computing the area of tibial cartilage that intersected the femoral cartilage.[27] The cartilage contact deformation was then defined for each vertex of the articular surface mesh as the amount of cartilage surface intersection (in mm) (Figure 1) divided by the sum of the tibial and femoral cartilage surface thicknesses (in mm) multiplied by 100.[27] In this study, cartilage contact location was defined as the location of peak cartilage deformation, referenced to Cartesian coordinate systems on the tibial plateaus[23,25,29] (Figure 2). The origin of each coordinate system was located at the center of a circle, which was fit to the posterior edge of each tibial compartment. The anteroposterior and mediolateral axes split each tibial plateau into quadrants. In the anteroposterior direction, a location anterior to the mediolateral axis was considered positive. In the mediolateral direction, a location lateral to the anteroposterior axis was considered positive.

In a recent study of in vivo cartilage contact deformation in the healthy human tibiofemoral joint, a lack of agreement of 14 ± 11% (mean ± SD) was found between the combined dual fluoroscopic–MRI technique and a silicone casting technique in calculating the mean ± SD cartilage contact area of 244 ± 131 mm^2.[27] For the present study, we conducted an accuracy and precision analysis of the tibiofemoral cartilage reconstructions in which the measurement of cartilage thickness based on 3-D MRI–based knee models was compared with direct cartilage thickness measurement on calibrated digital images of cross-sections of specimens from the cadaver donors, and repeatedly measured for intra- and interobserver precision (see Appendix A). The average absolute difference between the cartilage thickness values based on the 3-D MRI–based knee models and those captured from the specimens from the cadaver donors was 0.04 ± 0.01 mm (mean ± SD), and excellent intra- and interobserver precision was obtained.

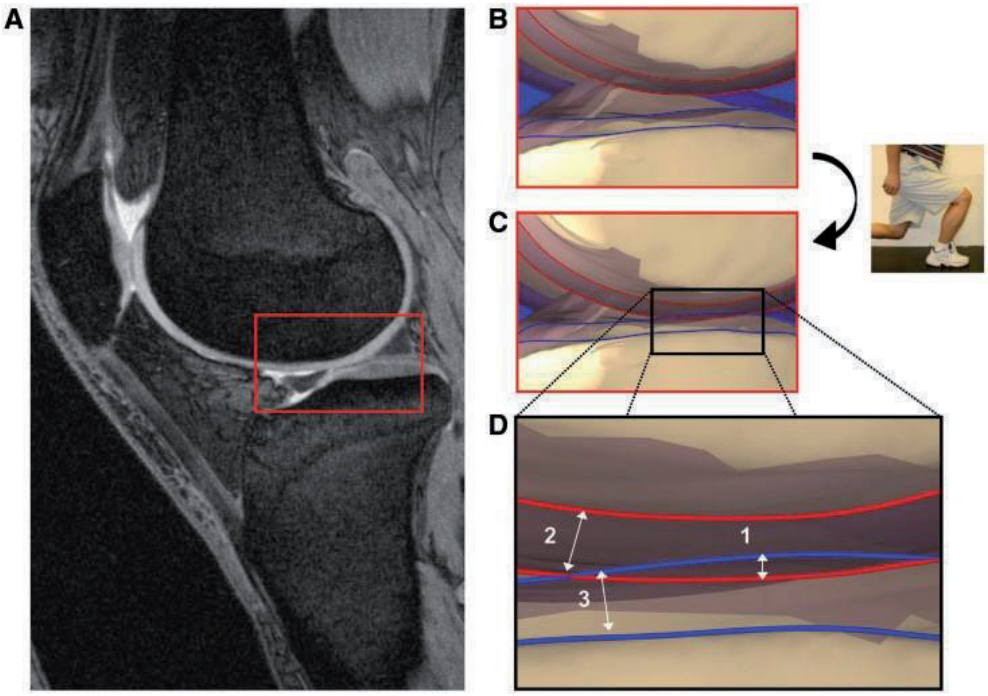

Figure 1. Illustration of the calculation of compartmental contact deformation. The MR images of the knee joint after ~1 h non-weight bearing (**A**) are used to determine the respective cartilage thicknesses of the femur (red outlines) and tibia (blue outlines) at rest (**B**). After matching the MR models to the fluoroscopic images captured during weight-bearing lunge (**C**), compartmental cartilage deformation is calculated by dividing the amount of penetration (1) by the sum of the femoral (2) and tibial (3) cartilage surface thicknesses, as illustrated in (**D**).

A two-way repeated-measures analysis of variance and the Student-Newman-Keuls post hoc test were used to determine statistically significant differences in location, contact area, thickness, and cartilage contact deformation between the intact contralateral knees and the ACL-deficient knees at each flexion angle. *P* values less than 0.05 were considered significant.

RESULTS

Location of cartilage contact. In general, the location of peak cartilage contact deformation on the tibial plateaus was more posterior and lateral in ACL-deficient knees as compared with healthy contralateral knees. In the medial compartment of ACL-deficient knees, cartilage contact shifted posteriorly by an average (±SD) of 6.3 ± 0.7 mm at 0° and 15° of flexion (Figure 2A) and laterally by an average of 4.7 ± 0.9 mm between 0° and 60° of flexion (Figure 2B), as compared with the location in the intact knees. In the lateral compartment, cartilage contact shifted posteriorly by an average of 3.6 ± 1.3 mm between 0° and 30° of flexion (Figure 2C) and shifted laterally by an average of 4.2 ± 0.6 mm between 0° and 60° of flexion (Figure 2D) following rupture of the ACL.

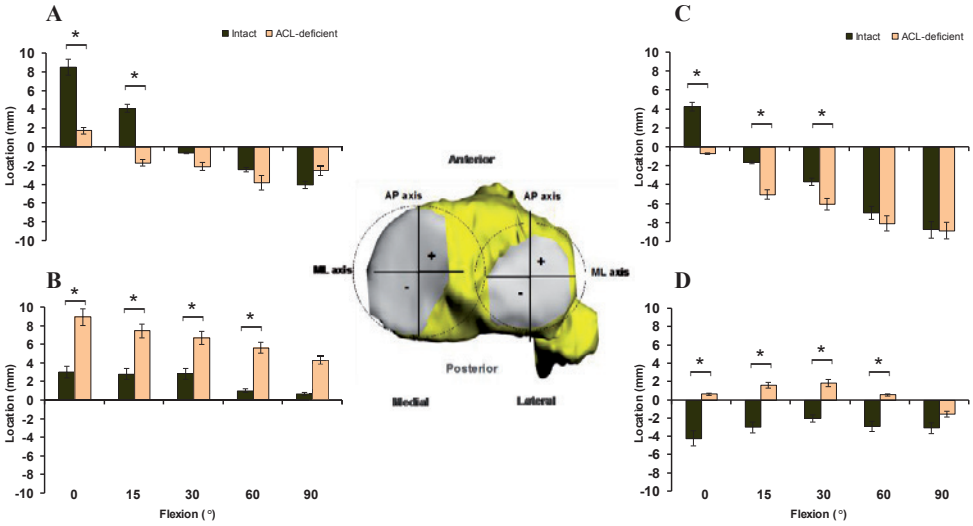

Figure 2. Location of cartilage contact on the medial tibial plateau in the anteroposterior (AP) (**A**) and mediolateral (ML) (**B**) directions and on the lateral tibial plateau in the AP (**C**) and ML (**D**) directions in intact and anterior cruciate ligament (ACL)-deficient knees as a function of knee flexion angle in 8 patients with acute, isolated rupture of the ACL. The central illustration shows the Cartesian coordinate system on the tibial plateau. Values are the mean ± SD. * = $P < 0.05$.

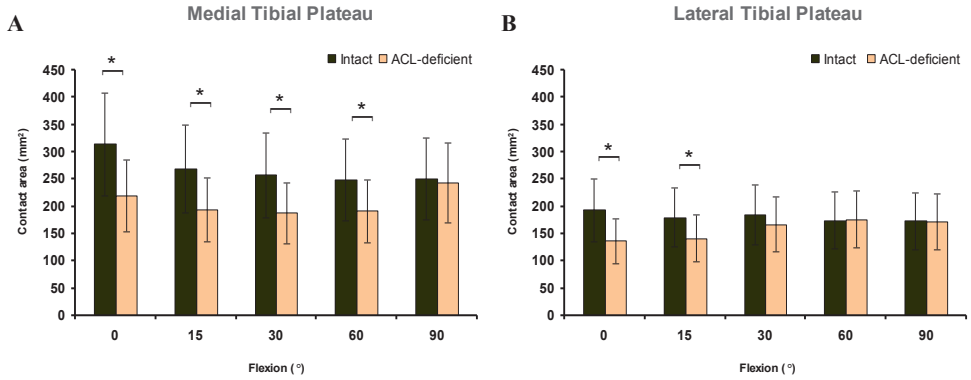

Figure 3. Cartilage contact area on the medial (**A**) and lateral (**B**) tibial plateaus in intact and anterior cruciate ligament (ACL)-deficient knees as a function of knee flexion angle in 8 patients with acute, isolated rupture of the ACL. Values are the mean ± SD. * = $P < 0.05$.

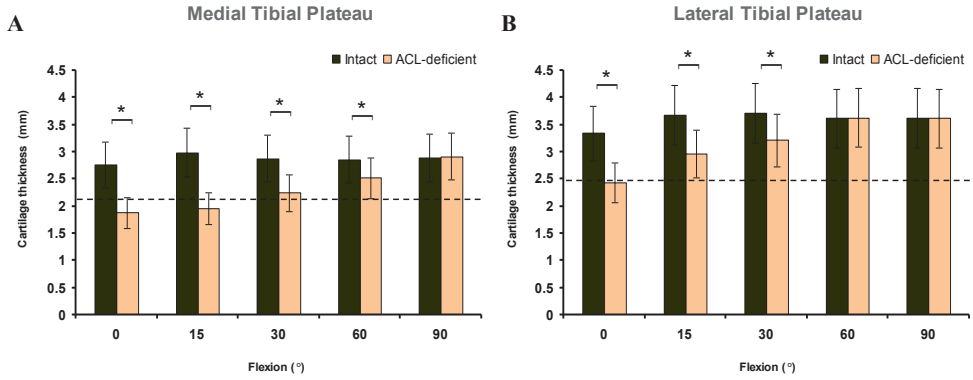

Figure 4. Thickness of cartilage in regions of contact on the medial (**A**) and lateral (**B**) tibial plateaus in intact and anterior cruciate ligament (ACL)-deficient knees as a function of knee flexion angle in 8 patients with acute, isolated rupture of the ACL. Values are the mean ± SD. * = $P < 0.05$.

Size of the contact area. In the medial compartment, the cartilage contact area in ACL-deficient knees was significantly smaller from 0° to 60° of flexion ($P < 0.05$) than that in the intact knees (Figure 3A). The maximum decrease in cartilage contact area after ACL rupture occurred at 0° of flexion (219.6 ± 69.4 mm^2 in the ACL-deficient knee versus 314.4 ± 113.6 mm^2 in the intact knee; $P = 0.0025$). In the lateral compartment, a decrease in contact area in ACL-deficient knees was observed at the lowest flexion angles (137.1 ±

64.1 mm^2 and 141.7 ± 48.7 mm^2 at 0° and 15° of flexion, respectively, in ACL-deficient knees versus 193.4 ± 75.2 mm^2 and 180.0 ± 46.8 mm^2, respectively, in intact knees [P = 0.0004 and P = 0.0041, respectively]) (Figure 3B).

Cartilage thickness at the contact area. The total average thickness of cartilage in the studied knees was 2.2 ± 0.4 mm (mean ± SD) and 2.5 ± 0.5 mm, respectively, in the medial and lateral tibial plateaus. In the intact contralateral knees, the cartilage thickness located in areas of contact was an average of 1.4 times greater than the total average thickness. In contrast, regions of contact for both the medial and lateral compartments in ACL-deficient knees were an average of 0.9 times thinner than the total average thickness. Cartilage thickness at contact was an average of 0.7 ± 0.3 mm thinner between 0° and 60° of flexion in the medial compartment (Figure 4A) and 0.7 ± 0.2 mm thinner between 0° and 30° of flexion in the lateral compartment (Figure 4B) as compared with the cartilage thickness at contact in the respective compartments of intact knees.

Magnitude of cartilage contact deformation. Rupture of the ACL significantly increased the deformation of cartilage between 0° and 60° of flexion in the medial compartment of the knee joint as compared with the intact knees (P < 0.05) (Figure 5A). The maximum increase in compartmental cartilage deformation after ACL rupture occurred at 0° of flexion (19 ± 4% intact knee, 29 ± 9% ACL-deficient knee, P = 0.0138). The increase in cartilage deformation that was observed after ACL rupture gradually lessened with flexion. At 90° of flexion, there was no significant difference in cartilage deformation between the healthy and ACL-deficient knee.

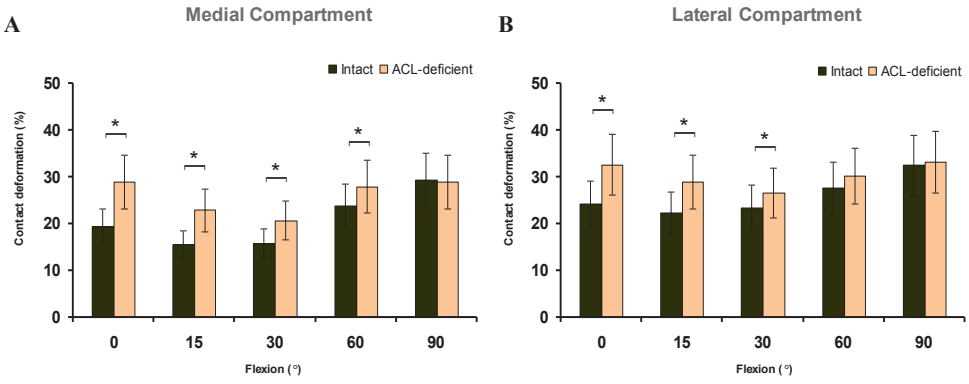

Figure 5. Peak cartilage contact deformation in the medial (**A**) and lateral (**B**) tibiofemoral compartments in intact and anterior cruciate ligament (ACL)-deficient knees as a function of knee flexion angle in 8 patients with acute, isolated rupture of the ACL. Values are the mean ± SD. * = P < 0.05.

In the lateral compartment, rupture of the ACL significantly increased the deformation of cartilage between 0° and 30° of knee flexion ($P < 0.05$) (Figure 5B). The maximum increase in cartilage deformation after ACL rupture occurred at 0° of flexion, where a mean ± SD percentage deformation of 24 ± 9% was found in the healthy knee and 33 ± 6% in the ACL-deficient knee ($P = 0.0033$).

DISCUSSION

Rupture of the ACL mostly affects patients under 30 years of age[30] and is associated clinically with an increased incidence,[3,4] an earlier onset,[4] and a faster progression[31] of knee OA. In vivo T1ρ quantitative assessment of knee cartilage after ACL injury using 3T MRI has previously demonstrated that cartilage abnormalities were already present following initial ACL injury in patients with underlying bone marrow edema–like lesions in the lateral tibia,[15] suggesting a role in the pathogenesis of OA in ACL deficiency.[32,33] Interestingly though, an increased prevalence of cartilage degeneration has been described in the medial compartment in the presence of an ACL injury,[34–37] whereas the bone marrow edema–like lesions are usually found in the lateral compartment of the knee.[38]

Based on theoretical models, it has been hypothesized that the persistent abnormal kinematic behavior that is seen in isolated ACL deficiency could alter the stress distributions in the cartilage over time, thereby predisposing the knee to degenerative changes.[39] This "wear and tear" theory could be supported by the efficacy of the classic animal models of knee OA, in which transection of the ACL, with consequent joint instability, but without injury to the other structures of the knee, triggers cartilage degeneration.[40,41] However, it remains poorly understood how, during in vivo weightbearing flexion of the knee, the minimal changes in cartilage contact kinematics observed in unstable knee joints without manifest initial cartilage or underlying bone lesions[25] could contribute to the initiation of OA.

In our previous in vivo analysis of the tibiofemoral joint kinematics in patients with ACL deficiency, we found an increased anterior translation (~3 mm) and internal rotation (~2°) of the tibia at low flexion angles as compared with the healthy control knee.[9] Similar findings have been well documented in the literature.[10,11] ACL deficiency also caused an increased medial tibial translation of ~1 mm. These changes in tibiofemoral kinematics after ACL injury were expected to lead to changes in the tibiofemoral cartilage contact characteristics. Specifically, the medial shift of the tibia after ACL deficiency would alter the contact stress distributions in the tibiofemoral cartilage near the medial tibial spine. Indeed, in the presence of ACL injury, the cartilage contact points shifted not only posteriorly, as was expected based on the increased anterior tibial translation, but also laterally on the surface of the tibial plateau.[25] In the medial compartment, the contact points shift toward the medial tibial spine, a region where degeneration is observed in patients

with chronic ACL injuries.[34] The question remained as to whether the ~2-mm shift in cartilage contact (determined based on the location of the centroid of the cartilage contact area) to incongruent articular regions of the knee joint affects the stress on the cartilage of the joint.

In the present study, we found a similar posterior and lateral shift in cartilage contact location on the surface of the tibial plateaus following ACL injury. However, when determining the location of cartilage contact based on the location where peak cartilage deformation occurred, we found that the magnitude of the posterior and lateral shift following ACL rupture (~5 mm) was greater than that previously reported.[25] A possible explanation for the discrepancy in the magnitude of shift based on measurement methodology could be found in the regional variations in cartilage thickness. When determining the cartilage contact location based on the closest interarticular distance between the bony surfaces of the tibiofemoral joint[24] or the centroid of the tibiofemoral cartilage contact area,[25] regional variations in the thickness of underlying cartilage are not taken into account. In the present study, the region of tibiofemoral cartilage contact was not only smaller following rupture of the ACL, but also had significantly thinner cartilage at contact in both the medial and lateral compartments as compared with the thickness at contact in the intact knees. In other words, the minimal shift in the location of the cartilage contact area to regions of thinner cartilage as reported previously[25] resulted in a considerable change in cartilage loading distribution within the knee joint.

The posterior and lateral shift in cartilage contact to thinner articular regions increased the magnitude of cartilage deformation in those regions. The maximum relative increase in cartilage contact deformation after ACL rupture occurred at full extension in the medial compartment, where deformation of 19 ± 4% was found in healthy knees and 29 ± 9% in ACL-deficient knees as compared with deformation of 24 ± 9% and 33 ± 6%, respectively, in the lateral compartment. The relatively greater increase in cartilage deformation in the medial compartment as compared with the lateral compartment relates to the increased development of OA in the medial compartment of the knee joint, as was observed during arthroscopic examination of 130 ACL-deficient patients.[35]

Due to the constraints of the imaging technique, motion and deformation of the meniscus were not detectable in the fluoroscopic images. For quantitative examination of the interaction of molecular changes in the meniscus and adjacent cartilage in ACL deficiency, recent developments in MRI techniques, such as T1ρ mapping, represent potential means.[42] However, based on our previous validation of the imaging technique,[27] the present limitation in examination of the meniscus by the dual fluoroscopic technique did not affect the determination of cartilage–cartilage contact, since articular surface mesh penetration was only recorded at the location of in vivo tibiofemoral cartilage contact. An additional constraint of the present methodology is that any possible underlying physiochemical activities (e.g., elevated cytokines in the joint fluid[43]) that might occur in the knee joint

following ACL rupture could not be analyzed, thereby restricting the formulation of inclusive insight into the pathogenesis of OA in knee joint instability. In addition, regional variations in the mechanical properties of the articular cartilage were not taken into account when computing the cartilage contact deformation. This may be a limitation, since in vitro compression of tibial cartilage explants obtained from distinct regions of the joint has demonstrated that chondrocytes displayed region-specific baseline gene expression and responded differently to in vitro mechanical loading.[44]

Patients with discernible cartilage lesions on 3T MRI at a mean ± SD of 4.5 ± 3 months of injury were excluded from the study. However, with our methodology, we were unable to appreciate the extent of potential cartilage softening that existed at the time of the analysis and were thus unable to resolve the "chicken-or-egg" issue. Were our measured deformation differentials attributable to the ACL-deficient knee cartilage being more compliant, rather than increased deformation being responsible for the subsequent degeneration onset? Future studies using a methodology similar to that used in this pilot study, with baseline and follow-up imaging biomarkers, such as T1ρ or delayed gadolinium-enhanced MRI of cartilage, should follow ACL-deficient patients who are treated conservatively for longer periods. Tibiofemoral contact deformation and the health of the cartilage could therefore be monitored over time to quantify any possible biomechanical relationships.

We acquired data from only 1 functional activity, a single leg lunge, using a goniometer to measure the flexion angle. Measurement of the forces and strains in human tissues is currently impracticable, which impedes the extrapolation of the current findings to other weightbearing activities. It is conceivable that the knee joint anteroposterior shear forces during the single leg lunge might be higher than during normal gait,[45] thus exaggerating the measured articular surface engagement differentials. However, it has been reported that the magnitude of the anteroposterior shear forces increase with knee flexion during the descent phase of a lunge performed with a 223-N (50-lb) barbell[46] and that the knee forces are minimal in the functional range between 0° and 50° of knee flexion.[47] In the present study, the largest deformation differential was observed around 0° of knee flexion. In future studies, other in vivo activities, such as walking, running, and stair climbing, should be considered in order to construct a comprehensive insight into the effect of ACL deficiency on cartilage during daily activities.

During performance of the lunge activity, our patients were asked to pause for 5 seconds at each flexion angle while simultaneous fluoroscopic images were taken. To the best of our knowledge, the real-time in vivo creep of tibiofemoral cartilage has not yet been studied. Based on the in vivo creep compression curves for ankle cartilage using similar assessment methodologies which showed that cartilage contact deformation continued to increase during the first 20 seconds of loading,[48] it might be possible that the present data represent a

conservative estimate of a potentially bigger differential if the patients were asked to pause longer at each flexion angle.

It should be noted that no ground reaction forces were measured in this study to document that global knee joint loading was replicated reproducibly for both the intact and the ACL-deficient knee. The patient performed the lunge activity with full body weight on the tested leg, while the untested leg was used for balance only, to ensure physiologic loading conditions.

Finally, the present analysis compared tibiofemoral cartilage contact deformation in ACL-deficient and intact knees at each flexion angle, thereby ignoring potential interactions among the measured cartilage deformation and various knee flexion angles. Further research involving a larger study sample needs to be performed to confirm the present findings. Nonetheless, we believe our results provided comprehensible insight into the changes in in vivo tibiofemoral cartilage contact deformation following injury of the ACL and identified important directions for future research.

We found that rupture of the ACL alters the in vivo cartilage contact biomechanics of the tibiofemoral joint by shifting the cartilage contact location to smaller regions of thinner cartilage and increasing the magnitude of cartilage contact deformation.

REFERENCES

1. Aspden RM, Scheven BA, Hutchison JD. Osteoarthritis as a systemic disorder including stromal cell differentiation and lipid metabolism. Lancet 2001;357:1118–20.
2. Brandt K, Lohmander L, Doherty M. The concept of osteoarthritis as failure of the diarthrodial joint. In: Brandt K, Doherty M, Lohmander L, editors. Osteoarthritis. Oxford: Oxford University Press; 1998. p. 70–4.
3. Fithian DC, Paxton LW, Goltz DH. Fate of the anterior cruciate ligament-injured knee. Orthop Clin North Am 2002;33:621–36, v.
4. Roos H, Adalberth T, Dahlberg L, Lohmander LS. Osteoarthritis of the knee after injury to the anterior cruciate ligament or meniscus: the influence of time and age. Osteoarthritis Cartilage 1995;3:261–7.
5. Felson DT, Lawrence RC, Dieppe PA, Hirsch R, Helmick CG, Jordan JM, et al. Osteoarthritis: new insights. Part 1: the disease and its risk factors [review]. Ann Intern Med 2000;133:635–46.
6. Marshall KW, Chan AD. Arthroscopic anterior cruciate ligament transection induces canine osteoarthritis. J Rheumatol 1996;23: 338–43.
7. Brandt KD, Myers SL, Burr D, Albrecht M. Osteoarthritic changes in canine articular cartilage, subchondral bone, and synovium fifty-four months after transection of the anterior cruciate ligament. Arthritis Rheum 1991;34:1560–70.
8. Hunter DJ, Sharma L, Skaife T. Alignment and osteoarthritis of the knee. J Bone Joint Surg Am 2009;91 Suppl 1:85–9.
9. DeFrate LE, Papannagari R, Gill TJ, Moses JM, Pathare NP, Li G. The 6 degrees of freedom kinematics of the knee after anterior cruciate ligament deficiency: an in vivo imaging analysis. Am J Sports Med 2006;34:1240–6.
10. Georgoulis AD, Papadonikolakis A, Papageorgiou CD, Mitsou A, Stergiou N. Three-dimensional tibiofemoral kinematics of the anterior cruciate ligament-deficient and reconstructed knee during walking. Am J Sports Med 2003;31:75–9.
11. Logan M, Dunstan E, Robinson J, Williams A, Gedroyc W, Freeman M. Tibiofemoral kinematics of the anterior cruciate ligament (ACL)-deficient weightbearing, living knee employing vertical access open "interventional" multiple resonance imaging. Am J Sports Med 2004;32:720–6.
12. Shepherd DE, Seedhom BB. Thickness of human articular cartilage in joints of the lower limb. Ann Rheum Dis 1999;58:27–34.
13. Jones G, Glisson M, Hynes K, Cicuttini F. Sex and site differences in cartilage development: a possible explanation for variations in knee osteoarthritis in later life. Arthritis Rheum 2000;43:2543–9.
14. Ateshian GA, Soslowsky LJ, Mow VC. Quantitation of articular surface topography and cartilage thickness in knee joints using stereophotogrammetry. J Biomech 1991;24:761–76.

15. Bolbos RI, Ma CB, Link TM, Majumdar S, Li X. In vivo T1p quantitative assessment of knee cartilage after anterior cruciate ligament injury using 3 Tesla magnetic resonance imaging. Invest Radiol 2008;43:782–8.

16. Saadat E, Jobke B, Chu B, Lu Y, Cheng J, Li X, et al. Diagnostic performance of in vivo 3-T MRI for articular cartilage abnormalities in human osteoarthritic knees using histology as standard of reference. Eur Radiol 2008;18:2292–302.

17. Samosky JT, Burstein D, Eric Grimson W, Howe R, Martin S, Gray ML. Spatially-localized correlation of dGEMRIC-measured GAG distribution and mechanical stiffness in the human tibial plateau. J Orthop Res 2005;23:93–101.

18. Taylor C, Carballido-Gamio J, Majumdar S, Li X. Comparison of quantitative imaging of cartilage for osteoarthritis: T2, T1p, dGEMRIC and contrast-enhanced computed tomography. Magn Reson Imaging 2009:27:779–84.

19. Freeman MA, Pinskerova V. The movement of the knee studied by magnetic resonance imaging. Clin Orthop Relat Res 2003: 35–43.

20. Hinterwimmer S, Gotthardt M, von Eisenhart-Rothe R, Sauerland S, Siebert M, Vogl T, et al. In vivo contact areas of the knee in patients with patellar subluxation. J Biomech 2005;38:2095–101.

21. Wretenberg P, Ramsey DK, Nemeth G. Tibiofemoral contact points relative to flexion angle measured with MRI. Clin Biomech (Bristol, Avon) 2002;17:477–85.

22. Asano T, Akagi M, Tanaka K, Tamura J, Nakamura T. In vivo three-dimensional knee kinematics using a biplanar image-matching technique. Clin Orthop 2001:157–66.

23. Li G, DeFrate LE, Park SE, Gill TJ, Rubash HE. In vivo articular cartilage contact kinematics of the knee: an investigation using dual-orthogonal fluoroscopy and magnetic resonance image-based computer models. Am J Sports Med 2005;33:102–7.

24. Dennis DA, Mahfouz MR, Komistek RD, Hoff W. In vivo determination of normal and anterior cruciate ligament-deficient knee kinematics. J Biomech 2005;38:241–53.

25. Li G, Moses JM, Papannagari R, Pathare NP, DeFrate LE, Gill TJ. Anterior cruciate ligament deficiency alters the in vivo motion of the tibiofemoral cartilage contact points in both the antero-posterior and mediolateral directions. J Bone Joint Surg Am 2006;88:1826–34.

26. Irrgang JJ, Anderson AF, Boland AL, Harner CD, Kurosaka M, Neyret P, et al. Development and validation of the International Knee Documentation Committee subjective knee form. Am J Sports Med 2001;29:600–13.

27. Bingham JT, Papannagari R, Van de Velde SK, Gross C, Gill TJ, Felson DT, et al. In vivo cartilage contact deformation in the healthy human tibiofemoral joint. Rheumatology (Oxford) 2008; 47:1622–7.

28. Li G, Van de Velde SK, Bingham JT. Validation of a non-invasive fluoroscopic imaging technique for the measurement of dynamic knee joint motion. J Biomech 2008;41:1616–22.

29. Li G, Park SE, DeFrate LE, Schutzer ME, Ji L, Gill TJ, et al. The cartilage thickness distribution in the tibiofemoral joint and its correlation with cartilage-to-cartilage contact. Clin Biomech (Bristol, Avon) 2005;20:736–44.

30. Griffin LY, Agel J, Albohm MJ, Arendt EA, Dick RW, Garrett WE, et al. Noncontact anterior cruciate ligament injuries: risk factors and prevention strategies. J Am Acad Orthop Surg 2000; 8:141–50.

31. Kannus P, Jarvinen M. Posttraumatic anterior cruciate ligament insufficiency as a cause of osteoarthritis in a knee joint. Clin Rheumatol 1989;8:251–60.

32. Hernandez-Molina G, Guermazi A, Niu J, Gale D, Goggins J, Amin S, et al. Central bone marrow lesions in symptomatic knee osteoarthritis and their relationship to anterior cruciate ligament tears and cartilage loss. Arthritis Rheum 2008;58:130–6.

33. Li X, Ma BC, Bolbos RI, Stahl R, Lozano J, Zuo J, et al. Quantitative assessment of bone marrow edema-like lesion and overlying cartilage in knees with osteoarthritis and anterior cruciate ligament tear using MR imaging and spectroscopic imaging at 3 Tesla. J Magn Reson Imaging 2008;28:453–61.

34. Fairclough JA, Graham GP, Dent CM. Radiological sign of chronic anterior cruciate ligament deficiency. Injury 1990;21: 401–2.

35. Murrell GA, Maddali S, Horovitz L, Oakley SP, Warren RF. The effects of time course after anterior cruciate ligament injury in correlation with meniscal and cartilage loss. Am J Sports Med 2001;29:9–14.

36. Amin S, Guermazi A, LaValley MP, Niu J, Clancy M, Hunter DJ, et al. Complete anterior cruciate ligament tear and the risk for cartilage loss and progression of symptoms in men and women with knee osteoarthritis. Osteoarthritis Cartilage 2008;16:897–902.

37. Hill CL, Seo GS, Gale D, Totterman S, Gale ME, Felson DT. Cruciate ligament integrity in osteoarthritis of the knee. Arthritis Rheum 2005;52:794–9.

38. Fowler PJ. Bone injuries associated with anterior cruciate ligament disruption. Arthroscopy 1994;10:453–60.

39. Andriacchi TP, Mundermann A, Smith RL, Alexander EJ, Dyrby CO, Koo S. A framework for the in vivo pathomechanics of osteoarthritis at the knee. Ann Biomed Eng 2004;32:447–57.

40. Brandt KD. Transection of the anterior cruciate ligament in the dog: a model of osteoarthritis. Semin Arthritis Rheum 1991;21 Suppl 2:22–32.

41. Lozano J, Saadat E, Li X, Majumdar S, Ma CB. Magnetic resonance T(1ρ) imaging of osteoarthritis: a rabbit ACL transection model. Magn Reson Imaging 2009;27:611–6.

42. Bolbos RI, Link TM, Benjamin Ma C, Majumdar S, Li X. T1 ρ relaxation time of the meniscus and its relationship with T1 ρ of adjacent cartilage in knees with acute ACL injuries at 3 T. Osteoarthritis Cartilage 2009;16:12–8.

43. Cameron M, Buchgraber A, Passler H, Vogt M, Thonar E, Fu F, et al. The natural history of the anterior cruciate ligament-deficient knee. Changes in synovial fluid cytokine and keratin sulfate concentrations. Am J Sports Med 1997;25:751–4.

44. Bevill SL, Briant PL, Levenston ME, Andriacchi TP. Central and peripheral region tibial plateau chondrocytes respond differently to in vitro dynamic compression. Osteoarthritis Cartilage 2009;17: 980–7.

45. Shelburne KB, Torry MR, Pandy MG. Muscle, ligament, and joint-contact forces at the knee during walking. Med Sci Sports Exerc 2005;37:1948–56.

46. Stuart MJ, Meglan DA, Lutz GE, Growney ES, An KN. Comparison of intersegmental tibiofemoral joint forces and muscle activity during various closed kinetic chain exercises. Am J Sports Med 1996;24:792–9.

47. Escamilla RF. Knee biomechanics of the dynamic squat exercise. Med Sci Sports Exerc 2001;33:127–41.

48. Li G, Wan L, Kozanek M. Determination of real-time in-vivo cartilage contact deformation in the ankle joint. J Biomech 2008; 41:128–36.

49. Raynauld JP, Kauffmann C, Beaudoin G, Berthiaume MJ, de Guise JA, Bloch DA, et al. Reliability of a quantification imaging system using magnetic resonance images to measure cartilage thickness and volume in human normal and osteoarthritic knees. Osteoarthritis Cartilage 2003;11:351–60.

APPENDIX - ACCURACY AND PRECISION OF TIBIOFEMORAL CARTILAGE THICKNESS MEASUREMENT BY 3T MR IMAGING

Assessment of the accuracy and precision of cartilage thickness measurement based on 3-D meshed knee models created with 3T MR images is critical for the appreciation of biomechanical parameters such as in vivo cartilage contact deformation. In a validation study, we used calibrated digital images of a series of cartilage cross- sections from cadaver donors as the gold standard since the actual cartilage boundaries can be clearly delineated from the specimens (Figure A1 en A2).

Two fresh-frozen knee specimens from cadaver donors (right knee from a 48-year-old man; left knee from a 48-year-old woman) were selected. Specimens were stored at -20°C prior to testing and were thawed at room temperature for 24 hours before experimentation. Discernible cartilage damage in each specimen was ruled out by fluoroscopic, MRI, and visual examinations. Both knee specimens, with surrounding soft tissues intact, were then imaged with a 3T MRI scanner to create 3-D meshed models of the tibia, femur, and articulating cartilage layers using the protocol described previously.

Following MRI, the knee specimens were stripped of all surrounding soft tissues and disarticulated, leaving only the individual bones and articular cartilage surfaces. The bones were successively installed in a rigid cylinder with the shaft centered and osteotomized through the midsagittal planes of the articulating surfaces of the medial and lateral condyles. Between each osteotomy/digital image capturing of the pertinent cross-section, the specimens were wrapped in a moist dressing to prevent desiccation of the articular

cartilage. Eight cartilage cross-sections from the 2 specimens were measured (i.e., 2 cross-sections of each tibia and each femur). Digital images of the cross-sections were captured and were calibrated using a fluoroscopic image calibration protocol designed in our laboratory.

We next determined the same cross-section of the respective tibial and femoral cartilage layers in the 3-D surface mesh models. The osteotomized bones were CT scanned (LightSpeed Pro16 scanner; GE, Waukesha, WI). High-resolution axial-plane images were obtained (thickness 0.625 mm, gap 0.625 mm, and resolution 512 X 512 pixels). The CT images were then imported into MatLab (MathWorks, Natick, MA), and the contours of the osteotomized bones were digitized for each CT image based on a modified Canny edge detection method that combined pixel magnitude to construct a 3-D anatomic mesh model of the osteotomized bones. The osteotomized bone models were then mapped to the MRI-based models of the knee specimens using a customized code implemented in MatLab, based on the iterative closest point method. A plane was constructed along the cutting cross-section of the CT bone model. This plane was used to separate the MRI model at the location of the osteotomy.

The calibrated digital images of cartilage cross-sections were then matched to the respective cross-sectional planes of the MRI models. Thus, cartilage thickness could be measured at the same location on both the digital image and the MRI model. Ten equally distributed locations on each of the 8 cartilage cross-sections were measured and compared using Student's paired t-test, with significance set at $P < 0.05$.

For the first specimen, the average cartilage thickness values measured from the digital images versus the MRI models were 2.03 + 0.26 mm (mean + SD) versus 2.04 + 0.27 mm for the medial femoral condyle (absolute difference 0.05 + 0.03 mm; $P = 0.789$), 2.00 + 0.31 mm versus 2.02 + 0.30 mm for the lateral femoral condyle (absolute difference 0.05 + 0.03 mm; $P = 0.527$), 2.24 + 0.51 mm versus 2.26 + 0.48 mm for the medial tibial condyle (absolute difference 0.05 + 0.03 mm; $P = 0.378$), and 2.16 + 0.98 mm versus 2.18 + 1.00 mm for the lateral tibial condyle (absolute difference 0.04 + 0.03 mm; $P = 0.354$).

For the second specimen, the average cartilage thickness values measured from the digital images versus the MRI models were 2.15 + 0.29 mm versus 2.17 + 0.30 mm for the medial femoral condyle (absolute difference 0.04 + 0.03 mm; $P = 0.357$), 2.52 + 0.49 mm versus 2.52 + 0.48 mm for the lateral femoral condyle (absolute difference 0.03 + 0.02 mm; $P = 0.826$), 2.06 + 0.22 mm versus 2.04 + 0.23 mm for the medial tibial condyle (absolute difference 0.04 + 0.01 mm; $P = 0.447$), and 3.15 + 0.81 mm versus 3.17 + 0.80 mm for the lateral tibial condyle (absolute difference 0.03 + 0.02 mm; $P = 0.521$).

The average absolute difference in cartilage thickness, as measured at the 10 locations along the 8 section planes, between the direct measurement of the specimens and the MRI-based models was 0.04 + 0.01 mm (corresponding to a 1.8 + 1.6% difference). This

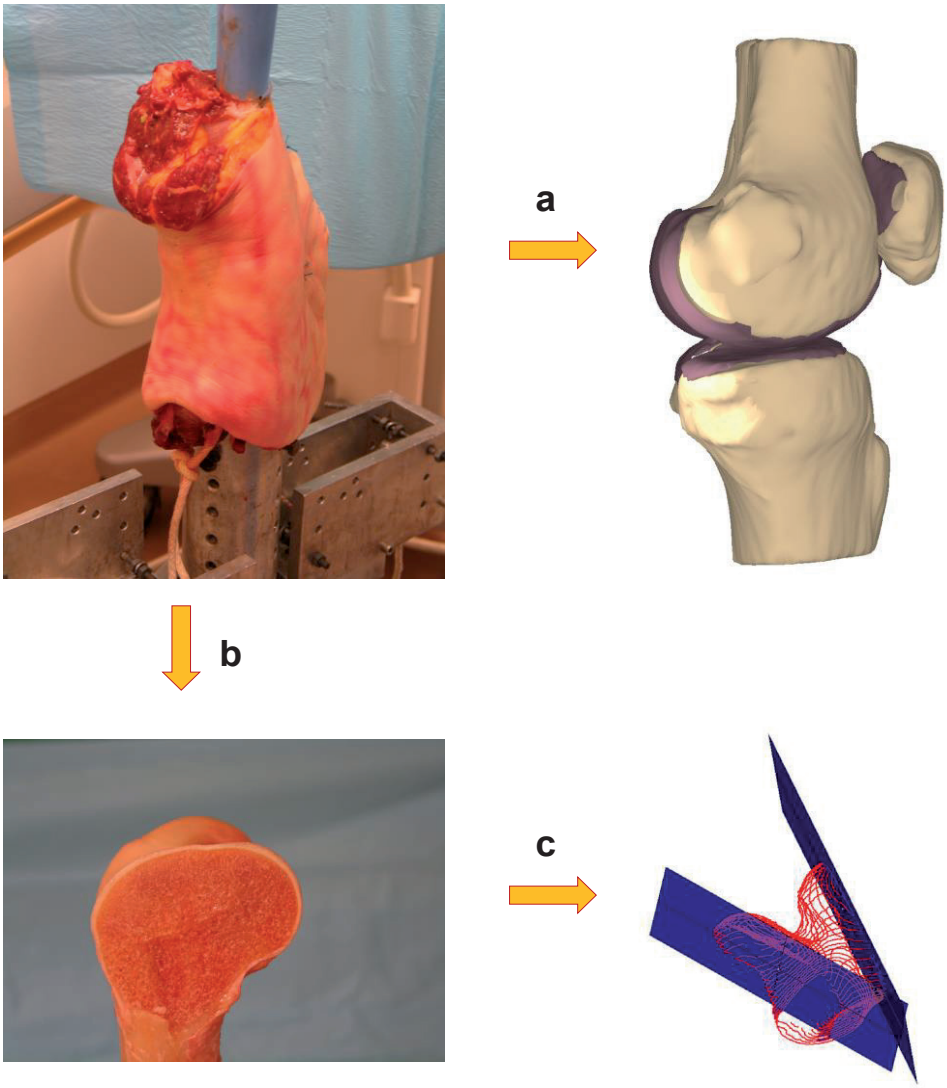

Figure A1. (**a**) 3T MR images were used to create 3D models of the cadaver knees; (**b**) digital images of osteotomized condyles were captured for gold standard measurement; (**c**) CT images of osteotomized bones were used to determine the location of the osteotomies.

demonstrated that the MRI-based cartilage model was close to the actual cartilage and was sufficiently accurate for the determination of cartilage contact deformation differentials between intact and ACL- deficient knee joints.

To test the intraobserver precision of the tibiofemoral cartilage thickness measurement using the MRI protocol and computer modeling, the cartilage layers that corresponded to the cutting planes were independently digitized 10 times by 3 observers (SKVdV, AH, and MK), with 1 day separating each re-segmentation. Cartilage thickness was determined at the 10 locations on each of the 8 cartilage cross-sections. The analyses were based on the

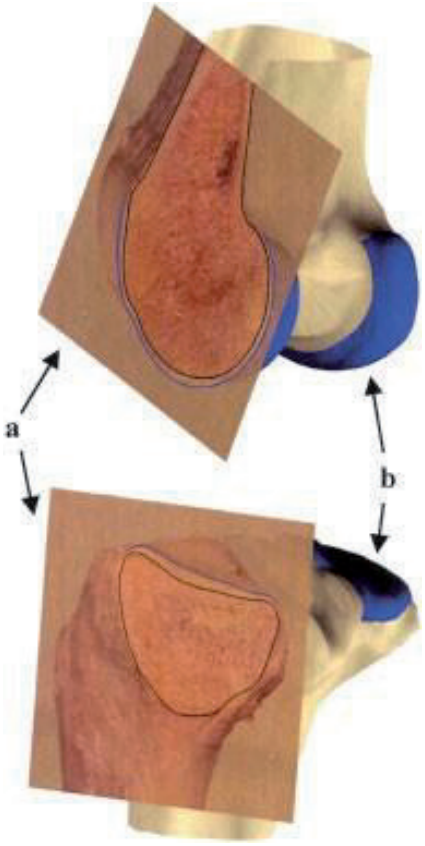

Figure A2. Comparison of direct measurement of the thickness of cartilage cross-sections from cadaver donors with measurement on MRI-based models. Digital images of osteotomies (**a**) were matched to the respective cross-sectional planes of the MRI models (**b**). The black (bone mesh) and blue (cartilage mesh) lines on the digital images indicate the intersection of the cartilage mesh models with the digital image at the location of the osteotomy. Only 2 cross-sections are shown.

maximum differences between the digitizations provided by each observer (results from the largest value minus the smallest value for each location). Intraobserver precision was assessed with Pearson's correlation coefficients and Student's t-tests of the paired differences of the observations. Correlations between the 10 digitizations were found to be excellent. Pearson's correlation coefficients for intraobserver precision at the measured locations were >0.984 ($P < 0.0001$) for each of the 3 readers.

Interobserver agreement was assessed by determining whether there were significant differences between the cartilage thickness measurements (thickness values from the first digitization session were selected) made by the 3 observers, using intraclass correlation coefficients (ICCs). Interobserver agreement was very high, with ICCs of 0.989–0.999 ($P < 0.0001$). These data are consistent with the values reported in the literature (49) and indicate that the cartilage thickness measurement using MRI-based cartilage models could be performed with great precision.

6

CHAPTER

Analysis of tibiofemoral cartilage deformation in the posterior cruciate ligament-deficient knee.

Samuel K. Van de Velde
Jeffrey T. Bingham
Thomas J. Gill, IV
Guoan Li

J Bone Joint Surg Am. 2009 Jan;91(1):167-75.

ABSTRACT

Background: Degeneration of the tibiofemoral articular cartilage often develops in patients with posterior cruciate ligament deficiency, yet little research has focused on the etiology of this specific type of cartilage degeneration. In this study, we hypothesized that posterior cruciate ligament deficiency changes the location and magnitude of cartilage deformation in the tibiofemoral joint.

Methods: Fourteen patients with a posterior cruciate ligament injury in one knee and the contralateral side intact participated in the study. First, both knees were imaged with use of a specific magnetic resonance imaging sequence to create three-dimensional knee models of the surfaces of the bone and cartilage. Next, each patient performed a single leg lunge as images were recorded with a dual fluoroscopic system at 0°, 30°, 60°, 75°, 90°, 105°, and 120° of knee flexion. Finally, the three-dimensional knee models and fluoroscopic images were used to reproduce the in vivo knee position at each flexion angle with use of a previously described image-matching method. With use of these series of knee models, the location and magnitude of peak tibiofemoral cartilage deformation at each flexion angle were compared between the intact contralateral and posterior cruciate ligament-deficient knees.

Results: In the medial compartment of the posterior cruciate ligament-deficient knees, the location and magnitude of peak cartilage deformation were significantly changed, compared with those in the intact contralateral knees, between 75° and 120° of flexion, with a more anterior and medial location of peak cartilage deformation on the tibial plateau as well as increased deformation of the cartilage. In the lateral compartment, no significant differences in the location or magnitude of peak cartilage deformation were found between the intact and posterior cruciate ligament-deficient knees.

Conclusions: The altered kinematics associated with posterior cruciate ligament deficiency resulted in a shift of the tibiofemoral contact location and an increase in cartilage deformation in the medial compartment beyond 75° of knee flexion. The magnitude of the medial contact shift in the posterior cruciate ligament-deficient knee was on the same order as that of the anterior contact shift.

Clinical Relevance: The observed changes in the location and magnitude of cartilage deformation in the tibiofemoral joint provide insight about the development of degeneration of the tibiofemoral joint cartilage in patients with posterior cruciate ligament deficiency. Our data also suggest that recreating mediolateral stability of posterior cruciate ligament-deficient knees might be of importance in addition to surgically improving anteroposterior translation.

INTRODUCTION

Clinically, rupture of the posterior cruciate ligament is associated with posterior instability, patellar pain, and an increased prevalence of knee osteoarthritis.[1-6] These complications have led some clinicians and researchers in the past to advocate surgical reconstruction of the posterior cruciate ligament.[3,7,8] However, many studies have documented articular cartilage lesions and premature degenerative changes after posterior cruciate ligament reconstruction, even though posterior stability was successfully restored.[8-12] As a result, a substantial amount of research on intact, posterior cruciate ligament-deficient, and surgically reconstructed knees has been performed, in the hopes of developing new and improved strategies for the treatment of posterior cruciate ligament deficiency.

The posterior cruciate ligament is thought to act as the primary restraint to posterior tibial translation of the knee at higher flexion angles.[13-22] Apparently, the posterior cruciate ligament is not only oriented anteriorly with respect to the tibia to constrain posterior tibial translation, it is also oriented medially from its tibial to femoral attachment region so that it also constrains lateral translation of the tibia.[23,24] These findings could explain why posterior cruciate ligament deficiency not only increased posterior tibial translation and external tibial rotation[16,25-27] but also increased lateral translation in our in vivo study of eight patients with posterior cruciate ligament deficiency.[24]

Despite the progress in our understanding of the anatomy and biomechanics of the posterior cruciate ligament, it remains unclear how and to what extent the subtle changes in in vivo joint kinematics that have been observed in posterior cruciate ligament-deficient knees contribute to the initiation of osteoarthritis. If a goal of the treatment of posterior cruciate ligament deficiency is the prevention of destruction of the tibiofemoral cartilage, then the impact of posterior cruciate ligament deficiency on the contact biomechanics of the cartilage needs to be understood.

The objective of this study was to investigate, with the use of a combined dual orthogonal fluoroscopic and magnetic resonance imaging technique, the effect of posterior cruciate ligament deficiency on the location of tibiofemoral cartilage contact as well as the magnitude of in vivo cartilage contact deformation during weight-bearing knee flexion.[28-30] We hypothesized that posterior cruciate ligament deficiency changes the location and magnitude of peak cartilage deformation in the tibiofemoral joint.

MATERIALS AND METHODS

Fourteen patients (ten men and four women ranging in age from nineteen to sixty-four years old) with nine right and five left knees with a posterior cruciate ligament rupture documented by clinical examination (a positive posterior drawer test as measured by the senior author [T.J.G.]) and demonstrated by magnetic resonance imaging were included in

this study. All subjects had a healthy contralateral knee. Injury to other ligaments, noticeable cartilage lesions, and injury to the underlying bone were reasons for exclusion from the study. Patients with a meniscal injury requiring removal of <50% of the meniscus were included in this study, since patients with an isolated posterior cruciate ligament injury and no damage to the meniscus are relatively rare and it is difficult to precisely quantify the extent to which the meniscus is damaged without arthroscopic examination. The purpose of the study was explained in detail to all of the subjects at the time of recruitment. Each subject signed a consent form that had been approved by our institutional review board. Eight of these fourteen subjects had been included in our previous study of the six-degrees-of-freedom tibiofemoral kinematics in patients with posterior cruciate ligament deficiency.[24]

Magnetic resonance and dual orthogonal fluoroscopic imaging techniques have been described in detail and validated in previous studies.[28,31-33] In brief, a protocol established in our laboratory was used to image both the left and the right knee with a magnetic resonance imaging scanner to create three-dimensional meshed models of the knees.[31] Each anatomic knee model included the osseous geometry of the femur, tibia, and fibula as well as the tibial and femoral cartilage layers. After the magnetic resonance image-based computer models were constructed, both knees of each subject were simultaneously imaged with use of two orthogonally placed fluoroscopes as the patient performed a single leg quasistatic lunge at 0°, 30°, 60°, 75°, 90°, 105°, and 120° of flexion while the upper body remained upright. Next, the fluoroscopic images were imported into solid-modeling software and

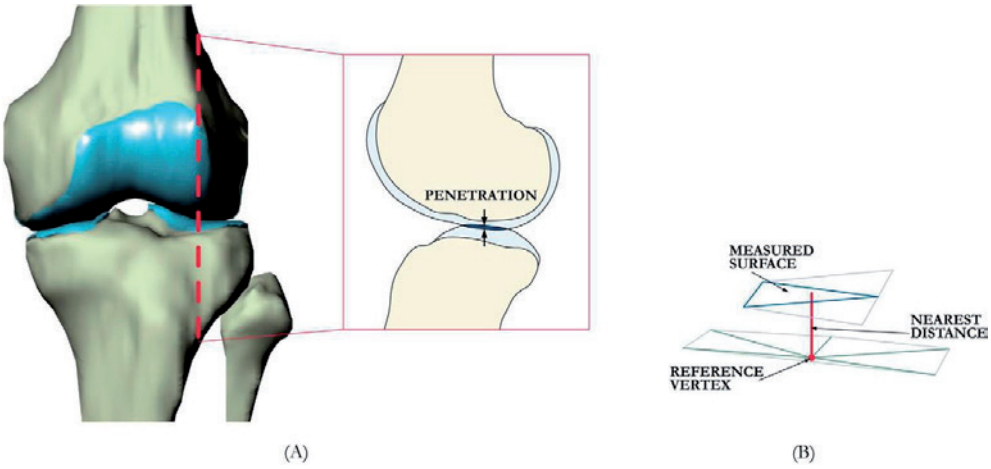

Figure 1. A: Sagittal section of a left knee, illustrating cartilage penetration (defined in this study as cartilage deformation). **B:** Method of measuring cartilage thickness and penetration depth from meshed surfaces.

placed in the orthogonal planes on the basis of the position of the fluoroscopes during the imaging of the patient. In the following step, the three-dimensional magnetic resonance image-based knee model of the patient was imported into the same software, viewed from the two orthogonal directions corresponding to the orthogonal fluoroscopic setup used to acquire the images, and independently manipulated in six degrees of freedom inside the software until the projections of the model matched the outlines of the fluoroscopic images. When the projections match the outlines of the images made during in vivo knee flexion, the model reproduces the in vivo position of the knee. Finally, the relative positions of the cartilage layers on the femur and tibia were determined from the series of models used to reproduce knee motion. When cartilage contact occurred during knee flexion, the articular surface meshes of the tibia and femur overlapped.

In this study, cartilage deformation was defined for each vertex of the articular surface mesh as the amount of penetration (Fig. 1, A) divided by the sum of the tibial and femoral cartilage surface thicknesses.[33,34] The cartilage thickness was calculated by finding the smallest Euclidian distance connecting a vertex of the articular surface to the cartilage-bone interface (Fig. 1, B).

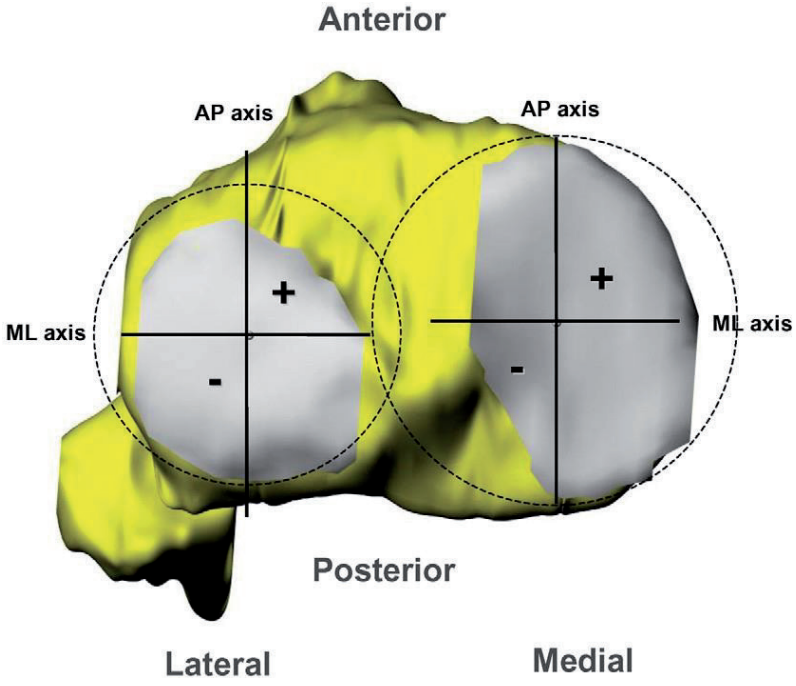

Figure 2. The Cartesian coordinate system for the tibial plateau. In the anteroposterior (AP) direction, a location anterior to the mediolateral axis was considered positive. In the mediolateral (ML) direction, a location medial to the anteroposterior axis was considered positive.

The locations of peak cartilage deformation were referenced to Cartesian coordinate systems on the tibial plateaus, as has been described in detail in previous publications (Fig. 2).[30,32,35] The origin of each coordinate system was located by the center of a circle, which was fit to the posterior edge of each tibial compartment. The anteroposterior and mediolateral axes split each tibial plateau into quadrants. In the anteroposterior direction, a location anterior to the mediolateral axis was considered positive. In the mediolateral direction, a location medial to the anteroposterior axis was considered positive.

A one-way repeated-measures analysis of variance and the Student-Newman-Keuls test were used to compare the location and magnitude of peak cartilage deformation of the intact contralateral knees with those of the posterior cruciate ligament-deficient knees. Differences were considered significant at the level of $p < 0.05$.

RESULTS

Location of Peak Cartilage Deformation

Healthy Contralateral Knees

In the medial tibial plateau, peak deformation moved posteromedially with flexion, from a mean (and standard deviation) of 6.7 ± 2.1 mm anterior to the mediolateral axis and 5.1 ± 1.4mm medial to the anteroposterior axis at 0° to a mean of 20.5 ± 0.2 mm posterior to the mediolateral axis (Fig. 3, A) and 2.0 ± 0.3 mm medial to the anteroposterior axis (Fig. 3, B) at 60°, where it remained for the rest of flexion.

In the lateral tibial plateau, peak deformation moved posteriorly throughout flexion, from a mean of 1.4 ± 2.3 mm anterior to the mediolateral axis at 0° to a mean of 27.6 ± 2.1 mm posterior to the mediolateral axis at 120° (Fig. 4, A). Peak deformation moved laterally in the lateral tibial plateau until 30°, at which point it was 1.9 ± 4.4 mm from the anteroposterior axis; peak deformation then moved medially until 90°, reaching a value of 4.6 ± 2.2 mm from the anteroposterior axis (Fig. 4, B).

Posterior Cruciate Ligament-Deficient Knees

In the medial compartment, posterior cruciate ligament deficiency significantly changed the location of peak cartilage deformation between 75° and 120° of flexion, with the posterior cruciate ligament-deficient knee having a more anterior and medial cartilage contact location as compared with the intact knee. During flexion of ≥75°, contact in the medial compartment shifted anteriorly by an average of 2.2 ± 0.4 mm (Fig. 3, A) and medially by an average of 1.9 ± 0.4 mm (Fig. 3, B) as compared with the location in the intact knees. These values include the data of the four subjects with a partial meniscectomy. Contact in the medial compartments of the four posterior cruciate ligament-deficient knees with partial

meniscectomy shifted anteriorly by an average of 2.1 ± 0.5 mm and medially by an average of 2.0 ± 0.5 mm between 75° and 120° of flexion.

In the lateral compartment, no significant differences in the anteroposterior and mediolateral motion of cartilage contact were observed between the intact and posterior cruciate ligament-deficient knees (Fig. 4, A and B).

Magnitude of Peak Cartilage Deformation

Healthy Contralateral Knees

In the medial compartment, peak deformation increased with flexion, from a mean of 0.17

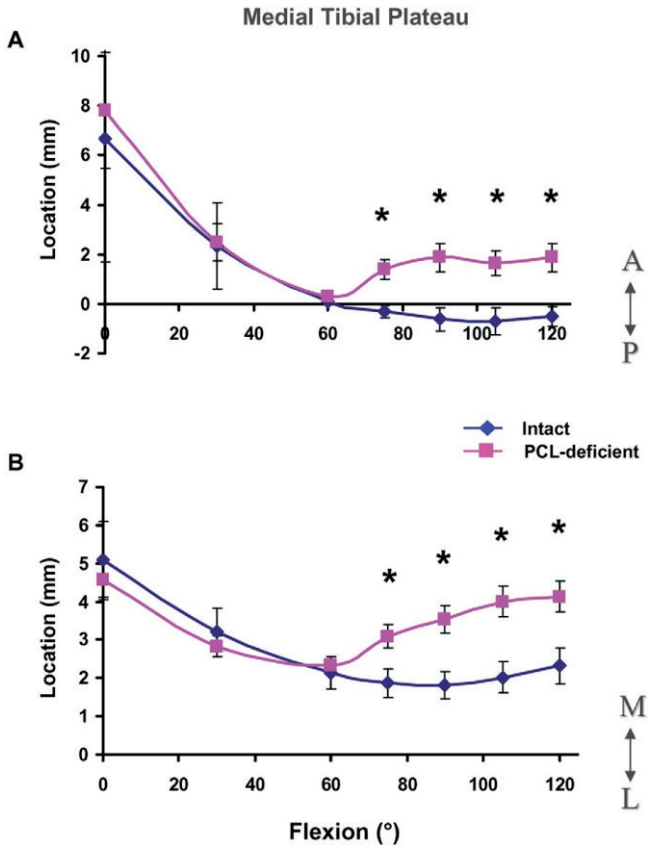

Figure 3. Location of peak cartilage deformation on the medial tibial plateau in the anteroposterior (**A**) and mediolateral (**B**) directions in the intact and posterior cruciate ligament (PCL)-deficient knees as a function of knee flexion angle. A = anterior to mediolateral axis, P = posterior to mediolateral axis, M = medial to anteroposterior axis, and L = lateral to anteroposterior axis. The values are given as the mean and standard deviation. *P < 0.05 as determined with one-way repeated-measures analysis of variance.

± 0.09 mm/mm at full extension to a mean of 0.20 ± 0.07 mm/mm at 120° of flexion (Fig. 5, A). In the lateral compartment, a similar increase in peak deformation was observed, with mean values of 0.17 ± 0.08 mm/mm at full extension and 0.22 ± 0.07 mm/mm at 120° of flexion (Fig. 5, B).

Posterior Cruciate Ligament-Deficient Knees

In the medial compartment, rupture of the posterior cruciate ligament caused a significant gradual increase in cartilage deformation, as compared with that in the intact knees, from 75° to 120° of flexion (Fig. 5, A). The maximum increase in cartilage deformation after

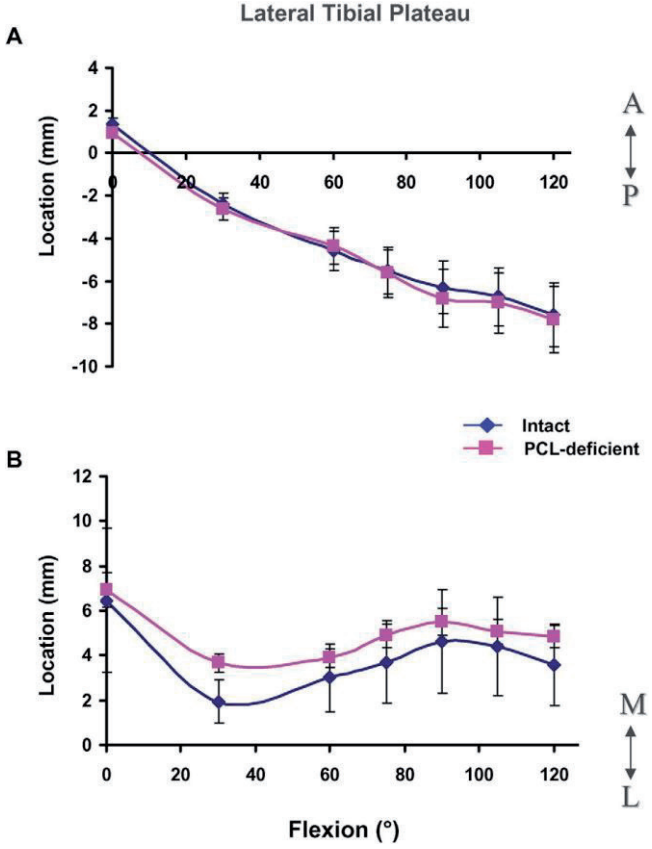

Figure 4. Location of peak cartilage deformation on the lateral tibial plateau in the anteroposterior (**A**) and mediolateral (**B**) directions in the intact and posterior cruciate ligament (PCL)-deficient knees as a function of knee flexion angle. A = anterior to mediolateral axis, P = posterior to mediolateral axis, M = medial to anteroposterior axis, and L = lateral to anteroposterior axis. The values are given as the mean and standard deviation.

posterior cruciate ligament rupture occurred at 120° of flexion (0.20 ± 0.07 mm/mm in the intact knee compared with 0.28 ± 0.08 mm/mm in the posterior cruciate ligament-deficient knee).We did not detect significant differences in cartilage deformation from 0° to 60° of flexion between the healthy and posterior cruciate ligament-deficient knees.

In the lateral compartment, we did not detect any significant differences in cartilage deformation between the intact and posterior cruciate ligament-deficient knees throughout the range of flexion (Fig. 5, B).

DISCUSSION

In this study, we investigated the location and magnitude of tibiofemoral cartilage deformation in posterior cruciate ligament-deficient knees. In the medial compartment of these knees, the location and magnitude of peak cartilage deformation were significantly changed, as compared with the findings in the intact contralateral knees, between 75° and

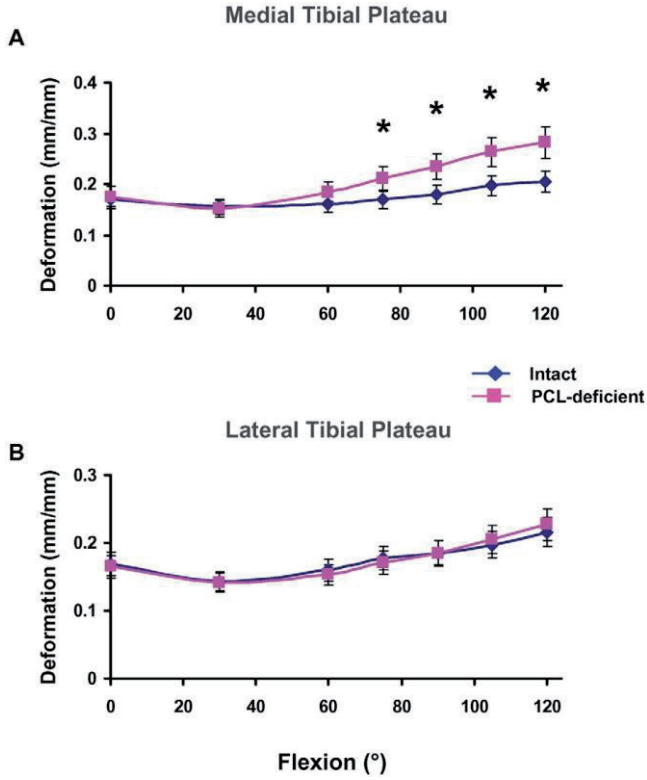

Figure 5. Magnitude of peak cartilage deformation on the medial (A) and lateral (B) tibial plateaus in the intact and posterior cruciate ligament (PCL)-deficient knees. *P < 0.05 as determined with one-way repeated-measures analysis of variance.

120° of flexion, with a more anterior and medial location as well as an increased magnitude. In the lateral compartment, no significant differences were found in the location or magnitude of peak tibiofemoral cartilage deformation between the intact and posterior cruciate ligament-deficient knees.

In our previous in vivo analysis of tibiofemoral joint kinematics, posterior cruciate ligament-deficient knees displayed increased posterior tibial translation beyond 30° of flexion compared with that in healthy control knees.[24] Similar findings have been well documented in the literature.[16,25-27,36]

However, posterior cruciate ligament deficiency also resulted in an average 1.1-mm increase in lateral tibial translation at 90° of flexion. The findings of the present analysis of cartilage deformation in posterior cruciate ligament-deficient knees are consistent with these altered tibiofemoral joint kinematics, as the increased posterior and lateral tibial translation could be related, respectively, to the increased anterior and medial locations of cartilage deformation on the medial tibial plateau.

In normal knees, cartilage is up to 50% thicker in regions where cartilage-to-cartilage contact is present.[35] Healthy cartilage is believed to adapt to mechanical stimuli[37,38] and ultimately become dependent on the maintenance of the mechanical stimulus for normal tissue function.[39] The thicker cartilage within the cartilage-to-cartilage contact area may result in a reduced contact stress, as was demonstrated by a three-dimensional finite-element analysis suggesting that thicker cartilage bears a lower peak contact stress than thinner cartilage under the same loading conditions.[40] In the present study, we found that posterior cruciate ligament deficiency significantly altered tibiofemoral cartilage contact in both the anteroposterior and the mediolateral direction in the medial compartment of the knee at higher flexion angles. In the presence of posterior cruciate ligament injury, cartilage contact not only shifted anteriorly, as was expected on the basis of increased posterior tibial translation, but also medially on the surface of the tibial plateau in flexion positions of ≥75°, forcing the femur to ride up the upslope of the medial tibial plateau, a region of thinner cartilage.[34,41] This medial shift of the location of cartilage contact after posterior cruciate ligament rupture to incongruent, thinner articular regions increased the cartilage deformation in those regions (Fig. 6). Increased cartilage deformation is associated with increased mechanical loading of the articular contact region within the knee, which in turn has been linked to higher rates of progression of osteoarthritis.[42] The relatively greater increase of cartilage deformation in the medial compartment compared with that in the lateral compartment observed in the posterior cruciate ligament-deficient knees in the present study is consistent with the reported increased development of osteoarthritis in the medial compartment of the knee joint following posterior cruciate ligament injury.[2,4]

As the presented data were obtained during only one functional in vivo activity—namely, the single leg lunge—we advise caution when extrapolating the data to other functional

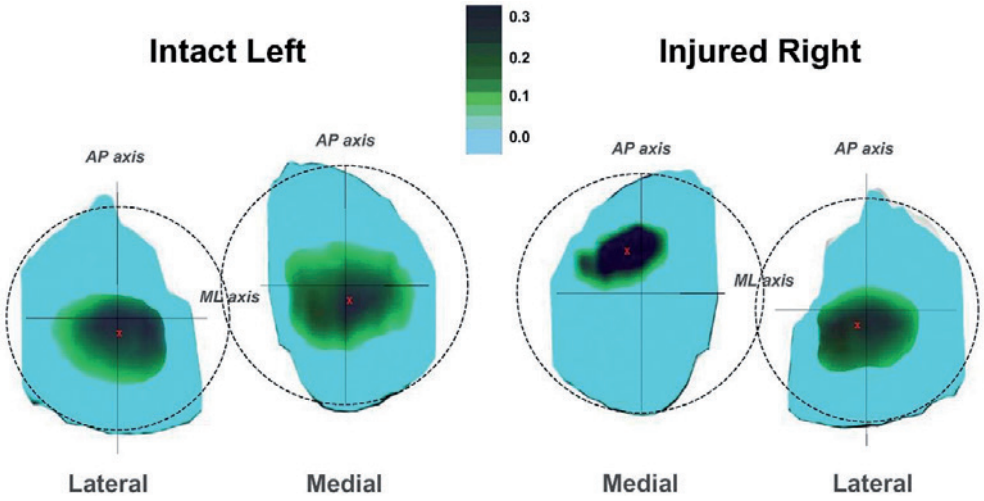

Figure 6. Color map of the cartilage deformation in the intact (left) and posterior cruciate ligament-deficient (right) knees of a typical subject with the knees in 105° of flexion, illustrating the effect of posterior cruciate ligament deficiency on the location and magnitude of cartilage deformation at flexion angles beyond 75°. The red X on the cartilage surfaces indicates the location of peak cartilage de- formation. Note the more anterior (relative to the mediolateral axis) and medial (relative to the anteroposterior axis) contact location of cartilage deformation in the medial compartment of the posterior cruciate ligament-deficient knee. The darker color depicts a higher magnitude of peak cartilage deformation (in millimeters). The illustrative color map was created by assigning an increasingly darker color value to each increased value of cartilage deformation for each vertex of the articular surface mesh. AP = anteroposterior, and ML = mediolateral.

activities. Nevertheless, we believe that these findings might be useful for the design of improved treatment protocols for posterior cruciate ligament deficiency. First, as we did not detect differences in the cartilage biomechanics between the intact and posterior cruciate ligament-deficient knees during the single leg lunge between 0° and 60° of flexion, our findings suggest that rehabilitation exercises might be safely performed in this range of flexion. On the other hand, repetitive deep knee squats should be avoided by subjects with posterior cruciate ligament deficiency, so as not to increase the tibiofemoral cartilage deformation. Second, it is interesting to note that the magnitude of medial contact shift in the posterior cruciate ligament-deficient knees was on the same order as the magnitude of the anterior contact shift. This suggests that, when a posterior cruciate ligament reconstruction is performed with either a single or a double-bundle graft, recreation of the mediolateral stability of posterior cruciate ligament-deficient knees may be as important as the surgical improvement of anteroposterior translation. Finally, in a recent cadaver study,

Giffin et al. demonstrated, with a robotic testing system, that increasing the tibial slope with a sagittal osteotomy successfully reduced the abnormal tibial sag in the posterior cruciate ligament-deficient knee, shifting the resting position of the tibia anteriorly.[43] On the basis of our data, it could be theorized in future studies that the osteotomy should include a varus component, possibly reducing the abnormal medial shift following posterior cruciate ligament injury and thereby possibly reducing the increase in cartilage deformation.

This study had limitations. As a result of the constraints of the imaging technique, motion and deformation of the meniscus were not detectable on the fluoroscopic images. However, on the basis of our previous validation of the imaging technique,[32] we do not believe that this limitation affected the cartilage-cartilage contact data, as articular surface mesh penetration was recorded only at the location of in vivo tibiofemoral cartilage contact. In addition, as mentioned earlier, we acquired data during only one functional activity, a single leg lunge. Other in vivo activities such as walking, running, and stair climbing should be considered in future studies. Furthermore, it should be noted that no ground reaction forces were measured in this study. In the future, a force-plate will be incorporated into the system. Since isolated posterior cruciate ligament injuries are rare, we included some patients who had a partial tear of one of the menisci. Because there were only fourteen subjects in our study, there was not enough statistical power for us to analyze the effect of partial removal of the meniscus as well. The findings from this study might therefore have been affected by the meniscal tears. Another limitation is that the patients were investigated at different time intervals after the injury. In future studies, patients in whom posterior cruciate ligament deficiency has been treated conservatively should be followed for longer periods with use of a methodology similar to that employed in our study. Tibiofemoral contact and the health of the cartilage could therefore be monitored over time to quantify any possible biomechanical relationships.

In conclusion, the altered kinematics caused by posterior cruciate ligament deficiency resulted in a shift of the tibiofemoral contact location and an increase in the in vivo deformation beyond 75° of flexion in the medial compartment. This injurious ‘‘jab-and-cross combo’’ provides insight about the development of degeneration of tibiofemoral joint cartilage in patients with posterior cruciate ligament deficiency. If the prevention of osteoarthritis in patients with posterior cruciate ligament deficiency is a goal of the treating physician, the function of the injured ligament should be restored as closely to normal as possible, in both the anteroposterior and mediolateral directions, thereby possibly better normalizing the cartilage biomechanics of the knee.

REFERENCES

1. Boynton MD, Tietjens BR. Long-term followup of the untreated isolated posterior cruciate ligament-deficient knee. Am J Sports Med. 1996;24:306-10.
2. Clancy WG Jr, Shelbourne KD, Zoellner GB, Keene JS, Reider B, Rosenberg TD. Treatment of knee joint instability secondary to rupture of the posterior cruciate ligament. Report of a new procedure. J Bone Joint Surg Am. 1983;65:310-22.
3. Cross MJ, Powell JF. Long-term followup of posterior cruciate ligament rupture: a study of 116 cases. Am J Sports Med. 1984;12:292-7.
4. Keller PM, Shelbourne KD, McCarroll JR, Rettig AC. Nonoperatively treated isolated posterior cruciate ligament injuries. Am J Sports Med. 1993; 21:132-6.
5. Parolie JM, Bergfeld JA. Long-term results of nonoperative treatment of isolated posterior cruciate ligament injuries in the athlete. Am J Sports Med. 1986; 14:35-8.
6. Shelbourne KD, Davis TJ, Patel DV. The natural history of acute, isolated, nonoperatively treated posterior cruciate ligament injuries. A prospective study. Am J Sports Med. 1999;27:276-83.
7. Schulte KR, Chu ET, Fu FH. Arthroscopic posterior cruciate ligament reconstruction. Clin Sports Med. 1997;16:145-56.
8. Moore HA, Larson RL. Posterior cruciate ligament injuries. Results of early surgical repair. Am J Sports Med. 1980;8:68-78.
9. Marks PH, Cameron M, Fu FH. [Reconstruction of the cruciate ligaments with allogeneic transplants. Techniques, results and perspectives]. Orthopade. 1993;22:386-91. German.
10. Hughston JC, Bowden JA, Andrews JR, Norwood LA. Acute tears of the posterior cruciate ligament. Results of operative treatment. J Bone Joint Surg Am. 1980;62:438-50.
11. Pournaras J, Symeonides PP, Karkavelas G. The significance of the posterior cruciate ligament in the stability of the knee. An experimental study in dogs. J Bone Joint Surg Br. 1983;65:204-9.
12. Richter M, Kiefer H, Hehl G, Kinzl L. Primary repair for posterior cruciate ligament injuries. An eight-year followup of fifty-three patients. Am J Sports Med. 1996;24:298-305.
13. Butler DL, Noyes FR, Grood ES. Ligamentous restraints to anterior-posterior drawer in the human knee. A biomechanical study. J Bone Joint Surg Am. 1980;62:259-70.
14. Fanelli GC, Giannotti BF, Edson CJ. The posterior cruciate ligament arthroscopic evaluation and treatment. Arthroscopy. 1994;10:673-88.
15. Fox RJ, Harner CD, Sakane M, Carlin GJ, Woo SL. Determination of the in situ forces in the human posterior cruciate ligament using robotic technology. A cadaveric study. Am J Sports Med. 1998;26:395-401.
16. Gollehon DL, Torzilli PA, Warren RF. The role of the posterolateral and cruciate ligaments in the stability of the human knee. A biomechanical study. J Bone Joint Surg Am. 1987;69:233-42.

17. Markolf KL, Slauterbeck JR, Armstrong KL, Shapiro MS, Finerman GA. A biomechanical study of replacement of the posterior cruciate ligament with a graft. Part II: forces in the graft compared with forces in the intact ligament. J Bone Joint Surg Am. 1997;79:381-6.

18. Noyes FR, Stowers SF, Grood ES, Cummings J, VanGinkel LA. Posterior subluxations of the medial and lateral tibiofemoral compartments. An in vitro ligament sectioning study in cadaveric knees. Am J Sports Med. 1993;21:407-14.

19. Fukubayashi T, Torzilli PA, Sherman MF, Warren RF. An in vitro biomechanical evaluation of anterior-posterior motion of the knee. Tibial displacement, rotation, and torque. J Bone Joint Surg Am. 1982;64:258-64.

20. Race A, Amis AA. The mechanical properties of the two bundles of the human posterior cruciate ligament. J Biomech. 1994;27:13-24.

21. Girgis FG, Marshall JL, Monajem A. The cruciate ligaments of the knee joint. Anatomical, functional and experimental analysis. Clin Orthop Relat Res. 1975;106:216-31.

22. Carlin GJ, Livesay GA, Harner CD, Ishibashi Y, Kim HS, Woo SL. In-situ forces in the human posterior cruciate ligament in response to posterior tibial loading. Ann Biomed Eng. 1996;24:193-7.

23. Papannagari R, Defrate LE, Nha KW, Moses JM, Moussa M, Gill TJ, Li G. Function of posterior cruciate ligament bundles during in vivo knee flexion. Am J Sports Med. 2007;35:1507-12.

24. Li G, Papannagari R, Li M, Bingham JT, Nha KW, Allred D, Gill TJ. Effect of posterior cruciate ligament deficiency on in vivo translation and rotation of the knee during weightbearing flexion. Am J Sports Med. 2008;36:474-9.

25. Gill TJ, DeFrate LE, Wang C, Carey CT, Zayontz S, Zarins B, Li G. The biomechanical effect of posterior cruciate ligament reconstruction on knee joint function. Kinematic response to simulated muscle loads. Am J Sports Med. 2003;31:530-6.

26. Li G, Gill TJ, DeFrate LE, Zayontz S, Glatt V, Zarins B. Biomechanical consequences of PCL deficiency in the knee under simulated muscle loads—an in vitro experimental study. J Orthop Res. 2002;20:887-92.

27. Li G, Most E, DeFrate LE, Suggs JF, Gill TJ, Rubash HE. Effect of the posterior cruciate ligament on posterior stability of the knee in high flexion. J Biomech. 2004;37:779-83.

28. Li G, Wuerz TH, DeFrate LE. Feasibility of using orthogonal fluoroscopic images to measure in vivo joint kinematics. J Biomech Eng. 2004;126:314-8.

29. DeFrate LE, Sun H, Gill TJ, Rubash HE, Li G. In vivo tibiofemoral contact analysis using 3D MRI-based knee models. J Biomech. 2004;37:1499-504.

30. Li G, DeFrate LE, Park SE, Gill TJ, Rubash HE. In vivo articular cartilage contact kinematics of the knee: an investigation using dual-orthogonal fluoroscopy and magnetic resonance image-based computer models. Am J Sports Med. 2005;33:102-7.

31. Defrate LE, Papannagari R, Gill TJ, Moses JM, Pathare NP, Li G. The 6 degrees of freedom kinematics of the knee after anterior cruciate ligament deficiency: an in vivo imaging analysis. Am J Sports Med. 2006;34:1240-6.

32. Li G, Moses JM, Papannagari R, Pathare NP, DeFrate LE, Gill TJ. Anterior cruciate ligament deficiency alters the in vivo motion of the tibiofemoral cartilage contact points in both the anteroposterior and mediolateral directions. J Bone Joint Surg Am. 2006;88:1826-34.

33. Li G, Wan L, Kozanek M. Determination of real-time in-vivo cartilage contact deformation in the ankle joint. J Biomech. 2008;41:128-36.

34. Bingham JT, Papannagari R, Van de Velde SK, Gross C, Gill TJ, Rubash HE, Li G. In-vivo cartilage contact deformation in the healthy human tibiofemoral joint. Rheumatology (Oxford). 2008;47:1622-7.

35. Li G, Park SE, DeFrate LE, Schutzer ME, Ji L, Gill TJ, Rubash HE. The cartilage thickness distribution in the tibiofemoral joint and its correlation with cartilage-to-cartilage contact. Clin Biomech (Bristol, Avon). 2005;20:736-44.

36. Logan M, Williams A, Lavelle J, Gedroyc W, Freeman M. The effect of posterior cruciate ligament deficiency on knee kinematics. Am J Sports Med. 2004;32:1915-22.

37. Arokoski JP, Jurvelin JS, Vaatainen U, Helminen HJ. Normal and pathological adaptations of articular cartilage to joint loading. Scand J Med Sci Sports. 2000;10:186-98.

38. Smith RL, Donlon BS, Gupta MK, Mohtai M, Das P, Carter DR, Cooke J, Gibbons G, Hutchinson N, Schurman DJ. Effects of fluid-induced shear on articular chondrocyte morphology and metabolism in vitro. J Orthop Res. 1995;13:824-31.

39. Carter DR, Beaupre´ GS, Giori NJ, Helms JA. Mechanobiology of skeletal regeneration. Clin Orthop Relat Res. 1998;355 Suppl:S41-55.

40. Li G, Lopez O, Rubash H. Variability of a three-dimensional finite element model constructed using magnetic resonance images of a knee for joint contact stress analysis. J Biomech Eng. 2001;123:341-6.

41. Donahue TL, Hull ML, Rashid MM, Jacobs CR. A finite element model of the human knee joint for the study of tibiofemoral contact. J Biomech Eng. 2002;124:273-80.

42. Miyazaki T, Wada M, Kawahara H, Sato M, Baba H, Shimada S. Dynamic load at baseline can predict radiographic disease progression in medial compartment knee osteoarthritis. Ann Rheum Dis. 2002;61:617-22.

43. Giffin JR, Stabile KJ, Zantop T, Vogrin TM, Woo SL, Harner CD. Importance of tibial slope for stability of the posterior cruciate ligament deficient knee. Am J Sports Med. 2007;35:1443-9.

7

CHAPTER

The effect of anterior cruciate ligament deficiency and reconstruction on the patellofemoral joint.

Samuel K. Van de Velde
Thomas J. Gill, IV
Louis E. DeFrate
Ramprasad Papannagari
Guoan Li

Am J Sports Med. 2008 Jun;36(6):1150-9.

ABSTRACT

Background: Little is known about the impact of anterior cruciate ligament deficiency and reconstruction on the patellofemoral joint.

Hypothesis: Anterior cruciate ligament deficiency changes the patellofemoral joint biomechanics. Reconstruction of the ligament does not restore the altered patellofemoral joint function.

Study Design: Controlled laboratory study.

Methods: Eight patients with an acute anterior cruciate ligament injury in 1 knee and the contralateral side intact were included in the study. Magnetic resonance and dual-orthogonal fluoroscopic imaging techniques were used to compare the patellofemoral joint function during a single-leg lunge between the intact, the anterior cruciate ligament–injured, and the anterior cruciate ligament–reconstructed knee. Data on the patellar tendon apparent elongation and orientation, patellar tracking, and patellofemoral cartilage contact location were collected preoperatively and at 6 months after reconstruction.

Results: Anterior cruciate ligament deficiency caused a significant apparent elongation and change in orientation of the patellar tendon. It decreased the flexion and increased the valgus rotation and tilt of the patella. Anterior cruciate ligament injury caused a proximal and lateral shift in patellofemoral cartilage contact location. Anterior cruciate ligament reconstruction reduced the abnormal apparent elongation but not the orientation of the patellar tendon, and it restored the patellar flexion and proximal shift in contact. The abnormal patellar rotation, tilt, and lateral shift in cartilage contact persisted after reconstruction.

Conclusion: The altered function of the patellar tendon in anterior cruciate ligament deficiency resulted in an altered patellar tracking and patellofemoral cartilage contact. Persistent changes in patellofemoral joint function after anterior cruciate ligament reconstruction imply that reconstruction of the anterior cruciate ligament does not restore the normal function of the patellofemoral joint.

Clinical Relevance: The abnormal kinematics of the patellofemoral joint might predispose the patellofemoral cartilage to degenerative changes associated with anterior cruciate ligament deficiency, even if the ligament is reconstructed in a way that restores anteroposterior knee laxity.

INTRODUCTION

Patients with ACL deficiency often develop alterations in quadriceps muscle performance with weakness and atrophy[5,7,38,41] and degeneration of the patellofemoral joint (PFJ) cartilage.[32] In patients who have undergone ACL reconstruction with a bone–patellar tendon–bone (BPTB) graft, some of the most prevalent complications are persistent patellar irritability,[36] patellofemoral pain,[1,4,10,15-17,30,36] and quadriceps weakness.[15,36] Yet little research has focused on the PFJ in ACL deficiency, and there is even less on the PFJ after ACL reconstruction. Hsieh et al[20,21] hypothesized that patellofemoral kinematics and contact characteristics are different in the ACL-deficient knee, causing patellofemoral problems. Excision of the ACL in cadaveric knees resulted in an increased lateral shift and tilt of the patella[20] and decreased patellofemoral contact area and pressure.[21] Reconstruction of the ACL restored the abnormal biomechanics to normal levels in both in vitro studies.

To our knowledge, no data have been reported on the PFJ function in ACL deficiency under in vivo weightbearing conditions. Furthermore, the effect of ACL reconstruction on the patellofemoral function under weightbearing conditions is unknown.

The objective of this study was to investigate the effects of ACL deficiency and reconstruction on the 3-dimensional (3D) behavior of the patellar tendon, the patellofemoral kinematics, and the contact characteristics of the PFJ during an in vivo weightbearing activity. In this study, we hypothesized that ACL deficiency changes the 3D behavior of the patellar tendon, the patellar tracking, and subsequently the cartilage contact location of the PFJ. Furthermore, we hypothesized that contemporary ACL reconstruction does not restore the normal PFJ function, although anteroposterior laxity of the knee under anterior tibial loads is restored.

MATERIALS AND METHODS

Subject Recruitment and Exclusion Criteria

Eight patients (6 men and 2 women; age range, 19-38 years) were included in the study.[12,25,34,39] The included patients were diagnosed with an acute, isolated ACL injury, documented by clinical examination (8-mm Lachman test with no end point and a grade 2 pivot-shift test measured by the same orthopaedic surgeon) and MRI and had no injuries to the contralateral knee. Four patients had an injury of the left knee, and 4 had an injury of the right knee. Subjects had been injured within a mean 4.5 ± 3 months of testing. Injury to other ligaments, distinguishable cartilage lesions, and injury to the underlying bone were reasons for exclusion from the study. However, patients with minimal meniscal injury were allowed in this study because patients with an isolated ACL injury and absolutely no damage to the meniscus are relatively rare, and it is difficult to precisely quantify the extent to which the meniscus is damaged without arthroscopic examination. However, the status

of the meniscus was documented during subsequent arthroscopic reconstruction of the ACL. If removal of more than 50% of the medial or lateral meniscus was required during reconstruction, the patient was excluded. Three patients had no significant damage to the meniscus, 1 patient had a partial- thickness tear of the lateral meniscus, and the remaining 4 patients had injuries requiring partial removal of the lateral meniscus (10%, 15%, 30%, and 40% removal of the lateral meniscus).[12,25,34,39]

The purpose of the present study was explained in detail to all of the subjects at the time of recruitment. Each subject signed a consent form that had been approved by our institutional review board.

The ACL Reconstruction Technique

The subjects underwent arthroscopic surgical reconstruction of the ACL of the injured knee. All surgeries were performed by 1 orthopaedic surgeon. A diagnostic arthroscopy was performed before graft placement. During surgery, the status of each patient's menisci was documented. Reconstruction was performed in a standard fashion using a central 10-mm BPTB autograft. A 10-mm tibial tunnel was drilled using a 55° guide (Linvatec-Conmed, Largo, Fla) centered at a point 7 mm anterior to the PCL on the downslope of the medial tibial spine. A 10-mm femoral tunnel was drilled using a 6-mm femoral offset guide (Arthrex, Naples, Fla) centered at the 10:30 position for right knees (1:30 for left). The graft was passed in retrograde fashion, and the femoral and tibial bone blocks were secured with titanium interference screws (Guardsman, Linvatec-Conmed). The femoral screw length was 25 mm and was placed with the knee in maximal flexion. The tibial screw length was 30 mm. The graft was fully tensioned with the knee in full extension. Screw diameter was determined based on graft-tunnel fit. Examination confirmed that there was no notch impingement, and cycling of the knee revealed less than 2 mm of graft motion in all cases. The anterior laxity of the reconstructed knee as measured with the KT-1000 arthrometer was similar to that of the intact contralateral knee.[34]

The MRI Scan and 3D Knee Model

Before the ACL reconstruction, both knees were imaged with a magnetic resonance (MR) scanner using a 1.5-T magnet (General Electric, Waukesha, Wis) and a fat-suppressed 3D spoiled gradient-recalled sequence.[13,24] The patients were lying horizontally with the knee in a relaxed, extended position. The MR scans spanned the medial and lateral extremes of the knee and were used to generate parallel sagittal plane images (resolution 512 × 512 pixels) with a field of view of 16 × 16 cm and a spacing of 1 mm. For each knee, the MR scanning time was approximately 12 minutes. Approximately 120 sagittal plane images were obtained for each knee. The MRIs were used to create 3D models of the knees in a solid modeling software (Rhinoceros, Robert McNeel and Associates, Seattle, Wash) using a protocol established in our laboratory.[13,23] The contours of the bone and cartilage surfaces of the femur, tibia, and patella were digitized within each image. The digitized spatial data

(x, y, and z coordinates) were then linked using B-spline curves to reproduce the contours of the femur, tibia, and patella. Bone and cartilage surfaces of the femur, tibia, and patella were created from the contours with the use of nonuniform rational B-splines. In addition to the bone and cartilage surface contours, the attachment areas of the patellar tendon on the tibial tubercle and the apex of the patella were delineated.

Dual-Orthogonal Fluoroscopic Imaging of the Knee During a Weightbearing Activity

After the MRI-based computer models were constructed, both knees of each subject were simultaneously imaged using 2 orthogonally placed fluoroscopes as the patient performed a single-leg quasi-static lunge at 0°, 15°, 30°, 60°, and 90° of flexion. Flexion angle of the knee was monitored using a handheld goniometer. The subject kept the knee stable for 1 second at each target flexion angle, so that the fluoroscopes captured the knee position, and then flexed the knee to the next target position. At each selected flexion angle, the subject supported his or her body weight on the leg being scanned, while the other leg was used to help balance the body. Data were collected preoperatively and at 6 months after single-bundle ACL reconstruction. These images were used to quantify the in vivo knee position at each of the targeted flexion angles.

Measurement of In Vivo 6 Degrees of Freedom Knee Kinematics Using Image-Matching Technique[28]

The orthogonal images were imported into a solid modeling software and placed in the orthogonal planes based on the position of the fluoroscopes during the imaging of the patient. The contours of the femur, tibia, and patella were outlined on each fluoroscopic image. The 3D MRI–based model of the patient was then imported into the software and viewed from the 2 orthogonal directions corresponding to the orthogonal fluoroscopic setup used to acquire the images. The models were independently manipulated in 6 degrees of freedom inside the software until the projections of the models matched the outlines of the images. When the projections matched the outlines of the images taken during in vivo knee

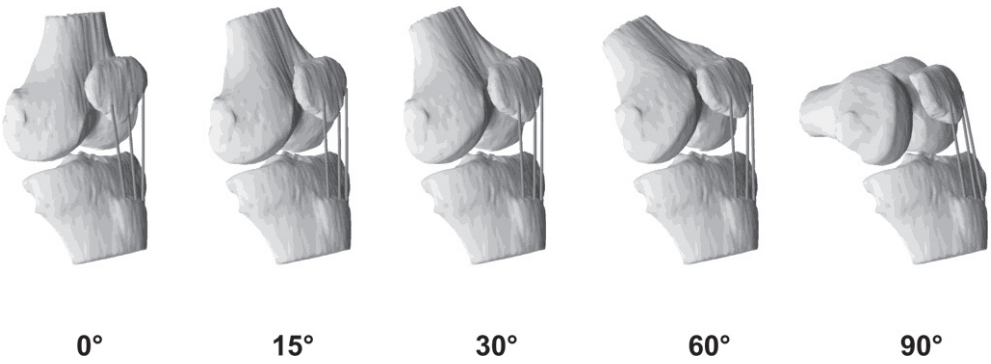

Figure 1. The knee models for a typical subject at 0°, 15°, 30°, 60°, and 90° of flexion.

flexion, the model reproduced the in vivo position of the knee. A series of knee models that reproduce knee positions at all target flexion angles re- created the in vivo knee flexion from full extension to 90° of flexion (Figure 1).

Magnetic resonance and dual-orthogonal fluoroscopic imaging techniques have been described in detail in previous publications. This system has an accuracy of less than 0.1 mm in measuring tibiofemoral joint kinematics.[12,28] The procedure was further validated for measuring the patellofemoral kinematics.[33] The methodology has an error of less than 0.1 ± 0.2 mm in measuring patellar shift and 0.2° ± 0.1° in patellar tilt.[33]

Description of the Biomechanical Function of the Patellar Tendon

The kinematics of the patellar tendon were measured from the series of bone models representing the kinematics of the knee.[11] The attachment sites of the patellar tendon on the patella and tibial tubercle were divided into thirds: a medial portion, a central portion, and a lateral portion. The apparent elongation of each portion of the patellar tendon was defined as the length of the line connecting the attachment sites on the patellar apex and tibial tubercle. The sagittal plane angle was defined as the angle formed between the long axis of the tibia and the projection of the patellar tendon on the sagittal plane of the tibia (Figure

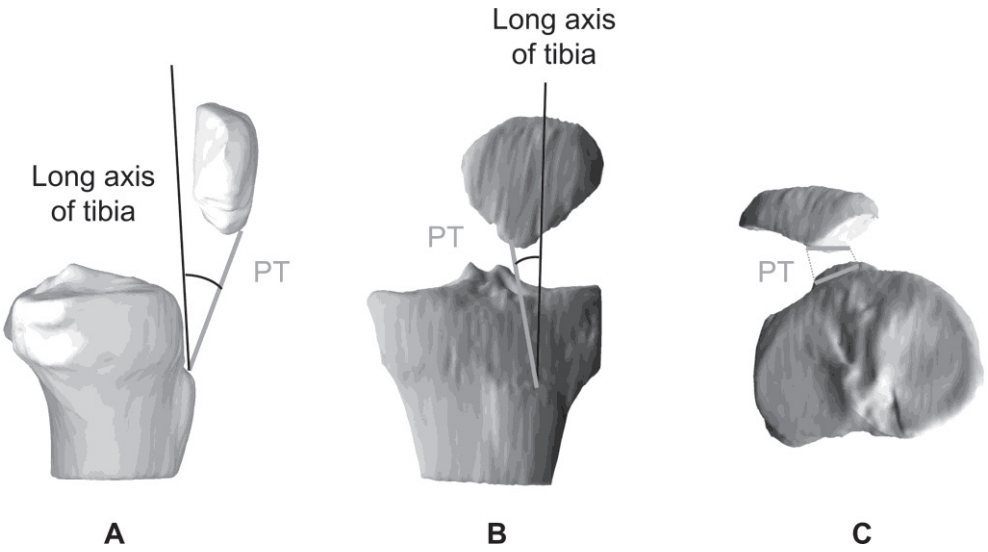

Figure 2. The sagittal plane angle (**A**), measured in the sagittal plane between the patellar tendon (PT) and the long axis of the tibia; the coronal plane angle (**B**), measured in the coronal plane between the PT and the long axis of the tibia; and twist (**C**), measured in the transversal plane between the patellar and tibial attachment of the PT.

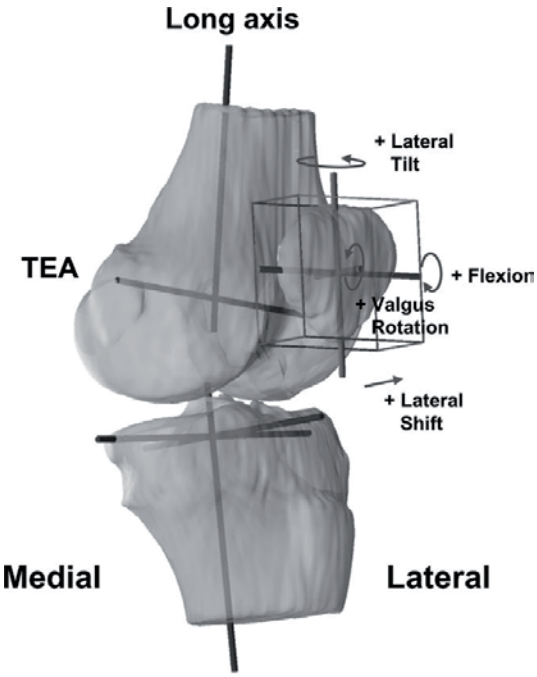

Figure 3. Coordinate systems used to quantify the patella tracking. The femoral coordinate system consisted of the transepicondylar axis (TEA) and the long axis intersecting at the center of the knee joint (midpoint of TEA). A cuboid was enclosed around the patella to determine the patellar center. The patellar coordinate system consisted of the proximodistal, anteroposterior, and mediolateral axes. Patellar flexion, shift, tilt, and rotation are considered positive as shown in the figure.

2A). A positive sagittal plane angle corresponded to an anterior orientation of the patellar tendon (patellar attachment anterior to the tibial attachment) relative to the long axis of the tibia, and negative values correspond to a posterior orientation. The coronal plane angle was defined as the angle between the long axis of the tibia and the projection of the patellar tendon on the coronal plane of the tibia (Figure 2B). Positive coronal plane angles corresponded to a medial orientation of the patellar tendon (patellar attachment medial to the tibial attachment) relative to the long axis of the tibia, whereas negative values corresponded to a lateral orientation. In this fashion, the kinematics of the patellar tendon were quantified for each subject as a function of flexion. Twist of the patellar tendon was defined as the angle measured in the transversal plane between the patellar and tibial attachment sites (Figure 2C).

Description of Patellar Tracking

After reproducing the in vivo knee positions along the flexion path, the patellar tracking was measured from the series of knee models.[33] A joint coordinate system[19] was established for each knee to describe the motion of the patella. Two axes were drawn on the femur: the long axis along the posterior femoral shaft surface in sagittal plane and the transepicondylar axis (TEA) connecting the epicondyle extremes of the medial and lateral femoral condyles.[31] The knee center was defined as the midpoint of the TEA. An axis parallel to the posterior wall of the tibial shaft was defined as the long axis of the tibia. The flexion angle of the knee was defined as the angle between the long axes of the femur and tibia in the

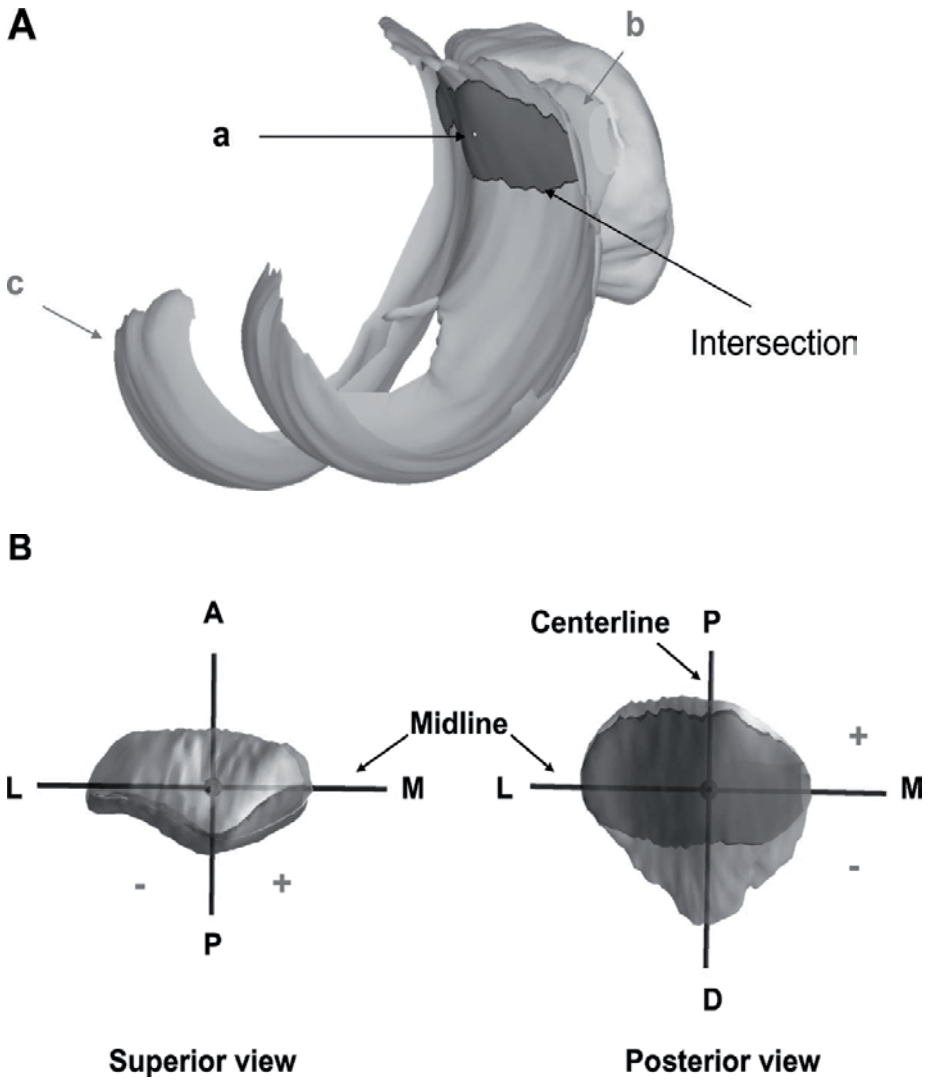

Figure 4. A, the centroid (a) of the intersection of the patellar (b) and femoral (c) cartilage was used to determine the patellofemoral contact locations. **B**, the coordinate system on the patellar cartilage surface for patellofemoral cartilage contact analysis. The proximal (P)–distal (D) axis was called the centerline. The medial (M)–lateral (L) axis was called the midline. Contact proximal to the midline and medial to the centerline was positive. A, anterior.

sagittal plane. To reduce the variability in creating patellar coordinate systems, a cuboid was used to enclose the patella so that it touched the proximodistal, anteroposterior, and mediolateral borders of the patella.[26,33] The center of the cuboid was defined as the origin of the patella. The long axis of the patella was defined as the line along the superior-inferior direction.

Patellar flexion was defined as the rotation of the patella about the TEA of the femur (Figure 3).[8] Patellar shift was defined as the medial or lateral movement of the center of the patella along the TEA of the femur (Figure 3). A positive shift corresponded to the lateral movement of the patellar center with respect to the knee center along the TEA of the femur. Patellar tilt was defined as the rotation of the patella about its long axis, where lateral tilt followed the direction of external femoral rotation (Figure 3). Patellar rotation is the rotation of the patella about the anteroposterior axis of the patella, where valgus rotation follows the direction of valgus rotation in tibiofemoral motion (Figure 3), that is, an outward angulation of the distal segment of the patella. In this fashion, the patellar tracking was quantified for each subject as a function of flexion of the knee.

Description of Patellofemoral Cartilage Contact Points

The contact points on the patellar cartilage were calculated by finding the centroid of the intersection of the patellar and femoral cartilage layers.[13,22,25] From the series of models used to reproduce knee motion, the relative positions of the cartilage layers on the femur and patella were determined. The overlap of the 2 cartilage layers was used to approximate the cartilage contact area (Figure 4A). The solid modeling software automatically outlined the intersection of the patellar and femoral cartilage layers and calculated the centroid of the enclosed area. The centroid of this contact area was defined as the contact point. To describe the motion of the cartilage contact points, a coordinate system was created on the surface of the patella (Figure 4B). The center of the vertical ridge of the patella was the origin of the coordinate system. In this coordinate system, the proximodistal axis was called the centerline, and the mediolateral axis was called the midline. In the proximodistal direction, the contact point was positive if it was proximal to the midline and negative if it was distal to the midline. In the mediolateral direction, a contact point was positive if it was on the medial side of the centerline and negative if it was on the lateral side of the centerline.

Statistical Methods

A 1-way repeated-measures analysis of variance was used to compare the biomechanical function of the patellar tendon (apparent elongation, sagittal plane angle, coronal plane angle, and twist), the patellar tracking (patellar flexion, shift, tilt, and rotation), and the position of the patellofemoral contact points on the patellar cartilage of the ACL-deficient, ACL-reconstructed, and intact (contralateral) knees. The Student-Newman-Keuls post hoc

test was performed to isolate statistically significant differences between groups. The level of significance was set at $P < .05$.

RESULTS

Biomechanical Function of the Patellar Tendon

In the healthy knee, all 3 portions of the patellar tendon deformed similarly with flexion. The apparent elongation of the lateral, central, and medial portions of the patellar tendon increased from 64.9 ± 10.1 mm, 53.7 ± 6.9 mm, and 62.2 ± 7.9 mm, respectively, at 0° to 70.8 ± 8.6 mm, 57.9 ± 7.2 mm, and 66.6 ± 8.2 mm, respectively, at 30° of flexion, after which no marked change in apparent elongation was observed in the portions (Figure 5A). Anterior cruciate ligament deficiency caused an apparent elongation of all 3 portions of the patellar tendon, which was significant at most flexion angles. The effect of ACL deficiency on the apparent elongation of the patellar tendon was greatest at 0° of flexion in the lateral portion; an increase of 8.1% was noticed, compared to the healthy knee ($P < .05$). Anterior cruciate ligament reconstruction decreased the abnormal apparent elongation of the patellar tendon in all 3 portions to levels not significantly different from those of the intact knee.

In the sagittal plane (Figure 5B), the angle between the patellar tendon and the long axis of the tibia decreased with flexion from 21.8° ± 4.7°, 25.1° ± 5.6°, and 23.4° ± 4.8° at 0° of flexion to –4.7° ± 4.0°, –2.3° ± 4.0°, and –0.5° ± 3.4° at 90° of flexion in the lateral, central, and medial portions, respectively, of the healthy patellar tendon. In the flexion range from 0° to 30°, ACL deficiency decreased the sagittal plane angle by approximately 3°. The greatest decrease in sagittal plane angle occurred at 0° in the central portion of the patellar tendon: from 25.1° ± 5.6° to 20.8° ± 5.1°. At 0° of knee flexion, ACL reconstruction did not significantly change the sagittal plane angle, compared to the ACL-deficient knee. In the lateral and central portions, the sagittal plane angle remained significantly decreased in the ACL-reconstructed knee compared with the intact knee at 0° of knee flexion ($P < .05$). The ACL reconstruction reduced the abnormal sagittal plane angles in all the patellar tendon portions at 15° and 30° of knee flexion to levels not significantly different from those of the intact knee. At 60° of knee flexion, ACL reconstruction significantly increased the sagittal plane angle in the medial and central portion compared to the healthy knee; at 90° of knee flexion, ACL reconstruction significantly increased the sagittal plane angle in all the patellar tendon portions.

In the coronal plane (Figure 5C), the 3 portions of the healthy patellar tendon exhibited a similar trend of gradually decreasing coronal plane angles with flexion: from 9.0° ± 1.8°, 13.2° ± 3.4°, and 16.0° ± 4.6° at 0° of flexion to 1.3° ± 2.8°, 2.3° ± 3.1°, and 5.0° ± 3.5° at 90° of flexion in the lateral, central, and medial portions, respectively. In the ACL-deficient knee, the patellar tendon showed a similar trend of a gradually decreasing coronal plane

angle with flexion, but the coronal plane angle was less deviated to the medial side compared to the healthy knee, with a maximal difference of 7.6° at 0° of flexion in the central portion of the patellar tendon. The coronal plane angle in the ACL-deficient knee decreased from 3.0° ± 3.2°, 5.6° ± 6.4°, and 9.1° ± 5.4° at 0° of flexion to –3.0° ± 4.0°, –1.6° ± 4.2°, and 2.6° ± 4.5° at 90° of flexion in the lateral, central, and medial portions, respectively. The decrease in the coronal plane angle after ACL deficiency was significant at all angles and in all 3 portions of the patellar tendon, except at 90° of knee flexion in the central portion and between 30° and 90° in the medial portion. The ACL reconstruction was unable to restore the normal coronal plane angle. The coronal plane angle in the ACL-reconstructed knee varied from –0.4° ± 4.8°, 5.4° ± 5.8°, and 10.4° ± 4.9° at 0° of flexion to –5.8° ± 4.2°, –2.6° ± 4.9°, and 2.4° ± 4.1° at 90° of flexion in the lateral, central, and medial portions, respectively.

The healthy patellar tendon demonstrated a gradually increasing external rotation of its patellar attachment site relative to the tibial attachment site with flexion (Figure 5D): from 0.6°± 4.7° at 0° of flexion to –8.6°± 6.5° at 90° of flexion. In the ACL-deficient knee, the patellar attachment site was about 3° more externally twisted relative to the tibial attachment site compared to the healthy knee: from –3.8°± 6.4° at 0° of flexion to –11.6°± 7.9° at 90° of flexion. The ACL reconstruction did not significantly reduce the increased external twist of the patellar tendon that was observed in the ACL-deficient knee: from –4.5° ± 4.5° at 0° of flexion to –13.5° ± 8.3° at 90° of flexion.

Patellar Tracking

Anterior cruciate ligament injury significantly decreased the flexion angle between the patella and femur at 0° and 15° of flexion (Figure 6A) ($P < .05$). In the healthy knee, the patellar flexion angle measured 9.7° ± 5.6° at 0° of knee flexion and increased to 16.2° ± 6.9° at 15° of knee flexion. In ACL-deficient knees, patellar flexion at 0° was 3.2° ± 4.4° and increased to 9.1° ± 3.2° at 15° of knee flexion. On average, ACL deficiency reduced the patellar flexion angle by 6.6° throughout the measured range of motion. Anterior cruciate ligament reconstruction reduced the abnormal patellar flexion. At 0° of knee flexion, the patellar flexion was 7.5° ± 5.8° and increased to 13.6° ± 5.7° at 15° of knee flexion in ACL-reconstructed knees. On average, patellar flexion remained 3.1° less than

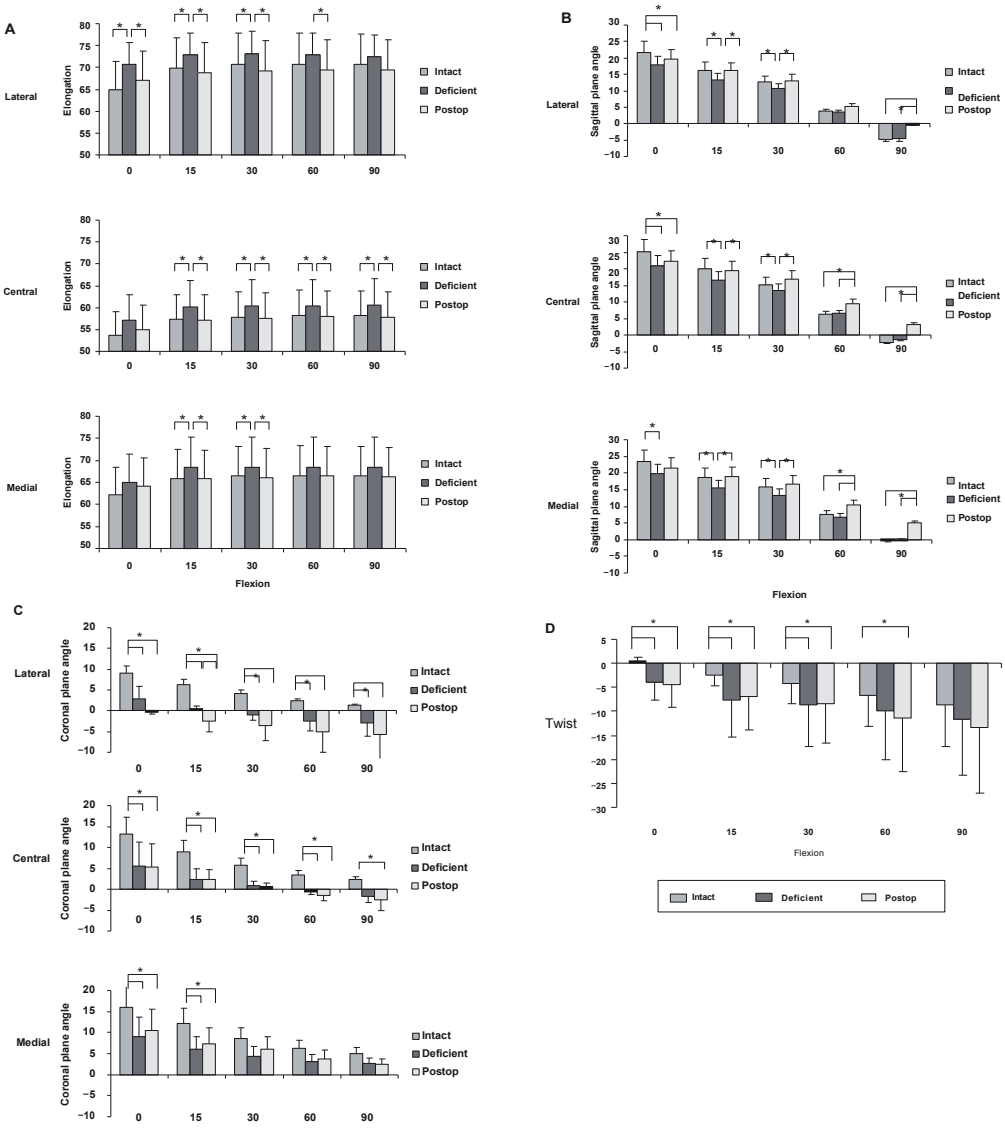

Figure 5. The biomechanical function of the patellar tendon. **A**, apparent elongation; **B**, sagittal plane angle; **C**, coronal plane angle; and **D**, twist of the patellar tendon as a function of knee flexion angle. Central, central portion of the patellar tendon; Deficient, ACL-deficient knee; Intact, intact knee; Lateral, lateral portion of the patellar tendon; Medial, medial portion of the patellar tendon; Postop, postoperative ACL-reconstructed knee. Mean ± SD; *P < .05.

that of the control knee; however, this residual decrease in flexion was not significantly different from the intact or ACL-deficient knee.

The patella in ACL-deficient knees shifted significantly more laterally at 0° of knee flexion, and reconstruction of the ACL did not reduce the abnormal shift (Figure 6B). At 0° of flexion, the patella was 7.2 ± 4.6 mm, 8.9 ± 4.2 mm, and 9.2 ± 3.9 mm lateral to the knee center along the TEA of the femur in the healthy, ACL-deficient, and ACL- reconstructed knees, respectively.

Anterior cruciate ligament deficiency significantly changed the patellar rotation at 15° of knee flexion, and ACL reconstruction was unable to restore the values to normal (Figure 6C). In the ACL-deficient knee, the patella was approximately 2° more valgusly rotated. Anterior cruciate ligament reconstruction was not only unable to restore the normal rotation pattern of the patella but actually further increased the valgus rotation between 0° and 30° of knee flexion.

The effect of ACL deficiency was more pronounced on the patellar tilt (Figure 6D). Between 0° and 60° of knee flex- ion, ACL deficiency increased the lateral tilt of the patella by nearly 5°. The maximum effect of ACL deficiency occurred at 0° of knee flexion; the lateral tilt increased from 2.2° ± 6.0° to 7.4° ± 3.4° after ACL deficiency. Reconstruction of the ACL did not have an effect on the abnormal tilt of the patella, as there was no significant difference in tilt detected between the ACL-deficient and reconstructed knees. At 0° of knee flexion, the patella was 7.0° ± 3.5° tilted in the ACL-reconstructed knees.

Patellofemoral Cartilage Contact Points

We did not observe any contact between the femoral and patellar cartilage in the healthy, ACL-deficient, and ACL-reconstructed knees at 0° of knee flexion. Articular cartilage contact in the healthy knee moved from 5.3 ± 3.6 mm distal of the midline at 15° of knee flexion to 4.8 ± 4.4 mm proximal of the midline at 90° of knee flexion (Figure 7A) and was located along the vertical ridge (centerline) of the patellar surface (Figure 7B).

Rupture of the ACL caused a significant proximal and lateral shift of the cartilage contact between 15° and 90° of flexion. On average, the contact point location in the ACL-deficient knees was 4.8 mm more proximal than in the healthy knee joint (Figure 7A). The maximum effect was observed at 15° of flexion, at which ACL deficiency caused a 5.0 ± 3.9 mm proximal shift. The effect of ACL deficiency was more pronounced in the mediolateral direction (Figure 7B). A lateral shift of 6.5 ± 2.4 mm minimum (at 15° of flexion) to 7.2 ± 2.9 mm maximum (at 60° of flexion) was measured along the midline.

Reconstruction of the ACL reduced the abnormal contact location in the proximodistal direction, but a significant proximal shift remained compared with the intact knee, except at 90° (Figure 7A). Between 15° and 60° of knee flexion, a significant residual 2.5-mm

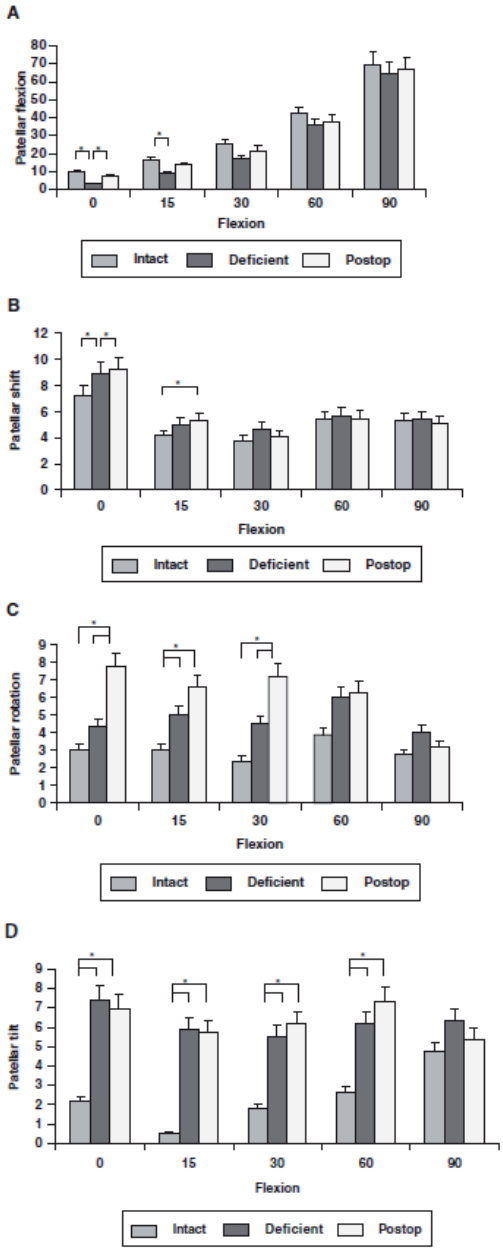

Figure 6. Patellar tracking. **A**, flexion; **B**, shift; **C**, rotation; and **D**, tilt of the patella as a function of knee flexion angle. Deficient, ACL-deficient knee; Intact, intact knee; Postop, postoperative ACL-reconstructed knee. Mean ± SD; **P* < .05.

proximal shift remained after ACL reconstruction. In the mediolateral direction, ACL reconstruction did not restore normal contact kinematics (Figure 7B). A lateral shift of minimum 6.5 ± 2.2 mm (at 15° of flexion) to maximum 8.1 ± 1.9 mm (at 30° of flexion) persisted along the midline.

DISCUSSION

We used a combined MR and dual-orthogonal fluoroscopic imaging technique to compare the 3D behavior of the patellar tendon, the patellofemoral kinematics, and the contact characteristics of the PFJ between the intact, ACL- injured, and ACL-reconstructed knees. Data were collected preoperatively and at 6 months after single-bundle ACL reconstruction with a BPTB autograft. The anterior laxity of the reconstructed knees as measured with the

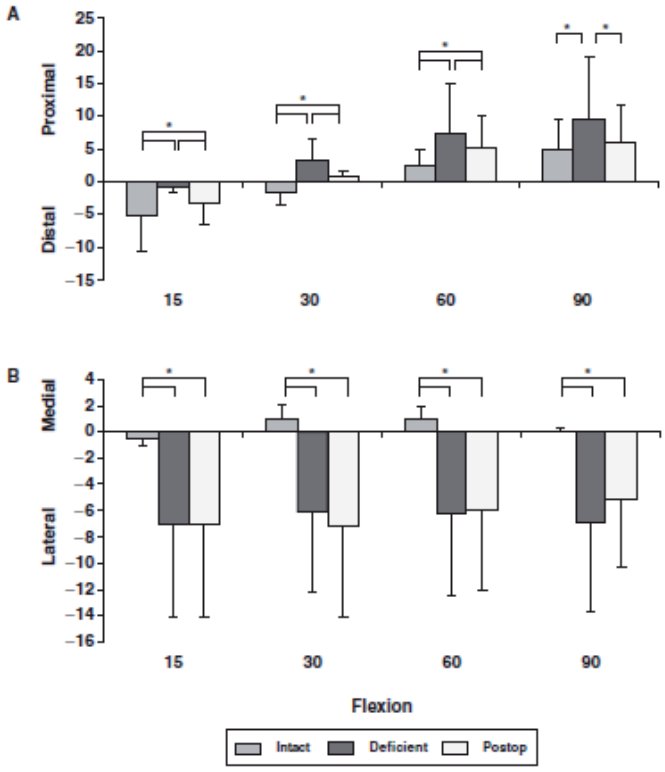

Figure 7. Patellofemoral cartilage contact points. Cartilage contact in the (**A**) proximodistal and (**B**) mediolateral direction as a function of knee flexion angle. Deficient, ACL-deficient knee; Intact, intact knee; Postop, postoperative ACL-reconstructed knee. Mean ± SD; *$P <$ .05.

KT-1000 arthrometer was similar to that of the intact contralateral knee.

Anterior cruciate ligament injury caused an increase in the apparent elongation of the patellar tendon. The increased apparent elongation of the patellar tendon in ACL-deficient knees could be responsible for the quadriceps muscle weakness associated with ACL injury. The patellar tendon length was found to influence considerably the mechanical behavior of the patellar articulation.[40] An increased length of the patellar tendon, an essential element of the knee extensor mechanism, implies an increase in quadriceps slack length, thus decreasing the quadriceps mechanical advantage.[14]

We found that ACL injury caused a decreased sagittal and coronal plane angle and an increased external twist. This altered orientation of the patellar tendon is understandable because the PFJ is not an isolated unit in the knee. Instead, a kinematic coupling exists between the patellofemoral and the tibiofemoral articulations, connected by the patellar tendon.[26] In the tibiofemoral joint of ACL-deficient patients, an increased anterior translation and internal rotation of the tibia[2,18,29,35] as well as an increased medial tibial translation[12] are observed. The increased anteroposterior tibial translation could explain the decreased sagittal plane angle, as the anterior tibial translation moves the tibial attachment of the patellar tendon forward, bringing the patellar tendon more parallel to the tibial shaft in the sagittal plane. Similarly, an increased medial tibial translation in ACL deficiency[12] will move the tibial attachment of the patellar tendon more medial relative to its patellar attachment, effectively reducing the angle between the patellar tendon and the tibia in the coronal plane. Finally, the increased internal rotation of the tibia that is observed in ACL deficiency could explain the increased twist of the patella that we found.

The abnormal orientation of the patellar tendon after ACL injury implies an alteration in patellar tracking, as the patellar tendon links the tibiofemoral joint and the PFJ. This investigation has demonstrated that ACL injury decreased the flexion and increased the valgus rotation and lateral tilt of the patella. Furthermore, the patella in ACL-deficient knees shifted significantly more laterally at 0° of knee flexion. These findings are consistent with the in vitro study results obtained by Hsieh et al,[20] in which they showed that excision of the ACL resulted in increases in lateral patellar tilt and in lateral patellar shift.20 An alteration in patellar tracking after ACL injury would be expected to lead to changes in patellofemoral articular contact biomechanics.

Because of the high congruency of the PFJ, small changes in patellar tracking were expected to result in major changes in patellofemoral contact characteristics. Indeed, we found that rupture of the ACL caused a significant proximal and lateral shift of the articular cartilage contact on the patellar cartilage surface. A proximal shift in articular cartilage contact could be explained by the decreased patellar flexion. The lateral patellar shift and increased lateral tilt of the patella could be responsible for the large lateral shift in cartilage contact and may help to explain the onset of anterior knee pain in patients with ACL

deficiency. It is interesting to note that the lateral shift in cartilage contact was more pronounced than was the proximal shift. This finding can be attributed to the geometry of the femoral trochlear groove and articular surface of the patella. Study of our MRIs showed that the vertical ridge of the patella had thicker cartilage than that of the medial and lateral aspect of the patellar cartilage surface. In the healthy knee, cartilage contact occurred along this vertical ridge of the patellar cartilage surface. This is consistent with the cartilage contact characteristics of the tibiofemoral joint, in which it was found that cartilage is up to 50% thicker in regions where cartilage-to-cartilage contact is present.[6,27] Healthy cartilage adapts to mechanical stimuli[3,37] and ultimately becomes dependent on the maintenance of the mechanical stimulus for normal tissue function.[9] The thicker cartilage within the cartilage-to-cartilage contact area may result in a reduced contact stress, as was demonstrated by a 3D finite element analysis suggesting that thicker cartilage bears a lower peak contact stress than does thinner cartilage under the same loading conditions.[24] A subtle change in patellar tracking will create a large shift in cartilage contact, moving the articular loading away from the vertical ridge toward the lateral aspect of the patellar cartilage. This abnormal loading of unconditioned PFJ chondrocytes might predispose the patellofemoral cartilage to degenerative changes associated with ACL injury. Future studies will follow up the patients to examine the correlation between cartilage degeneration and changes in PFJ contact kinematics.

Anterior cruciate ligament reconstruction reduced the abnormal apparent elongation and sagittal plane angle of the patellar tendon. Furthermore, ACL reconstruction restored the patellar flexion and proximal shift in contact. These findings suggest that there might be an improvement in anteroposterior tibiofemoral stability after reconstruction. In our previous study of tibiofemoral kinematics after ACL reconstruction that included the patients of this study,[34] the anterior laxity of the reconstructed knee as measured with the arthrometer was similar to that of the intact contralateral knee. Once the anteroposterior knee stability is improved, the tibial tubercle moves more posteriorly relative to the patellar apex, returning the sagittal plane angle to a level similar to that of the healthy knee. A restored sagittal plane angle will reduce the abnormal patellar flexion, as the inferior pole of the patella is no longer pulled anteriorly relative to the femur. Once the patellar flexion is normalized, the cartilage contact in proximodistal direction returns to normal.

However, the abnormal coronal plane angle and twist of the patellar tendon persisted after ACL reconstruction. As the patellar tendon links the tibiofemoral joint and the PFJ, it was not surprising to find that the persistent abnormal coronal plane angle and twist of the patellar tendon that were observed in ACL-reconstructed knees resulted in abnormal patellar rotation and tilt after the reconstruction. Consequently, the lateral shift in cartilage contact that was detected in ACL-deficient knees did not improve after ACL reconstruction. These findings demonstrate that the surgical reconstruction of the ACL does not restore the rotational stability of the knee, as the coronal plane angle and twist of the patellar tendon

are likely a function of tibiofemoral rotation. This persistent abnormal motion of the PFJ might predispose the patellofemoral cartilage to degenerative changes and may explain the onset of patellofemoral pain after reconstruction. Our observations differ somewhat from the study by Hsieh et al,[21] which demonstrated that intra-articular reconstruction of the ACL completely returned the normal PFJ contact characteristics. The difference between the data might be owing to the differences between the in vitro and in vivo loading conditions applied in the studies. During the in vivo knee function, the quadriceps and hamstring forces may be higher and more complicated than are the simulated muscle loads.

Our study has several limitations. We measured only 1 functional activity, namely a single-leg lunge, using a goniometer to control the flexion angle. Other in vivo activities such as walking, running, and stair climbing should be considered in future studies. This study evaluated the PFJ only at 6 months after surgery. In the future, patients should be followed up at various time intervals to investigate the change in kinematics over time. This might also provide insight into the relationship between altered joint behavior and joint degeneration. In addition, this study approximated the function of the patellar tendon using 3 straight lines. However, these lines did not penetrate into the tibia, and the differences in deformations between the 3 regions were relatively small, indicating a relatively uniform deformation of the patellar tendon. In addition, the unstrained (reference) length of the patellar tendon was not known, so it is difficult to quantify the strains experienced by the patellar tendon from these data. Furthermore, this study did not measure the ground reaction force. Future studies should incorporate a load cell into the system, so that the moment applied to the joint might be estimated. The cartilage contact position was determined as the centroid of the intersection area formed by the tibial and femoral cartilage surfaces. Cartilage deformation was not considered during calculation of the contact point. We included some patients who had partial tears of the lateral meniscus. Therefore, the explanation of our data should be based on the patient condition as indicated in the Materials and Methods section. Eight patients were investigated in this study. A larger patient population should be included in future studies, so that the effects of various combined meniscal injuries and ACL reconstruction on the PFJ function can be investigated.

In conclusion, we found that the altered tibiofemoral joint kinematics associated with ACL injury changed the apparent elongation and orientation of the patellar tendon. The disturbed function of the patellar tendon corresponded to an altered patellar tracking and patellofemoral cartilage contact. Anterior cruciate ligament reconstruction reduced the abnormal apparent elongation and abnormal orientation of the patellar tendon in the sagittal plane, as well as the abnormal patellar flexion and the superior shift in cartilage contact. These findings imply that ACL reconstruction improved the PFJ function. However, the abnormal orientation in the coronal plane and twist of the patellar tendon, as well as the abnormal patellar rotation, tilt, and lateral shift in PFJ cartilage contact, demonstrate that

ACL reconstruction did not fully restore the rotational stability of the knee. This abnormal loading of the PFJ may predispose the patellofemoral cartilage to degenerative changes associated with ACL injury and might help to explain the onset of patellofemoral pain after reconstruction, even if the ACL is reconstructed in a way that restores the clinical anteroposterior stability of the knee.

REFERENCES

1. Aglietti P, Giron F, Buzzi R, Biddau F, Sasso F. Anterior cruciate ligament reconstruction: bone–patellar tendon–bone compared with double semi-tendinosus and gracilis tendon grafts. A prospective, randomized clinical trial. J Bone Joint Surg Am. 2004;86(10):2143-2155.
2. Andriacchi TP, Dyrby CO. Interactions between kinematics and loading during walking for the normal and ACL deficient knee. J Biomech. 2005;38(2):293-298.
3. Arokoski JP, Jurvelin JS, Vaatainen U, Helminen HJ. Normal and pathological adaptations of articular cartilage to joint loading. Scand J Med Sci Sports. 2000;10(4):186-198.
4. Asano H, Muneta T, Shinomiya K. Evaluation of clinical factors affecting knee pain after anterior cruciate ligament reconstruction. J Knee Surg. 2002;15(1):23-28.
5. Baugher WH, Warren RF, Marshall JL, Joseph A. Quadriceps atrophy in the anterior cruciate insufficient knee. Am J Sports Med. 1984;12(3):192-195.
6. Bingham JT, Papannagari R, Gross C, et al. In-vivo cartilage contact deformation in the healthy human tibiofemoral joint. Osteoarthritis Cartilage. In press.
7. Bonamo JJ, Fay C, Firestone T. The conservative treatment of the anterior cruciate deficient knee. Am J Sports Med. 1990;18(6):618-623.
8. Bull AM, Katchburian MV, Shih YF, Amis AA. Standardisation of the description of patellofemoral motion and comparison between different techniques. Knee Surg Sports Traumatol Arthrosc. 2002;10(3):184-193.
9. Carter DR, Beaupre GS, Wong M, Smith RL, Andriacchi TP, Schurman DJ. The mechanobiology of articular cartilage development and degeneration. Clin Orthop Relat Res. 2004;427(suppl):S69-S77.
10. Corry IS, Webb JM, Clingeleffer AJ, Pinczewski LA. Arthroscopic reconstruction of the anterior cruciate ligament: a comparison of patellar tendon autograft and four-strand hamstring tendon autograft. Am J Sports Med. 1999;27(4):444-454.
11. Defrate LE, Nha KW, Papannagari R, Moses JM, Gill TJ, Li G. The bio- mechanical function of the patellar tendon during in-vivo weight- bearing flexion. J Biomech. 2007;40(8):1716-1722.
12. Defrate LE, Papannagari R, Gill TJ, Moses JM, Pathare NP, Li G. The 6 degrees of freedom kinematics of the knee after anterior cruciate ligament deficiency: an in vivo imaging analysis. Am J Sports Med. 2006;34(8):1240-1246.
13. DeFrate LE, Sun H, Gill TJ, Rubash HE, Li G. In vivo tibiofemoral con- tact analysis using 3D MRI-based knee models. J Biomech. 2004;37(10):1499-1504.
14. Draganich LF, Andriacchi TP, Andersson GB. Interaction between intrinsic knee mechanics and the knee extensor mechanism. J Orthop Res. 1987;5(4):539-547.
15. Feller JA, Webster KE. A randomized comparison of patellar tendon and hamstring tendon anterior cruciate ligament reconstruction. Am J Sports Med. 2003;31(4):564-573.

16. Fox JA, Nedeff DD, Bach BR Jr, Spindler KP. Anterior cruciate ligament reconstruction with patellar autograft tendon. Clin Orthop Relat Res. 2002;402:53-63.

17. Freedman KB, D'Amato MJ, Nedeff DD, Kaz A, Bach BR Jr. Arthroscopic anterior cruciate ligament reconstruction: a meta-analysis comparing patellar tendon and hamstring tendon autografts. Am J Sports Med. 2003;31(1):2-11.

18. Georgoulis AD, Papadonikolakis A, Papageorgiou CD, Mitsou A, Stergiou N. Three-dimensional tibiofemoral kinematics of the anterior cruciate ligament–deficient and reconstructed knee during walking. Am J Sports Med. 2003;31(1):75-79.

19. Grood ES, Suntay WJ. A joint coordinate system for the clinical description of three-dimensional motions: application to the knee. J Biomech Eng. 1983;105(2):136-144.

20. Hsieh YF, Draganich LF, Ho SH, Reider B. The effects of removal and reconstruction of the anterior cruciate ligament on patellofemoral kinematics. Am J Sports Med. 1998;26(2):201-209.

21. Hsieh YF, Draganich LF, Ho SH, Reider B. The effects of removal and reconstruction of the anterior cruciate ligament on the contact characteristics of the patellofemoral joint. Am J Sports Med. 2002;30(1):121-127.

22. Li G, DeFrate LE, Park SE, Gill TJ, Rubash HE. In vivo articular cartilage contact kinematics of the knee: an investigation using dual- orthogonal fluoroscopy and magnetic resonance image–based computer models. Am J Sports Med. 2005;33(1):102-107.

23. Li G, DeFrate LE, Sun H, Gill TJ. In vivo elongation of the anterior cruciate ligament and posterior cruciate ligament during knee flexion. Am J Sports Med. 2004;32(6):1415-1420.

24. Li G, Lopez O, Rubash H. Variability of a three-dimensional finite element model constructed using magnetic resonance images of a knee for joint contact stress analysis. J Biomech Eng. 2001;123(4): 341-346.

25. Li G, Moses JM, Papannagari R, Pathare NP, DeFrate LE, Gill TJ. Anterior cruciate ligament deficiency alters the in vivo motion of the tibiofemoral cartilage contact points in both the anteroposterior and mediolateral directions. J Bone Joint Surg Am. 2006;88(8):1826-1834.

26. Li G, Papannagari R, Nha KW, DeFrate LE, Gill TJ, Rubash HE. The coupled motion of the femur and patella during in-vivo weightbearing knee flexion. J Biomech Eng. 2007;129(6):937.

27. Li G, Park SE, DeFrate LE, et al. The cartilage thickness distribution in the tibiofemoral joint and its correlation with cartilage-to-cartilage contact. Clin Biomech (Bristol, Avon). 2005;20(7):736-744.

28. Li G, Wuerz TH, DeFrate LE. Feasibility of using orthogonal fluoroscopic images to measure in vivo joint kinematics. J Biomech Eng. 2004;126(2):314-318.

29. Logan M, Dunstan E, Robinson J, Williams A, Gedroyc W, Freeman M. Tibiofemoral kinematics of the anterior cruciate ligament (ACL)–deficient weightbearing, living knee employing vertical access open "interventional" multiple resonance imaging. Am J Sports Med. 2004;32(3):720-726.

30. Matsumoto A, Yoshiya S, Muratsu H, et al. A comparison of bone–patellar tendon–bone and bone–hamstring tendon–bone auto- grafts for anterior cruciate ligament reconstruction. Am J Sports Med. 2006;34(2):213-219.

31. Most E, Axe J, Rubash H, Li G. Sensitivity of the knee joint kinematics calculation to selection of flexion axes. J Biomech. 2004;37(11): 1743-1748.

32. Murrell GA, Maddali S, Horovitz L, Oakley SP, Warren RF. The effects of time course after anterior cruciate ligament injury in correlation with meniscal and cartilage loss. Am J Sports Med. 2001;29(1):9-14.

33. Nha KW, Papannagari R, Gill TJ, et al. In-vivo patellar tracking: clinical motions and patellofemoral indices. J Orthop Res. In press.

34. Papannagari R, Gill TJ, Defrate LE, Moses JM, Petruska AJ, Li G. In vivo kinematics of the knee after anterior cruciate ligament reconstruction: a clinical and functional evaluation. Am J Sports Med. 2006;34(12):2006-2012.

35. Ristanis S, Giakas G, Papageorgiou CD, Moraiti T, Stergiou N, Georgoulis AD. The effects of anterior cruciate ligament reconstruction on tibial rotation during pivoting after descending stairs. Knee Surg Sports Traumatol Arthrosc. 2003;11(6):360-365.

36. Sachs RA, Daniel DM, Stone ML, Garfein RF. Patellofemoral problems after anterior cruciate ligament reconstruction. Am J Sports Med. 1989;17(6):760-765.

37. Smith RL, Donlon BS, Gupta MK, et al. Effects of fluid-induced shear on articular chondrocyte morphology and metabolism in vitro. J Orthop Res. 1995;13(6):824-831.

38. Tsepis E, Vagenas G, Ristanis S, Georgoulis AD. Thigh muscle weak- ness in ACL-deficient knees persists without structured rehabilitation. Clin Orthop Relat Res. 2006;450:211-218.

39. Van de Velde SK, DeFrate LE, Gill TJ, Moses JM, Papannagari R, Li G. The effect of anterior cruciate ligament deficiency on the in vivo elongation of the medial and lateral collateral ligaments. Am J Sports Med. 2007;35(2):294-300.

40. van Eijden TM, Kouwenhoven E, Weijs WA. Mechanics of the patellar articulation: effects of patellar ligament length studied with a mathematical model. Acta Orthop Scand. 1987;58(5):560-566.

41. Wojtys EM, Huston LJ. Neuromuscular performance in normal and anterior cruciate ligament–deficient lower extremities. Am J Sports Med. 1994;22(1):89-104.

8

CHAPTER

Dual fluoroscopic analysis of the posterior cruciate ligament-deficient patellofemoral joint during lunge.

Samuel K. Van de Velde
Thomas J. Gill, IV
Guoan Li

Med Sci Sports Exerc. 2009 Jun;41(6):1198-205.

ABSTRACT

Purpose: To investigate the effect of posterior cruciate ligament (PCL) deficiency on the kinematics and the cartilage contact characteristics of the patellofemoral joint during an in vivo single-leg lunge.

Methods: Ten patients with an isolated PCL injury in one knee and the contralateral side intact participated in the study. Magnetic resonance and dual fluoroscopic imaging techniques were used to analyze the patellofemoral kinematics and cartilage contact of the intact and the PCL-deficient knee during a quasi-static single-leg lunge from 0 degrees to 120 degrees of flexion.

Results: PCL deficiency significantly changed the patellofemoral kinematics between 90 degrees and 120 degrees of knee flexion ($P < 0.007$): an increased patellar flexion angle by 10.7 degrees on average and a decreased lateral shift (on average -1.9 mm), patellar tilt (approximately -2.7 degrees), and valgus rotation (approximately -1.8 degrees) were observed in the PCL-deficient knee compared with the intact contralateral joint. The changes in patellofemoral kinematics resulted in significant changes in patellofemoral cartilage contact ($P < 0.007$). PCL deficiency caused a distal (approximately -3.3 mm) and medial (approximately + 2.7 mm) shift of cartilage contact from 75 degrees to 120 degrees of flexion.

Conclusion: The altered tibiofemoral kinematics that were previously described in PCL deficiency resulted in changes in patellofemoral joint function at flexion angles greater than 75 degrees. This abnormal loading of the patellofemoral joint might predispose the patellofemoral cartilage to degenerative changes. Because we did not detect differences in the patellofemoral joint behavior of the intact and the PCL-deficient knee between 0 degrees and 60 degrees of flexion, rehabilitation exercises might be safely performed in this range of flexion. On the other hand, repetitive deep knee squats should be avoided in PCL-deficient patients, so as not to excessively disturb the patellofemoral cartilage contact kinematics.

INTRODUCTION

The posterior displacement of the tibia that occurs after rupture of the posterior cruciate ligament (PCL) is associated with degeneration of both the patellofemoral and the medial tibiofemoral joint compartments.[7,28,35] Parolie and Bergfeld[33] reported on 25 patients with PCL injury that were treated conservatively at 6 years of follow-up. Patellofemoral symptoms were present in 12 patients (48%), medial joint line tenderness in 3 patients (12%), and radiographic evidence of osteoarthritis in 9 patients (36%) total, eight patients (32%) of the medial and four patients (16%) of the patellofemoral compartment. Clancy et al.[6] reported that 90% of patients with PCL injuries for longer than 4 years had grade 3 or 4 osteoarthritis of the medial femoral condyle, whereas only 31% of patients had preoperative radiographic changes. Dandy and Pusey[8] reported on 20 PCL-deficient patients treated nonoperatively after approximately 7 years. Fourteen patients (70%) continued to have pain while walking, 11 patients (55%) had patellofemoral symptoms, whereas 9 patients (45%) had episodic giving-way. Similarly, Boynton et al.[1] reported that 81% of patients with isolated PCL-deficient knees had at least occasional pain and 17 patients (56%) had at least occasional swelling at a mean follow-up of 13.4 years. Cross and Powell[7] evaluated 116 patients at a mean duration of follow-up of 5 years: 40% of their patients had patellofemoral symptoms, whereas 20% had osteoarthritis of the medial compartment.

For the last three decades, most research on PCL deficiency has been directed predominantly at the tibiofemoral joint. This focus is comprehensible because restraining posterior tibial translation is the primary function of the PCL in the intact knee.[3] Both in vitro and in vivo studies have documented an increased posterior tibial translation[3,5,12,15,16,25,27,31,32,34] as well as an increased external tibial rotation[16,21,24] and lateral translation[25] of the tibia after rupture of the PCL. In our recent in vivo study of 14 PCL-deficient patients, we found that these altered tibiofemoral kinematics in PCL deficiency resulted in a shift of the normal tibiofemoral contact location with a subsequent increase in cartilage deformation in the medial compartment, providing a possible explanation for the medial joint compartment cartilage degeneration.[38]

In contrast, little is known about the patellofemoral joint in PCL deficiency. In vitro studies by Skyhar et al.[37] and Gill et al.[13] found that sectioning of the PCL in cadaveric studies resulted in elevated patellofemoral contact pressures. However, to our knowledge, no data have been reported on the patellofemoral joint function in PCL deficiency under in vivo weight-bearing conditions. This knowledge could be used to provide a scientific insight in the possible pathogenesis of patellofemoral complications after injury to the PCL and to formulate concrete guidelines for the development of potentially safer rehabilitation regimens for PCL-deficient patients after surgical or conservative treatment.

In this study, we hypothesized that PCL deficiency changes the patellofemoral kinematics and, subsequently, the cartilage contact point location of the patellofemoral joint. The objective of this study was to investigate the effects of PCL deficiency on the kinematics (patellar flexion, shift, tilt, and rotation) and the contact characteristics of the patellofemoral joint during an in vivo weight-bearing activity using the combined dual-orthogonal fluoroscopic and magnetic resonance (MR) imaging technique.[30,39]

MATERIALS AND METHODS

Subject recruitment and exclusion criteria

Ten patients (average age = 34 ± 14 years, age range = 19–51 years; average weight = 80 ± 12 kg, weight range = 54–97 kg; average height = 173 ± 10 cm, height range = 165–180 cm; six males, four females; seven right injured knees, three left injured knees; active on a minimal to moderate athletic level before injury) with a PCL rupture documented by clinical examination (positive posterior drawer test measured by the senior author (TJG) and MR imaging were included in this study). The average time between injury and analysis was 4.9 ± 3 months. All subjects had healthy contralateral knees. Injury to other ligaments or capsule, noticeable cartilage lesions, meniscal injury requiring partial meniscectomy, and injury to the underlying bone were reasons for exclusion from the study. The 10 included patients were studied previously as part of a larger sample of 14 PCL-deficient patients for the analysis of tibiofemoral cartilage deformation in PCL deficiency.[38]

The purpose of the present study was explained in detail to all of the patients at the time of recruitment. Each patient signed a consent form that had been approved by our institutional review board.

MR imaging scan and three-dimensional knee model

With the patients supine and the knee in a relaxed, extended position, both the left and the right knee were imaged with an MR scanner using a 3-T magnet (Magnetom Trio®; Siemens, Erlangen, Germany) and a fat-suppressed three-dimensional (3D) spoiled gradient-recalled echo sequence. The MR scans spanned the medial and the lateral boundaries of the knee. Parallel sagittal and coronal plane images (resolution = 512 × 512 pixels) with a field of view of 16 × 16 cm and a spacing of 1 mm were taken. For each knee, the MR scanning time was approximately 12 min. These MR images were used to create 3D meshed models of the knees using a protocol established in our laboratory.[10] Each anatomic knee model included the bony geometry of the femur, the tibia, the fibula, and the patella as well as the patellar and the femoral cartilage layers (Fig. 1A).

Dual fluoroscopic imaging of the knee during a weight-bearing activity

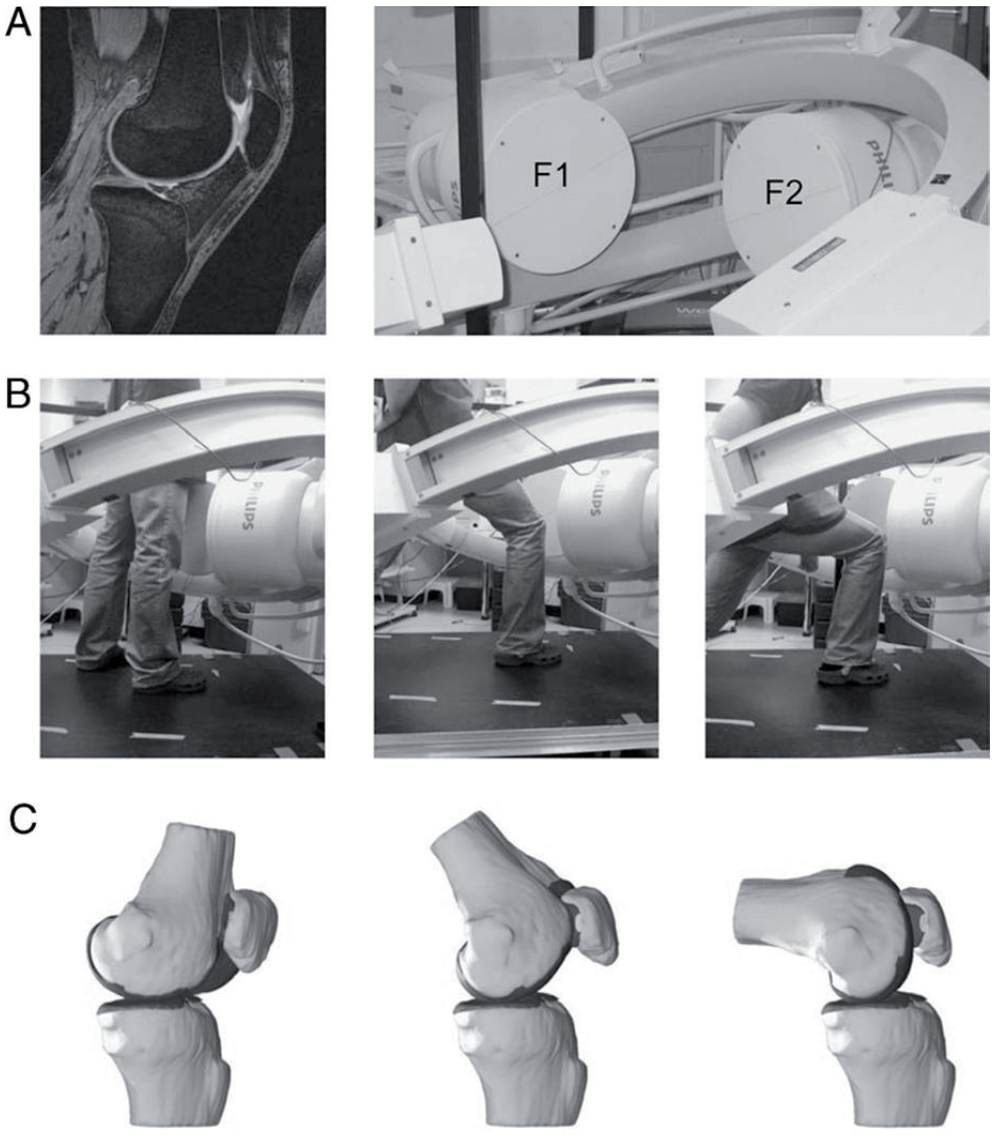

Figure 1. A, The combined MR and dual fluoroscopic imaging technique, in which 3D knee models are created from a series of sagittal MR images (image left), and the motion of the patient's tested knee is recorded using two orthogonally placed fluoroscopes (image right). **B**, In the present study, the tested activity was a single-leg quasi-static lunge at 0°, 30°, 60°, 75°, 90°, 105°, and 120° of flexion while the upper body remained upright (only three flexion angles are shown for illustrative purposes). **C**, The 3D meshed knee models and the series of dual fluoroscopic images were combined to reproduce the knee positions. F1, fluoroscope 1; F2, fluoroscope 2.

Both knees of each patient were simultaneously imaged using two orthogonally placed fluoroscopes (Fig. 1A; BV Pulsera; Philips, Eindhoven, The Netherlands) set to generate an 8-ms width x-ray pulses with a dose rate of 13 μGy per scanning as the patient performed a single-leg quasi-static lunge at 0°, 30°, 60°, 75°, 90°, 105°, and 120° of flexion while their upper body remained upright. Flexion angle of the knee was monitored using a handheld goniometer. The patient kept the knee stable for one second at each target flexion angle so that the fluoroscopes captured the knee position and then flexed the knee to the next target position. At each selected flexion angle, the patient supported his or her body weight on the leg being scanned while the other leg was used to help balance the body (Fig. 1B).

Measurement of in vivo knee kinematics using image-matching technique

The fluoroscopic images were imported into a solid modeling software (Rhinoceros; Robert McNeel and Associates, Seattle, WA) and placed in the orthogonal planes based on the

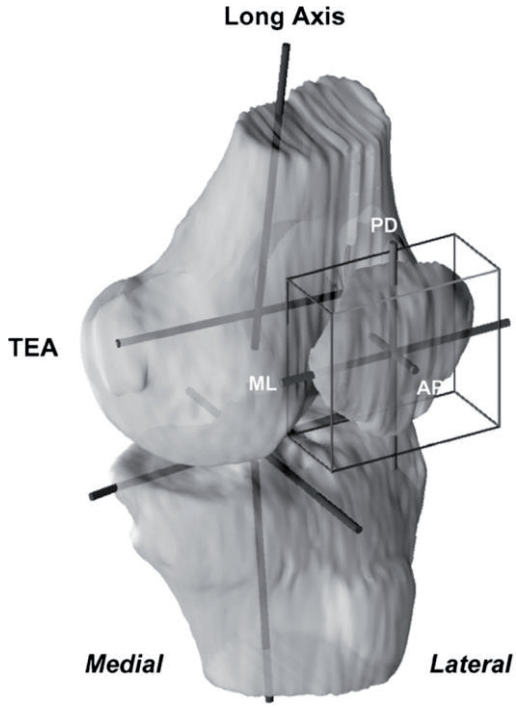

Figure 2. Coordinate systems used to quantify the patellofemoral kinematics. The femoral coordinate system consisted of the trans-epicondylar axis (TEA) and the long axis intersecting at the center of the knee joint (midpoint of TEA). A cuboid was enclosed around the patella to determine the patellar center. The patellar coordinate system consisted of the proximodistal (PD), the anteroposterior (AP), and the mediolateral (ML) axes.

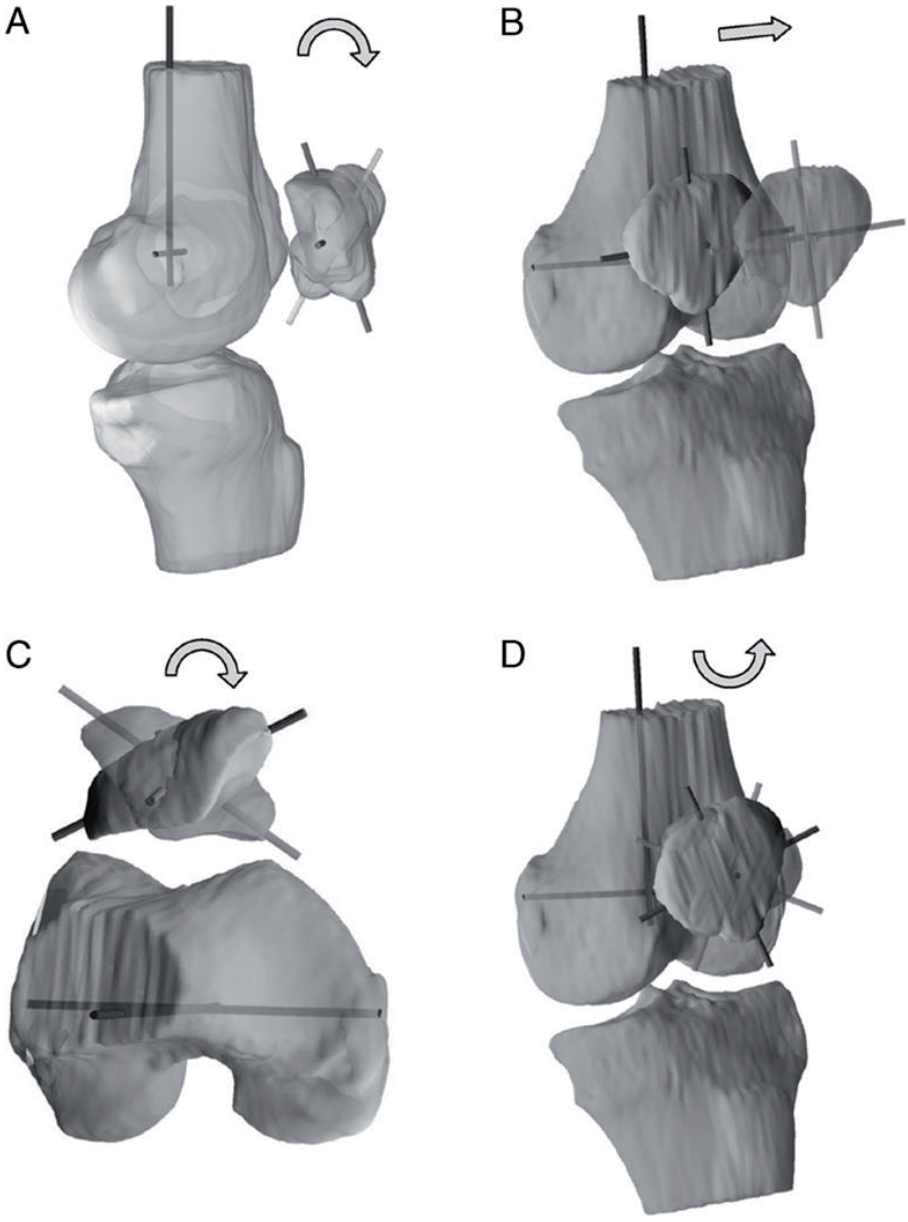

Figure 3. The definition of patellofemoral kinematics, illustrated on a left knee model. Patellar flexion in sagittal view (**A**), patellar shift in coronal view (**B**), patellar tilt in axial view (**C**), and patellar rotation in coronal view (**D**). The arrows indicate the direction of positive value.

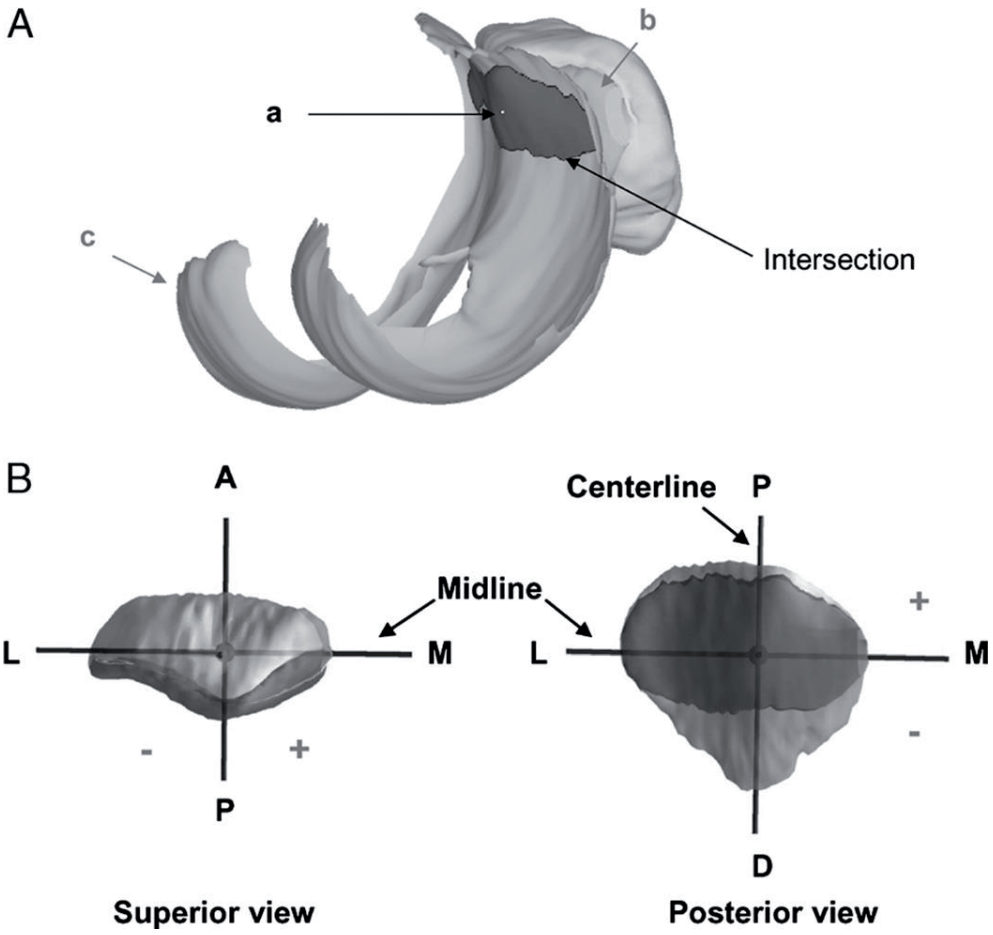

Figure 4. A, The centroid (a) of the intersection of the patellar (b) and femoral (**c**) cartilage was used to determine the patellofemoral contact locations. **B**, The coordinate system on the patellar cartilage surface for patellofemoral cartilage contact analysis. The proximal (P)–distal (D) axis was called the centerline. The medial (M)–lateral (L) axis was called the midline. Contact proximal to the midline and medial to the centerline was positive. Reprinted with permission from Van de Velde et al. *Am J Sports Med*. 2008 Jun;36(6):1150–9.

position of the fluoroscopes during the imaging of the patient. In the following step, the 3D MR image-based knee model of the patient was imported into the same software, viewed from the two orthogonal directions corresponding to the orthogonal fluoroscopic setup used to acquire the images, and manually manipulated in six degrees of freedom inside the software until the projections of the model matched the outlines of the fluoroscopic images.

When the projections matched the outlines of the images taken during in vivo knee flexion, the model reproduced the in vivo position of the knee (Fig. 1C). MR and dual fluoroscopic imaging techniques have been described in detail in previous publications. This system has an error of less than 0.1 mm and 0.3° in measuring tibiofemoral joint translations and rotations, respectively.[10] The procedure was further validated for measuring the patellofemoral kinematics. The methodology has an error of less than 0.1 ± 0.2 mm in measuring patellar shift and 0.1° ± 0.2° in patellar tilt.[30]

Description of patellofemoral kinematics

After reproducing the in vivo knee positions along the flexion path, the patellofemoral kinematics were measured from the series of knee models.[30,39] A joint coordinate system[17] was established for each knee to describe the motion of the patella (Fig. 2). Two axes were drawn on the femur: the long axis along the posterior femoral shaft surface in sagittal plane and the transepicondylar axis (TEA) connecting the epicondyle extremes of the medial and the lateral femoral condyles.[29] The knee center was defined as the midpoint of the TEA. An axis parallel to the posterior wall of the tibial shaft was defined as the long axis of the tibia. The flexion angle of the knee was defined as the angle between the long axes of the femur and the tibia in sagittal plane. To reduce the variability in creating patellar coordinate systems, a cuboid was used to enclose the patella so that it touched the proximodistal, the anteroposterior, and the mediolateral borders of the patella.[26,30] The center of the cuboid was defined as origin of the patella. The long axis of the patella was defined as the line along the superior-inferior direction.

Patellar flexion was defined as the rotation of the patella about the TEA of the femur (Fig. 3A).[2] Patellar shift was defined as the medial or the lateral movement of the center of the patella along the TEA of the femur (Fig. 3B). A positive shift corresponded to the lateral movement of the patellar center with respect to the knee center along the TEA of the femur. Patellar tilt was defined as the rotation of the patella about the long axis of the femur, where lateral tilt followed the direction of external femoral rotation (Fig. 3C). Patellar rotation is the rotation of the patella about the anteroposterior axis of the femur, where valgus rotation follows the direction of valgus rotation in tibiofemoral motion (Fig. 3D), that is, an outward angulation of the distal segment of the patella. In this fashion, the patellofemoral kinematics were quantified for each subject as a function of flexion of the knee.

Description of patellofemoral cartilage contact points

The contact points on the patellar cartilage were calculated by finding the centroid of the intersection of the patellar and the femoral cartilage layers.[11,20,23,39] From the series of models used to reproduce knee motion, the relative positions of the cartilage layers on the femur and patella were determined. The overlap of the two cartilage layers was used to approximate the cartilage contact area (Fig. 4A). The solid modeling software automatically outlined the intersection of the patellar and the femoral cartilage layers and calculated the

centroid of the enclosed area. The centroid of this contact area was defined as the contact point. To describe the motion of the cartilage contact points, a coordinate system was created on the surface of the patella (Fig. 4B). The center of the vertical ridge of the patella was the origin of the coordinate system. In this coordinate system, the proximodistal axis was called the centerline, and the mediolateral axis was called the midline. In the proximodistal direction, the contact point was positive if it was proximal to the midline and negative if it was distal to the midline. In the mediolateral direction, a contact point was positive if it was on the medial side of the centerline and negative if it was on the lateral side of the centerline.

Statistical methods

At each flexion angle, the Wilcoxon signed rank test was used to compare the patellofemoral joint function (patellar flexion, shift, tilt, rotation, and position of the patellofemoral contact points on the patellar cartilage) of the PCL-deficient and intact (contralateral) knees. A Bonferroni correction factor (1/7) was used to account for multiple comparisons (at seven flexion angles). Differences at each flexion angle between the PCL-deficient and the intact knees were considered significant for $P < 0.007$.

RESULTS

Patellofemoral kinematics

Between 90° and 120° of flexion, PCL deficiency increased the patellar flexion angle by 10.7° on average (Fig. 5A). The maximum difference occurred at 90° (intact knee = 65.2° ± 8.1°, PCL-deficient knee = 79.5° ± 6.1°, $P < 0.001$).

The patella in PCL-deficient knees shifted significantly less laterally between 90° and 120° of knee flexion (Fig. 5B; $P < 0.007$). In the PCL-deficient knee, the patella was on average 1.9 mm less lateral to the knee center along the TEA compared with the healthy knee between 90° and 120° of knee flexion, with a maximum difference occurring at 105° (intact knee = 8.2 ± 3.9 mm, PCL-deficient knee = 6.2 ± 2.4 mm, $P < 0.007$).

Between 90° and 120° of knee flexion, PCL deficiency significantly decreased the lateral tilt of the patella by nearly 2.7° (Fig. 5C; $P < 0.007$). The maximum effect of PCL deficiency occurred at 120° of knee flexion: the lateral tilt decreased from 5.1° ± 2.7° to 1.9° ± 2.6° after PCL deficiency ($P < 0.001$).

PCL deficiency significantly changed the patellar rotation between 90° and 120° of knee flexion (Fig. 5D; $P < 0.007$). In the PCL-deficient knee, the patella was approximately 1.8° less valgusly rotated between 90° and 120° of knee flexion.

Patellofemoral cartilage contact point location

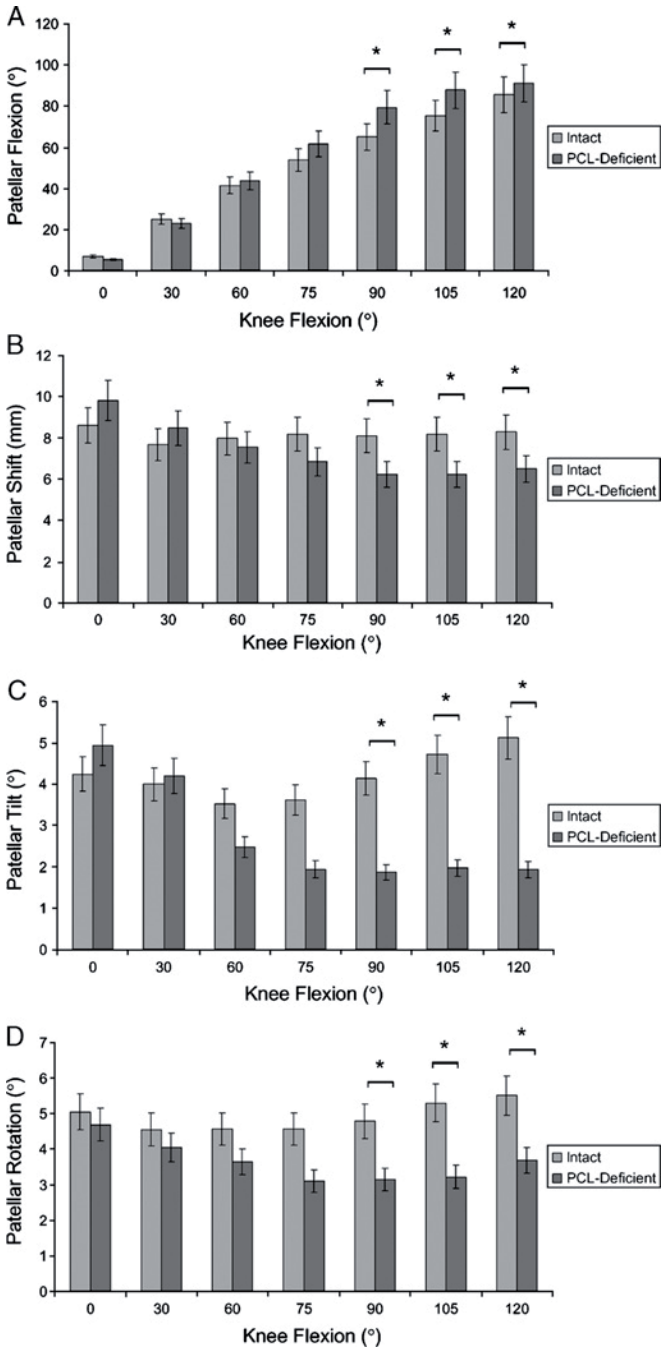

Figure 5. Patellofemoral kinematics. Patellar flexion (**A**), patellar shift (**B**), patellar tilt (**C**), and patellar rotation (**D**) as a function of knee flexion angle (mean ± SD; **P* values <0.007 determined with the Wilcoxon signed rank test).

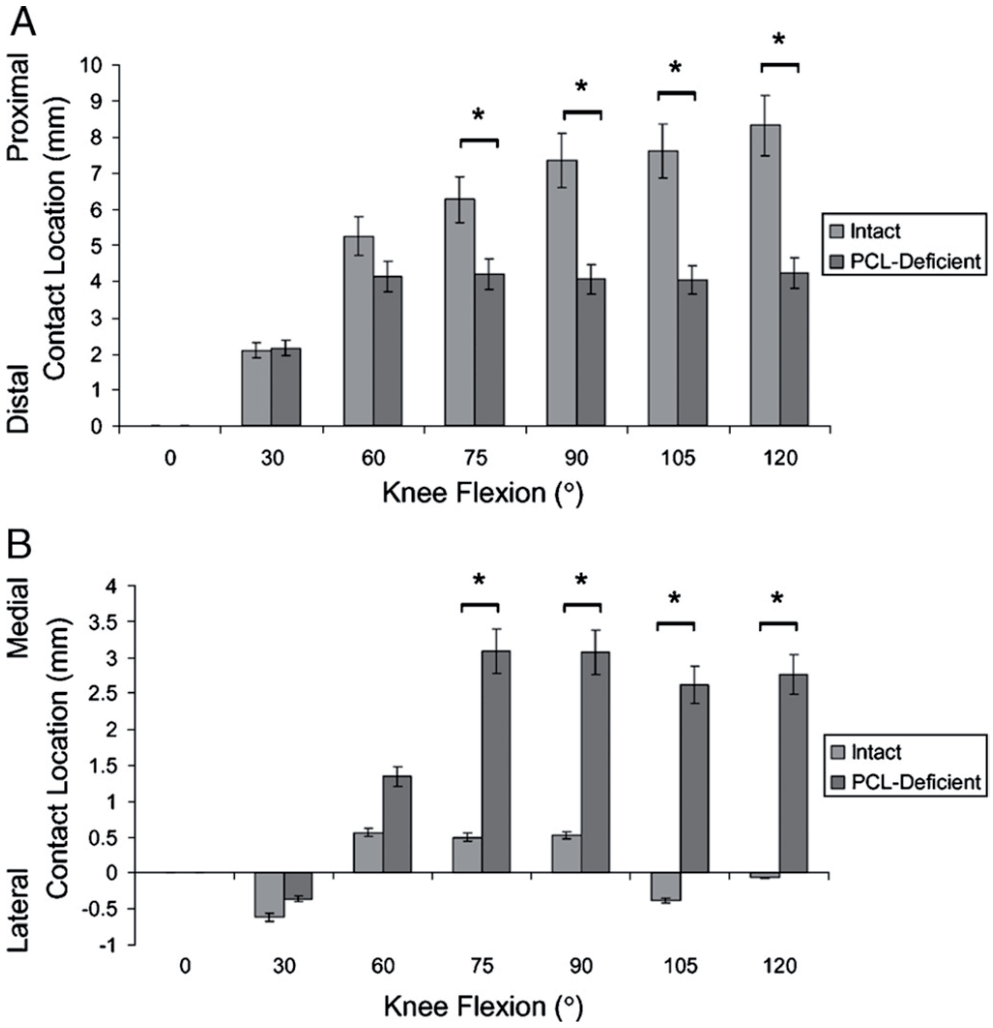

Figure 6. Location of patellofemoral cartilage contact on the patellar surface. Cartilage contact in the proximodistal (**A**) and the mediolateral (**B**) direction as a function of knee flexion angle (mean ± SD; **P* values <0.007 determined with the Wilcoxon signed rank test).

We did not observe any contact between the femoral and the patellar cartilage in the healthy and the PCL-deficient knees at 0° of knee flexion. At 30° of knee flexion, the patellofemoral cartilage contact point on the patellar cartilage surface was 2.1 ± 1.0 and 2.2 ± 1.4 mm proximal to the midline in the healthy and the PCL-deficient knee, respectively ($P = 0.75$), and was 0.6 ± 1.4 and 0.4 ± 1.3 mm lateral from the centerline in the healthy and the PCL-deficient knee, respectively ($P = 0.52$). At 60° of knee flexion, the

patellofemoral cartilage contact point on the patellar cartilage surface was 5.3 ± 1.6 and 4.1 ± 1.3 mm proximal to the midline in the healthy and the PCL-deficient knee, respectively ($P = 0.04$), and was 0.6 ± 1.0 and 1.3 ± 1.1 mm medial from the centerline in the healthy and the PCL-deficient knee, respectively ($P = 0.02$).

Between 75° and 120° of knee flexion, PCL deficiency caused a significant distal and medial shift of patellofemoral cartilage contact point location (Fig. 6; $P < 0.007$). Articular cartilage contact in the healthy knee moved along the centerline from 6.3 ± 1.7 mm proximal to the midline at 75° of knee flexion to 8.3± 1.3 mm proximal to the midline at 120° of knee flexion. In PCL deficiency, the patellofemoral contact point on the patellar cartilage surface remained in the same region, approximately 2.9 mm medial to the centerline and 4.1 mm proximal to the midline between 60° and 120° of knee flexion. The maximum difference between the healthy and the PCL-deficient knee was observed at 120° of knee flexion in the proximodistal direction (intact knee = 8.3 ± 1.3 mm, PCL-deficient knee = 4.2 ± 1.7 mm, $P < 0.001$; Fig. 6A) and at 105° of knee flexion in the mediolateral direction (intact knee = −0.4 ± 0.7 mm, PCL-deficient knee = 2.6 ± 1.7 mm, $P < 0.001$; Fig. 6B).

DISCUSSION

An increased prevalence of quadriceps weakness and atrophy, patellofemoral crepitus, and degeneration of the patellofemoral joint cartilage has been described in PCL-deficient patients.[1,19,36] In the present study, we found that PCL deficiency increased the patellar flexion angle and decreased the lateral shift, tilt, and valgus rotation of the patella at flexion angles 90° and greater. Due to the congruency of the patellofemoral joint, these changes in patellofemoral kinematics resulted in changes in the location of the patellofemoral cartilage contact point. PCL deficiency caused a distal and medial shift of cartilage contact point from 75° to 120° of flexion.

It is challenging to formulate an explanation for the observed changes in patellofemoral kinematics after rupture of the PCL due to the complex interaction of muscle loading patterns, ligament and capsule deformation, and contact stress distribution on articular cartilage that occurs during in vivo weight-bearing knee flexion to stabilize the patella within the femoral trochlea. It was brought to our attention in response to our study of the patellofemoral joint in anterior cruciate ligament deficiency[39] that the abnormal patellofemoral kinematics could in theory be attributed to changes in neuromuscular stabilization resulting in atrophy of the quadriceps, hereby altering the normal patellar tracking (Daniel Walz, M.D., personal communication, University Clinic München). Others have suggested that the degeneration of the patellofemoral joint cartilage is the result of an increased quadriceps activity and concomitant increased patellofemoral pressures as a compensation for the increased posterior tibial translation.[4,7] On the basis our own analysis

of the in vivo knee joints,[26] we found that a kinematic coupling exist between the tibiofemoral and the patellofemoral joint, and consequently that tibiofemoral changes should be considered when investigating patellar pathologies.[26] In the tibiofemoral joint of PCL-deficient patients, an increased posterior tibial translation as well as an increased external tibial rotation[16,21,24] and lateral translation[25] has been documented. Because the effect of tibiofemoral kinematic changes on patellofemoral kinematics is likely combined, isolating a particular tibial translation or rotation to a corresponding patellofemoral degree-of-freedom is difficult. Nevertheless, the increased posterior tibial translation could potentially explain the increased patellar flexion angle and subsequent distal shift in patellofemoral cartilage contact by moving the tibial tubercle more posteriorly and increasing the angle between the patellar tendon and the tibia in the sagittal plane. Conversely, the increased external tibial rotation observed in PCL deficiency would theoretically decrease the normal patellar tendon twist,[9] explaining the decreased patellar tilt observed in the present study. The increased lateral translation of the tibia after PCL injury would move the tibial attachment of the patellar tendon more laterally relative to its patellar attachment, effectively increasing the coronal plane angle of the patellar tendon[9] and pushing the patella medially. The combination of decreased lateral shift and tilt could explain the medial shift of cartilage contact point from 75° to 120° of flexion that was observed in PCL deficiency. The kinetic coupling between the tibiofemoral and the patellofemoral joints implies that the optimal treatment of PCL injury, either surgical or conservative, should ideally restore the normal tibiofemoral kinematics, hereby possibly normalizing the patellofemoral function and potentially preventing long-term patellofemoral complications.

In our present study, cartilage contact area and deformation were not considered during the calculation of the cartilage contact point, hereby impeding the calculation of contact pressure changes within the patellofemoral joint. Nevertheless, the documented changes in patellofemoral joint kinematics and cartilage contact after isolated rupture of the PCL might provide an insight in the possible pathogenesis of the patellofemoral complications observed in PCL deficiency. In the healthy knee joint, the cartilage contact point location occurred along the centerline, that is, the vertical ridge of the patella. Previous study showed that the vertical ridge of the patella had thicker cartilage than the medial and the lateral articulating aspect of the patellar cartilage surface.[39] The thicker cartilage within the normal cartilage-to-cartilage contact area may result in a reduced contact stress, as was demonstrated by a 3D finite element analysis, suggesting that thicker cartilage bears a lower peak contact stress than does thinner cartilage under the same loading conditions.[22] The abnormal shift of the cartilage contact point to thinner regions of patellar cartilage would therefore theoretically increase the peak contact stress in the patellofemoral joint, which is consistent with the elevated patellofemoral contact pressures that were found after sectioning of the PCL in cadaveric studies.[14,37]

When combining the present patellofemoral joint data with our previous analysis of the in vivo PCL function,[32] the tibiofemoral kinematics,[25] and the cartilage contact deformation in PCL deficiency,[38] it becomes apparent that a target range of motion could be formulated for PCL-deficient patients in which knee motion might be safely performed. During the single-leg lunge between 0°and 60° of knee flexion, we did not detect differences in either tibiofemoral or patellofemoral joint biomechanics of the intact and the PCL-deficient knee. Therefore, rehabilitation exercises might be safely performed in this range of flexion. On the other hand, repetitive deep knee squats should be avoided in PCL-deficient subjects, so as not to excessively alter normal patellofemoral cartilage loading. We would like to emphasize that the present findings were obtained during a quasi-static lunge activity. As most daily activities are dynamic, other in vivo activities such as walking, running, and stair climbing[18] should be considered in future studies to define the definite safe range of motion for PCL-deficient patients.

Our study has several limitations. As mentioned above, data were acquired during only one functional activity, namely, a single-leg lunge. Another limitation is that the patients were investigated at different time intervals from injury. Future studies should also follow PCL-deficient patients who are treated conservatively for longer periods using a methodology similar to that used in this study. The patellofemoral cartilage contact behavior and the health of the cartilage could therefore be monitored with time to quantify any possible biomechanical relationships. This study did not measure the ground reaction force. Future studies should incorporate a load cell into the system as well as a whole body motion analysis system to ensure that the performed functional activities are fully uniform among the tested limbs. The cartilage contact position was determined as the centroid of the intersection area formed by the patellar and femoral cartilage surfaces. Cartilage contact area and deformation were not considered during calculation of the contact point, impeding the calculation of contact pressure changes. Finally, the present analysis compared the patellofemoral joint function of the PCL-deficient and intact knees at each flexion angle, hereby ignoring potential interactions among the patellar rotational and the translational degrees of freedom and various knee flexion angles. Future research involving a larger study sample needs to be performed to confirm the present findings. Nonetheless, we believe that the current findings provided a comprehensible insight in the patellofemoral changes after injury of the PCL and identified important directions for future research.

In summary, the altered tibiofemoral kinematics that were previously described in PCL deficiency resulted in changes in patellofemoral joint kinematics and cartilage contact at flexion angles greater than 60°. This abnormal loading of the patellofemoral joint might predispose the patellofemoral cartilage to degenerative changes associated with PCL injury.

REFERENCES

1. Boynton MD, Tietjens BR. Long-term followup of the untreated isolated posterior cruciate ligament-deficient knee. Am J Sports Med. 1996;24(3):306–310.
2. Bull AM, Katchburian MV, Shih YF, Amis AA. Standardization of the description of patellofemoral motion and comparison between different techniques. Knee Surg Sports Traumatol Arthrosc. 2002;10(3):184–193.
3. Butler DL, Noyes FR, Grood ES. Ligamentous restraints to anterior-posterior drawer in the human knee. A biomechanical study. J Bone Joint Surg Am. 1980;62(2):259–270.
4. Cain TE, Schwab GH. Performance of an athlete with straight posterior knee instability. Am J Sports Med. 1981;9(4):203–208.
5. Carlin GJ, Livesay GA, Harner CD, Ishibashi Y, Kim HS, Woo SL. In-situ forces in the human posterior cruciate ligament in response to posterior tibial loading. Ann Biomed Eng. 1996;24(2):193–197.
6. Clancy WG, Jr., Shelbourne KD, Zoellner GB, Keene JS, Reider B, Rosenberg TD. Treatment of knee joint instability secondary to rupture of the posterior cruciate ligament. Report of a new procedure. J Bone Joint Surg Am. 1983;65(3):310–322.
7. Cross MJ, Powell JF. Long-term followup of posterior cruciate ligament rupture: a study of 116 cases. Am J Sports Med. 1984;12(4):292–297.
8. Dandy DJ, Pusey RJ. The long-term results of unrepaired tears of the posterior cruciate ligament. J Bone Joint Surg Br. 1982;64(1):92–94.
9. Defrate LE, Nha KW, Papannagari R, Moses JM, Gill TJ, Li G. The biomechanical function of the patellar tendon during in-vivo weight-bearing flexion. J Biomech. 2007;40(8):1716–1722.
10. Defrate LE, Papannagari R, Gill TJ, Moses JM, Pathare NP, Li G. The 6 degrees of freedom kinematics of the knee after anterior cruciate ligament deficiency: an in vivo imaging analysis. Am J Sports Med. 2006;34(8):1240–1246.
11. DeFrate LE, Sun H, Gill TJ, Rubash HE, Li G. In vivo tibiofemoral contact analysis using 3D MRI-based knee models. J Biomech. 2004;37(10):1499–1504.
12. Fox RJ, Harner CD, Sakane M, Carlin GJ, Woo SL. Determination of the in situ forces in the human posterior cruciate ligament using robotic technology. A cadaveric study. Am J Sports Med. 1998;26(3):395–401.
13. Gill TJ, DeFrate LE, Wang C, et al. The biomechanical effect of posterior cruciate ligament reconstruction on knee joint function. Kinematic response to simulated muscle loads. Am J Sports Med. 2003;31(4):530–536.
14. Gill TJ, DeFrate LE, Wang C, et al. The effect of posterior cruciate ligament reconstruction on patellofemoral contact pressures in the knee joint under simulated muscle loads. Am J Sports Med. 2004;32(1):109–115.

15. Girgis FG, Marshall JL, Monajem A. The cruciate ligaments of the knee joint. Anatomical, functional and experimental analysis. Clin Orthop. 1975;(106):216–231.

16. Gollehon DL, Torzilli PA, Warren RF. The role of the posterolateral and cruciate ligaments in the stability of the human knee. A biomechanical study. J Bone Joint Surg Am. 1987;69(2):233–242.

17. Grood ES, Suntay WJ. A joint coordinate system for the clinical description of three-dimensional motions: application to the knee. J Biomech Eng. 1983;105(2):136–144.

18. Iwata S, Suda Y, Nagura T, et al. Clinical disability in posterior cruciate ligament deficient patients does not relate to knee laxity, but relates to dynamic knee function during stair descending. Knee Surg Sports Traumatol Arthrosc. 2007;15(4):335–342.

19. Keller PM, Shelbourne KD, McCarroll JR, Rettig AC. Nonoperatively treated isolated posterior cruciate ligament injuries. Am J Sports Med. 1993;21(1):132–136.

20. Li G, DeFrate LE, Park SE, Gill TJ, Rubash HE. In vivo articular cartilage contact kinematics of the knee: an investigation using dual-orthogonal fluoroscopy and magnetic resonance image-based computer models. Am J Sports Med. 2005;33(1):102–107.

21. Li G, Gill TJ, DeFrate LE, Zayontz S, Glatt V, Zarins B. Biomechanical consequences of PCL deficiency in the knee under simulated muscle loads–an in vitro experimental study. J Orthop Res. 2002;20(4):887–892.

22. Li G, Lopez O, Rubash H. Variability of a three-dimensional finite element model constructed using magnetic resonance images of a knee for joint contact stress analysis. J Biomech Eng. 2001;123(4):341–346.

23. Li G, Moses JM, Papannagari R, Pathare NP, DeFrate LE, Gill TJ. Anterior cruciate ligament deficiency alters the in vivo motion of the tibiofemoral cartilage contact points in both the anteroposterior and mediolateral directions. J Bone Joint Surg Am. 2006;88(8):1826–1834.

24. Li G, Most E, DeFrate LE, Suggs JF, Gill TJ, Rubash HE. Effect of the posterior cruciate ligament on posterior stability of the knee in high flexion. J Biomech. 2004;37(5):779–783.

25. Li G, Papannagari R, Li M, et al. Effect of posterior cruciate ligament deficiency on in vivo translation and rotation of the knee during weightbearing flexion. Am J Sports Med. 2008;36(3):474–479.

26. Li G, Papannagari R, Nha KW, Defrate LE, Gill TJ, Rubash HE. The coupled motion of the femur and patella during in vivo weightbearing knee flexion. J Biomech Eng. 2007;129(6):937–943.

27. Markolf KL, Slauterbeck JR, Armstrong KL, Shapiro MS, Finerman GA. A biomechanical study of replacement of the posterior cruciate ligament with a graft. Part 1: isometry, pretension of the graft, and anterior-posterior laxity. J Bone Joint Surg Am. 1997;79(3):375–380.

28. Moore HA, Larson RL. Posterior cruciate ligament injuries. Results of early surgical repair. Am J Sports Med. 1980;8(2):68–78.

29. Most E, Axe J, Rubash H, Li G. Sensitivity of the knee joint kinematics calculation to selection of flexion axes. J Biomech. 2004;37(11):1743–1738.

30. Nha KW, Papannagari R, Gill TJ, et al. In vivo patellar tracking: clinical motions and patellofemoral indices. J Orthop Res. 2008;26(8):1067–1074.

31. Noyes FR, Stowers SF, Grood ES, Cummings J, VanGinkel LA. Posterior subluxations of the medial and lateral tibiofemoral compartments. An in vitro ligament sectioning study in cadaveric knees. Am J Sports Med. 1993;21(3):407–414.

32. Papannagari R, DeFrate LE, Nha KW, et al. Function of posterior cruciate ligament bundles during in vivo knee flexion. Am J Sports Med. 2007;35(9):1507–1512.

33. Parolie JM, Bergfeld JA. Long-term results of nonoperative treatment of isolated posterior cruciate ligament injuries in the athlete. Am J Sports Med. 1986;14(1):35–38.

34. Race A, Amis AA. Loading of the two bundles of the posterior cruciate ligament: an analysis of bundle function in a-P drawer. J Biomech. 1996;29(7):873–879.

35. Schulte KR, Chu ET, Fu FH. Arthroscopic posterior cruciate ligament reconstruction. Clin Sports Med. 1997;16(1):145–156.

36. Shelbourne KD, Davis TJ, Patel DV. The natural history of acute, isolated, nonoperatively treated posterior cruciate ligament injuries. A prospective study. Am J Sports Med. 1999;27(3):276–283.

37. Skyhar MJ, Warren RF, Ortiz GJ, Schwartz E, Otis JC. The effects of sectioning of the posterior cruciate ligament andthe posterolateral complex on the articular contact pressures within the knee. J Bone Joint Surg Am. 1993;75(5):694–699.

38. Van de Velde SK, Bingham JT, Gill TJ, Li G. Analysis of tibiofemoral cartilage deformation in posterior cruciate ligament-deficient knee. J Bone Joint Surg Am. 2009;91(1):167–175.

39. Van de Velde SK, Gill TJ, DeFrate LE, Papannagari R, Li G. The effect of anterior cruciate ligament deficiency and reconstruction on the patellofemoral joint. Am J Sports Med. 2008;36(6):1150–1159.

9

CHAPTER

The effect of anterior cruciate ligament deficiency on the in vivo elongation of the medial and lateral collateral ligaments.

Samuel K. Van de Velde
Louis E. DeFrate
Thomas J. Gill, IV
Jeremy M. Moses
Ramprasad Papannagari
Guoan Li

Am J Sports Med. 2007 Feb;35(2):294-300.

ABSTRACT

Background: Although anterior cruciate ligament deficiency has been shown to lead to joint degeneration, few quantitative data have been reported on its effect on soft tissue structures surrounding the knee joint.

Hypothesis: Anterior cruciate ligament deficiency will alter the deformation of both collateral ligaments during in vivo weightbearing knee function from 0° to 90°.

Study Design: Controlled laboratory study.

Methods: Six patients who had acute anterior cruciate ligament injury in 1 knee with the contralateral side intact participated in this study. Using magnetic resonance and dual orthogonal fluoroscopic imaging techniques, we measured the length of the fiber bundles of the superficial medial collateral ligament, deep medial collateral ligament, and lateral collateral ligament of the 6 patients; the healthy contralateral knee of each patient served as a control.

Results: Anterior cruciate ligament injury caused a significant elongation of the fiber bundles of the superficial and deep medial collateral ligament at every flexion angle. In contrast, the lateral collateral ligament fiber bundles shortened after anterior cruciate ligament injury.

Conclusion: The altered deformations of the collateral ligaments associated with the changes in tibiofemoral joint kinematics after anterior cruciate ligament injury demonstrate that deficiency of 1 of the knee joint structures upsets the in vivo knee homeostasis.

Clinical Relevance: Restoring normal knee kinematics after anterior cruciate ligament reconstruction is critical to restore the normal function of the collateral ligaments.

INTRODUCTION

Rupture of the anterior cruciate ligament (ACL) is a common injury. Up to 77% of patients evaluated with acute traumatic hemarthrosis of the knee are estimated to have an injury of the ACL, often without clinically noticeable abnormal joint laxity.[5,16,26,30] Acute rupture of the ACL is often associated with meniscal tears, chondral damage, and injury to the medial collateral ligament (MCL).[5,8,16,26,30] As the ACL injury becomes more chronic, an increasing incidence of joint swelling, instability, and meniscal tears is found, eventually resulting in progressive osteoarthritis.[2,13,27,28] In combined ACL and MCL injuries, the MCL does not heal as well as it does in isolated MCL injuries.[6,17,25,32,41]

A potential explanation for the poor outcome after ACL injury is that the changes in tibiofemoral joint kinematics associated with ACL injury disturb the normal function of other tissue structures of the knee.[3,12,18,25,36,38] Numerous in vivo studies have demonstrated that the ACL plays an important role in restraining anterior translation and internal rotation of the tibia at low flexion angles.[4,14,24,35] In addition, ACL injury was recently shown to cause a medial translation of the tibia during in vivo weightbearing flexion.[9] Transection of the ACL in cadaveric knees significantly increased the in situ forces in the MCL,[12,18,25,36,38] medial meniscus,[3] and the bony surface[36] under an anterior tibial load. Furthermore, studies using finite-element modeling predicted higher MCL strains after ACL transection under anterior tibial loads.[12]

In this study, we hypothesized that injury to the ACL alters the deformation of the collateral ligaments during an in vivo functional activity. We used magnetic resonance (MR) and dual orthogonal fluoroscopic imaging techniques to analyze the effects of injury to the ACL on the length of the collateral ligaments during in vivo knee flexion from 0° to 90°, with the healthy contralateral knee of each patient serving as a control.

MATERIALS AND METHODS

Six patients (5 men and 1 woman; age range, 19-38 years old; active on a moderate athletic level before injury and with no previous abnormal condition of the knee or lower limb) with complaints of knee laxity were included in the study. The protocol was approved by the Institutional Review Board at our institute. The included patients had diagnosed unilateral ACL injuries documented by clinical examination (8 mm Lachman with no end point and a grade 2 pivot shift measured by the same orthopaedic surgeon) and MR imaging. The patients had minimal associated injuries to other knee ligaments and cartilage and had healthy contralateral knees. Two patients had no significant damage to the menisci, 1 patient had a partial-thickness tear of the lateral meniscus, and the remaining 3 patients had injuries requiring up to 30% removal of the lateral meniscus at time of ACL reconstruction. Subjects had been injured within an average of 4.5 ± 3 months of testing. With the patients

supine and the knee in a relaxed, extended position, both knees were imaged with an MR scanner using a 1.5-tesla magnet (General Electric, Waukesha, Wis) and a fat-suppressed 3D spoiled gradient-recalled sequence. The MR scans spanned the medial and lateral extremes of the knee and were used to generate parallel sagittal plane images (resolution, 512 × 512 pixels) with a field of view of 16 × 16 cm and a spacing of 1 mm. These images were used to create 3D models of the knees in a solid modeling software (Rhinoceros, Robert McNeel and Associates, Seattle, Wash). Each anatomical knee model included the geometry of the femur and tibia, as well as the attachment sites of the superficial medial collateral ligament (SMCL), deep medial collateral ligament (DMCL), and lateral collateral ligament (LCL) (Figure 1). The ligament attachment sites were directly obtained from the MR images with the assistance of anatomical studies.[7,40,42]

After the MR image–based computer models were constructed, both knees of each subject were imaged using 2 orthogonally placed fluoroscopes as the patient performed a

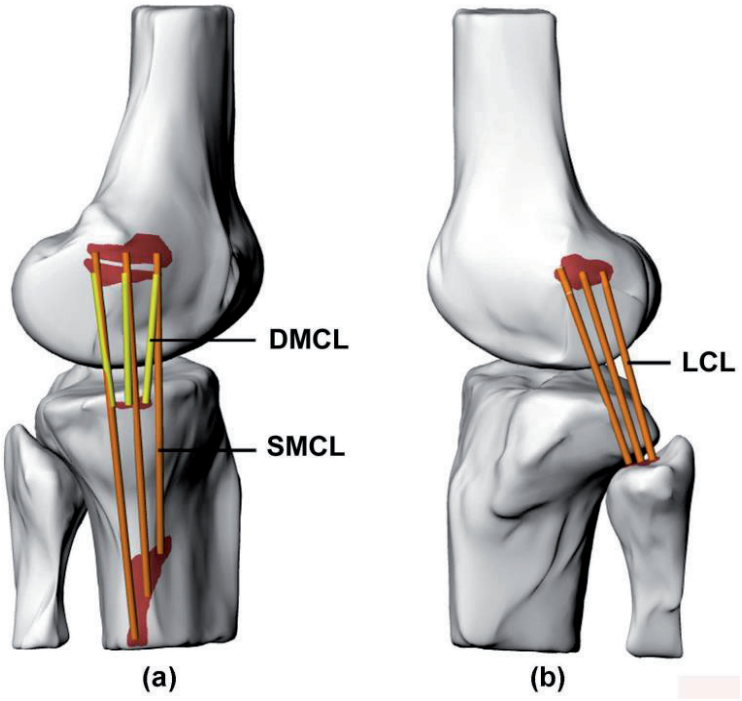

Figure 1. A typical 3D model of the knee created from sagittal plane MR images. (**A**) the attachment sites of the superficial medial collateral ligament (SMCL) and deep medial collateral ligament (DMCL); (**B**) the attachment sites of the lateral collateral ligament (LCL)

quasistatic single-legged lunge at 0°, 15°, 30°, 60°, and 90° of flexion. Flexion angle was verified with a goniometer as subjects stood upright on the platform with the fluoroscopes positioned in the horizontal plane. These images were used to quantify the in vivo knee position at each of the targeted flexion angles. The orthogonal images were imported into a solid modeling software and placed in the orthogonal planes based on the position of the fluoroscopes. The MR image–based knee models were viewed from 2 orthogonal directions corresponding to the views of the fluoroscopes. The models were manually manipulated in 6 degrees of freedom inside the software until the projections of the models matched the outlines of the images. When the projections matched the outlines of the images taken during in vivo knee flexion, the model reproduced the in vivo position of the knee. A series of knee models that reproduce knee positions at all target flexion angles re-created the in vivo knee flexion from full extension to 90° of flexion.

These imaging techniques have been described in detail in previous publications.[9,10,19-23,33] This system has an accuracy within 0.1 mm and 0.1° in determining the position and orientation of regularly shaped solid objects.[23] Recently, the procedure was further validated using a cadaveric knee, and the accuracy of measuring translation was less than 0.1 mm, whereas the repeatability was less than 0.1 mm and 0.3°.[9] The digitized attachment sites of the collateral ligaments from the MR images are not exactly the same for the pair of knees of each subject. To quantify the effect of ACL injury on length change of the

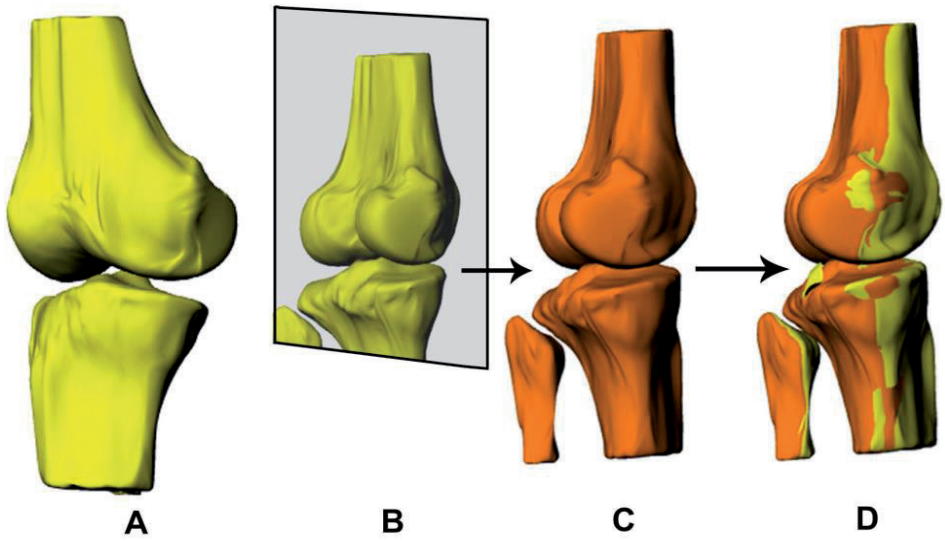

Figure 2. (**A**) a typical 3D model of the right knee; (**B**) the mirrored right knee model; (**C**) the 3D model of the left knee; (**D**) the mirrored right knee model is overlapped with the left knee model.

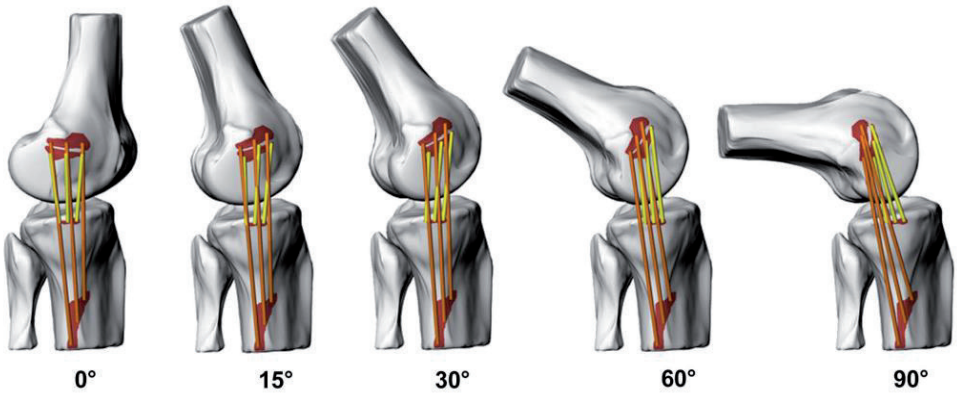

Figure 3. The knee models for a typical subject at 0°, 15°, 30°, 60°, and 90° of flexion during a quasistatic lunge.

collateral ligaments, we chose to use the centroids of the ligament attachment sites of the left knee for measurement of the bundle lengths of the collateral ligaments for both the ACL-injured and intact contralateral knees for each subject. The 3D model of the right knee was mirrored to create a "left" knee model.[9,22] The mirrored right knee was then overlapped with the 3D model of the left knee so that the centroids of the ligament attachment sites could be created on both knees simultaneously. The variability of the measurements due to differences in digitized ligament attachment sites is reduced because the same ligament attachment sites were used for both knees.[9] Figure 2 shows a patient's left knee model and the mirrored right knee.

The knee models for a typical subject at different flexion angles are shown in Figure 3. From the knee models, the relative positions of the SMCL, DMCL, and LCL attachment sites on the femur, tibia, and fibula were determined. The lengths of the collateral ligaments were directly measured from these models at each flexion angle. The insertion areas of each ligament were separated into 3 equal portions, creating 3 equal fiber bundles: the anterior bundle, the middle bundle, and the posterior bundle. The centroids of each portion were calculated. The length of ligaments was defined as the shortest distance between the centroids of the insertion areas. Because the collateral ligaments wrap around the femoral condyles and the tibial plateau, the direct line connecting the area centers was projected on the bony surfaces to create a curved ligament path (Figure 4). The length of this projected curve was measured as ligament length. At each flexion angle, the Wilcoxon signed rank test was used to compare the length of the fiber bundles between the intact and ACL-injured knees. Statistical significance was set at $P < .05$.

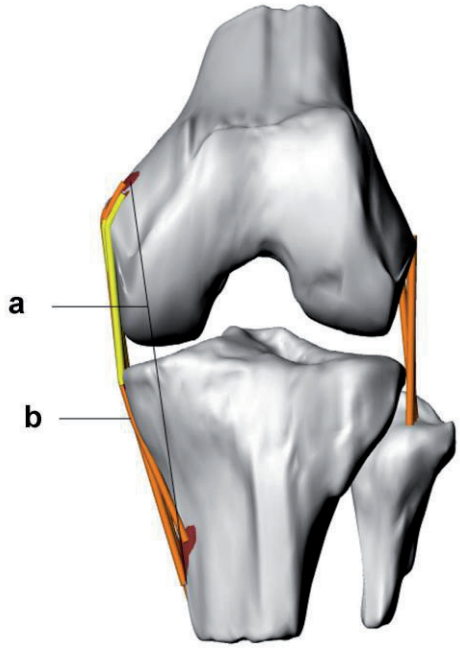

Figure 4. An anterior view of a typical knee model. (**a**) the direct line connecting the ligament area centers; (**b**) the direct line was projected on the bony surfaces to create a curved ligament path.

RESULTS

Superficial Medial Collateral Ligament

The ACL injury caused significant lengthening ($P < .05$) of all the fiber bundles of the SMCL at every target flexion angle (Figure 5). In the intact knee, the length of the anterior bundle at 0° was 78.8 ± 5.8 mm and increased gradually to 86.0 ± 8.2 mm at 90°. In the ACL-injured knee, the anterior bundle measured 80.2 ± 5.9 mm at 0° and 87.0 ± 7.7 mm at 90°. The middle bundle of the intact knee was 91.4 ± 6.1 mm long at 0°, increased slightly to 91.7 ± 6.0 mm at 30°, and then decreased to 89.2 ± 7.1 mm at 90°. A similar pattern of deformation was observed in the ACL-injured knee, but injury to the ACL caused a 1.5% increase in length ($P < .05$) at every flexion angle. In the intact knee, the length of the posterior bundle decreased from 103.3 ± 6.7 mm at 0° to 92.2 ± 6.2 mm at 90°. In the injured knee, the posterior bundle was 104.7 ± 7.0 mm long at 0° and decreased to 94.0 ± 6.4 mm at 90°.

Deep Medial Collateral Ligament

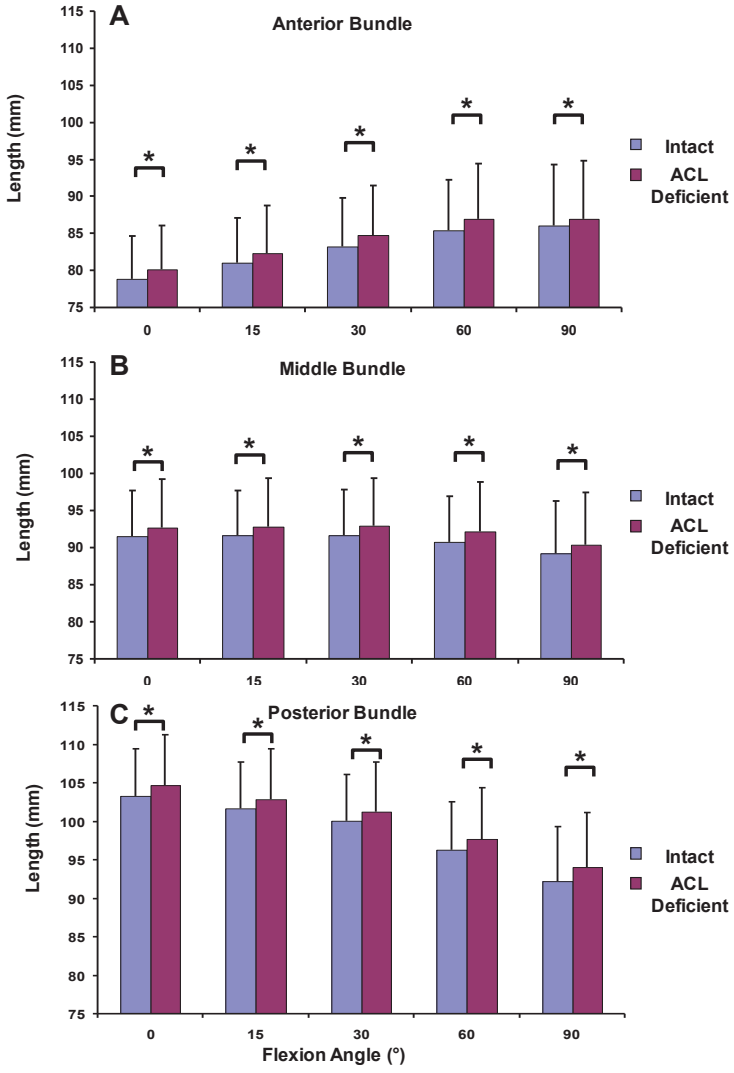

Figure 5. The length of the anterior (**A**), middle (**B**), and posterior (**C**) bundles of the superficial medial collateral ligament (SMCL) as a function of flexion for the intact and ACL-deficient knees. *Statistically significant difference ($P < .05$).

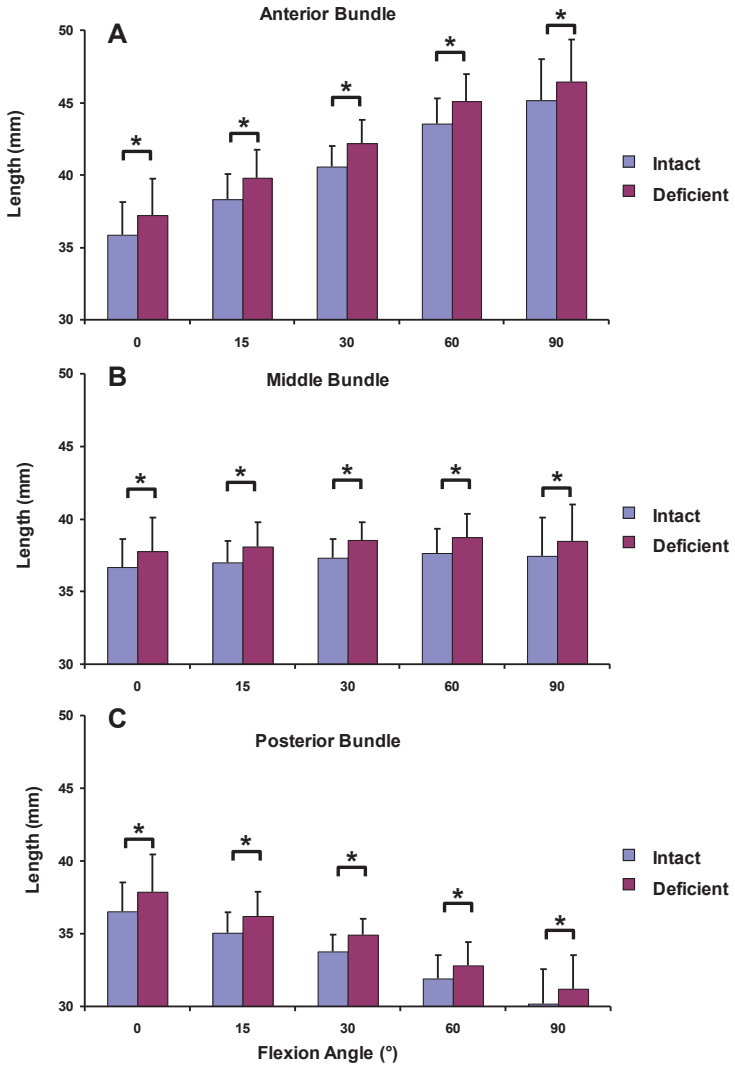

Figure 6. The length of the anterior (**A**), middle (**B**), and posterior (**C**) bundles of the deep medial collateral ligament (DSMCL) as a function of flexion for the intact and ACL-deficient knees. *Statistically significant difference ($P < .05$).

The ACL injury caused significant lengthening ($P < .05$) of all the fiber bundles of the DMCL at every flexion angle (Figure 6). In the intact knee, the length of the anterior bundle at 0° was 35.9 ± 2.2 mm and increased gradually to 45.2 ± 2.8 mm at 90°. In the ACL-injured knee, the anterior bundle measured 37.2 ± 2.5 mm at 0° and 46.5 ± 2.9 mm at 90°. The effect of ACL injury was maximal at 30° of flexion, with a 3.9% increase in length compared to the length of the same bundle in the intact knee. The middle bundle of the intact knee was 36.7 ± 1.9 mm long at 0° and increased slightly to 37.4 ± 2.6 mm at 90°. In the ACL-injured knee, the middle bundle was 37.6 ± 2.3 mm at 0° and 38.5 ± 2.5 mm at 90°. The length of the posterior bundle in the intact knee decreased from 36.5 ± 2.0 mm at 0° to 30.2 ± 2.3 mm at 90°. In the injured knee, the posterior bundle was 37.9 ± 2.5 mm long at 0° and decreased to 31.2 ± 2.2 mm at 90°, a 3.4% increase relative to the healthy ligament.

Lateral Collateral Ligament

A relative shortening of the fiber bundles of the LCL was observed after ACL injury. From 0° to 90° of flexion, ACL injury decreased the length of the anterior bundle significantly ($P < .05$). In the intact knee, the anterior bundle lengthened from 52.2 ± 8 mm at 0° to 54.0 ± 8.8 mm at 30°, and from 50.3 ± 7.8 mm to 52.5 ± 9 mm at 30° in the injured knee. Similar increases in length with further flexion of the intact and injured knee were observed, with statistically significant decreases for the ACL-deficient knee. The ACL injury decreased the length of the bundles of the middle and posterior bundles of the LCL significantly ($P < .05$) at every flexion angle. The length of the middle bundle remained relatively constant along the flexion path in the intact and injured knee. The middle bundle at 0° measured 51.1 ± 7.9 mm and 49.3 ± 7.8 mm in the intact and injured knee, respectively. At 90°, the middle bundle measured 50.4 ± 9.1 mm and 49.2 ± 9.6 mm in the intact and injured knee, respectively. The length of the posterior bundle in the intact knee decreased from 49.7 ± 7.7 mm at 0° to 43.4 ± 9.2 mm at 90°. In the injured knee, the posterior bundle was 47.8 ± 7.8 mm long at 0° and decreased in length to 42.0 ± 9.8 mm at 90°. The maximal significant difference between the intact and injured knee was at 15°, at which the length of the posterior bundle measured 48.2 ± 8.1 mm and 46.2 ± 8.4 mm, respectively.

DISCUSSION

This study quantified the effects of injury to the ACL on the collateral ligaments during an in vivo quasistatic lunge from 0° to 90° of knee flexion. The lengths of the fiber bundles of the SMCL, DMCL, and LCL of 6 patients with unilateral ACL injury were measured using MR and dual orthogonal fluoroscopic imaging techniques, with the healthy contralateral knee of each patient serving as control.

In the healthy contralateral knees, the elongation patterns of the fiber bundles of the collateral ligaments described in our study followed similar trends throughout the flexion path as the elongation patterns previously described in healthy subjects.[33] In the knees with ACL injury, the SMCL fiber bundles of the knee were significantly lengthened. The fiber bundles of the SMCL lengthened around 1.5% compared with the healthy knee. All the fiber bundles of the DMCL were significantly lengthened after ACL injury at every flexion angle. The effect of ACL injury was maximal at 30° of flexion in the anterior bundle of the DMCL, with a 3.9% increase in length compared to the length of the same bundle in the intact knee.

The ACL injury resulted in significant shortening of the LCL bundles. The maximal difference between the intact and injured knee occurred at 15°, where the length of the posterior bundle was 3.9% shorter compared with the length of the same bundle in the intact knee.

The changes in tibiofemoral joint kinematics associated with ACL injury are the key to the altered elongation patterns of the collateral ligaments during in vivo knee flexion. Numerous studies have demonstrated that the ACL plays an important role in restraining anterior translation and internal rotation of the tibia.[4,9,11,14,24,35,37] Andriacchi and Dyrby[4] observed a decrease in the external tibial rotation before heel strike in patients with ACL injury. DeFrate et al[9] found that ACL injury not only caused a statistically significant anterior shift (approximately 3 mm) and internal rotation of the tibia (approximately 2°) at low flexion angles but also caused a medial tibial translation of approximately 1 mm from 15° to 90° of flexion. An ACL injury might also cause an increased valgus rotation compared with the intact knee.[9] These findings might help to explain the increased elongation of the MCLs and the shortened length of the LCL in the ACL-injured knees observed in our study. For example, we observed that the orientation of the SMCL and DMCL is approximately parallel to the tibial shaft at full extension, whereas the LCL passes from anterior proximally to posterior distally, as shown in Figure 1. Therefore, the increased internal tibial rotation associated with ACL injury will elongate the SMCL and DMCL and shorten the LCL.

Previous in vitro studies have examined the effect of injury to the ACL on other tissue structures of the joint.[3,12,15,18,25,36,38,39] For example, transection of the ACL in cadaveric knees significantly increased the in situ forces in the MCL.[12,18,25,36,38] The in situ forces in the MCL increased by 63% at 30° of knee flexion under a 134-N anterior tibial load in the ACL-deficient knee.[18] A finite-element modeling study predicted significantly higher MCL strains after ACL transection under anterior tibial loads.[12] Combined musculoskeletal modeling and computer simulation calculated a peak force in the MCL that was 3 times greater in the ACL-deficient knee than in the ACL-intact knee during walking.[38] Even though a direct comparison of our data and those from the in vitro studies is difficult

because of the differences between in vivo and in vitro studies, they showed similar effects of ACL injury on the function of the MCL.

These data suggest that because of the altered role of the MCL in maintaining knee joint stability, the MCL is at greater risk of secondary injury after isolated ACL injury. This suggestion is supported by the observation that there is an increased incidence of MCL tears in ACL-injured knees compared to uninjured knees.[31] Tissue strain analysis in a rat MCL indicated that necrotic fibroblast damage was induced at ligament strain levels significantly below the structural damage threshold.[34] In our study, up to 3.9% lengthening of the medial collateral fiber bundles occurred in the ACL-injured knee, which might have a negative effect on the biomechanical function of the MCL.

Traumatic rupture of the ACL is frequently associated with injury of the MCL.[29] Numerous animal studies have demonstrated that the mechanical properties of the healing MCL are inferior in a combined ACL and MCL injury as compared with an isolated MCL injury.[6,17,25,32,41] For example, at 6 weeks after ACL and MCL transection in a goat model, the tensile strength of the healing MCL was only 10% of the tensile strength of controls.[1] Excessive loads across the MCL as a result of the combined ACL and MCL injury have been thought to decrease the ability of the MCL to heal. The findings of the present study suggest that there might be higher loads on the MCLs after ACL injury, potentially impeding MCL healing.

It is interesting to note that ACL injury resulted in significant shortening of the LCL bundles, which might indicate that ACL injury alters the biomechanical function of the posterolateral structures. The impact of this finding is currently unclear. Further research is necessary to investigate the effect of ACL injury on the stabilizing structures of the lateral knee compartment, such as the popliteus tendon, the popliteofibular ligament, and the lateral meniscus.

One of the limitations of this study was that we measured the length of the collateral ligament fiber bundles as the distance between the bundle insertion centroids on the tibia and femur. These data cannot be directly related to ligament strains because the reference lengths of the ligaments (zero-load length) are unknown. Furthermore, we only examined the effect of ACL injury during a quasistatic single-legged lunge using a goniometer to control the flexion angle. In the future, the effects of injury to the ACL on the elongation during other in vivo activities such as gait and stair ascent and descent should also be investigated.

In conclusion, injury to the ACL altered the lengths of the collateral ligaments during in vivo knee flexion. The ACL injury caused a significant elongation of the fiber bundles of the SMCL and DMCL at every flexion angle. Throughout most of the range of motion, ACL injury resulted in significant shortening of the LCL bundles. These altered length patterns of the collateral ligaments, associated with the changes in tibiofemoral joint

kinematics after ACL injury, demonstrate that deficiency of the ACL upsets the in vivo knee homeostasis and puts the associated joint environment at greater risk of secondary injury. The altered deformations of the collateral ligaments associated with ACL injury stress the importance for ACL reconstruction techniques to restore knee kinematics in 6 degrees of freedom. Restoring knee kinematics might prevent secondary injury to other tissue structures around the knee joint and improve the healing process of the associated structures in the event of a combined ligament injury.

REFERENCES

1. Abramowitch SD, Yagi M, Tsuda E, Woo SL. The healing medial collateral ligament following a combined anterior cruciate and medial collateral ligament injury: a biomechanical study in a goat model. J Orthop Res. 2003;21:1124-1130.
2. Aichroth PM, Patel DV, Zorrilla P. The natural history and treatment of rupture of the anterior cruciate ligament in children and adolescents: a prospective review. J Bone Joint Surg Br. 2002;84:38-41.
3. Allen CR, Wong EK, Livesay GA, Sakane M, Fu FH, Woo SL. Importance of the medial meniscus in the anterior cruciate ligament-deficient knee. J Orthop Res. 2000;18:109-115.
4. Andriacchi TP, Dyrby CO. Interactions between kinematics and loading during walking for the normal and ACL deficient knee. J Biomech. 2005;38:293-298.
5. Bomberg BC, McGinty JB. Acute hemarthrosis of the knee: indications for diagnostic arthroscopy. Arthroscopy. 1990;6:221-225.
6. Bray RC, Doschak MR, Gross TS, Zernicke RF. Physiological and mechanical adaptations of rabbit medial collateral ligament after anterior cruciate ligament transection. J Orthop Res. 1997;15:830-836.
7. Brinkman JM, Schwering PJ, Blankevoort L, Kooloos JG, Luites J, Wymenga AB. The insertion geometry of the posterolateral corner of the knee. J Bone Joint Surg Br. 2005;87:1364-1368.
8. Butler JC, Andrews JR. The role of arthroscopic surgery in the evaluation of acute traumatic hemarthrosis of the knee. Clin Orthop Relat Res. 1988;228:150-152.
9. DeFrate LE, Ramprasad P, Gill TJ, et al. The six degrees of freedom kinematics of the knee after ACL deficiency: an in-vivo imaging analysis. Am J Sports Med. 2006;34:1240-1246.
10. DeFrate LE, Sun H, Gill TJ, Rubash HE, Li G. In vivo tibiofemoral contact analysis using 3D MRI-based knee models. J Biomech. 2004;37: 1499-1504.
11. Dennis DA, Mahfouz MR, Komistek RD, Hoff W. In vivo determination of normal and anterior cruciate ligament-deficient knee kinematics. J Biomech. 2005;38:241-253.
12. Ellis BJ, Lujan TJ, Dalton MS, Weiss JA. Medial collateral ligament insertion site and contact forces in the ACL-deficient knee. J Orthop Res. 2006;24:800-810.
13. Fithian DC, Paxton LW, Goltz DH. Fate of the anterior cruciate ligament-injured knee. Orthop Clin North Am. 2002;33:621-636.
14. Georgoulis AD, Papadonikolakis A, Papageorgiou CD, Mitsou A, Stergiou N. Three-dimensional tibiofemoral kinematics of the anterior cruciate ligament-deficient and reconstructed knee during walking. Am J Sports Med. 2003;31:75-79.
15. Haimes JL, Wroble RR, Grood ES, Noyes FR. Role of the medial structures in the intact and anterior cruciate ligament-deficient knee: limits of motion in the human knee. Am J Sports Med. 1994;22:402-409.
16. Hardaker WT Jr, Garrett WE Jr, Bassett FH III. Evaluation of acute traumatic hemarthrosis of the knee joint. South Med J. 1990;83:640-644.

17. Hart DP, Dahners LE. Healing of the medial collateral ligament in rats: the effects of repair, motion, and secondary stabilizing ligaments. J Bone Joint Surg Am. 1987;69:1194-1199.

18. Kanamori A, Sakane M, Zeminski J, Rudy TW, Woo SL. In-situ force in the medial and lateral structures of intact and ACL-deficient knees. J Orthop Sci. 2000;5:567-571.

19. Li G, DeFrate LE, Park SE, Gill TJ, Rubash HE. In vivo articular cartilage contact kinematics of the knee: an investigation using dual-orthogonal fluoroscopy and magnetic resonance image-based computer models. Am J Sports Med. 2005;33:102-107.

20. Li G, DeFrate LE, Rubash HE, Gill TJ. In vivo kinematics of the ACL during weight-bearing knee flexion. J Orthop Res. 2005;23:340-344.

21. Li G, DeFrate LE, Sun H, Gill TJ. In vivo elongation of the anterior cruciate ligament and posterior cruciate ligament during knee flexion. Am J Sports Med. 2004;32:1415-1420.

22. Li G, Moses JM, Papannagari R, Pathare NP, Defrate LE, Gill TJ. Anterior cruciate ligament deficiency alters in vivo tibiofemoral cartilage contact patterns in both anteroposterior and mediolateral directions. J Bone Joint Surg Am. 2006;88:1826-1834.

23. Li G, Wuerz TH, DeFrate LE. Feasibility of using orthogonal fluoroscopic images to measure in vivo joint kinematics. J Biomech Eng. 2004;126:314-318.

24. Logan M, Dunstan E, Robinson J, Williams A, Gedroyc W, Freeman M. Tibiofemoral kinematics of the anterior cruciate ligament (ACL)-deficient weightbearing, living knee employing vertical access open “interventional” multiple resonance imaging. Am J Sports Med. 2004;32:720-726.

25. Ma CB, Papageogiou CD, Debski RE, Woo SL. Interaction between the ACL graft and MCL in a combined ACL+MCL knee injury using a goat model. Acta Orthop Scand. 2000;71:387-393.

26. Maffulli N, Binfield PM, King JB, Good CJ. Acute haemarthrosis of the knee in athletes: a prospective study of 106 cases. J Bone Joint Surg Br. 1993;75:945-949.

27. Murrell GA, Maddali S, Horovitz L, Oakley SP, Warren RF. The effects of time course after anterior cruciate ligament injury in correlation with meniscal and cartilage loss. Am J Sports Med. 2001;29:9-14.

28. Nebelung W, Wuschech H. Thirty-five years of follow-up of anterior cruciate ligament-deficient knees in high-level athletes. Arthroscopy. 2005;21:696-702.

29. Nielsen AB, Yde J. Epidemiology of acute knee injuries: a prospective hospital investigation. J Trauma. 1991;31:1644-1648.

30. Noyes FR, Bassett RW, Grood ES, Butler DL. Arthroscopy in acute traumatic hemarthrosis of the knee: incidence of anterior cruciate tears and other injuries. J Bone Joint Surg Am. 1980;62:687-695, 757.

31. Oates KM, Van Eenenaam DP, Briggs K, Homa K, Sterett WI. Comparative injury rates of uninjured, anterior cruciate ligament-deficient, and reconstructed knees in a skiing population. Am J Sports Med. 1999;27: 606-610.

32. Ohno K, Pomaybo AS, Schmidt CC, Levine RE, Ohland KJ, Woo SL. Healing of the medial collateral ligament after a combined medial collateral and anterior cruciate ligament injury and reconstruction of

the anterior cruciate ligament: comparison of repair and nonrepair of medial collateral ligament tears in rabbits. J Orthop Res. 1995;13:442-449.

33. Park SE, DeFrate LE, Suggs JF, Gill TJ, Rubash HE, Li G. The change in length of the medial and lateral collateral ligaments during in vivo knee flexion. Knee. 2005;12:377-382.

34. Provenzano PP, Heisey D, Hayashi K, Lakes R, Vanderby R Jr. Subfailure damage in ligament: a structural and cellular evaluation. J Appl Physiol. 2002;92:362-371.

35. Ristanis S, Giakas G, Papageorgiou CD, Moraiti T, Stergiou N, Georgoulis AD. The effects of anterior cruciate ligament reconstruction on tibial rotation during pivoting after descending stairs. Knee Surg Sports Traumatol Arthrosc. 2003;11:360-365.

36. Sakane M, Livesay GA, Fox RJ, Rudy TW, Runco TJ, Woo SL. Relative contribution of the ACL, MCL, and bony contact to the anterior stability of the knee. Knee Surg Sports Traumatol Arthrosc. 1999;7:93-97.

37. Scarvell JM, Smith PN, Refshauge KM, Galloway HR, Woods KR. Comparison of kinematic analysis by mapping tibiofemoral contact with movement of the femoral condylar centres in healthy and anterior cruciate ligament injured knees. J Orthop Res. 2004;22:955-962.

38. Shelburne KB, Pandy MG, Torry MR. Comparison of shear forces and ligament loading in the healthy and ACL-deficient knee during gait. J Biomech. 2004;37:313-319.

39. Sullivan D, Levy IM, Sheskier S, Torzilli PA, Warren RF. Medial restraints to anterior-posterior motion of the knee. J Bone Joint Surg Am. 1984; 66:930-936.

40. Warren LF, Marshall JL. The supporting structures and layers on the medial side of the knee: an anatomical analysis. J Bone Joint Surg Am. 1979;61:56-62.

41. Woo SL, Young EP, Ohland KJ, Marcin JP, Horibe S, Lin HC. The effects of transection of the anterior cruciate ligament on healing of the medial collateral ligament: a biomechanical study of the knee in dogs. J Bone Joint Surg Am. 1990;72:382-392.

42. Wymenga AB, Kats JJ, Kooloos J, Hillen B. Surgical anatomy of the medial collateral ligament and the posteromedial capsule of the knee. Knee Surg Sports Traumatol Arthrosc. 2006;14:229-234.

10

CHAPTER

In vivo length changes of the anterolateral ligament and related extra-articular reconstructions

Samuel K. Van de Velde
William A. Kernkamp
Ali Hosseini
Robert F. LaPrade
Ewoud R. van Arkel
Guoan Li

Am J Sports Med. 2016, in press.

Background: Based on little in vitro biomechanical data with considerable variability, both anatomic anterolateral ligament (ALL) and non-anatomic anterolateral reconstructions are performed to improve the stability of anterior cruciate ligament (ACL)-deficient patients. However, no in vivo biomechanical data are available, which is essential for safe and effective reconstruction techniques.

Purpose: To measure the theoretical length change patterns of the ALL and various anterolateral extra-articular reconstructions in healthy and ACL-deficient knees during in vivo weight-bearing flexion.

Study Design: Descriptive In Vivo Laboratory Study

Methods: Ten patients with an ACL injury in one knee and the contralateral side intact were included. Using MR and dual fluoroscopic imaging techniques, the changes in length of the ALL, **modelled** with its femoral attachment either anterior or posterior-proximal to the fibular collateral ligament (FCL) attachment, and non-anatomic extra-articular reconstructions were measured as a function of knee flexion, and compared between the intact and ACL-deficient knees.

Results: The ALL, with its femoral attachment anterior to the FCL attachment, showed a consistent length increase of approximately 50% from 0° to 90° of knee flexion. The length change of the ALL was 20% when its femoral attachment was placed posterior-proximal to the FCL. ACL deficiency did not affect ALL length.

An extra-articular reconstruction with the femoral attachment proximal to the lateral epicondyle and the tibial attachment on Gerdy's tubercle increased 15% in length from 0° to 60° and shortened at 90° of flexion. When the tibial fixation of the anatomical ALL with its femoral attachment posterior to the FCL was moved to Gerdy's tubercle, a 30% length increase over 90 degrees occurred, without the drop in length at 90°. A significant length increase of both theoretical reconstruction grafts was seen at 0° in ACL-deficient knees.

Conclusion: An anatomic ALL reconstruction as modelled based on recent anatomical studies was not isometric during in vivo knee flexion, and was not affected by ACL deficiency. The non-anatomic extra-articular reconstructions demonstrated more biomechanically favorable length change patterns with the smallest percent increase in elongation during knee flexion.

Clinical Relevance: This study presents the first in vivo biomechanical data on the ALL, both in healthy and ACL-deficient knees, and provides surgical information for restoring normal anterolateral stability.

INTRODUCTION

Several studies have documented the anterolateral ligament (ALL) in cadaveric knees and its possible role in controlling rotational stability, together with the anterior cruciate ligament (ACL). Most researchers agree, based on the anatomic location and some exploratory cadaveric testing, that the ALL might be an important stabilizer of internal tibial rotation.[2, 4, 11, 16, 19, 22, 23, 27, 30] However, the actual length change pattern of the ALL, and thus the flexion angle at which the ALL might perform its stabilizing function, remain unclear. According to the measurements by Dodds et al., the ALL was close to isometric between 0° and 60° of flexion, and shortened from 60° to 90° of flexion.[4] In contrast, Zens et al. described the ALL as a non-isometric structure which increased in length with increasing knee flexion.[30] In the study by Parsons et al., the ALL was an important stabilizer of internal rotation at flexion angles greater than 35°.[19] This is in conflict with the study by Saiegh et al., in which adding an ALL lesion in ACL-deficient cadaveric knees did not increase tibiofemoral instability in any of the testing conditions.[20]

Given the considerable discrepancy between these in vitro measurements, it is not surprising that the recommendations for surgical restoration of anterolateral knee stability vary widely as well. Some groups have advised securing the ALL tenodesis in extension,[21] others argued for tensioning and fixation of the ALL graft at 90° of flexion,[30] yet others have reasoned against performing an anatomic ALL reconstruction altogether.[10, 12, 22] Based on possible unacceptable graft strains at higher knee flexion[12] and overconstraining the lateral compartment,[10] the traditional, non-anatomic lateral extra-articular reconstructions might actually be biomechanically more favorable and more effective at controlling anterolateral laxity than an anatomic ALL reconstruction.[12, 22]

A possible explanation for the above-mentioned contradictory biomechanical results and recommendations for anterolateral reconstruction might be the variability in the anatomic landmarks used for ALL measurement in the cadaveric studies – more specifically the femoral attachment of the ALL. Some investigators reported that the femoral attachment of the ALL was anterior-distal with respect to the attachment of the fibular collateral ligament (FCL),[2, 8, 28] while others described the femoral ALL attachment as more posterior and proximal of the FCL origin.[4, 11, 16] Even minor shifts in position around the rotational axis of the femur would result in contrary ligament kinematic patterns.[18] Another explanation might be that ligament kinematics are highly dependent on the loading conditions, and subsequent tibiofemoral biomechanics, of the knee during testing. Even the most advanced in vitro experiments are limited by the difficulty in simulating the complex physiological loading conditions that occur during weight-bearing knee flexion.[24] It is therefore difficult to extrapolate the biomechanical behavior of the ALL and related anterolateral reconstructions that were measured during variable loading conditions in cadaveric studies to the length change patterns that would be seen in the knees of either healthy or ACL-deficient patients during in vivo weight-bearing knee flexion.

The purpose of the present study was to measure the theoretical length change pattern of the ALL and various anterolateral extra-articular reconstructions in healthy knees and ACL-deficient knees during in vivo weight-bearing flexion of the knee using magnetic resonance (MR) and dual fluoroscopic imaging techniques.

MATERIAL AND METHODS

Patient Selection

Ten patients (six men and four women; age range 19-38 years old; active on a moderate athletic level before injury and with no previous abnormal condition of the knee or lower limb) with complaints of knee instability were included in the study. The patients had a diagnosis of an acute ACL rupture, as documented by clinical examination findings (8-mm Lachman test with weak end point and a grade 2 pivot-shift test) and findings of an isolated ACL tear on MR imaging. All patients had healthy contralateral knees. Patients had been injured within a mean ± SD of 4.5 ± 3 months of testing. Patients with injury to other ligaments, noticeable cartilage lesions, and injury to the underlying bone were excluded from the study. Six patients had no significant damage to the menisci, one patient had a partial-thickness tear of the lateral meniscus, and the remaining three patients had injuries requiring up to 30% removal of the lateral meniscus at time of ACL reconstruction. Five of these 10 patients were included in our previous studies of the 6 degrees-of-freedom tibiofemoral kinematics,[3] elongation of the collateral ligaments,[26] and tibiofemoral cartilage contact deformation[25] in ACL deficiency.

Each patient signed a consent form that had been approved by our Institutional Review Board.

Imaging Procedure

The MR and dual fluoroscopic imaging techniques for the measurement of ligament kinematics have been described in detail previously.[14,18, 26] Briefly, both the left and right knees were imaged with a MR scanner to create 3-dimensional (3-D) meshed models of the knees, using a protocol established in our laboratory.[3] Patients were asked to lie supine, with the knee in a relaxed, extended position while sagittal plane images were acquired with a 1.5T MRI scanner (Siemens, Malvern, PA). The MR scanner was equipped with a surface coil and used a 3-D double-echo water excitation sequence (field of view 16 X 16 X 12 cm, voxel resolution 0.31 X 0.31 X 1.00 mm, repetition time [TR] 24 msec, echo time [TE] 6.5 msec, and flip angle 25°). Each scan lasted for approximately 12 minutes. The images were then imported into solid modeling software (Rhinoceros; Robert McNeel and Associates, Seattle, WA) to construct 3-D surface mesh models of the tibia, fibula and femur. The meshes were assembled using a point density of 80 vertices/cm2 and triangular facets, with an average aspect ratio of 2. The attachment sites of the FCL were identified as

previously described and included in the 3-D knee model.[26] On these anatomical knee models the attachment sites of the anatomic ALL and theoretical extra-articular reconstructions were presented as points. The femoral attachment sites of the ALL were positioned based both on the description by Claes et al. (i.e. slightly anterior-distal with respect to the attachment of the FCL)[2] and the description by Kennedy et al. (posterior and proximal of the FCL origin).[11] The tibial attachment site of the ALL was positioned midway between the center of Gerdy's tubercle and the anterior margin of the fibular head.[2, 11] A more proximal over-the-top (OTT) extra-articular reconstruction position was chosen based on the descriptions by Zarins and Rowe[29] and Kittle et al.[12] To minimize intra-subject variability in positioning the attachment sites for the ALL and extra-articular reconstructions, the 3-D model of the right knee was mirrored to create a "left" knee model. The mirrored right knee was then overlapped with the 3-D model of the left knee so that the attachment sites could be created on both knees simultaneously.[26]

After the MRI-based computer models were constructed, both knees of each patient were simultaneously imaged using 2 orthogonally placed fluoroscopes (OEC 9800; GE Healthcare, Salt Lake City, UT) as the patient performed a single-leg quasistatic lunge at 0°, 15°, 30°, 60°, and 90° of flexion. At each flexion angle, the patient paused for 5 seconds while simultaneous fluoroscopic images were obtained. Throughout the experiment, the leg being tested supported the patient's body weight, while the other leg provided stability.

Next, the fluoroscopic images were imported into solid modeling software and placed in the orthogonal planes based on the position of the fluoroscopes during imaging of the patient. Finally, the 3-D MRI–based knee model of each patient was imported into the same software, viewed from the 2 orthogonal directions corresponding to the orthogonal fluoroscopic setup used to acquire the images, and independently manipulated in 6 degrees of freedom inside the software until the projections of the model matched the outlines of the fluoroscopic images. When the projections matched the outlines of the images taken during in vivo knee flexion, the model reproduced the in vivo position of the knee. This system has a reported error of <0.1 mm and 0.3° in measuring tibiofemoral joint translations and rotations, respectively.[3, 15]

Measurement of Length Change of the ALL and Extra-Articular Reconstructions

The changes in length of the ALL and extra-articular reconstructions were measured as a function of knee flexion with several combinations of the tibiofemoral attachment points (Figure 1). The length of the ALL and theoretical grafts was defined as the shortest distance between the attachment site points. Because the structures wrap around the femoral condyles and the tibial plateau, a direct line connecting the attachment sites was projected on the bony surfaces to create a curved ligament path to avoid penetration of the connecting line through bone.[14, 26] The length of this projected curve was measured as length of the ligament or theoretical graft. For the analysis of anatomic ALL length change, the tibial

point midway between the center of Gerdy's tubercle and the anterior margin of the fibular head was connected with either (1) the femoral point slightly anterior-distal with respect to the attachment of the FCL (Claes et al.)[2], or (2) the femoral point posterior and proximal to the FCL origin (Kennedy et al.)[11]. For the analysis of theoretical non-anatomic extra-articular reconstruction grafts, the tibial point on Gerdy's tubercle was connected with

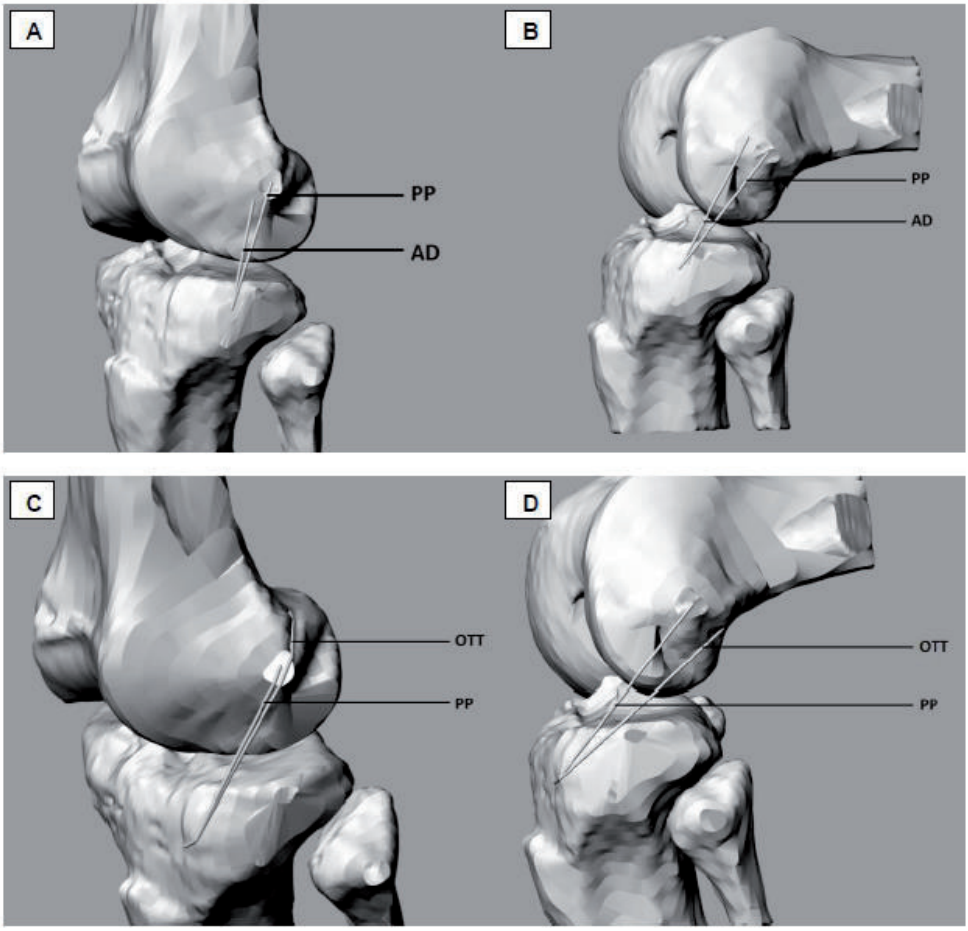

Figure 1. 3-D MR knee models illustrating the anatomic anterolateral ligament (ALL) with the femoral attachment anterior-distal (AD) and posterior-proximal (PP) with respect to the attachment of the fibular collateral ligament (FCL) at 0° (**A**) and 90° (**B**) of knee flexion; non-anatomic extra-articular grafts with the tibial attachment at Gerdy tubercle and with the femoral attachment over-the-top (OTT) and posterior-proximal (PP) with respect to the attachment of the FCL at 0° (**C**) and 90° (**D**) of knee flexion.

either (1) the more proximal OTT extra-articular reconstruction position on the lateral femur with the connecting curve always projected so that the theoretical graft intersected with the FCL, or (2) the femoral point of the ALL posterior and proximal to the FCL origin.

Statistical Analysis

Changes in the length of the anatomic ALL, based on the descriptions by both Claes et al.[2] and Kennedy et al.[11], and the theoretical extra-articular reconstruction grafts caused by flexion of the knee were examined using one-way analysis of variance with pairwise comparisons, having the Newman-Keuls procedure for multiple comparisons. A two-way repeated-measures analysis of variance and the Newman-Keuls post hoc test were used to determine statistically significant differences in length between the intact contralateral knees and the ACL-deficient knees at each flexion angle. *P*-values less than 0.05 were considered significant.

RESULTS

Anatomic ALL length change (Figure 2).

The ALL as described by Claes et al.[2] demonstrated a consistent, significant increase in length with increasing flexion, from 32.8 ± 2.5 mm at 0° to 48.5 ± 4.6 mm at 90° ($P<0.001$). This increase was approximately a 50% increase over 90° of flexion. The ALL as described by Kennedy et al.[11] also showed a consistent increase with flexion, but with only a 20 % increase during knee flexion from 0° to 90°, from 40.0 ± 2.4 mm at 0° to 48 ± 3.6 mm at 90° of flexion ($P<0.001$). ACL deficiency did not significantly affect the **length** in either group at any of the flexion angles.

Non-anatomic anterolateral reconstructions (Figure 3).

The OTT position on the femur, tunneled under the FCL, and attached to Gerdy's tubercle, resulted in only a 15% increase in length from 0° to 60° but then decreased again at 90° of flexion. In the OTT measurements, ACL deficiency did cause a significant length increase of the reconstruction around 0° (68.5 ± 2.9 mm versus 70.5 ± 2.4 mm in intact and ACL deficient knees, respectively, $P=0.019$). When the anatomical ALL as described by Kennedy et al.[11] was modified by leaving the femoral point identical, but moving the tibia fixation to Gerdy's tubercle, a similar significant graft elongation effect of ACL deficiency was noticed at 0° of flexion (51 ± 2.1 mm versus 53.8 ± 2.2 mm in intact and ACL deficient knees, respectively, $P=0.037$). A 30% increase in length over 90 degrees was seen, without the drop in length at 90°.

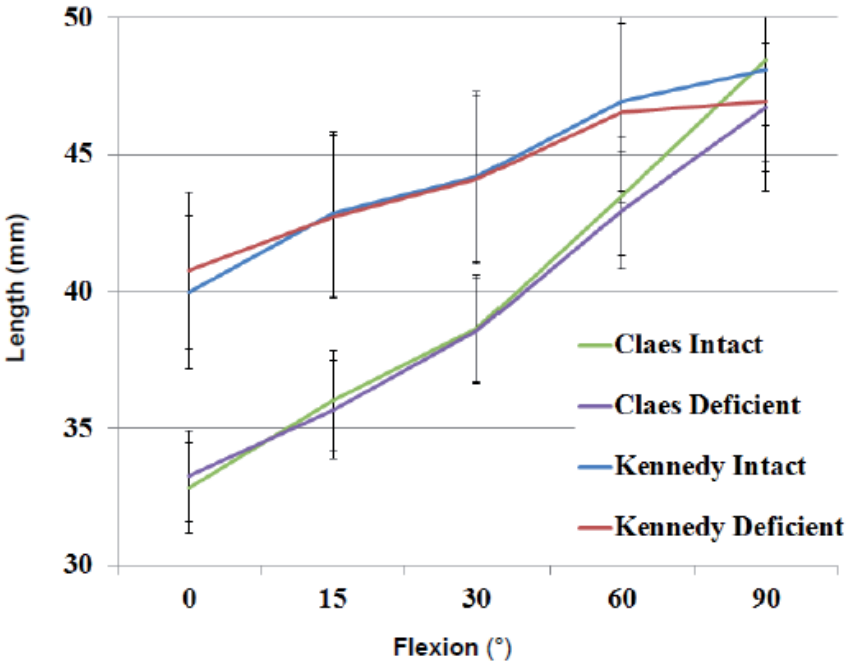

Figure 2. Anterolateral ligament (ALL) length (mm) in intact and anterior cruciate ligament (ACL)-deficient knees (femoral attachment of the ALL based on Claes et al.,[2] bottom lines; femoral attachment of the ALL based on based on Kennedy et al.,[11] top lines) as function of flexion (°) in 10 patients with acute, isolated rupture of the ACL. Values are mean ± SD.

DISCUSSION

The most important findings of this study were that the ALL was not isometric between any of the flexion angles and was not affected by ACL deficiency, and that the non-anatomic extra-articular reconstructions demonstrated more biomechanically favorable length change patterns with the smallest percent length increase during knee flexion. There are several recent studies that have elucidated the anatomy and biomechanical role of the ALL in cadaveric knees. Based on these in vitro data, reconstruction techniques are proposed to improve anterolateral stability in ACL-deficient knees. However, there is an ongoing debate on what might be the most optimal reconstruction, due to the variability in the results of these cadaveric studies. The present study is the first in vivo biomechanical analysis of the ALL and related anterolateral reconstructions. We described the length change patterns of the anatomic ALL and various non-anatomic anterolateral extra-articular reconstructions in

healthy and ACL-deficient knees during in vivo weight-bearing flexion, using combined MR and dual fluoroscopic imaging techniques.

In the present study, the ALL as described by the Claes et al.[2] was not isometric between any of the flexion angles, as was believed based on some cadaveric work.[4] This finding is consistent with the in vitro study by Kittl et al., which measured a similar length increase of the ALL from full extension to 90° of flexion of 19%.[12] However, in the present study, the length increase of the ALL during in vivo weight bearing was actually closer to 50% at 90° of flexion. Such increase during knee flexion suggests that an anatomic reconstruction of this structure as described at this femoral attachment might likely be biomechanically unfavorable. Specifically, an anatomic ALL graft with its femoral fixation slightly anterior and distal to the attachment of the FCL would be either slack in extension, where it is intended to correct rotational instability,[1, 5] or too tight in flexion, potentially causing

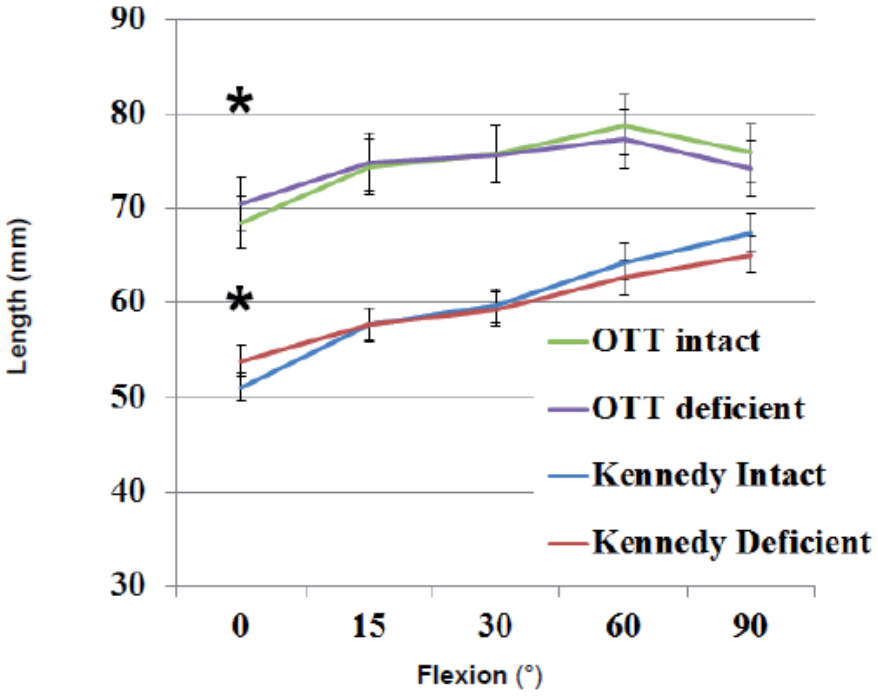

Figure 3. Length of non-anatomic extra-articular reconstructions (mm) in intact and anterior cruciate ligament (ACL)-deficient knees with the tibial attachment on Gerdy tubercle and the femoral attachment over-the-top proximal to the lateral epicondyle (OTT, top lines) and femoral attachment posterior to the FCL (modified Kennedy, bottom lines) as a function of flexion (°) in 10 patients with acute, isolated rupture of the ACL. Values are mean ± SD. * = $P < 0.05$

overconstraint of the lateral compartment. Interestingly, when the femoral attachment of the anatomic ALL was moved only a few mm posterior and proximal to the FCL attachment, as described in the anatomic study by Kennedy et al,[11] the same length change pattern persisted, but with only a 20 % increase during knee flexion from 0° to 90°.

The length change patterns of the non-anatomic extra-articular reconstructions that were modelled on the 3-D models of healthy knees in the present study demonstrated more biomechanically favorable behavior, analogous to the in vitro biomechanical benefits of the traditional extra-articular reconstructions described several decades ago.[6, 7, 17] Particularly, the theoretical graft attached to Gerdy's tubercle, tunneled under the FCL and attached proximally to an OTT position showed only a 15% length increase from 0° to 90° of flexion. This finding corroborates the conclusion of the recent biomechanical study by Spencer et al. in which it was not an anatomic ALL reconstruction, but rather a non-anatomic lateral extra-articular tenodesis which was able to control both anterior and rotational laxity.[22] However, this graft reconstruction would be simultaneously the longest reconstruction, therefore possibly resulting in a less stiff reconstruction. In addition, there might be concern about interference of the OTT graft tenodesis with the femoral tunnel of the ACL reconstruction. An alternative to the OTT reconstruction, based on the present findings, would be to modify the anatomic ALL reconstruction based on the description by Kennedy et al,[11] by leaving the femoral point identical but moving the tibia fixation anteriorly to Gerdy's tubercle. This reconstruction was slightly less isometric than the OTT reconstruction, but could be performed with a shorter, hence stiffer, graft and would evade the possible interference with the femoral tunnel of the ACL reconstruction.

Because anatomic ALL and non-anatomic extra-articular reconstructions are intended to control the anterolateral subluxation of the tibia seen in some ACL-deficient patients, we determined which of the length change patterns of the various reconstruction options were affected by ACL deficiency, thereby indirectly indicating which reconstruction option would have the capability at offering the most efficient control of the kinematic changes seen in ACL deficiency. In the present study, ACL deficiency did not affect the anatomic ALL length at any of the flexion angles. It should be noted that an effect of ACL deficiency might have been noticed if forced internal rotation or during pivot maneuvers were tested rather than knee flexion in neutral rotation.[16, 19] Interestingly though, ACL deficiency did cause a significant increase in graft length at 0° of flexion in the non-anatomic theoretical reconstruction grafts during the loading condition used in the present study. This finding could be explained by the altered angle of the graft on the tibia, hereby exacerbating the effect of the minor increase in internal rotation that is seen in ACL deficient knees during weight-bearing flexion.

We acknowledge some limitations to this study. We acquired data during only one functional activity, a single leg lunge. Other in vivo activities such as walking and stair climbing should be considered in future studies. In the present study, we measured the

length of the ALL and related extra-articular reconstructions as the shortest distance between the attachment site points on the 3-D models projected to the bony surfaces. These data cannot be directly related to ligament strains because the reference lengths of the ligaments (zero-load length) are unknown. On the available 1.5T MR images, we could not identify the ALL, and by no means its precise attachment anatomy, with the same certainty as described by others.[9, 13] We therefore used the meticulously performed anatomic descriptions by Claes et al.[2] and Kennedy et al.[11] instead to position the ALL attachment sites on the 3-D knee models. In addition, no actual non-anatomic reconstructions were performed in this study. Rather, the length measurements for these reconstructions were performed between theoretical points as proposed in previous studies.[12] As mentioned above, weight bearing flexion of the knee was performed with the foot in neutral position. We could therefore not assess what the effect of forced internal rotation would be on the elongation behavior of the ALL.

As the presented data were obtained during only one functional in vivo activity—namely, the single leg lunge—we advise caution when extrapolating the data to other functional activities. Nevertheless, we believe that these findings might be useful for the design of improved treatment protocols for anterolateral instability in ACL deficient patients. On the basis of our data, it could be theorized in future studies that for optimal anterolateral reconstructions one could choose either an OTT to Gerdy's tubercle reconstruction fixed at 60° of flexion (i.e., the smallest percent length increase, but longer graft hence less stiff reconstruction, with a drop at 90° of flexion, and possible interference with ACL tunnel), or a modified ALL reconstruction (i.e., femur attachment proximal and posterior to the FLC attachment and tibia attachment at Gerdy's, fixed at 90°) with slightly less isometry, but without the drop in length at 90°, no risk of interference with the ACL tunnel, and a shorter graft.

In conclusion, this study presents the first in vivo data on the ALL and related anterolateral reconstructions, both in healthy knees and ACL-deficient knees. The anatomic ALL reconstruction was not isometric between any of the flexion angles, and was not affected by ACL deficiency. The non-anatomic extra-articular reconstructions showed more biomechanically favorable length change patterns with the smallest percent increase in length during knee flexion.

REFERENCES

1. Carson WG Jr. Extra-articular reconstruction of the anterior cruciate ligament: lateral procedures. Orthop Clin North Am. 1985;16:191-211.
2. Claes S, Vereecke E, Maes M, Victor J, Verdonk P, Bellemans J. Anatomy of the anterolateral ligament of the knee. J Anat. 2013;223:321-328.
3. Defrate LE, Papannagari R, Gill TJ, Moses JM, Pathare NP, Li G. The 6 degrees of freedom kinematics of the knee after anterior cruciate ligament deficiency: an in vivo imaging analysis. Am J Sports Med. 2006;34:1240-1246.
4. Dodds A, Halewood C, Gupte C, Williams A, Amis A. The anterolateral ligament anatomy, length changes and association with the Segond fracture. Bone Joint J. 2014;96(3):325-331.
5. Dodds AL, Gupte CM, Neyret P, Williams AM, Amis AA. Extraarticular techniques in anterior cruciate ligament reconstruction: a literature review. J Bone Joint Surg Br. 2011;93:1440-1448.
6. Draganich LF, Reider B, Ling M, Samuelson M. An in vitro study of an intraarticular and extraarticular reconstruction in the anterior cruciate ligament deficient knee. Am J Sports Med. 1990;18:262-266.
7. Engebretsen L, Lew WD, Lewis JL, Hunter RE. The effect of an iliotibial tenodesis on intraarticular graft forces and knee joint motion. Am J Sports Med. 1990;18:169-176.
8. Helito CP, Demange MK, Bonadio MB, et al. Anatomy and histology of the knee anterolateral ligament. Orthop J Sports Med. 2013;1(7):2325967113513546.
9. Helito CP, Helito PV, Costa HP, Bordalo-Rodrigues M, Pecora JR, Camanho GL, Demange MK. MRI evaluation of the anterolateral ligament of the knee: assessment in routine 1.5-T scans. Skeletal Radiol. 2014;43:1421-1427.
10. Imbert P, Belvedere C, Leardini A. Knee laxity modifications after ACL rupture and surgical intra- and extra-articular reconstructions: intra-operative measures in reconstructed and healthy knees. Knee Surg Sports Traumatol Arthrosc. 2015 Jun 3.
11. Kennedy MI, Claes S, Fuso FA, et al. The Anterolateral Ligament: An Anatomic, Radiographic, and Biomechanical Analysis. Am J Sports Med. 2015;43:1606-1615.
12. Kittl C, Halewood C, Stephen JM, Gupte CM, Weiler A, Williams A, Amis AA. Length change patterns in the lateral extra-articular structures of the knee and related reconstructions. Am J Sports Med. 2015;43:354-62.
13. Kosy JD, Mandalia VI, Anaspure R. Characterization of the anatomy of the anterolateral ligament of the knee using magnetic resonance imaging. Skeletal Radiol. 2015;44:1647-1653.
14. Kozanek M, Fu EC, Van de Velde SK, Gill TJ, Li G. Posterolateral structures of the knee in posterior cruciate ligament deficiency. Am J Sports Med. 2009;37:534-541.
15. Li G, Van de Velde SK, Bingham JT. Validation of a non-invasive fluoroscopic imaging technique for the measurement of dynamic knee joint motion. J Biomech. 2008;41:1616-1622.

16. Lutz C, Sonnery-Cottet B, Niglis L, Freychet B, Clavert P, Imbert P. Behavior of the anterolateral structures of the knee during internal rotation. Orthop Traumatol Surg Res. 2015;101:523-528.

17. Noyes F, Barber S. The effect of an extra-articular procedure on allograft reconstructions for chronic ruptures of the anterior cruciate ligament. J Bone Joint Surg Am. 1991;73:882-892.

18. Park SE, DeFrate LE, Suggs JF, Gill TJ, Rubash HE, Li G. The change in length of the medial and lateral collateral ligaments during in vivo knee flexion. Knee. 2005;12:377-382.

19. Parsons EM, Gee AO, Spiekerman C, Cavanagh PR. The biomechanical function of the anterolateral ligament of the knee. Am J Sports Med. 2015;43:669-674.

20. Saiegh YA, Suero EM, Guenther D, et al. Sectioning the anterolateral ligament did not increase tibiofemoral translation or rotation in an ACL-deficient cadaveric model. Knee Surg Sports Traumatol Arthrosc. 2015 Sep 16.

21. Sonnery-Cottet B, Thaunat M, Freychet B, Pupim BH, Murphy CG, Claes S. Outcome of a Combined Anterior Cruciate Ligament and Anterolateral Ligament Reconstruction Technique With a Minimum 2-Year Follow-up. Am J Sports Med. 2015;43:1598-1605.

22. Spencer L, Burkhart TA, Tran MN, Rezansoff AJ, Deo S, Caterine S, Getgood AM. Biomechanical Analysis of Simulated Clinical Testing and Reconstruction of the Anterolateral Ligament of the Knee. Am J Sports Med. 2015;43:2189-2197.

23. Terry GC, Norwood LA, Hughston JC, Caldwell KM. How iliotibial tract injuries of the knee combine with acute anterior cruciate ligament tears to influence abnormal anterior tibial displacement. Am J Sports Med. 1993;21:55-60.

24. Van de Velde SK, Gill TJ, Li G. Evaluation of kinematics of anterior cruciate ligament-deficient knees with use of advanced imaging techniques, three-dimensional modeling techniques, and robotics. J Bone Joint Surg Am. 2009;91 Suppl 1:108-14.

25. Van de Velde SK, Bingham JT, Hosseini A, Kozanek M, DeFrate LE, Gill TJ, Li G. Increased tibiofemoral cartilage contact deformation in patients with anterior cruciate ligament deficiency. Arthritis Rheum. 2009;60:3693-3702.

26. Van de Velde SK, DeFrate LE, Gill TJ, Moses JM, Papannagari R, Li G. The effect of anterior cruciate ligament deficiency on the in vivo elongation of the medial and lateral collateral ligaments. Am J Sports Med. 2007;35:294-300.

27. Vieira ELC, Vieira EA, Teixeira da Silva R, dos Santos Berlfein PA, Abdalla RJ, Cohen M. An anatomic study of the iliotibial tract. Arthroscopy. 2007;23:269-274.

28. Vincent J-P, Magnussen RA, Gezmez F, et al. The anterolateral ligament of the human knee: an anatomic and histologic study. Knee Surg Sports Traumatol Arthrosc. 2012;20:147-152.

29. Zarins B, Rowe C. Combined anterior cruciate-ligament reconstruction using semitendinosus tendon and iliotibial tract. J Bone Joint Surg Am. 1986;68:160-177.

30. Zens M, Niemeyer P, Ruhhammer J, et al. Length Changes of the Anterolateral Ligament During Passive Knee Motion: A Human Cadaveric Study. Am J Sports Med. 2015;43:2545-2552.

CHAPTER 11

General discussion

BACKGROUND

The distress that is caused by cruciate ligament injury is substantial, particularly in the young and active population. It has been estimated that of those patients that are evaluated with acute traumatic hemarthrosis of the knee up to 77% and 37% have an injury of the ACL and the PCL, respectively.[8,33,56,65] Acute rupture of one of the cruciate ligaments is associated with meniscal tears, chondral damage, and injury to the collateral ligaments.[8,12,28,33,56,65,77] As the ligamentous injury becomes more chronic, an increasing incidence of joint swelling, instability, and meniscal tears is found.[2,10,20,25,38,59,61] Patients with cruciate ligament deficiency often develop alterations in quadriceps muscle performance with weakness and atrophy[6,9,78,85] and degeneration of the patellofemoral joint cartilage.[17,59] Ultimately, rupture of either the ACL or the PCL is associated clinically with an increased incidence,[10,17,25,38,71] an earlier onset,[71] and a faster progression[37] of knee OA.

Each year ~200,000 ACL deficient patients opt for ACL reconstruction in the United States,[11] drawn by the excellent postoperative stability, health-related quality of life, and the ability to return to sports.[5,46] However, in patients who have undergone ACL reconstruction with a bone–patellar tendon–bone graft, some of the most prevalent complications are persistent patellar irritability,[72] patellofemoral pain,[1,4,16,24,26,27,57,72] and quadriceps weakness.[24,72] In addition, a lack of rotational stability, confirmed by a positive pivot-shift test, often persists even after the most recent ACL reconstruction techniques.[14] Eventually, no long-term difference in OA prevalence has been detected between patients that opted for conservative treatment and those that opted for surgery.[54]

Compared to the annual volume of ACL reconstructions, only a fraction of the relative number of surgical procedures for PCL deficiency is performed. Clinicians have traditionally advocated nonoperative treatment of a torn PCL because many patients with isolated PCL deficiency have good functional results.[18,66] However, others have supported surgical reconstruction based on long-term follow-up studies revealing an association between the increased posterior displacement of the tibia and joint degeneration in PCL deficient knees.[10,17,44,73] Unfortunately, analogous to the inability of ACL reconstruction to prevent long-term joint degeneration, OA has been reported in 20% to 60% of patients after PCL reconstruction as well.[17,35,70]

A tremendous amount of research has been done on the healthy, injured, and surgically reconstructed joint biomechanics, in the hopes of developing new and improved treatment strategies that would counter both short-term and long-term complications of cruciate ligament deficiency. In orthopaedic surgery, it is widely assumed that the reconstruction technique that would generate the most optimal biomechanical joint environment is believed to result in a clinically satisfactory stable knee and avert the long-term articular cartilage degeneration. For example, performing a double-bundle ACL or PCL reconstruction has been advocated as an alternative to standard single-bundle

reconstruction, as the former would be more capable at controlling rotational deviations seen in cruciate ligament deficient patients. Similarly, more anatomic placement of the graft tunnels has been stressed lately as this might restore native kinematics closer to normal. More recently in ACL surgery, emphasis has shifted to the extra-articular structures of the knee that might be injured during ACL rupture. Several recent studies have documented the anterolateral ligament (ALL) in cadaveric knees and its possible role in controlling rotational stability, together with the anterior cruciate ligament.[15,22,39] An unrecognized injury to the ALL might be responsible for residual internal rotation and a positive pivot shift after ACL reconstruction.[68] Based on little in vitro biomechanical data with considerable variability both anatomic ALL and non-anatomic anterolateral reconstructions are now performed in the hopes of improving the stability of ACL-deficient patients.

To understand possible link between postoperative knee biomechanics and postoperative clinical outcome, an accurate, minimally invasive method to analyze the in vivo joint biomechanics was needed. However, measuring knee biomechanics and its subtle changes after injury and the various proposed reconstruction options of the cruciate ligaments with an acceptable degree of accuracy has been technically challenging. Historically, joint kinematics have been studied using cadaveric specimens. Knowledge obtained from these studies was vital for our current approach to the treatment of various articular pathologies. However, due to the complexity of muscle loading patterns, the simulation of the human joint function under physiological loads remains difficult in in vitro conditions. Furthermore, factors such as graft healing and postoperative rehabilitation cannot be addressed in vitro. Out of this context, the quest for an accurate, minimally invasive method to analyze the in vivo joint biomechanics was initiated.

Multiple video cameras have been used to track the 3D motions of reflective markers fixed to the skin of study subjects.[13,69] Due to the relative motion between the skin and the underlying bones, as well as the difficulty in identifying external landmarks on the tested joint, there is a certain degree of inaccuracy associated with this technique.[7] One solution that has been proposed to reduce the artifact associated with non-rigid body movement of points placed on the skin during gait analysis was based on uniformly distributing a cluster of points on the limb segment.[3] To entirely eliminate the effect of skin motion, reflective markers have been fixed directly to knee or ankle bones using intracortical pins.[45,84] Another technique, roentgen stereophotogrammatric analysis (RSA), was developed to measure the motion of roentgen opaque markers embedded within bone, which are captured using dual X-ray images.[55,83] The accuracy of kinematic measurements greatly improved. Unfortunately the enhanced precision could only be attained through disruption of the joint, limiting the clinical implementations in the investigation of healthy and cruciate ligament deficient knees.

Recently, CT and MR imaging techniques have been introduced into in vivo musculoskeletal joint biomechanics studies.[34,60,74] These techniques offer 3D quantification

of in vivo morphology and positions of the joint without using invasive markers. Within the imaging equipment however, joint motion is restricted, thereby limiting the flexibility to study various functional activities.

Due to its accessibility, low radiation dosage, and greater freedom of unrestricted motion of the joint, single plane fluoroscopy combined with joint shape-matching has been used extensively for the analysis of articular biomechanics.[58,64,67,86] However, while 3D model matching can theoretically be achieved using a single image, it was found that the use of a single image may not result in the same accuracy in the out-of-plane degrees-of-freedom compared to the in-plane motion.[42,52]

Over the past decade, the research of joint biomechanics in our laboratory has gone through an evolution from in vitro simulation to in vivo measurements.[81] The overall goal of our project was to develop a non-invasive methodology that would not only be capable of capturing joint kinematics in all degrees-of-freedom, but would also be sufficiently accurate for the detailed analysis of subtle articular contact changes during physiologic loading. Furthermore, the methodology would incorporate unmodified and commercially available imaging hardware, so that – once automated algorithms for the various processes are refined – the in vivo analysis of joint biomechanics could be employed in routine clinical settings. Our approach was to combine the benefits of fluoroscopy (i.e. in vivo joint motion) and magnetic resonance imaging (i.e. joint anatomy), while reducing the innate limitations of the techniques in isolation.

PURPOSE

The first purpose of the present thesis was to describe the development and validation of a combined MR and dual fluoroscopic imaging technique to measure in vivo knee joint biomechanics.

The second purpose of the thesis was to present some of the clinical implementation work performed with the imaging methodology, providing a comprehensive insight in (1) the biomechanical impact of ACL and PCL injury on the tibiofemoral cartilage biomechanics, (2) the alterations of the patellofemoral joint in cruciate ligament deficient knees, and finally (3) the effect of intra-articular changes following cruciate ligament deficiency on the surrounding extra-articular structures, including the medial collateral ligaments and the anterolateral structures.

METHODOLOGY

A patient cohort with complaints of knee instability was selected for our clinical studies. These patients had either a diagnosis of acute, isolated ACL rupture or isolated PCL

rupture, as documented by clinical examination findings and findings on MRI. All patients had healthy contralateral knees. Patients had been injured within approximately 4 months of testing. Patients with injury to other ligaments, noticeable cartilage lesions, and injury to the underlying bone were excluded from the study.

The first step of the procedure is the acquisition of a 3D model of the joint that includes the anatomical structures relevant to the study including bones, plus respective cartilage layers[29] or ligament insertion sites.[80] The joint is scanned with a 1.5 or 3.0 Tesla MR scanner, and the acquired images are imported into commercially available solid modeling software (Rhinoceros®, Robert McNeel and Associates, Seattle, WA) to construct 3D surface mesh models. The 3D models are created by digitizing the contours of the anatomical structures within each MR image.

To examine the tissue responses under in vivo loading, the knee is subsequently imaged from two directions during the in vivo motion. Our earliest setup used one 3D fluoroscope (ISO3D, Siemens) for the imaging.[52] This setup was later improved by using an additional fluoroscope[19] to facilitate the investigation of dynamic joint motion. The fluoroscopes that are used for the imaging are commercially available and unmodified (BV Pulsera®, Philips, Bothell, WA). The fluoroscopes have a clearance of approximately one meter between the X-ray source and the image intensifier, allowing the investigated knee to be simultaneously imaged throughout the entire range of motion by the fluoroscopes as the patient performs a wide range of weightbearing activities (such as lunge, treadmill gait and stair ascending-descending.[82]

The fluoroscopic images are then imported in the solid modeling software and placed in the position of the intensifiers of the virtual fluoroscopes. In the following step, the 3D joint model is imported in the same modeling file, placed in the 3D space between the points that replicate the respective fluoroscopes (i.e. placed between the “virtual fluoroscopes”, much like the placement of the patient’s joint between the real fluoroscopes), and viewed from the source points (by setting at origin of the view at the source point and directed at the intensifier point), effectively projecting the 3D model onto the fluoroscopic images. With the modeling file’s viewing screen set to multiple planes, the 3D model can be simultaneously translated and rotated in all degrees-of-freedom in a controlled manner in indefinitely small increments, until the 3D model matches the bony contours on both fluoroscopic images.

By repeating this matching process at selected intervals of the investigated joint motion, a series of joint models that replicate the in vivo 6DOF articular motion is created which form the basis for further biomechanical analysis: parameters such as joint kinematics, location and magnitude of cartilage deformation, and relative ligament elongation and orientation could be derived from the matched sequences.

VALIDATION

For the complicated 6DOF biomechanics of the knee, it is a challenge to determine exactly the joint motion in space and use it as a gold standard to validate a biomechanics measurement technique. We performed a series of validation studies to appreciate the capabilities and limitations of the dual fluoroscopy to analyze the function, dysfunction, and treatment of the knee.

Tibiofemoral kinematics.

First, we used standard geometric spheres made from ceramic, steel, and tungsten rolling down a slope to demonstrate the capability of the imaging technique to determine the object positions under changing speeds. The translational pose of the spheres could be recreated to less than 0.15 ± 0.09 mm for velocities below 300 mm/s.

Next, tantalum beads were inserted into the femur and tibia of two fresh frozen cadaver knees to compare the dynamic kinematics measured by matching knee models to the kinematics from the tantalum bead matching — a technique similar to RSA. Each cadaveric knee was attached to the crosshead of a tensile testing machine (MTS QTest 5, Eden Prairie, MN), which has an accuracy of 0.001 mm in translation, and was vertically translated at a rate of 16.66 mm/s while images were captured with the fluoroscopes. Subsequently, the tibia was held fixed and the femur manually flexed from full extension to 90° of flexion, as the fluoroscopes acquired images. In vitro translation of the cadaver knee using the tensile testing machine deviated from predicted values by 0.08 ± 0.14 mm for the matched knee models. The difference between matching the knee and tantalum bead models during the dynamic flexion–extension motion of the knee was 0.1 ± 0.65°/s in flexion speed; 0.24 ± 0.16 mm in posterior femoral translation; and 0.16 ± 0.61° in internal–external tibial rotation.

Finally, we applied the method to investigate the knee kinematics of a living subject during a step ascent and treadmill gait. High repeatability was demonstrated for the in vivo application. Thus, the combined MR and dual fluoroscopy imaging technique provides an easy and powerful tool for accurately determining 6DOF positions of the tibiofemoral joint when performing daily functional activities.

Patellofemoral kinematics.

The method using imbedded spherical beads was used for the validation of 6DOF patellofemoral kinematics measurement as well. Patellar tracking obtained using the fluoroscopic technique and the RSA-like method was very similar. On average, the difference of the two methods was 0.09 ± 0.16mm in patellar shift along the flexion path of the knee. The difference in patellar rotation was 0.13 ± 0.32°, and 0.12 ± 0.21° in patellar tilt between the two methods.[63]

Cartilage measurement.

Assessment of the accuracy and precision of cartilage thickness measurement based on 3-D meshed knee models created with 3T MR images is critical for the appreciation of biomechanical parameters such as in vivo cartilage contact deformation. In a validation study, we used calibrated digital images of a series of cartilage cross-sections from cadaver donors as the gold standard since the actual cartilage boundaries can be clearly delineated from the specimens. We found that the average absolute difference between the cartilage thickness values based on the 3-D MRI–based knee models and those captured from the specimens from the cadaver donors was 0.04 ± 0.01 mm – sufficiently accurate for the determination of clinically significant cartilage contact deformation differentials. With Pearson correlation coefficients of >0.984 (P<0.0001) and ICC coefficients ranging from 0.989 to 0.999 (P<0.0001), excellent intra- and interobserver precision was obtained.

We finally compared the in vivo kinematics of the uninjured contralateral knees of patients with cruciate ligament deficiency with knee kinematics of age-matched patients without joint injury and found no differences across the groups in all rotations and translations during weightbearing flexion. This finding assured that the healthy, contralateral knee of cruciate ligament deficient patients might be used as a reliable normal kinematic control.[43]

IMPLEMENTATION

In a previous in vivo analysis of the tibiofemoral joint kinematics in patients with ACL deficiency, an increased anterior translation (~3 mm) and internal rotation (~2°) of the tibia at low flexion angles as compared with the healthy control knee were found.[19] Similar findings have been well documented in the literature.[29,53] ACL deficiency also caused an increased medial tibial translation of ~1 mm. These changes in tibiofemoral kinematics after ACL injury were expected to lead to changes in the tibiofemoral cartilage contact characteristics. Specifically, the medial shift of the tibia after ACL deficiency would alter the contact stress distributions in the tibiofemoral cartilage near the medial tibial spine. Indeed, in the presence of ACL injury, cartilage contact points shifted not only posteriorly, as was expected based on the increased anterior tibial translation, but also laterally on the surface of the tibial plateau.[48] In the medial compartment, the contact points shift toward the medial tibial spine, a region where degeneration is observed in patients with chronic ACL injuries.[23]

Analogous to the changes in tibiofemoral kinematics following ACL injury, changes in tibiofemoral kinematics have been described in PCL deficiency: PCL deficiency was found not only to increase posterior tibial translation and external tibial rotation,[32,31,47,49] but also increased lateral translation of the tibia.[50]

The question remained as to how and to what extent the subtle changes in in vivo joint kinematics affect the cartilage contact biomechanics of the cruciate ligament deficient knee.

Tibiofemoral joint biomechanics in ACL deficiency and PCL deficiency.

In our study of cartilage biomechanics in patients with ACL deficiency, we found a posterior and lateral shift in cartilage contact location on the surface of the tibial plateaus following ACL injury as described before.[79] However, when determining the location of cartilage contact based on the location where peak cartilage deformation occurred, we found that the magnitude of the posterior and lateral shift following ACL rupture (~5 mm) was greater than that previously reported.[48] A possible explanation for the discrepancy in the magnitude of shift based on measurement methodology could be found in the regional variations in cartilage thickness. When determining the cartilage contact location based on the closest interarticular distance between the bony surfaces of the tibiofemoral joint[21] or the centroid of the tibiofemoral cartilage contact area,[48] regional variations in the thickness of underlying cartilage are not taken into account. In the present study, the region of tibiofemoral cartilage contact was not only smaller following rupture of the ACL, but also had significantly thinner cartilage at contact in both the medial and lateral compartments as compared with the thickness at contact in the intact knees. In other words, the minimal shift in the location of the cartilage contact area to regions of thinner cartilage as reported previously[48] resulted in a considerable change in cartilage loading distribution within the knee joint.

The posterior and lateral shift in cartilage contact to thinner articular regions increased the magnitude of cartilage deformation in those regions. The maximum relative increase in cartilage contact deformation after ACL rupture occurred at full extension in the medial compartment, where deformation of 19 ± 4% was found in healthy knees and 29 ± 9% in ACL-deficient knees as compared with deformation of 24 ± 9% and 33 ± 6%, respectively, in the lateral compartment. The relatively greater increase in cartilage deformation in the medial compartment as compared with the lateral compartment relates to the increased development of OA in the medial compartment of the knee joint, as was observed during arthroscopic examination of 130 ACL-deficient patients.[59]

In our study on the location and magnitude of tibiofemoral cartilage deformation in PCL deficient knees, we found that in the medial compartment of these knees, the location and magnitude of peak cartilage deformation were significantly changed, as compared with the findings in the intact contralateral knees, between 75° and 120° of flexion, with a more anterior and medial location as well as an increased magnitude. In the lateral compartment, no significant differences were found in the location or magnitude of peak tibiofemoral cartilage deformation between the intact and posterior cruciate ligament-deficient knees.

As we did not detect differences in the cartilage biomechanics between the intact and PCL deficient knees during the single leg lunge between 0° and 60° of flexion, our findings

suggest that rehabilitation exercises might be safely performed in this range of flexion. On the other hand, repetitive deep knee squats should be avoided by subjects with PCL deficiency, so as not to increase the tibiofemoral cartilage deformation. Second, it is interesting to note that the magnitude of medial contact shift in the posterior cruciate ligament-deficient knees was on the same order as the magnitude of the anterior contact shift. This suggests that, when a PCL reconstruction is performed with either a single or a double-bundle graft, recreation of the mediolateral stability of posterior cruciate ligament-deficient knees may be as important as the surgical improvement of anteroposterior translation. Finally, in a recent cadaver study, Giffin et al. demonstrated, with a robotic testing system, that increasing the tibial slope with a sagittal osteotomy successfully reduced the abnormal tibial sag in the posterior cruciate ligament-deficient knee, shifting the resting position of the tibia anteriorly.[30] On the basis of our data, it could be theorized in future studies that the osteotomy should include a varus component, possibly reducing the abnormal medial shift following posterior cruciate ligament injury and thereby possibly reducing the increase in cartilage deformation.

Patellofemoral joint biomechanics in ACL deficiency and PCL deficiency.

The changes in tibiofemoral kinematics upon losing the cruciate ligament's function were found to upset the entire knee joint. It was already shown previously in our laboratory that the patellofemoral joint is not an isolated unit in the knee. Instead, a kinematic coupling was described between the patellofemoral and the tibiofemoral articulations, connected by the patellar tendon.[51] We were therefore not surprised to find that not only the tibiofemoral biomechanics but also the patellofemoral biomechanics were affected by cruciate ligament deficiency. For instance, we found in ACL deficient knees that the elongation of the patellar tendon was increased, and the orientation changed, compared to that of the patellar tendon in the healthy knee. The altered biomechanics of the patellar tendon subsequently resulted in a decreased flexion and increased valgus rotation and tilt of the patella, with a proximal and lateral shift in patellofemoral cartilage contact location as final result.

Similarly in PCL deficiency, we found that the changes seen in tibiofemoral kinematics following rupture of the ligament resulted in altered patellofemoral kinematics. PCL deficiency increased the patellar flexion angle and decreased the lateral shift, tilt, and valgus rotation of the patella at flexion angles 90° and greater. Due to the congruency of the patellofemoral joint, these changes in patellofemoral kinematics resulted in changes in the location of the patellofemoral cartilage contact point. PCL deficiency caused a distal and medial shift of cartilage contact point from 75° to 120° of flexion.

When combining the present patellofemoral joint data with our analysis of the cartilage contact deformation in PCL deficiency, it becomes apparent that a target range of motion could be formulated for PCL deficient patients in which knee motion might be safely performed. During the single-leg lunge between 0°and 60° of knee flexion, we did not

detect differences in either tibiofemoral or patellofemoral joint biomechanics of the intact and the PCL deficient knee. Therefore, rehabilitation exercises might be safely performed in this range of flexion. On the other hand, repetitive deep knee squats should be avoided in PCL deficient subjects, so as not to excessively alter normal patellofemoral cartilage loading.

Medial collateral ligament elongation in ACL deficiency.

The orientation of the MCL is approximately parallel to the tibial shaft at full extension.[80] Therefore, the increased internal tibial rotation associated with ACL injury would be expected to elongate the MCL throughout the range of flexion. Indeed, when we measured the apparent elongation of both superficial and deep fibers of the MCL in ACL deficient knees, at each flexion angle the apparent length of the MCL was significantly increased to that of the healthy, contralateral knees. These altered length patterns of the MCL, associated with the changes in tibiofemoral joint kinematics after ACL injury, demonstrate that deficiency of the ACL upsets the in vivo knee homeostasis and puts the associated joint environment at greater risk of secondary injury.

The anterolateral ligament and related reconstructions.

Whereas the above-cited studies were mainly of explanatory nature, providing the clinician with possible biomechanical substantiation for the clinical complaints and long-term complications seen in ACL deficiency and reconstruction, our study of the theoretical elongation patterns of anatomic ALL and non-anatomic lateral extra-articular reconstructions had a more direct, practical emphasis.

In 2013, Claes et al. described in great detail the anatomy of the ALL – a ligamentous structure at the anterolateral aspect of the knee originally described by Segond in 1879.[15] Several subsequent studies further elucidated the anatomy and biomechanical role of the ALL in cadaveric knees. Based on these in vitro data, reconstruction techniques were proposed to improve anterolateral stability in ACL deficient knees. However, a debate arose amongst surgeons and researchers on what might be the most optimal reconstruction, due to the variability in the results of these cadaveric studies. Some groups have advised securing the ALL tenodesis in extension,[75] others argued for tensioning and fixation of the ALL graft at 90° of flexion,[87] yet others have reasoned against performing an anatomic ALL reconstruction altogether.[36,41,76]

We published our own anatomic ALL tenodesis technique, using an autograft harvest from the iliotibial tract.[40] The graft was proximally attached slightly anterior to the origin of the lateral collateral ligament and proximal and posterior to the popliteus tendon, tunneled deep to the iliotibial tract, and distally secured midway between the tip of the fibular head and the Gerdy tubercle, with the knee in 90° of flexion and slight exorotation. Our initial enthusiasm for the anatomic ALL reconstruction was tempered though when we noticed

some early failures including pull-out from the tenodesis anchors. We therefore aimed to determine which anterolateral reconstruction, whether an anatomic ALL or a non-anatomic tenodesis, fixed at which flexion angle would be most biomechanically favorable.

To do so, we modeled the ALL and related extra-articular reconstructions and their apparent elongation pattern on the healthy and ACL deficient knees that were already analyzed in our previous studies. For the analysis of anatomic ALL length change, the tibial point midway between the center of Gerdy tubercle and the anterior margin of the fibular head was connected with either (1) the femoral point slightly anterior-distal with respect to the attachment of the FCL (Claes et al.),[15] or (2) the femoral point posterior and proximal to the FCL origin (Kennedy et al.).[39] For the analysis of theoretical non-anatomic extra-articular reconstruction grafts, the tibial point on Gerdy tubercle was connected with either (1) the more proximal OTT extra-articular reconstruction position on the lateral femur with the connecting curve always projected so that the theoretical graft intersected with the FCL, or (2) the femoral point of the ALL posterior and proximal to the FCL origin.

We found that the ALL was not isometric between any of the flexion angles and was not affected by ACL deficiency, and that the non-anatomic extra-articular reconstructions demonstrated more biomechanically favorable length change patterns with the smallest percent length increase during knee flexion. The length increase of the ALL during in vivo weight bearing was close to 50% at 90° of flexion. Such increase during knee flexion suggests that an anatomic reconstruction of this structure as described at this femoral attachment might likely be biomechanically unfavorable. Specifically, an anatomic ALL graft with its femoral fixation slightly anterior and distal to the attachment of the FCL would be either slack in extension, where it is intended to correct rotational instability, or too tight in flexion, potentially causing overconstraint of the lateral compartment. The most biomechanically favorable reconstruction was an over-the-top tenodesis, where the theoretical graft is attached to Gerdy tubercle, tunneled under the FCL and attached proximally to an OTT position – showing only a 15% length increase from 0° to 90° of flexion.

CURRENT AND FUTURE PERSPECTIVES

Current clinical practice is increasingly guided by evidence-based medicine, using patient reported outcomes as measures in properly designed prospectively randomized trials. We believe that the addition of the in vivo biomechanical analysis early on in the introduction phase of new surgical techniques for cruciate ligament deficiency has a valuable place in both detecting early unfavorable postoperative patterns (such as overconstraint following anatomic ALL reconstruction) and determining which intervention might be beneficial for patients in the long-term – analogous to the established predictive properties of RSA in the phased introduction of joint prosthesis.[62] Patient reported outcomes are of course necessary,

but they are limited by design to assessing the subjective cross-sectional perception of knee function. The biomechanical analysis of the knee, as outlined in this thesis, has the potential to intercept any underlying disturbance of joint homeostasis in response to various treatment modalities which would be detrimental if left untreated.

One of the main advantages of the combined MR and dual fluoroscopic imaging technique is that, in addition to its high accuracy, relatively low radiation and non-invasive nature, it places the in vivo dynamic analysis of various musculoskeletal joints within reach of virtually every researcher working in a routine clinical setting.

The biomechanical analysis of the healthy and cruciate ligament deficient knee that has been established in this thesis will be the baseline for several clinical studies, validating surgical interventions. For example, based on our theoretical modeling of the elongation pattern of the ALL and related lateral extra-articular reconstructions, we have modified our technique to match the lateral reconstruction which was most isometric throughout the range of flexion. We are currently conducting a randomized trial, measuring the tibiofemoral kinematics of ACL deficient patients with combined anterolateral instability in which the ACL reconstruction is performed with or without the modified lateral extra-articular tenodesis.

The biomechanics and the possible predictions based on these measurements will be coupled with economics parameters, and the most efficient and patient-centered treatment modality will be calculated (Figure 1).

Another exciting new direction will be the incorporation of advanced quantitative MR imaging within our methodology. We are currently unable to appreciate the extent of potential cartilage softening that existed at the time of the injury and were thus unable to resolve the “chicken-or-egg” issue. Were our measured cartilage deformation differentials attributable to the cruciate ligament deficient knee cartilage being more compliant, rather than increased deformation being responsible for the subsequent degeneration onset? Future studies using our imaging methodology, with baseline and follow-up imaging biomarkers, such as T1ρ or delayed gadolinium-enhanced MRI of cartilage incorporated, will follow cruciate ligament deficient patients who are treated conservatively for longer periods. Tibiofemoral contact deformation and the health of the cartilage could therefore be monitored over time to quantify any possible biomechanical relationships (Figure 2).

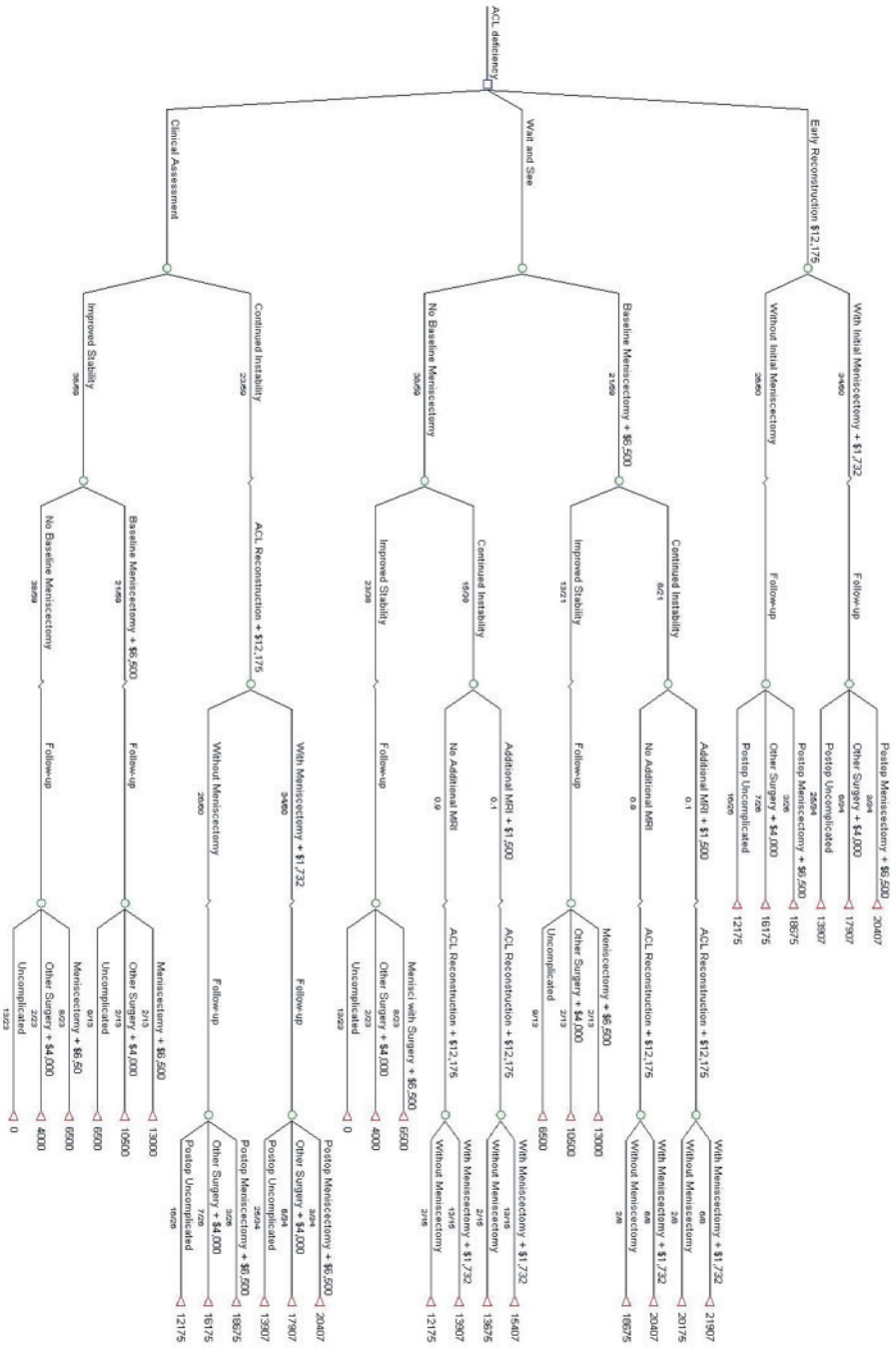

Figure 1. An example of a preliminary decision tree analysis for the calculation of most efficient treatment modality for ACL deficiency. The model can be expended to include additional procedures including lateral tenodesis, meniscal transplantation.

The high incidence of cruciate ligament injuries, especially among the young and active population, requires clinical treatments that will restore normal knee function and prevent long-term disability. Even a small increment of improvement in function would be valuable for this active population. The obtained data are necessary for establishing whether the proposed intervention, whether it is a double-bundle ACL or PCL reconstruction, a lateral extra-articular tenodesis, a meniscal repair, a meniscal transplantation or substitute, would be an advance in vivo, or a step in the wrong direction.

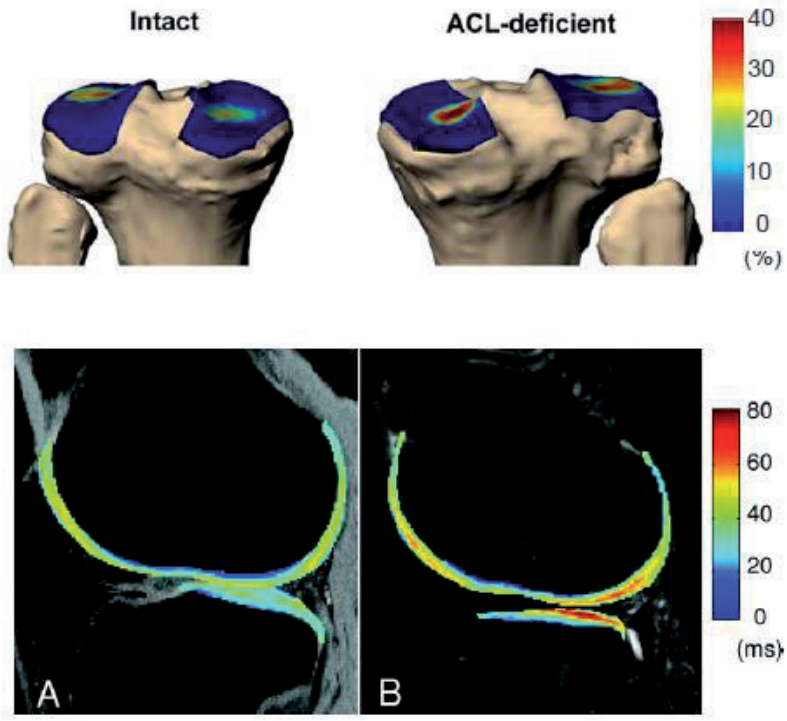

Figure 2. A. Color map of the cartilage deformation for the intact and ACL-deficient tibia at 15° of flexion of a typical subject, illustrating the effect of ACL deficiency on the magnitude of cartilage deformation at lower flexion angles. The darker color depicts a higher magnitude of peak cartilage deformation (%). **B.** Representative T1ρ color-coded map from the lateral side of a healthy control knee and representative T1ρ color-coded map from the lateral side of an ACL injured knee.

REFERENCES

1. Aglietti P, Giron F, Buzzi R, Biddau F, Sasso F. Anterior cruciate ligament reconstruction: bone–patellar tendon–bone compared with double semi-tendinosus and gracilis tendon grafts. A prospective, randomized clinical trial. J Bone Joint Surg Am. 2004;86(10):2143-2155.
2. Aichroth PM, Patel DV, Zorrilla P. The natural history and treatment of rupture of the anterior cruciate ligament in children and adolescents: a prospective review. J Bone Joint Surg Br. 2002;84:38-41.
3. Andriacchi TP, Alexander EJ, Toney MK, Dyrby C, Sum J. 1998. A point cluster method for in vivo motion analysis: applied to a study of knee kinematics. J Biomech Eng 120:743-9.
4. Asano H, Muneta T, Shinomiya K. Evaluation of clinical factors affecting knee pain after anterior cruciate ligament reconstruction. J Knee Surg. 2002;15(1):23-28.
5. Barenius B, Nordlander M, et al. Quality of life and clinical outcome after ACL reconstruction using patellar tendon graft or quadrupled semitendinosus graft: an 8-year follow-up of a randomized controlled trial. Am J Sports Med. 2010; 38:1533–1541.
6. Baugher WH, Warren RF, Marshall JL, Joseph A. Quadriceps atrophy in the anterior cruciate insufficient knee. Am J Sports Med. 1984;12(3):192-195.
7. Benoit DL, Ramsey DK, Lamontagne M et al. 2006. Effect of skin movement artifact on knee kinematics during gait and cutting motions measured in vivo. Gait Posture 24:152-64.
8. Bomberg BC, McGinty JB. Acute hemarthrosis of the knee: indications for diagnostic arthroscopy. Arthroscopy. 1990;6:221-225.
9. Bonamo JJ, Fay C, Firestone T. The conservative treatment of the anterior cruciate deficient knee. Am J Sports Med. 1990;18(6):618-623.
10. Boynton MD, Tietjens BR. Long-term followup of the untreated isolated posterior cruciate ligament-deficient knee. Am J Sports Med. 1996;24(3):306-310.
11. Brophy RH, Wright RW, et al. Cost analysis of converting from single-bundle to double-bundle anterior cruciate ligament reconstruction. Am J Sports Med. 2009; 37:683–687.
12. Butler JC, Andrews JR. The role of arthroscopic surgery in the evaluation of acute traumatic hemarthrosis of the knee. Clin Orthop Relat Res. 1988;228:150-152.
13. Chao EY. 1986. Biomechanics of the human gait. Frontiers in Biomechanics, in Zweifach B, New York, NY: Springer-Verlag 225-219.
14. Chouliaras V, Ristanis S, Moraiti C, Stergiou N, Georgoulis AD. Effectiveness of reconstruction of the anterior cruciate ligament with quadrupled hamstrings and bone-patellar tendon-bone autografts: an in vivo study comparing tibial internal-external rotation. Am J Sports Med. 2007;35(2):189-196.
15. Claes S, Vereecke E, Maes M, Victor J, Verdonk P, Bellemans J. Anatomy of the anterolateral ligament of the knee. J Anat. 2013;223:321-328.
16. Corry IS, Webb JM, Clingeleffer AJ, Pinczewski LA. Arthroscopic reconstruction of the anterior cruciate ligament: a comparison of patellar tendon autograft and four-strand hamstring tendon autograft. Am J Sports Med. 1999;27(4):444-454.

17. Cross MJ, Powell JF. Long-term followup of posterior cruciate ligament rupture: a study of 116 cases. Am J Sports Med. 1984; 12(4):292-297.

18. Dandy DJ, Pusey RJ. The long-term results of unrepaired tears of the posterior cruciate ligament. J Bone Joint Surg Br. 1982;64(1):92-94.

19. Defrate LE, Papannagari R, Gill TJ et al. 2006. The 6 degrees of freedom kinematics of the knee after anterior cruciate ligament deficiency: an in vivo imaging analysis. Am J Sports Med 34:1240-6.

20. Dejour H, Walch G, Peyrot J, Eberhard P. The natural history of rupture of the posterior cruciate ligament. Rev Chir Orthop Reparatrice Appar Mot. 1988;74(1):35-43.

21. Dennis DA, Mahfouz MR, Komistek RD, Hoff W. In vivo determination of normal and anterior cruciate ligament-deficient knee kinematics. J Biomech 2005;38:241–53.

22. Dodds A, Halewood C, Gupte C, Williams A, Amis A. The anterolateral ligament anatomy, length changes and association with the Segond fracture. Bone Joint J. 2014;96(3):325-331.

23. Fairclough JA, Graham GP, Dent CM. Radiological sign of chronic anterior cruciate ligament deficiency. Injury 1990;21: 401–2.

24. Feller JA, Webster KE. A randomized comparison of patellar tendon and hamstring tendon anterior cruciate ligament reconstruction. Am J Sports Med. 2003;31(4):564-573.

25. Fithian DC, Paxton LW, Goltz DH. Fate of the anterior cruciate ligament-injured knee. Orthop Clin North Am. 2002;33:621-636.

26. Fox JA, Nedeff DD, Bach BR Jr, Spindler KP. Anterior cruciate ligament reconstruction with patellar autograft tendon. Clin Orthop Relat Res. 2002;402:53-63.

27. Freedman KB, D'Amato MJ, Nedeff DD, Kaz A, Bach BR Jr. Arthroscopic anterior cruciate ligament reconstruction: a meta-analysis comparing patellar tendon and hamstring tendon autografts. Am J Sports Med. 2003;31(1):2-11.

28. Geissler WB, Whipple TL. Intraarticular abnormalities in association with posterior cruciate ligament injuries. Am J Sports Med. 1993;21(6):846-849.

29. Georgoulis AD, Papadonikolakis A, et al. Three-dimensional tibiofemoral kinematics of the ACL-deficient and reconstructed knee during walking. Am J Sports Med. 2003; 31:75–79.

30. Giffin JR, Stabile KJ, Zantop T, Vogrin TM, Woo SL, Harner CD. Importance of tibial slope for stability of the posterior cruciate ligament deficient knee. Am J Sports Med. 2007;35:1443-9.

31. Gill TJ, DeFrate LE, Wang C, Carey CT, Zayontz S, Zarins B, Li G. The biomechanical effect of posterior cruciate ligament reconstruction on knee joint function. Kinematic response to simulated muscle loads. Am J Sports Med. 2003;31:530-6.

32. Gollehon DL, Torzilli PA, Warren RF. The role of the posterolateral and cruciate ligaments in the stability of the human knee. A biomechanical study. J Bone Joint Surg Am. 1987;69:233-42.

33. Hardaker WT Jr, Garrett WE Jr, Bassett FH III. Evaluation of acute traumatic hemarthrosis of the knee joint. South Med J. 1990;83:640-644.

34. Hirsch BE, Udupa JK, Roberts D. 1989. Three-dimensional reconstruction of the foot from computed tomography scans. J Am Podiatr Med Assoc 79:384-94.

35. Hughston JC, Bowden JA, Andrews JR, Norwood LA. Acute tears of the posterior cruciate ligament: results of operative treatment. J Bone Joint Surg Am. 1980;62(3):438-450.

36. Imbert P, Belvedere C, Leardini A. Knee laxity modifications after ACL rupture and surgical intra- and extra-articular reconstructions: intra-operative measures in reconstructed and healthy knees. Knee Surg Sports Traumatol Arthrosc. 2015 Jun 3.

37. Kannus P, Jarvinen M. Posttraumatic anterior cruciate ligament insufficiency as a cause of osteoarthritis in a knee joint. Clin Rheumatol 1989;8:251–60.

38. Keller PM, Shelbourne KD, McCarroll JR, Rettig AC. Nonoperatively treated isolated posterior cruciate ligament injuries. Am J Sports Med. 1993;21(1):132-136.

39. Kennedy MI, Claes S, Fuso FA, et al. The Anterolateral Ligament: An Anatomic, Radiographic, and Biomechanical Analysis. Am J Sports Med. 2015;43:1606-1615.

40. Kernkamp WA, Van de Velde SK, Bakker EW, van Arkel E. Anterolateral extra-articular soft tissue reconstruction in persistent anterolateral rotatory instability of the knee after anterior cruciate ligament reconstruction. Arthroscopy Techniques, 2015 Dec;4(6):e863–e867.

41. Kittl C, Halewood C, Stephen JM, Gupte CM, Weiler A, Williams A, Amis AA. Length change patterns in the lateral extra-articular structures of the knee and related reconstructions. Am J Sports Med. 2015;43:354-62.

42. Komistek RD, Dennis DA, Mahfouz M. 2003. In vivo fluoroscopic analysis of the normal human knee. Clin Orthop 69-81.

43. Kozanek, M, Van de Velde SK, Gill TJ, Li G: The Contralateral Knee Joint in Cruciate Ligament Deficiency. Am J Sports Med. 2008 Nov;36(11):2151-7.

44. L'Insalata JC, Harner CD. Treatment of acute and chronic posterior cruciate ligament deficiency: new approaches. Am J Knee Surg. 1996;9(4):185-193.

45. Lafortune MA, Cavanagh PR, Sommer HJ, 3rd, Kalenak A. 1992. Three-dimensional kinematics of the human knee during walking. J Biomech 25:347-57.

46. Lewis PB, et al. Systematic review of single-bundle ACL reconstruction outcomes: a baseline assessment for consideration of double-bundle techniques. AJSM. 2008; 36:2028–2036.

47. Li G, Gill TJ, DeFrate LE, Zayontz S, Glatt V, Zarins B. Biomechanical consequences of PCL deficiency in the knee under simulated muscle loads—an in vitro experimental study. J Orthop Res. 2002;20:887-92.

48. Li G, Moses JM, Papannagari R, Pathare NP, DeFrate LE, Gill TJ. Anterior cruciate ligament deficiency alters the in vivo motion of the tibiofemoral cartilage contact points in both the antero-posterior and mediolateral directions. J Bone Joint Surg Am 2006;88:1826–34.

49. Li G, Most E, DeFrate LE, Suggs JF, Gill TJ, Rubash HE. Effect of the posterior cruciate ligament on posterior stability of the knee in high flexion. J Biomech. 2004;37:779-83.

50. Li G, Papannagari R, Li M, Bingham JT, Nha KW, Allred D, Gill TJ. Effect of posterior cruciate ligament deficiency on in vivo translation and rotation of the knee during weightbearing flexion. Am J Sports Med. 2008;36:474-9.

51. Li G, Papannagari R, Nha KW, DeFrate LE, Gill TJ, Rubash HE. The coupled motion of the femur and patella during in-vivo weightbearing knee flexion. J Biomech Eng. 2007;129(6):937.
52. Li G, Wuerz TH, DeFrate LE. 2004. Feasibility of using orthogonal fluoroscopic images to measure in vivo joint kinematics. J Biomech Eng 126:314-8.
53. Logan M, Dunstan E, Robinson J, Williams A, Gedroyc W, Freeman M. Tibiofemoral kinematics of the anterior cruciate ligament (ACL)-deficient weightbearing, living knee employing vertical access open "interventional" multiple resonance imaging. Am J Sports Med 2004;32:720–6.
54. Lohmander LS, Englund PM, et al. The long-term consequence of anterior cruciate ligament and meniscus injuries: osteoarthritis. Am J Sports Med. 2007; 35:1756–1769. [PubMed: 17761605]
55. Lundberg A, Goldie I, Kalin B, Selvik G. 1989. Kinematics of the ankle/foot complex: plantarflexion and dorsiflexion. Foot Ankle 9:194-200.
56. Maffulli N, Binfield PM, King JB, Good CJ. Acute haemarthrosis of the knee in athletes: a prospective study of 106 cases. J Bone Joint Surg Br. 1993;75:945-949.
57. Matsumoto A, Yoshiya S, Muratsu H, et al. A comparison of bone–patellar tendon–bone and bone–hamstring tendon–bone auto- grafts for anterior cruciate ligament reconstruction. Am J Sports Med. 2006;34(2):213-219.
58. Moro-oka TA, Hamai S, Miura H et al. 2008. Dynamic activity dependence of in vivo normal knee kinematics. J Orthop Res 26:428-34.
59. Murrell GA, Maddali S, Horovitz L, Oakley SP, Warren RF. The effects of time course after anterior cruciate ligament injury in correlation with meniscal and cartilage loss. Am J Sports Med. 2001;29:9-14.
60. Nakagawa S, Kadoya Y, Todo S et al. 2000. Tibiofemoral movement 3: full flexion in the living knee studied by MRI. J Bone Joint Surg Br 82:1199-200.
61. Nebelung W, Wuschech H. Thirty-five years of follow-up of anterior cruciate ligament-deficient knees in high-level athletes. Arthroscopy. 2005;21:696-702.
62. Nelissen RG, Pijls BG, Kärrholm J, Malchau H, Nieuwenhuijse MJ, Valstar ER. RSA and registries: the quest for phased introduction of new implants.J Bone Joint Surg Am. 2011 Dec 21;93 Suppl 3:62-5.
63. Nha KW, Papannagari R, Gill TJ, Van de Velde SK, Freiberg AA, Rubash HE, Li G: In-vivo Patellar Tracking: Clinical Motions and Patellofemoral Indices. J Orthop Res. 2008 Aug;26(8):1067-74.
64. Nishinaka N, Tsutsui H, Mihara K et al. 2008. Determination of in vivo glenohumeral translation using fluoroscopy and shape-matching techniques. J Shoulder Elbow Surg 17:319-22.
65. Noyes FR, Bassett RW, Grood ES, Butler DL. Arthroscopy in acute traumatic hemarthrosis of the knee: incidence of anterior cruciate tears and other injuries. J Bone Joint Surg Am. 1980;62:687-695, 757.
66. Patel DV, Allen AA, Warren RF, Wickiewicz TL, Simonian PT. The nonoperative treatment of acute, isolated (partial or complete) posterior cruciate ligament-deficient knees: an intermediate-term follow-up study. HSS J. 2007;3(2):137-146.
67. Pfirrmann CW, Huser M, Szekely G, Hodler J, Gerber C. 2002. Evaluation of complex joint motion with computer-based analysis of fluoroscopic sequences. Invest Radiol 37:73-6.

68. Rasmussen MT, Nitri M, Williams BT, Moulton SG, Cruz RS, Dornan GJ, Goldsmith MT, LaPrade RF. An In Vitro Robotic Assessment of the Anterolateral Ligament, Part 1: Secondary Role of the Anterolateral Ligament in the Setting of an Anterior Cruciate Ligament Injury. Am J Sports Med. 2015 Dec 18

69. Reinschmidt C, van Den Bogert AJ, Murphy N, Lundberg A, Nigg BM. 1997. Tibiocalcaneal motion during running, measured with external and bone markers. Clin Biomech (Bristol, Avon) 12:8-16.

70. Richter M, Kiefer H, Hehl G, Kinzl L. Primary repair for posterior cruciate ligament injuries: an eight-year followup of fifty-three patients. Am J Sports Med. 1996;24(3):298-305.

71. Roos H, Adalberth T, Dahlberg L, Lohmander LS. Osteoarthritis of the knee after injury to the anterior cruciate ligament or meniscus: the influence of time and age. Osteoarthritis Cartilage 1995;3:261–7.

72. Sachs RA, Daniel DM, Stone ML, Garfein RF. Patellofemoral problems after anterior cruciate ligament reconstruction. Am J Sports Med. 1989;17(6):760-765.

73. Schulte KR, Chu ET, Fu FH. Arthroscopic posterior cruciate ligament reconstruction. Clin Sports Med. 1997;16(1):145-156.

74. Sheehan FT, Zajac FE, Drace JE. 1998. Using cine phase contrast magnetic resonance imaging to non-invasively study in vivo knee dynamics. J Biomech 31:21-6.

75. Sonnery-Cottet B, Thaunat M, Freychet B, Pupim BH, Murphy CG, Claes S. Outcome of a Combined Anterior Cruciate Ligament and Anterolateral Ligament Reconstruction Technique With a Minimum 2-Year Follow-up. Am J Sports Med. 2015;43:1598-1605.

76. Spencer L, Burkhart TA, Tran MN, Rezansoff AJ, Deo S, Caterine S, Getgood AM. Biomechanical Analysis of Simulated Clinical Testing and Reconstruction of the Anterolateral Ligament of the Knee. Am J Sports Med. 2015;43:2189-2197.

77. Strobel MJ, Weiler A, Schulz MS, Russe K, Eichhorn HJ. Arthroscopic evaluation of articular cartilage lesions in posterior-cruciate-ligament deficient knees. Arthroscopy. 2003;19(3):262-268.

78. Tsepis E, Vagenas G, Ristanis S, Georgoulis AD. Thigh muscle weak- ness in ACL-deficient knees persists without structured rehabilitation. Clin Orthop Relat Res. 2006;450:211-218.

79. Van de Velde SK, Bingham JT, Hosseini A et al. 2009. Increased tibiofemoral cartilage contact deformation in patients with anterior cruciate ligament deficiency. Arthritis Rheum 60:3693-702.

80. Van de Velde SK, DeFrate LE, Gill TJ, Moses JM, Papannagari R, Li G. The effect of anterior cruciate ligament deficiency on the in vivo elongation of the medial and lateral collateral ligaments. Am J Sports Med. 2007;35:294-300.

81. Van de Velde SK, Gill TJ, Li G. 2009. Evaluation of kinematics of anterior cruciate ligament-deficient knees with use of advanced imaging techniques, three-dimensional modeling techniques, and robotics. J Bone Joint Surg Am 91 Suppl 1:108-14.

82. Van de Velde SK, Hosseini A, Kozanek M, Gill TJ, Rubash HE, Li G: Application guidelines for dynamic knee joint analysis with a dual fluoroscopic imaging system. Acta Orthop Belg. 2010 Feb;76(1):107-13.

83. van Dijk R, Huiskes R, Selvik G. 1979. Roentgen stereophotogrammetric methods for the evaluation of the three dimensional kinematic behaviour and cruciate ligament length patterns of the human knee joint. J Biomech 12:727-31.

84. Westblad P, Hashimoto T, Winson I, Lundberg A, Arndt A. 2002. Differences in ankle-joint complex motion during the stance phase of walking as measured by superficial and bone-anchored markers. Foot Ankle Int 23:856-63.

85. Wojtys EM, Huston LJ. Neuromuscular performance in normal and anterior cruciate ligament–deficient lower extremities. Am J Sports Med. 1994;22(1):89-104.

86. Yamaguchi S, Sasho T, Kato H, Kuroyanagi Y, Banks SA. 2009. Ankle and subtalar kinematics during dorsiflexion-plantarflexion activities. Foot Ankle Int 30:361-6.

87. Zens M, Niemeyer P, Ruhhammer J, et al. Length Changes of the Anterolateral Ligament During Passive Knee Motion: A Human Cadaveric Study. Am J Sports Med. 2015;43:2545-2552.

SUMMARY

This thesis offers an overview of the development, validation and application of a non-invasive imaging methodology to capture the in vivo biomechanics of cruciate ligament deficient knees.

By combining dual fluoroscopy to capture the in vivo joint motion and magnetic resonance (MR) imaging to reconstruct the joint anatomy (***Chapter 2***), we obtained a comprehensive insight in both tibiofemoral as well as patellofemoral kinematics and cartilage biomechanics of healthy knees under various loading conditions. These baseline measurements helped us comprehend the alterations in biomechanics seen in knees after injury of the cruciate ligaments, which in turn generated clinically useful data for the improvement of our surgical reconstruction techniques.

The first step of the imaging procedure is the acquisition of a 3D surface mesh model of the joint that includes the anatomical structures relevant to the study including bones, plus respective cartilage layers or ligament insertion sites. To accomplish this, the joint is scanned with an MR scanner, the acquired images are imported into solid modeling software, and the contours of the anatomical structures are digitized within each MR image. Next, the knee is simultaneously imaged with two fluoroscopes during in vivo motion. The fluoroscopic images are then imported in the solid modeling software and placed in the position of the intensifiers of the virtual fluoroscopes. In the following step, the 3D joint model is imported in the same modeling file, placed in the 3D space between the points that replicate the respective fluoroscopes and translated and rotated in all degrees-of-freedom until the 3D model matches the bony contours on both fluoroscopic images. By repeating this matching process at selected intervals of the investigated joint motion, a series of joint models that replicate the in vivo 6DOF articular motion is created which form the basis for further biomechanical analysis (***Chapter 3***).

A thorough understanding of the capabilities and limitations of the analysis system is necessary to investigate the knee joint motion with the technique. When comparing the results of the imaging technique with the 'gold standard' in joint kinematics analysis, namely the highly accurate but invasive RSA technique, we found an excellent agreement in all degrees-of-freedom that were determined by the two methods. The difference in reproduction of tibiofemoral kinematics during dynamic flexion-extension between the imaging technique and the RSA method was 0.1 ± 0.65°/second in flexion speed ; 0.24 ± 0.16 mm in posterior femoral translation; and 0.16 ± 0.61° in internal- external tibial rotation (***Chapter 4***).

The biomechanical data of ACL deficient and PCL deficient knees that were obtained with the combined MR and dual fluoroscopic imaging system are presented in the subsequent chapters. ***Chapter 5*** demonstrates how minimal alterations in tibiofemoral kinematics in ACL deficient knees result in significant abnormal cartilage contact biomechanics. Rupture

of the ACL changed the cartilage contact biomechanics between 0° and 60° of flexion in the medial compartment of the knee. Compared with the contralateral knee, the location of peak cartilage contact deformation on the tibial plateaus was more posterior and lateral, the contact area was smaller, the average cartilage thickness at the tibial cartilage contact area was thinner, and the resultant magnitude of cartilage contact deformation was increased. Similar changes were observed in the lateral compartment, with increased cartilage contact deformation from 0° to 30° of knee flexion in the presence of ACL deficiency.

The altered tibiofemoral kinematics that are seen upon loss of PCL function changed the cartilage contact biomechanics in PCL deficiency as well (***Chapter 6***). In the medial compartment of the PCL deficient knees, the location and magnitude of peak cartilage deformation were significantly changed, compared with those in the intact contralateral knees, between 75° and 120° of flexion, with a more anterior and medial location of peak cartilage deformation on the tibial plateau as well as increased deformation of the cartilage. In the lateral compartment, no significant differences in the location or magnitude of peak cartilage deformation were found between the intact and PCL deficient knees.

Cruciate ligament deficiency not only disturbed the tibiofemoral biomechanics but altered the patellofemoral joint as well. We observed a significant apparent elongation and change in orientation of the patellar tendon in ACL deficient knees. The altered function of the patellar tendon resulted in an altered patellar tracking and a proximal and lateral shift in patellofemoral cartilage contact location (***Chapter 7***).

Similarly in PCL deficiency, we found that the changes seen in tibiofemoral kinematics following rupture of the ligament resulted in altered patellofemoral kinematics (***Chapter 8***). PCL deficiency increased the patellar flexion angle and decreased the lateral shift, tilt, and valgus rotation of the patella at flexion angles 90° and greater. Due to the congruency of the patellofemoral joint, these changes in patellofemoral kinematics resulted in changes in the location of the patellofemoral cartilage contact point. PCL deficiency caused a distal and medial shift of cartilage contact point from 75° to 120° of flexion.

In ***Chapter 9***, we show that injury to the ACL caused a significant elongation of the fiber bundles of the MCL at every flexion angle. These altered length patterns of the collateral ligaments, associated with the changes in tibiofemoral joint kinematics after ACL injury, demonstrate that deficiency of the ACL upsets the in vivo knee homeostasis and puts the associated joint environment at greater risk of secondary injury.

In ***Chapter 10,*** we argue against performing an anatomic reconstruction of the ALL. Of the various theoretical anterolateral reconstructions, an anatomic ALL graft was least isometric and was not affected by ACL deficiency. The length increase of the ALL during in vivo weight bearing from 0° to 90° of flexion was close to 50%. Such increase during knee flexion suggests that an anatomic reconstruction of this structure might likely be biomechanically unfavorable. Specifically, an anatomic ALL graft with its femoral fixation

slightly anterior and distal to the attachment of the FCL would be either slack in extension, where it is intended to correct rotational instability, or too tight in flexion, potentially causing overconstraint of the lateral compartment. The more traditional lateral extra-articular reconstructions that were described several decades ago showed more biomechanically favorable length change patterns with the smallest percent increase in length during knee flexion.

NEDERLANDSE SAMENVATTING

Dit manuscript geeft een overzicht van de ontwikkeling, validatie en toepassing van een niet-invasieve meetmethode die de in vivo biomechanica van de knie na een letsel van een van de kruisbanden evalueert.

Door de koppeling van twee beeldversterkers, die de in vivo beweging simultaan vastleggen, met magnetische resonantie (MR) beelden, die de anatomie van het gewricht reconstrueren (***Hoofdstuk 2***), hebben wij inzicht gekregen in zowel tibiofemorale als patellofemorale kinematica en kraakbeenbiomechica van gezonde knieën tijdens verschillende activiteiten. Met deze uitgangsmetingen in gezonde knieën konden de veranderingen in biomechanica die optreden in knieën na letsel van ofwel de voorste kruisband (VKB) of de achterste kruisband (AKB) bestudeerd worden. Het bestuderen van deze verschillen vormt de basis voor het verbeteren van de operatieve technieken van een gescheurde kruisband.

De eerste stap van de beeldvormingstechniek is het maken van een 3D oppervlakte model van de ossale structuren van de knie, inclusief de anatomische structuren die relevant zijn voor de betreffende studie, zoals kraakbeenlagen of ligamentaire aanhechting locaties. Een MRI scan van de knie vormt de basis van het 3D kniemodel, vervolgens worden deze beelden met software voor modelontwikkeling bewerkt. Binnen elk MRI beeld worden de contouren van de anatomische structuren gedigitaliseerd. In de volgende stap wordt de knie van de patiënt simultaan door twee beeldversterkers doorlicht tijdens een in vivo activiteit. Deze doorlichtingsbeelden worden ook in deze software ingevoerd en in de positie geplaatst van de beeldversterkers. Het 3D kniemodel wordt in deze virtuele testomgeving gebracht en zodanig gepositioneerd dat het past binnen alle translaties en rotaties van het gewricht op beide doorlichtingsbeelden. Door dit proces te herhalen voor meerdere discrete punten van de in vivo activiteit wordt een serie anatomische modellen gecreëerd die deze in vivo activiteit reproduceert (***Hoofdstuk 3***). Hierop kunnen dan de gewenste metingen verricht worden.

Inzicht in de mogelijkheden en beperkingen (i.e. validatie) van beide beeldvormings-technieken (doorlichting en MRI) is essentieel voordat een analyse van de knie biomechanica met deze techniek kan starten. Dit werd gedaan door de beeldvormingstechniek te vergelijken met de ‘gouden standaard’ wat betreft accurate analyse van gewrichtskinematica, namelijk de Röntgen Stereophotogrammetrische Analyse (RSA). In alle rotatie- en translatiemogelijkheden zagen wij een excellent resultaat. Het verschil in de reproductie van tibiofemorale kinematica tussen de twee meetmethoden was 0.1 ± 0.65°/seconden voor flexie snelheid; 0.24 ± 0.16 mm voor posterieure femorale translatie; en 0.16 ± 0.61° voor interne- externe tibiale rotatie (***Hoofdstuk 4***).

In de volgende hoofdstukken worden de biomechanica data van VKB-insufficiënte en AKB-insufficiënte knieën gepresenteerd die met de gecombineerde MRI en beeldversterker

techniek werden gegenereerd. In ***Hoofdstuk 5*** beschrijven wij hoe minimale veranderingen in tibiofemorale kinematica van VKB-insufficiënte knieën leiden tot significante veranderingen in kraakbeenbiomechanica. Een VKB ruptuur veranderde de kraakbeenbiomechanica tussen 0° en 60° flexie in het mediale compartiment van de knie. In vergelijking met de gezonde contralaterale knie was het punt van maximale kraakbeendeformatie op de tibiaplateaus meer posterior en lateraal gelokaliseerd. Het contactoppervlakte was kleiner en het kraakbeen was dunner ter hoogte van de contactregio. Tezamen resulteerde dit in een verhoogde kraakbeendeformatie. Vergelijkbare bevindingen werden gezien in het laterale compartiment van de VKB-insufficiënte knie tussen 0° en 30° flexie.

De veranderingen in tibiofemorale kinematica die optreden na het verlies van de functie van de AKB zorgden ook voor veranderingen in de kraakbeenbiomechanica van AKB-insufficiënte knieën (***Hoofdstuk 6***). In het mediale compartiment van AKB-insufficiënte knieën waren de locatie en grootte van kraakbeendeformatie significant gewijzigd in vergelijking met deze van de gezonde contralaterale knieën tussen 75° en 120° flexie, met een meer anterieure en mediale locatie van maximale kraakbeendeformatie op het mediale tibiaplateau alsook een verhoogde kraakbeendeformatie. In het laterale compartiment, daarentegen, zagen wij geen effect van AKB insufficiëntie op de kraakbeenbiomechanica.

Insufficiëntie van de kruisbanden heeft niet alleen een negatieve impact op het tibiofemorale gewricht. Ook de kinematica van het patellofemorale gewricht worden beïnvloed door een ruptuur van de kruisband. Er was een significante elongatie en verandering in oriëntatie van de patellapees in VKB-insufficiënte knieën. Deze veranderde functie van de patellapees verstoorde de normale sporing van de patella, resulterend in een proximale en laterale verplaatsing van kraakbeencontact tussen patella en femur (***Hoofdstuk 7***).

Ook in AKB-insufficiënte knieën beïnvloedde de gewijzigde tibiofemorale kinematica het patellofemorale gewricht (***Hoofdstuk 8***). Een toename in patellaflexie en een afname in laterale verplaatsing (shift), kanteling (tilt) en valgus rotatie van de patella werden gezien vanaf 90° flexie in AKB-insufficiënte knieën. Door de congruentie van het patellofemorale gewricht leidden de veranderingen in patellofemorale kinematica tot een meer distale en mediale locatie van kraakbeenbelasting op de patella in AKB-insufficiënte knieën.

In ***Hoofdstuk 9*** beschrijven wij hoe een ruptuur van de VKB leidt tot een significante elongatie van het mediale collaterale ligament (MCL) tijdens buiging van de knie. Deze bevinding demonstreert hoe VKB insufficiëntie de in vivo homeostase van de knie verstoort en de geassocieerde stabiliserende structuren van de knie een verhoogd risico hebben op secundaire schade.

Tenslotte, wordt in ***Hoofdstuk 10*** onderbouwd hoe anatomische reconstructie van het anterolaterale ligament (ALL) bij verschillende chirurgische anterolaterale ligamentaire

reconstructies biomechanisch functioneert binnen onze beeldverwerkings methodiek. Een anatomische ALL reconstructie was namelijk niet isometrisch en werd bovendien niet beïnvloed door VKB insufficiëntie. Tussen 0° en 90° flexie nam het ALL 50% toe in lengte. Een dergelijke toename van een graftlengte leidt tot biomechanisch falen. Ofwel zou de graft te laks zijn in extensie van de knie (waar de rotatoire instabiliteit van de knie het meest uitgesproken is in VKB insufficiëntie), ofwel te strak in flexie met mogelijk overbelasting van het laterale compartiment. De traditionele anterolaterale reconstructies die decennia geleden reeds beschreven zijn, lieten een biomechanisch normaler elongatiepatroon zien, waarbij de meeste isometrie gedurende knieflexie aanwezig was.

ACKNOWLEDGEMENTS

None of the data presented in this thesis would have been possible without the work of the co-authors. A special thanks goes to Drs. Guoan Li, Louis DeFrate and Thomas Gill IV for introducing me to the world of orthopaedic biomechanical research.

I thank Prof. dr. Rob Nelissen and Dr. Ewoud van Arkel whose never-failing encouragement is responsible for this thesis.

The administrative help of Anika Hoogenstraaten was greatly appreciated.

Finally, I would like to thank Dr. Suzanne Yandow for showing me that Oahu has more to boast than beaches and pineapple plantations, namely intriguing pediatric hip disorders.

CURRICULUM VITAE

Samuel Van de Velde was born on July 13th 1978, in Mechelen, Belgium. After studying Latin and Greek at the Sint Romboutscollege in Mechelen, Belgium, he started his medical training at the Catholic University of Louvain, Belgium. During medical training, he completed a clinical rotation with Dr. Suzanne Yandow at the University of Hawaii/Shriners Hospital for Children. There, he studied protrusio acetabuli in children with certain connective tissue disorders – such as Marfan syndrome and Congenital Contractural Arachnodactyly.

After graduating *cum laude* from medical school in 2003 and clinical internships in orthopaedics and general surgery in Amsterdam and Leiden, the Netherlands, he joined the Bioengineering Laboratory at the Massachusetts General Hospital in Boston, Massachusetts (USA), as a postdoctoral research fellow in 2005. With Prof. Guoan Li, he initiated the study into the biomechanical pathogenesis of posttraumatic osteoarthritis following rupture of one of the cruciate ligaments in the knee joint, as outlined in this thesis. He was promoted to research faculty at Harvard Medical School in 2009. Some of the accolades of his stay in Boston include the O'Donoghue Sports Injury Research Award, a master's degree from the Harvard School of Public Health, and the Ruth Kirschstein Fellowship Award from the National Institutes of Health.

In 2011, he returned to the Netherlands to commence his Orthopaedic residency at Leiden University Medical Center, Leiden, and Medical Center Haaglanden – Bronovo, The Hague, under the supervision of Prof. dr. Rob Nelissen and Dr. Ewoud van Arkel. He is currently completing his final year of orthopaedic training.

In January 2017, he will complete a six-month visiting scholarship with Prof. dr. Mininder Kocher at Boston Children's Hospital. Here he will study the clinic and biomechanics of pediatric anterior cruciate ligament injury and reconstruction. In July 2017, he will move to Toronto, Canada, for the one-year Pediatric Orthopaedic Fellowship at The Hospital for Sick Children.

He lives in The Hague with his wife Jolie and three children, Svea, Finnegan and Beckett.

PUBLICATIONS

Publications related to this thesis

Van de Velde SK, Gill TJ, Li G: Evaluation of kinematics of anterior cruciate ligament-deficient knees with use of advanced imaging techniques, three-dimensional modeling techniques, and robotics. J Bone Joint Surg Am. 2009 Feb;91 Suppl 1:108-14.

Van de Velde SK, Hosseini A, Kozanek M, Gill TJ, Rubash HE, Li G: Application guidelines for dynamic knee joint analysis with a dual fluoroscopic imaging system. Acta Orthop Belg. 2010 Feb;76(1):107-13.

Li G, **Van de Velde SK**, and Bingham JT: Validation of a Non-invasive Fluoroscopic Imaging Technique for the Measurement of Dynamic Knee Joint Motion. J Biomech. 2008;41(7):1616-22.

Van de Velde SK, Bingham JT, Hosseini A, Kozanek M, DeFrate LE, Gill TJ, Li G: Increased in-vivo tibiofemoral cartilage contact deformation in anterior cruciate ligament-deficiency. Arthritis Rheum. 2009 Dec;60(12):3693-702.

Van de Velde SK, Bingham JT, Gill TJ, Li G: Analysis of tibiofemoral cartilage deformation in the posterior cruciate ligament-deficient knee. J Bone Joint Surg Am. 2009 Jan;91(1):167-75.

Van de Velde SK, Gill TJ, DeFrate LE, Papannagari R, Li G: The effect of anterior cruciate ligament deficiency and reconstruction on the patellofemoral joint. Am J Sports Med. 2008 Jun;36(6):1150-9.

Van de Velde SK, Gill TJ, Li G: Dual Fluoroscopic Analysis of the PCL-Deficient Patellofemoral Joint During Lunge. Med Sci Sports Exerc. 2009 Jun;41(6):1198-205.

Van de Velde SK, DeFrate LE, Gill TJ, Moses JM, Papannagari R, Li G: The effect of anterior cruciate ligament deficiency on the in vivo elongation of the medial and lateral collateral ligaments. Am J Sports Med. 2007 Feb;35(2):294-300.

Van de Velde SK, Kernkamp WA, Hosseini A, LaPrade RF, van Arkel E, Li G. In Vivo Elongation of the Anterolateral Ligament and Related Extra-Articular Reconstructions. Am J Sports Med, *in press*.

Other Publications

Van de Velde S, Fillman R, Yandow S: Protrusio Acetabuli in Marfan Syndrome: Indication for Surgery in a Skeletally Immature Marfan Patient. J Pediatr Orthop. 2005 Sep-Oct;25(5):603-6.

Van de Velde S, Fillman R, Yandow S: Current Concepts – Protrusio Acetabuli in Marfan Syndrome: History, Diagnosis, and Treatment. J Bone Joint Surg Am. 2006 Mar;88(3):639-46.

Van de Velde S, Fillman R, Yandow S: The aetiology of protrusio acetabuli. Literature review from 1824 to 2006. Acta Orthop Belg. 2006 Oct;72(5):524-9.

McClure SD, **Van de Velde S**, Fillman R, Yandow S: New Finding of Protrusio Acetabuli in Two Families with Congenital Contractural Arachnodactyly. J Bone Joint Surg Am. 2007 Apr;89(4):849-54.

Zarins B, **Van de Velde SK**, and Gill TJ: Advances in ACL Reconstruction: Current Concepts and Controversies in ACL Surgery. The Orthopaedic Journal at Harvard Medical School, epub Dec 2007.

Nha KW, Papannagari R, Gill TJ, **Van de Velde SK**, Freiberg AA, Rubash HE, Li G: In-vivo Patellar Tracking: Clinical Motions and Patellofemoral Indices. J Orthop Res. 2008 Aug;26(8):1067-74.

Bingham JT, Papannagari R, **Van de Velde SK**, Gross C, Gill TJ, Felson DT, Rubash HE, Li G: In vivo cartilage contact deformation in the healthy human tibiofemoral joint. Rheumatology (Oxford). 2008 Nov;47(11):1622-7.

Kozanek, M, **Van de Velde SK**, Gill TJ, Li G: The Contralateral Knee Joint in Cruciate Ligament Deficiency. Am J Sports Med. 2008 Nov;36(11):2151-7.

Kozanek, M, Fu EC, **Van de Velde SK**, Gill TJ, Li G: Posterolateral Structures of the Knee in Posterior Cruciate Ligament Deficiency. Am J Sports Med. 2009 Mar;37(3):534-41.

Van de Velde SK, Pearle AD. Section VI: Malalignment and ligamentous injury. J Bone Joint Surg Am. 2009 Feb;91 Suppl 1:77.

Li G, Hosseini A, Liu F, **Van de Velde SK**, Kozanek M: New Fluoroscopic Imaging Technique for Investigation of 6DOF Knee Kinematics during Treadmill Gait. J Orthop Surg Res. 2009 Mar 13;4:6.

Kozanek M, Hosseini A, **Van de Velde SK**, Liu F, Gill TJ, Rubash HE, Li G: Tibiofemoral kinematics and condylar motion during the stance phase of gait. J Biomech. 2009 Aug 25;42(12):1877-84.

Gill TJ, **Van de Velde SK**, Wing DW, Oh LS, Li G: 2009 AOSSM O'Donoghue Sports Injury Research Award paper: Tibiofemoral and Patellofemoral Kinematics Following Reconstruction of an Isolated Posterior Cruciate Ligament Injury. Am J Sports Med. 2009 Dec;37(12):2377-85.

Liu F, Hosseini A, Kozanek M, **Van de Velde SK**, Gill TJ, Rubash HE, Li G: In-vivo Tibiofemoral Cartilage Deformation during the Stance Phase of Gait. J Biomech. 2010 Mar 3;43(4):658-65.

Hosseini A, **Van de Velde SK**, Kozanek M, Gill TJ, Grodzinsky AJ, Rubash HE, Li G. In-vivo time-dependent creep articular cartilage contact behavior of the tibiofemoral joint. Osteoarthritis Cartilage. 2010 Jul;18(7):909-16.

Ferry AT, **Van de Velde SK**, Li G, Asnis P, Zarins B, Gill TJ. Revision anterior cruciate ligament reconstruction: preoperative planning and technical considerations. The Orthopaedic Journal at Harvard Medical School, epub Dec 2010.

Kozanek M, **Van de Velde SK**, Hosseini A, Gill TJ, Li G. Biomechanics of ACL Deficiency and Contemporary Reconstruction Techniques. In Anterior Cruciate Ligament (ACL): Causes of Injury, Adverse Effects and Treatment Options (Ed. Yeager CR), 2010;29-60.

Van de Velde SK, Li G, Oh LS, Robertson W, Gill TJ. The improvement of outcomes in posterior cruciate ligament reconstruction: a case for joint biomechanics. Minerva Ortop Traumatol, 2010;61:353-64.

Van de Velde SK, Gill TJ. Treatment for acute anterior cruciate ligament tear. N Engl J Med. 2010 Nov 4;363(19):1871-2.

Hosseini A, Gill TJ, **Van de Velde SK**, Li G. Estimation of in vivo ACL force changes in response to increased weightbearing. J Biomech Eng. 2011 May;133(5):051004.

Kozanek, M, Hosseini A, **Van de Velde SK**, Moussa ME, Gill TJ, Li G. Kinematic Evaluation of the Step-up Exercise in Anterior Cruciate Ligament Deficiency. Clin Biomech (Bristol, Avon). 2011 Nov;26(9):950-4.

Hosseini A, Lodhia P, **Van de Velde SK**, Asnis PD, Zarins B, Gill TJ, Li G. Tunnel position and graft orientation in failed anterior cruciate ligament reconstruction: a clinical and imaging analysis. Int Orthop. 2012 Apr;36(4):845-52.

Gill TJ, **Van de Velde SK**, Carroll K, Robertson WJ, Heyworth B. Surgical technique: Aperture fixation in PCL reconstruction: applying biomechanics to surgery. Clin Orthop Relat Res. 2012 Mar;470(3):853-60.

Van de Velde SK. Behind Enemy Lines – A Year at the Harvard School of Public Health. The Harvard Orthopaedic Journal at Harvard Medical School, epub Dec 2011.

Hosseini A, **Van de Velde SK**, Gill TJ, Li G. Tibiofemoral cartilage contact biomechanics in patients after reconstruction of a ruptured anterior cruciate ligament. J Orthop Res. 2012 Nov;30(11):1781-8.

Carroll KM, Cvetanovich G, Heyworth BE, **Van de Velde S**, Gill TJ. Approach to Management of the Patient with the Multiligament-Injured Knee. Harvard Orthopaedic Journal. 2013 Dec;15:54-64.

Kornaat PR, **Van de Velde SK**. Bone Marrow Edema Lesions in the Professional Athlete. Am J Sports Med. 2014 May;42(5):1242-6.

Schaasberg W, van der Steenhoven TJ, **Van de Velde SK**, Valstar ER, Nelissen RGHH. Feasibility of Osteosynthesis of Fractured Cadaveric Hips Following Preventive Elastomer Femoroplasty. Clin Biomech (Bristol, Avon). 2014 Aug;29(7):742-6.

Van der Steenhoven TJ, Staffhorst B, **Van de Velde SK**, Nelissen RGHH, Verhofstad MH. Complications and institutionalization are almost doubled after second hip fracture surgery in the elderly patient. J Orthop Trauma. 2015 Mar;29(3):e103-8.

Kernkamp WA, **Van de Velde SK**, Bakker EW, van Arkel E. Anterolateral extra-articular soft tissue reconstruction in persistent anterolateral rotatory instability of the knee after anterior cruciate ligament reconstruction. Arthroscopy Techniques, 2015 Dec;4(6):e863–e867.

Van der Wal RJ, **Van de Velde SK**, van Arkel ER. The Approach to Meniscal Lesions in the Netherlands; A Paradigm Shift. Ned Tijd Orthop. 2016, 23(2).

Kernkamp WA, **Van de Velde SK**, Tsai TY, Hosseini A, van Arkel E, Li G. In Vivo Anterolateral Ligament Length Change in the Healthy Knee during Functional Activities - A Combined Magnetic Resonance and Dual Fluoroscopic Imaging Analysis. Arthroscopy. 2016, *in press*.

Kernkamp WA, Li G, **Van de Velde SK**. The Anterolateral Ligament: a Closed Chapter? Ann Trans Med. 2016, *in press*.

Abstracts, Poster Presentations and Exhibits Presented at Professional Meetings

DeFrate LE, **Van de Velde SK**, Papannagari R, Moses JM, Gill TJ, Li G: Injury to the Anterior Cruciate Ligament Alters the In Vivo Length of the Collateral Ligaments. In: 6th International Symposium on Ligaments & Tendons-VI, Chicago, IL, 2006.

Van de Velde SK, Papannagari R, DeFrate LE, Gill TJ, Moses JM, Li G: Reconstruction of the Injured Anterior Cruciate Ligament Does Not Restore Normal Patellofemoral Cartilage Contact Kinematics. In: 7th International Symposium on Ligaments & Tendons-VII, San Diego, CA, 2007.

Van de Velde SK, DeFrate LE, Papannagari R, Gill TJ, Moses JM, Li G: The In Vivo Elongation and Orientation of the Patellar Tendon After Injury to the Anterior Cruciate Ligament. In: Trans ORS; Feb, 2007, San Diego, CA.

Van de Velde SK, DeFrate LE, Papannagari R, Gill TJ, Moses JM, Li G: The In Vivo Patellofemoral Cartilage Contact Kinematics Changes After Anterior Cruciate Ligament Injury. In: Trans ORS; Feb, 2007, San Diego, CA.

Van de Velde SK, DeFrate LE, Papannagari R, Gill TJ, Moses JM, Li G: The Effect of Anterior Cruciate Ligament Injury on the In Vivo Elongation of the Medial and Lateral Collateral Ligaments. In: Trans ORS; Feb, 2007, San Diego, CA.

Van de Velde SK, DeFrate LE, Papannagari R, Gill TJ, Moses JM, Li G: The In Vivo Elongation and Orientation of the Patellar Tendon After Injury to the Anterior Cruciate Ligament. In: 4th Annual Meeting of the International Chinese Hard Tissue Society, San Diego, CA, 2007.

Li G, Bingham J, Papannagari R, **Van de Velde S**, Hosseini A: Validation of a Dual Fluoroscopic System for Measurement of Dynamic Knee Motion. In: Asian-Pacific Biomechanics Conference, 2007.

Van de Velde SK, Gill TJ, DeFrate LE, Papannagari R, Li G. Reconstruction of the Injured Anterior Cruciate Ligament Does Not Restore the Normal Patellofemoral Joint Function. In: American Orthopaedic Society for Sports Medicine Specialty Day; March, 2008; San Francisco, CA.

Van de Velde SK, Bingham JT, DeFrate LE, Gill TJ, Li G. Why does the ACL-deficient knee develop osteoarthritis? In: Trans ORS; March, 2008; San Francisco, CA.

Van de Velde SK, DeFrate LE, Gill TJ, Papannagari R, Li G. ACL Deficiency Alters Patellar Tracking. In: Trans ORS; March, 2008; San Francisco, CA.

Van de Velde SK, DeFrate LE, Gill TJ, Papannagari R, Li G. The Patellar Tendon after ACL Reconstruction with a Bone-patellar tendon-bone Autograft. In: Trans ORS; March, 2008; San Francisco, CA.

Bingham JT, **Van de Velde SK**, Li G. Validation of a Non-invasive Imaging Technique for the Accurate Measurement of Dynamic Knee Joint Motion. In: Trans ORS; March, 2008; San Francisco, CA.

Van de Velde SK, Gill TJ, DeFrate LE, Papannagari R, Li G. The Patellar Tendon After ACL Reconstruction With a Bone-Patellar Tendon-Bone Autograft. In: Trans ORS; March, 2008; San Francisco, CA.

Van de Velde SK, Bingham JT, DeFrate LE, Gill TJ, Li G. ACL-Reconstruction & Cartilage Deformation. In: 8th International Symposium on Ligaments & Tendons; March, 2008; San Francisco, CA.

Van de Velde SK, Bingham JT, DeFrate LE, Gill TJ, Li G. Cartilage Deformation in the ACL-Reconstructed Knee. In: Ann. Meeting of the American Orthopaedic Society for Sports Medicine; July, 2008; Orlando, FL.

Kozanek, M, Fu EC, **Van de Velde SK**, Gill TJ, Li G. Posterolateral Structures of the Knee in PCL Deficiency. In: 76th Annual Meeting of the American Academy of Orthopaedic Surgeons; March, 2009; Las Vegas, NV.

Kozanek, M, **Van de Velde SK**, Gill TJ, Li G. The Contralateral Knee Joint in Cruciate Ligament Deficiency. In: 76th Annual Meeting of the American Academy of Orthopaedic Surgeons; March, 2009; Las Vegas, NV.

Altman K, **Van de Velde SK**, Gill TJ, Bellemans J, Li G: Is the 'Normal' Contralateral Knee Still Normal, Two Years Following PCL Reconstruction? In: Trans ORS; Feb, 2009; Las Vegas, NV.

Van de Velde SK, Wing DW, Oh L, Gill TJ, Li G: PCL Reconstruction Successfully Restores the AP Translation of the Tibia. In: Trans ORS; Feb, 2009; Las Vegas, NV.

Van de Velde SK, Gill TJ, Li G. The Patellofemoral Joint in PCL Deficiency: Defining a Safe Range of Motion. In: Trans ORS; Feb, 2009; Las Vegas, NV.

Van de Velde SK, Bingham JT, Gill TJ, Li G. The Location and Magnitude of Cartilage Deformation in PCL Deficiency: an Injurious Jab and Cross Combo. In: Trans ORS; Feb, 2009; Las Vegas, NV.

Liu F, **Van de Velde SK**, Wing DW, Gill TJ, Li G. Patellar Tracking in the PCL-Reconstructed Knee. In: Trans ORS; Feb, 2009; Las Vegas, NV.

Kozanek M, Fu EC, **Van de Velde SK**, Gill TJ, Li G. PCL Deficiency Alters the Elongation of Posterolateral Structures of the Knee. In: Trans ORS; Feb, 2009; Las Vegas, NV.

Kozanek M, Hosseini A, Liu F, **Van de Velde SK**, Gill TJ, Rubash HE, Li G. Tibiofemoral Kinematics During the Stance Phase of Gait. In: Trans ORS; Feb, 2009; Las Vegas, NV.

Van de Velde SK, Bingham JT, DeFrate LE, Gill TJ, Li G. Cartilage Deformation, ACL reconstruction, and OA Development. In: Trans ORS; Feb, 2009; Las Vegas, NV.

Hosseini A, Kozanek M, Liu F, **Van de Velde SK**, Gill T, Li G. In-Vivo Kinematics of the Anterior Cruciate Ligament during Gait on Treadmill. In: Trans ORS; Feb, 2009; Las Vegas, NV.

Gill TJ, **Van de Velde SK**, Wing DW, Oh LS, Li G. Tibiofemoral and Patellofemoral Kinematics Following Reconstruction of an Isolated PCL Injury. In: Annual Meeting of the American Orthopaedic Society for Sports Medicine; July, 2009; Keystone, CO.

Van de Velde SK, Wing DT, O LS, Gill TJ, Li G. Analysis of Tibiofemoral Cartilage Deformation in the PCL-Reconstructed Knee. In: Trans ORS; March, 2010; New Orleans, LA.

Van de Velde SK, Hosseini A, Kozanek M, Li G. Accuracy and Precision of Tibiofemoral Cartilage Thickness Measurement by 3T MR Imaging. In: Trans ORS; March, 2010; New Orleans, LA.

Van de Velde SK, Gill TJ, Li G. Cartilage Contact Characteristics in ACL Deficiency. In: Trans ORS; March, 2010; New Orleans, LA.

Van de Velde SK, Gill TJ, Li G. The Location of Peak Cartilage Contact Deformation in ACL Deficiency. In: Trans ORS; March, 2010; New Orleans, LA.

Kozanek M, Hosseini A, **Van de Velde SK**, Kassel D, Fu E, Sutton K, Gill TJ, Li G. Does Anterior Cruciate Ligament Deficiency Alter Knee Motion during Low Impact Daily Activities? In: Trans ORS; March, 2010; New Orleans, LA.

Kozanek M, Hosseini A, **Van de Velde SK**, Sutton K, Passias P, Rubash HE, Gill TJ, Li G. In-vivo Tibiofemoral Kinematics during Daily Functional Activities. In: Trans ORS; March, 2010; New Orleans, LA.

Hosseini A, **Van de Velde SK**, Kozanek M, Gill TJ, Grodzinsky AJ, Rubash HE, Li G. In-vivo Creep Deformation of Tibiofemoral Articular Cartilage. In: Trans ORS; March, 2010; New Orleans, LA.

Hosseini A, Kozanek M, **Van de Velde SK**, Sutton K, Gill TJ, Li G. In-Vivo Kinematics of the Anteromedial and Posterolateral Bundles of the Anterior Cruciate Ligament during Low-Impact Daily Activities. In: Trans ORS; March, 2010; New Orleans, LA.

Liu F, Kozanek M, Hosseini A, **Van de Velde SK**, Gill TJ, Li G. In vivo Tibiofemoral Cartilage Contact Area and Deformation during the Stance Phase of Gait. In: Trans ORS; March, 2010; New Orleans, LA.

Liu F, Kozanek M, Hosseini A, **Van de Velde SK**, Gill TJ, Rubash HE, Li G. In Vivo Tibiofemoral Contact Kinematics during the Stance Phase of Walking. In: Trans ORS; March, 2010; New Orleans, LA.

Gill TJ, Robertson W, **Van de Velde SK**, Redford KM, Carroll K, Li G. Combined Proximal and Distal Tibial Fixation in PCL Reconstruction. In: Trans ORS; March, 2010; New Orleans, LA.

Van de Velde SK, Gill TJ, Li G. Elongation and Orientation Patterns of the Theoretical ACL Bundles Following Injury. In: Trans ORS; March, 2010; New Orleans, LA.

Hosseini A, Kozanek M, **Van de Velde SK**, Driscoll SJ, Garner C, Gill TJ, Li G. In-Vivo Kinematics of the ACL Bundles during Low-Impact Daily Activities. In: Trans ORS; Jan, 2011; Long Beach, CA.

Ferry AT, **Van de Velde SK**, LeBoff Williams A, Li G, Asnis P, Zarins B, Gill TJ. Revision Anterior Cruciate Ligament Reconstruction: A Review of 153 cases. In: Trans ORS; Jan, 2011; Long Beach, CA.

Van de Velde SK, Hosseini A, Kozanek M, Gill TJ, Li G. Tibiofemoral Cartilage Contact Biomechanics in Patients after ACL Reconstruction. In: Trans ORS; Jan, 2011; Long Beach, CA.

Kozanek M, Hosseini A, Moussa M, **Van de Velde SK**, Kassel D, Driscoll SJ, Gill TJ, Li G. To What Extent Does ACL Deficiency Alter Knee Motion during the Low-Impact Activity of Rising from a Chair? In: Trans ORS; Jan, 2011; Long Beach, CA.

Kozanek M, Hosseini A, **Van de Velde SK**, Moussa M, Rubash HE, Gill TJ, Li G. Medial versus Lateral Pivot of the Knee during Daily Weightbearing Activities. In: Trans ORS; Jan, 2011; Long Beach, CA.

Kozanek M, Hosseini A, **Van de Velde SK**, Driscoll SJ, Rubash HE, Gill TJ, Li G. Relationship of Knee Flexion and Motion in Secondary Degrees of Freedom during Daily Weightbearing Activities. In: Trans ORS; Jan, 2011; Long Beach, CA.

Hosseini, A, Kim CW, Lin L, Wang L, **Van de Velde SK**, Asnis PD, Li G. Contribution of the Anterolateral Ligament in Anterior Cruciate Ligament Deficiency and ACL Reconstruction. Poster presentation, 2016 ORS Annual Meeting, Orlanda, FL.

Van de Velde SK, Kernkamp WA, Hosseini A, LaPrade RF, van Arkel E, Li G. In Vivo Elongation of the Anterolateral Ligament and Related Extra-Articular Reconstructions. Podium Presentation, 2016 ORS Annual Meeting, Orlanda, FL.

Van de Velde SK, Kernkamp WA, Hosseini A, LaPrade RF, van Arkel E, Li G. In Vivo Elongation of the Anterolateral Ligament and Related Extra-Articular Reconstructions. Podium Presentation, 2016 ESSKA Annual Meeting, Barcelona, Spain.